EPA/635/R-24/031b
External Review Draft
www.epa.gov/iris

IRIS Toxicological Review of Perfluorononanoic Acid (PFNA) and Related Salts

Supplemental Information

CASRN 375-95-1

March 2024

Integrated Risk Information System
Center for Public Health and Environmental Assessment
Office of Research and Development
U.S. Environmental Protection Agency
Washington, DC

DISCLAIMER

This document is a preliminary draft for review purposes only. This information is distributed solely for the purpose of predissemination peer review under applicable information quality guidelines. It has not been formally disseminated by EPA. It does not represent and should not be construed to represent any Agency determination or policy. Mention of trade names or commercial products does not constitute endorsement or recommendation for use.

CONTENTS

TABLES

FIGURES

ABBREVIATIONS

ABP	androgen binding protein
AC50	activity concentration at 50%
ACE	America's Children and the Environment
ACOG	American College of Obstetricians and Gynecologists
ACTH	adrenocorticotropic hormone
ADHD	attention-deficit/hyperactivity disorder
ADME	absorption, distribution, metabolism, and excretion
AFFF	aqueous film-forming foam
A/G	albumin/globulin
AGD	anogenital distance
AIC	Akaike's information criterion
ALP	alkaline phosphatase
ALT	alanine aminotransferase
AMH	anti-Müllerian hormone
AOP	adverse outcome pathway
APD	anopenile distance
AR	androgen receptor
ASA	active systemic anaphylaxis
ASD	anoscrotal distance
ASD	autism spectrum disorder
AST	aspartate aminotransferase
ATSDR	Agency for Toxic Substances and Disease Registry
AUC	area-under-the-concentration-curve
BAF	bioaccumulation factor
BCF	bioconcentration factor
BCRP	breast cancer resistance protein
BMD	benchmark dose
BMDL	benchmark dose lower confidence limit
BMDS	Benchmark Dose Software
BMI	body mass index
BMR	benchmark response
BUN	blood urea nitrogen
BW	body weight
$BW^{3/4}$	body weight raised to ¾ power
CAR	constitutive androstane receptor
CASRN	Chemical Abstracts Service Registry Number
CDR	Chemical Reporting Data
CERAPP	Collaborative Estrogen Receptor Activity Prediction Project
CHO	Chinese hamster ovary (cell line cells)
CI	confidence interval
CL	confidence limit
CL	clearance
CL_H	human clearance
C_{max}	maximum concentration
CPAD	Chemical and Pollutant Assessment Division
CPHEA	Center for Public Health and Environmental Assessment
CYP450	cytochrome P450
DAF	dosimetric adjustment factor
DDEF	data-derived extrapolation factor
DEG	differentially expressed gene
DMSO	dimethylsulfoxide
DNA	deoxyribonucleic acid
E2	estradiol
EMEA	European Medicines Agency
EPA	Environmental Protection Agency
ER	estrogen receptor
ER	extra risk
ETI	equal-tailed interval
Fa	fraction absorbed
FDA	Food and Drug Administration
FSH	follicle-stimulating hormone
FSH-R	follicle-stimulating hormone receptor
FSIQ	full-scale intelligence quotient
FTOH	fluorotelomer alcohol
GD	gestation day
GDH	glutamate dehydrogenase
GDM	gestational diabetes mellitus
GF	glomerular filtration
GFR	glomerular filtration rate
GGT	γ-glutamyl transferase
GLDH	glutamate dehydrogenase
GLP	good laboratory practices
GM	geometric mean
GSH	glutathione
GST	glutathione-*S*-transferase
HAWC	Health Assessment Workplace Collaborative
HDL	high-density lipoprotein
HEC	human equivalent concentration
HED	human equivalent dose
HERO	Health and Environmental Research Online
HOMA	homeostatic model assessment
HTS	high-throughput screening
Ig	immunoglobulins
IGF-1	insulin like growth factor 1
i.p.	intraperitoneal
IPCS	International Programme on Chemical Safety
IQR	interquartile range
IRIS	Integrated Risk Information System
IUR	inhalation unit risk
i.v.	intravenous
LC_{50}	median lethal concentration
LD_{50}	median lethal dose

LDL	low-density lipoprotein
LDS	lactate dehydrogenase
L-FABP	liver fatty acid binding protein
LH	luteinizing hormone
LOAEL	lowest observed adverse effect level
LOD	limit of detection
LOQ	limit of quantitation
MAD	median absolute deviation
MDR	multidrug resistance-associated protein
MIS	Müllerian inhibiting substance
MOA	mode of action
Na+	sodium
NCI	National Cancer Institute
NH4	ammonium
NHANES	National Health and Nutrition Examination Survey
NIS	sodium-iodide symporter
NOAEL	no-observed-adverse-effect level
NPL	National Priorities List
NTP	National Toxicology Program
OATP	organic anion transporting polypeptide
OCTN2	organic cation/carnitine transporter 2
OECD	Organisation for Economic Co-operation and Development
OR	odds ratio
ORD	Office of Research and Development
OSF	oral slope factor
osRFD	organ/system-specific RfD
PBPK	physiologically based pharmacokinetic
PCOS	polycystic ovary syndrome
PD	pharmacodynamic
PECO	populations, exposures, comparators, and outcomes
PFAS	per- and polyfluoroalkyl substances
PFBA	perfluorobutanoic acid
PFCA	perfluoroalkyl carboxylic acids
PFDA	perfluorodecanoic acid
PFHxA	perfluorohexanoic acid
PFHxS	perfluorohexane sulfonate
PFNA	perfluorononanoic acid
PFOA	perfluorooctanoic acid
PFOS	perfluorooctane sulfonate
PFUnDA	perfluoroundecanoic acid
PIQ	performance IQ
PK	pharmacokinetic
PND	postnatal day
POD	point of departure
POI	primary ovarian insufficiency
PPARα	peroxisome proliferator-activated receptor alpha
PPARβ/δ	peroxisome proliferator-activated receptor beta/delta
PPARγ	peroxisome proliferator-activated receptor gamma
PVDF	polyvinylidene fluoride
PWS	public water system
PXR	pregnane X receptor
RBC	red blood cell
RD	relative deviation
RfC	inhalation reference concentration
RfD	oral reference dose
RNA	ribonucleic acid
RR	risk ratio
RT-PCR	reverse transcription polymerase chain reaction
RWT	relative wall thickness
RXR	retinoid X receptor
SD	Sprague Dawley
SD	standard deviation
SDH	sorbitol dehydrogenase
SDQ	strengths and difficulties questionnaire
SE	standard error
SGA	small for gestational age
SHBG	sex hormone binding globulin
SOD	superoxide dismutase
SREBP	sterol regulatory element-binding protein
StAR	steroidogenic acute regulatory
T3	3,5,3′-triiodothyronine
T4	thyroxine
TBG	thyroid-binding globulin
TH	thyroid hormone
TNFα	tumor necrosis factor alpha
TPO	thyroid peroxidase
TR	thyroid hormone receptor
TRH	thyrotropin-releasing hormone
TSCA	Toxic Substances Control Act
TSH	thyroid-stimulating hormone
TTR	transthyretin
TWA	time-weighted average
UA	uric acid
UCMR	Uncontaminated Monitoring Rule
UF	uncertainty factor
UFA	animal-to-human uncertainty factor
UFC	composite uncertainty factor
UFD	database deficiencies uncertainty factor
UFH	human variation uncertainty factor
UFL	LOAEL-to-NOAEL uncertainty factor
UFS	subchronic-to-chronic uncertainty factor
Vd	volume of distribution
VIQ	verbal IQ
WBC	white blood cell
WOS	Web of Science
WRAVMA	Wide Range Assessment of Visual Motor Abilities
WHO	World Health Organization
WT1	Wilms tumor gene

APPENDIX A. SYSTEMATIC REVIEW PROTOCOL

A single systematic review protocol was used to guide the development of five separate IRIS PFAS assessments (i.e., PFBA, PFHxA, PFHxS, PFNA, and PFDA). The "Systematic Review Protocol for the PFBA, PFHxA, PFHxS, PFNA, and PFDA (anionic and acid forms) IRIS Assessments" was initially released for public comment in 2019 and updated in 2021. The updated protocol and prior revisions can be found at the following location: http://cfpub.epa.gov/ncea/iris_drafts/recordisplay.cfm?deid=345065.

A.1. LITERATURE SEARCH AND SCREENING STRATEGY

Table A-1. Summary of detailed search strategies for PFNA (PubMed, Web of Science, Toxline, TSCATS)

Search	Search strategy	Date
PubMed		
Search Terms	"375-95-1"[rn] OR "2,2,3,3,4,4,5,5,6,6,7,7,8,8,9,9,9-heptadecafluorononanoic acid"[tw] OR "Nonanoic acid, 2,2,3,3,4,4,5,5,6,6,7,7,8,8,9,9,9-heptadecafluoro-"[tw] OR "Nonanoic acid, heptadecafluoro-"[tw] OR "Perfluoro-n-nonanoic acid"[tw] OR "Perfluorononan-1-oic acid"[tw] OR "Perfluorononanoate"[tw] OR "Perfluorononanoic acid"[tw] OR "Perfluorononanonic acid"[tw] OR "Perfluoropelargonic acid"[tw] OR "heptadecafluorononanoic acid"[tw] OR (("PFNA"[tw] OR "C 1800"[tw]) AND (fluorocarbon*[tw] OR fluorotelomer*[tw] OR polyfluoro*[tw] OR perfluoro-*[tw] OR perfluoroa*[tw] OR perfluorob*[tw] OR perfluoroc*[tw] OR perfluorod*[tw] OR perfluoroe*[tw] OR perfluoroh*[tw] OR perfluoron*[tw] OR perfluoroo*[tw] OR perfluorop*[tw] OR perfluoros*[tw] OR perfluorou*[tw] OR perfluorinated[tw] OR fluorinated[tw] OR PFAS [tw] OR PFOS[tw] OR PFOA[tw]))	No date limit–July 2017
Literature update search terms and additional PFNA synonyms	((("2,2,3,3,4,4,5,5,6,6,7,7,8,8,9,9,9-heptadecafluorononanoic acid" [tw] OR "Nonanoic acid, 2,2,3,3,4,4,5,5,6,6,7,7,8,8,9,9,9-heptadecafluoro-" [tw] OR "Nonanoic acid, heptadecafluoro-" [tw] OR "Perfluoro-n-nonanoic acid" [tw] OR "Perfluorononan-1-oic acid" [tw] OR "Perfluorononanoate" [tw] OR "Perfluorononanoic acid" [tw] OR "Perfluorononanonic acid" [tw] OR "Perfluoropelargonic acid" [tw] OR "heptadecafluorononanoic acid" [tw] OR "PFNA" [tw] OR "C 1800" [tw] OR "Methyl-n1-Perfluorononanoic acid" [tw] OR "PFNA-n1CH3" [tw] OR "EINECS 206-801-3" [tw] OR "Heptadecafluornonansaeure" [tw] OR "Heptadekafluornonansaeure" [tw] OR "Perfluornonansaeure" [tw] OR "Perfluorononanoic acid (PFNA)" [tw] OR "UNII-5830Z6S63M" [tw] OR "perfluoro-n-nonanoic acid" [tw] OR "perfluorononan-1-oic acid" [tw] OR "perfluorononanoic acid" [tw] OR "Ammonium Perfluorononanoate" [tw] OR "Ammonium perfluorononanoate" [tw] OR "PFNA-H3N" [tw])))) AND ("2017/01/01"[Date – Publication] : "3000"[Date – Publication])	2017–2022
Web of Science		
Search terms	((TS=PFNA OR TS="C 1800") AND TS=(fluorocarbon* OR fluorotelomer* OR polyfluoro* OR perfluoro-* OR perfluoroa* OR perfluorob* OR perfluoroc* OR perfluorod* OR perfluoroe* OR perfluoroh* OR perfluoron* OR perfluoroo* OR perfluorop* OR perfluoros* OR perfluorou* OR perfluorinated OR fluorinated OR PFAS OR PFOS OR PFOA)) OR TS="2,2,3,3,4,4,5,5,6,6,7,7,8,8,9,9,9-heptadecafluorononanoic acid" OR TS="Nonanoic acid, 2,2,3,3,4,4,5,5,6,6,7,7,8,8,9,9,9-heptadecafluoro-" OR TS="Nonanoic acid, heptadecafluoro-" OR TS="Perfluoro-n-nonanoic acid" OR TS="Perfluorononan-1-oic acid" OR TS="Perfluorononanoate" OR TS="Perfluorononanoic acid" OR TS="Perfluorononanonic acid" OR TS="Perfluoropelargonic acid" OR TS="heptadecafluorononanoic acid”	No date limit–July 2017

Search	Search strategy	Date
Literature update search terms and additional PFNA synonyms	(TS="PFNA" OR TS="C 1800" OR TS="2,2,3,3,4,4,5,5,6,6,7,7,8,8,9,9,9-heptadecafluorononanoic acid" OR TS="Nonanoic acid, 2,2,3,3,4,4,5,5,6,6,7,7,8,8,9,9,9-heptadecafluoro-" OR TS="Nonanoic acid, heptadecafluoro-" OR TS="Methyl-n1-Perfluorononanoic acid" OR TS="PFNA-n1CH3" OR TS="EINECS 206-801-3" OR TS="Heptadecafluornonansaeure" OR TS="Heptadekafluornonansaeure" OR TS="Perfluornonansaeure" OR TS="Perfluorononanoic acid (PFNA)" OR TS="UNII-5830Z6S63M" OR TS="perfluoro-n-nonanoic acid" OR TS="perfluorononan-1-oic acid" OR TS="perfluorononanoic acid" OR TS="Ammonium Perfluorononanoate" OR TS="Ammonium perfluorononanoate" OR TS="PFNA-H3N") AND PY=2017–2022	2017–2022
Toxline		
Search terms	(((pfna OR "c 1800") AND (fluorocarbon* OR fluorotelomer* OR polyfluoro* OR perfluoro* OR perfluorinated OR fluorinated OR pfas OR pfos OR pfoa)) OR "375-95-1" [rn] OR "2 2 3 3 4 4 5 5 6 6 7 7 8 8 9 9 9-heptadecafluorononanoic acid" OR "nonanoic acid 2 2 3 3 4 4 5 5 6 6 7 7 8 8 9 9 9-heptadecafluoro-" OR "nonanoic acid heptadecafluoro-" OR "perfluoro-n-nonanoic acid" OR "perfluorononan-1-oic acid" OR "perfluorononanoate" OR "perfluorononanoic acid" OR "perfluorononanonic acid" OR "perfluoropelargonic acid" OR "heptadecafluorononanoic acid") AND (ANEUPL [org] OR BIOSIS [org] OR CIS [org] OR DART [org] OR EMIC [org] OR EPIDEM [org] OR HEEP [org] OR HMTC [org] OR IPA [org] OR RISKLINE [org] OR MTGABS [org] OR NIOSH [org] OR NTIS [org] OR PESTAB [org] OR PPBIB [org]) AND NOT PubMed [org] AND NOT pubdart [org]	No date limit–July 2017
Literature update search terms and additional PFNA synonyms	@AND+@OR+(pfna+"c 1800"+fluorocarbon*+"2,2,3,3,4,4,5,5,6,6,7,7,8,8,9,9,9-heptadecafluorononanoic+acid"+"nonanoic+acid+2,2,3,3,4,4,5,5,6,6,7,7,8,8,9,9,9-heptadecafluoro-"+"nonanoic+acid+heptadecafluoro-"+"perfluoro-n-nonanoic+acid"+"perfluorononan-1-oic+acid"+perfluorononanoate+"perfluorononanoic+acid"+"perfluoropelargonic+acid"+"heptadecafluorononanoic+acid"+"Methyl-n1-Perfluorononanoic+acid"+"PFNA-n1CH3"+"EINECS 206-801-3"+"Heptadecafluornonansaeure"+"Heptadekafluornonansaeure"+"Perfluornonansaeure"+"Perfluorononanoic+acid (PFNA)"+"UNII-5830Z6S63M"+"perfluoro-n-nonanoic+acid"+"perfluorononan-1-oic+acid"+"perfluorononanoic+acid"+"Ammonium+Perfluorononanoate"+"Ammonium+perfluorononanoate"+"PFNA-H3N"+@TERM+@rn+375-95-1)+@RANGE+yr+2017+2018+2019+2020+2021+2022	2017–2022
TSCATS		
Search terms	"375-95-1" [rn] AND TSCATS [org]	No date limit–July 2017
Literature update search terms and additional PFNA synonyms	@TERM+@rn+375-95-1+@RANGE+yr+2017+2018+2019+2020+2021+2022	2017–2022

1

APPENDIX B. LITERATURE SEARCH STRATEGY

B.1. DOCUMENTATION OF LITERATURE SEARCH UPDATES AFTER APRIL 2022

Table B-2 documents the decisions regarding studies identified after April 2022, including a literature search update in April 2023 and studies identified in public comments received through the EPA docket on the draft IRIS PFDA and PFHxS assessments. The table focuses primarily on the new studies that met the assessment PECO criteria. Specifically, epidemiological studies that met the PECO criteria were identified; no experimental animal studies that met the PECO criteria were identified. Mechanistic studies from the 2023 search are currently incorporated into the assessment. Table B-2 provides EPA's disposition on the decision to incorporate the epidemiological studies into the assessment as defined in draft Peer Review Charge question 1 (i.e., only incorporating studies that may potentially change which hazards are identified, or notably affect the RfDs, or studies that directly inform the identified key science issues); the charge question asks the peer reviewers to weigh in on EPA's disposition. These same criteria were applied to certain categories of newly identified supplemental studies (i.e., ADME studies). Notably, the PFAS evidence base is rapidly evolving, particularly in the field of epidemiology; therefore, there are challenges to balancing the incorporation of the most current literature with advancing these urgently needed and rigorously reviewed assessments in a timely manner.

The decision to exclude other recently identified studies that meet these specific supplemental evidence categories is documented in HAWC. Recently identified studies that meet supplemental evidence categories other than those above (e.g., exposure-only) were not evaluated in this way and are tagged in HERO and HAWC along with other screening decisions (e.g., excluded studies).

Table B-1. Summary of decisions regarding studies identified after April 2022, including characterization of all epidemiological studies meeting PECO criteria and supplemental ADME studies

Reference	Source	Health outcome	Results summary	EPA disposition on incorporation and characterization of impact[a]
Immune effects				
Kaur et al. (2023)	Lit update	Antibody levels to SARS-COV2 in adults	Inverse but not statistically significant association (beta −0.22, 95% CI −0.62, 0.18)	No. Findings are consistent with existing epidemiological evidence and have no impact on the draft immunosuppression synthesis, particularly given that two of the new studies are in adults and the draft conclusions are primarily based on studies in children.
Porter et al. (2022)	Lit update	Antibody levels to SARS-COV2 in adults	Inverse but not statistically significant association with IgG and neutralizing antibodies in response to COVID vaccination	
Zhang et al. (2023b)	Lit update	Vaccine response	Inverse but not statistically significant association with mumps and measles antibodies in sub-population with lower folate	
Zhang et al. (2022)	Lit update	Infectious disease	Positive but not statistically significant association with common cold at 3–11 yr (OR 1.36, 95% CI 0.93, 1.98) but not 12–19 yr	No. Existing epidemiological evidence on infectious disease is inconsistent and new studies do not change the current draft synthesis judgment.
Huang et al. (2020)	Commenter (on PFHxS)	Infectious disease	No association with the number of respiratory tract infections in preschool children	
Pan et al. (2023)	Lit update	Asthma	No association with current asthma (OR 0.71, 95% CI 0.46, 1.11 in Q4 vs. Q1) or wheezing. Inverse association with asthma attacks and emergency visits.	No. Existing epidemiological evidence on asthma and other hypersensitivity outcomes is inconsistent and new studies do not change the current draft synthesis judgment.
Gaylord et al. (2019)	Commenter (on PFDA)	Asthma	Positive but not statistically significant association with asthma (OR 1.20, 95% CI 0.63, 2.27)	
Averina et al. (2019)	Commenter (on PFDA)	Hypersensitivity outcomes	No association with asthma, eczema, allergies	
Wen et al. (2019)	Commenter (on PFHxS)	Atopic dermatitis	Inverse but not statistically significant association with atopic dermatitis	

Reference	Source	Health outcome	Results summary	EPA disposition on incorporation and characterization of impact[a]
Ammitzbøll et al. (2019)	Commenter (on PFDA)	Multiple sclerosis	No association with multiple sclerosis overall, but an indication of interaction by sex (positive association in women, inverse association in men)	No. Null results for autoimmune conditions in new studies would not influence PFNA draft evidence synthesis or integration conclusions on immune effects.
Gaylord et al. (2020)	Commenter (on PFDA)	Celiac disease	No association with celiac disease (OR 0.89, 95% CI 0.55, 1.46)	
Qu et al. (2022)	Lit update	Rheumatoid arthritis	No association with rheumatoid arthritis	
Steenland et al. (2018b)	Commenter (on PFHxS)	Ulcerative colitis	Inverse association with ulcerative colitis	
Developmental effects				
Wang et al. (2023a)	Lit update	Fetal growth restriction (Birth length (BL); head circumference (HC); birthweight (BWT))	Few sex-specific associations were observed for birth length (BL), birth weight (BWT) and head circumference (HC) endpoints per each ln-unit PFNA increase. BL Male β = −0.023; 95% CI: −0.207, 0.162; BL Female β = −0.041; 95% CI: −0.469, 0.387; HC Male β = −0.223; 95% CI: −0.455, 0.010; HC Female β = −0.402; 95% CI: −0.717, −0.087; BWT Male β = −0.073; 95% CI: −0.284, 0.138; BWT Female β = −0.115; 95% CI: −0.434, 0.203.	No. Null results observed for fetal growth restriction endpoints (birth length and birth weight and head circumference) in both female and male neonates. Neither these null associations nor the inverse associations for head circumference would change the current draft synthesis judgment for the individual fetal growth restriction endpoint judgements or the overall one for developmental effects.
Peterson et al. (2022)	Lit update	Fetal growth restriction	Non-significant inverse associations were evident for Fetal Head Circumference and appeared to be driven by the high stress sub-group; null results for Fetal Biparietal Diameter) in relation to PFNA exposures.	No. Null results for fetal biometric endpoints would not change the current draft synthesis judgment for fetal growth restriction or for the overall developmental effects.
Wang et al. (2023b)	Lit update	Fetal growth restriction	Per each log10-unit PFNA increase, statistically significant increased weight for length z-	No.

Reference	Source	Health outcome	Results summary	EPA disposition on incorporation and characterization of impact[a]
			scores were detected for boys and the overall population, while non-significant decreases were seen among girls. The remaining results were largely null across the overall population and both sexes, although boys showed lower birth length z-scores, and girls had larger head circumference z-scores. None of these latter results were statistically significant as the confidence intervals all included the null value.	These findings are not consistent with the majority of studies showing evidence of fetal growth restriction, but they would not change the current draft synthesis judgment.
Mwapasa et al. (2023)	Lit update	Fetal growth restriction, gestational duration	Per each ln-unit PFNA increase, inverse associations were detected for all of the primary developmental endpoints such as Birth Weight (β = −171 g; 95% CI: −346, 3), Gestational Age (β = −0.083 wk; 95% CI: −0.141, −0.023), Head Circumference (β = −0.080 cm; 95% CI: −0.125, −0.035), and Birth Length (β = −0.033 cm; 95% CI: −0.057, −0.010).	No. Findings are consistent with existing evidence including some large associations including for birth weight. However, given the strength and consistency of that endpoint, these results would not change the current draft synthesis judgment.
Padula et al. (2023)	Lit update	Fetal growth restriction, gestational duration	Per each per ln-unit PFNA increase, elevated risks were detected for PTB (OR = 1.43; 95% CI: 0.93, 2.19), term LBW (OR = 1.67; 95% CI: 0.64, 4.35), but was null for SGA (OR = 1.09; 95% CI: 0.74, 1.60). Associations were also evident across fetal growth and gestational duration endpoints [birth weight for gestational age β = −0.22; 95% CI: −0.33, −0.10; gestational age β = −0.17; 95% CI: −0.38, 0.04]. Authors also reported a statistically significant mean birthweight for PFNA (−16 g; 95% CI: −30, −2).	No. Inverse associations between fetal growth and gestational duration endpoints as well as null results for SGA and increased risks for PTB and LBW would not change the current draft synthesis judgment for either gestational duration (*slight*) or fetal growth restriction (*robust*). This pooled estimate across several ECHO cohort also overlaps 4 other publications that have already been included in the evidence syntheses (Chang et al., 2022; Eick et al., 2020; Sagiv et al., 2018; Starling et al., 2017).

Reference	Source	Health outcome	Results summary	EPA disposition on incorporation and characterization of impact[a]
Ouidir et al. (2020)	Commenter (on PFDA)	Fetal growth restriction	Per each PFNA IQR increase, a statistically significant longitudinal increase in head circumference (β = 0.21 mm; *p*-value < 0.05), femur length (β = 0.06 mm; *p*-value: 0.001 to 0.01), and abdominal circumference (β = 0.28 mm; *p*-value < 0.05) were detected; while a decrease in longitudinal biparietal diameter (β = −0.12 mm; *p*-value: 0.001 to 0.01) was seen. Results for in utero occipital-frontal diameter changes (β = 0.04 mm) and estimated fetal growth (β = 3.27 g) were null; (*p*-value/CIs not provided).	No. Study population was previously reported in a publication already in the assessment (Buck Louis et al., 2018). New results for longitudinal in utero measurements from ultrasonography would not change the current draft synthesis judgments for fetal growth restriction or developmental effects.
Petroff et al. (2023)	Lit update	Gestational age	Non-significant inverse association between PFNA exposure and gestational age (β = −0.31 ± 0.19; *p* = 0.09).	No. Inverse associations for gestational age would not change the current draft synthesis judgment of *slight* for gestational duration even in conjunction with similar results from Padula et al. (2023).
Yu et al. (2022)	Lit update	Preterm birth	Statistically significant increases in risk detected for untransformed data (OR = 2.19; 95% CI: 1.23, 3.91 per each ng/mL increase) only; transformed results were null (OR = 1.36; 95% CI: 1.01, 1.83 per each ln-unit increase).	No. Increased risks here along with Padula et al. (2023) and null results in Liao et al. (2022b) would not change the current draft synthesis judgment of *slight* for gestational duration.
Liao et al. (2022b)	Lit update	Preterm birth	Results were null across quartiles although a small non-significant increased risk of preterm birth per each $\log_{10}$ increase (OR = 1.16; 95% CI: 0.69, 1.938).	No. These largely null results, combined with increased risk in two other new studies by Yu et al. (2022) and Padula et al. (2023), would not change the current draft synthesis judgment of *slight* for gestational duration.

Reference	Source	Health outcome	Results summary	EPA disposition on incorporation and characterization of impact[a]
Wang et al. (2016a)	Commenter (on PFDA)	Gestational duration	Slightly higher but non-significant PFNA concentrations in term compared to preterm births.	No. This study reported only mean exposure concentrations without control for confounding so this would not influence the current draft synthesis judgment.
Hong et al. (2022)	Lit update	Spontaneous abortion	Inverse association (OR 0.33, 95% CI 0.10,1.14)	No. Existing evidence is inconsistent, and this new study does not change the current draft synthesis judgment.
Li et al. (2022a)	Lit update	Anogenital distance	No association with anogenital distance	No. The null finding does not change the current draft synthesis judgment.
Hepatic				
Borghese et al. (2022)	Lit update	Liver enzymes	Positive association with AST, GGT, and ALP	Yes (already incorporated into the current assessment text). The previous judgment was borderline between *slight* and *moderate* evidence and new studies increase certainty in a judgment of *moderate*. Studies on liver disease fill an existing data gap.
Liao et al. (2023)	Lit update	Liver enzymes	Positive association with GGT but not ALT, AST, or bilirubin	
Kim et al. (2023b)	Lit update	Liver enzymes	Positive associations with ALT, AST, and GGT	
Yao et al. (2020)	Commenter (on PFDA)	Liver enzymes	Positive association with ALT, AST, GGT (statistically significant for GGT)	
Salihović et al. (2019)	Commenter (on PFDA)	Bile acid levels (liver)	Positive correlations with TLCA, GLCA, and LCA ($p < 0.05$). Inverse but not statistically significant correlations with other bile acids.	
Rantakokko et al. (2015)	Commenter (on PFDA)	Liver disease	Inverse association with lobular inflammation (OR 0.02, 95% CI <0.01, 0.53 for 2–4 foci per 200× field)	
E et al. (2023)	Lit update	Liver disease	Positive association with non-alcoholic fatty liver disease in women (OR 1.86, 95% CI 1.24, 2.79) but not men	

Reference	Source	Health outcome	Results summary	EPA disposition on incorporation and characterization of impact[a]
Cancer				
Feng et al. (2022b)	Lit update	Breast cancer	Positive but not statistically significant association with breast cancer (OR = 1.23, 95% CI: 0.89, 1.70) per unit increase in ln-transformed plasma PFNA levels.	No. The results were inconsistent across the newly identified breast cancer studies. In addition, one new breast cancer study reports results for the same study population as a publication already included in the assessment Wielsøe et al. (2017). The only study reporting on liver cancer reported a weak, non-significant association with PFNA. The weak association observed for renal cancer dissipated when controlled for other PFAS. The available epidemiologic evidence on PFNA and the risk of cancer remains inadequate; the new studies would not influence the draft synthesis judgment.
Li et al. (2022b)	Lit update	Breast cancer	Inverse but not statistically significant association breast cancer (OR = 0.84, 95% CI: 0.70, 1.01) per SD increase in ln-transformed PFNA.	
Wielsøe et al. (2018)	Commenter (on PFDA)	Breast cancer	Positive but not statistically significant association of PFNA with breast cancer (OR = 2.25, 95% CI 0.54, 9.35 in high vs. low exposure for one genotype)	
Lee et al. (2020)	Commenter (on PFDA)	Breast cancer	No association of PFNA with mammographic density (beta −0.12, *p*-value 0.7)	
Goodrich et al. (2022)	Lit update	Liver cancer	Positive but not statistically significant association with liver cancer (OR = 1.20, 95% CI: 0.52, 2.80) for PFNA greater than the 90th% vs. less than 90th%.	
Shearer et al. (2021)	Commenter (on PFDA)	Renal cancer	Positive but not statistically significant association with renal cell carcinoma (OR 1.19, 95% CI 0.91, 1.55) per SD increase in ln-transformed PFNA.	
Neurodevelopment				
Luo et al. (2022a)	Lit update	Broad neurodevelopmental scale	Inverse association with cognitive, language, motor, and social-emotional scores, but not adaptive behavior score	No. There is inconsistency for neurodevelopmental effects in the current

Reference	Source	Health outcome	Results summary	EPA disposition on incorporation and characterization of impact[a]
Oh et al. (2022b)	Lit update	Autism, developmental delay	No increase in odds of autism spectrum disorder, developmental delay	draft assessment, and the new studies showing overall mixed but some positive associations with PFNA would not influence the synthesis judgment of *slight* evidence.
Zhou et al. (2023)	Lit update	Broad neurodevelopmental scale	Inverse association with communication, motor, problem solving , and personal-social (latter not statistically significant) at 6 mo but not at other visits (2, 12, and 24 mo)	
Li et al. (2023c)	Lit update	Broad neurodevelopmental scale	Positive though not statistically significant association with persistently low trajectory for gross motor and problem solving ability, but not communication, fine motor, or personal-social skills	
Oulhote et al. (2019)	Commenter (on PFDA)	Broad neurodevelopmental scale	Positive association with total Strengths and Difficulties Questionnaire score. No association with Boston Naming Test results.	
van Larebeke et al. (2022)	Lit update	Broad neurodevelopmental scale	No association with a battery of neurocognitive and behavior tests	
Xie et al. (2022)	Lit update	Neurobehavior	Inverse association with somatic complaints but no association with other behavior measures	
Ames et al. (2023)	Lit update	Autism	Positive association with Social Responsiveness Scale score	
Kim et al. (2023a)	Lit update	ADHD scale	Positive though non-monotonic association with ADHD rating scale at 8 yr, dependent on age at exposure measurement	
Male reproductive				

Reference	Source	Health outcome	Results summary	EPA disposition on incorporation and characterization of impact[a]
Luo et al. (2022b)	Lit update	Semen parameters	Inverse but not statistically significant association with motility	No. Evidence is inconsistent in existing studies and the new studies would not influence the draft synthesis judgment.
Ma et al. (2021)	Commenter (on PFDA)	Semen parameters	Inverse association with sperm concentration and morphology (statistically significant for concentration) but not motility	
Pan et al. (2019)	Commenter (on PFDA)	Semen parameters	No association with concentration, motility, or morphology	
Rivera-Núñez et al. (2023)	Lit update	Reproductive hormones	Positive association with T and free T, inverse association with E3, no association with E1, E2	No. Evidence is inconsistent in existing studies and the new studies would not influence the draft synthesis judgment of *indeterminate* evidence.
Guo et al. (2023)	Lit update	Reproductive hormones	No association with testosterone or estradiol (included boys and girls)	
Nian et al. (2020)	Commenter (on PFDA)	Reproductive hormones	No association with total testosterone (beta −0.008, 95% CI −0.083, 0.066 per ln-unit change), FSH, or LH	
Female reproductive				
Hong et al. (2022)	Lit update	In vitro fertilization outcomes	No association with oocyte maturation rate, fertilization rate, high quality embryo rate. Inverse but not statistically significant (OR = 0.88, 95% CI 0.63–1.22) for clinical pregnancy	No. Evidence of an association with fecundity and infertility is primarily null across the newly identified studies and was inconsistent across the studies currently included in the assessment. Thus, the new studies would not change the draft synthesis judgment.
Cohen et al. (2023)	Lit update	Fecundity, pregnancy	No association with time to pregnancy or odds of clinical pregnancy	
Luo et al. (2022c)	Lit update	Fecundity, infertility	No association with fecundability (FR 1.03, 95% CI 0.88, 1.20) or infertility (OR = 0.91, 95% CI 0.68, 1.23)	
Tan et al. (2022)	Lit update	Infertility	Lower odds of infertility (non-monotonic across quartiles and not statistically significant)	

Reference	Source	Health outcome	Results summary	EPA disposition on incorporation and characterization of impact[a]
Whitworth et al. (2016)	Commenter (on PFDA)	Fecundity	No association (FR 1.1, 95% CI 0.92, 1.3)	
Buck Louis et al. (2013)	Commenter (on PFDA)	Fecundity	No association with reduced fecundability (FR 1.00, 95% CI 0.84,1.19)	
Ma et al. (2021)	Commenter (on PFDA)	In vitro fertilization outcomes, pregnancy	No association with number of oocytes, zygotes, embryos, or clinical pregnancies	
Petro et al. (2014)	Commenter (on PFHxS)	In vitro fertilization outcomes	No association with fertilization rate	
Wang et al. (2019)	Commenter (on PFDA)	Polycystic ovarian syndrome	Positive but not statistically significant association with PCOS-related infertility (OR 1.62, 95% CI 0.45, 5.80 in 3rd vs. 1st tertile)	No. Existing evidence on gynecological conditions is inconsistent and there is considerable uncertainty due to potential reverse causation. The new study does not inform this uncertainty and would not change the draft synthesis judgment.
Rivera-Núñez et al. (2023)	Lit update	Reproductive hormones	Positive association with FT, inverse but not statistically significant association with E1, no association with T, E2, E3	No. New studies on reproductive hormones are inconsistent and would not change the current draft synthesis judgment.
Nian et al. (2020)	Commenter (on PFDA)	Reproductive hormones	No association with total testosterone (beta −0.008, 95% CI −0.083, 0.066 per ln-unit change), FSH, or LH	
Liu et al. (2020a)	Commenter (on PFDA)	Reproductive hormones	Positive association with estradiol (11.8% change, 95% CI 6.2, 17.6)	
Ding et al. (2020)	Commenter (on PFHxS)	Menopause	Positive association with incident natural menopause (HR 1.12, 95% CI 1.01, 1.24 per doubling)	

Reference	Source	Health outcome	Results summary	EPA disposition on incorporation and characterization of impact[a]
Lin et al. (2022)	Lit update	Postpartum hemorrhage	Higher odds of postpartum hemorrhage (OR 2.79, 95% CI 0.85, 9.21) but imprecise	No. This is a single study of the outcome and there are stronger associations with other PFAS, raising the potential for confounding. This would not change the current draft synthesis judgment.
Urinary				
Liang et al. (2023)	Lit update	Glomerular filtration rate	Lower GFR particularly in women and smokers	No. There is considerable uncertainty in interpretation of these outcomes due to potential reverse causation. The new studies do not inform this uncertainty and would not change the synthesis judgment.
Sood et al. (2019)	Commenter (on PFDA)	Glomerular filtration rate	Inverse association with eGFR (beta −21.2, 95% CI −41.6, −0.8)	
Pan et al. (2017)	Commenter (on PFHxS)	Glomerular filtration rate	Inverse association with GFR in crude analysis	
Feng et al. (2022c)	Lit update	Hyperuricemia	Higher odds of hyperuricemia, though not statistically significant	
Yang et al. (2022b)	Lit update	Hyperuricemia	Positive but not statistically significant with hyperuricemia (OR 1.11, 95% CI 0.90, 1.38)	
Arrebola et al. (2019)	Commenter (on PFDA)	Hyperuricemia	Positive but not statistically significant association with hyperuricemia (OR 1.68, 95% CI 0.80, 3.61)	
Yao et al. (2020)	Commenter (on PFDA)	Uric acid	Positive association with uric acid (beta 3.66, 95% CI 0.42, 7.00)	
Cardiometabolic				
Donat-Vargas et al. (2019b)	Commenter (on PFDA)	Serum lipids, hypertension	No association with total cholesterol, triglycerides, or hypertension	No. Mixed results for serum lipids from the new studies do not change the current draft synthesis judgment.
Batzella et al. (2022)	Lit update	Serum lipids	Positive association with total cholesterol (beta 6.61, 95% CI 5.72, 7.51) and LDL-cholesterol	

Reference	Source	Health outcome	Results summary	EPA disposition on incorporation and characterization of impact[a]
Morgan et al. (2023)	Lit update	Serum lipids	No association with total cholesterol or LDL-cholesterol (crude analysis only)	
Rosen et al. (2022)	Lit update	Serum lipids	Positive but not statistically significant association with total cholesterol, LDL, and triglycerides	
Fan et al. (2020)	Commenter (on PFHxS)	Serum lipids	Positive but not statistically significant association with total and LDL cholesterol	
Li et al. (2019)	Commenter (on PFHxS)	Serum lipids	No association with total cholesterol or triglycerides	
Jain (2014)	Commenter (on PFHxS)	Serum lipids, adiposity	No association with serum lipids; inverse association with BMI but small effect size	
Fassler et al. (2019)	Commenter (on PFHxS)	Serum lipids, adiposity, insulin resistance	No association with BMI, insulin resistance, or serum lipids	
Yao et al. (2020)	Commenter (on PFDA)	Serum lipids, blood glucose	Positive association with total cholesterol (beta 5.09, 95% CI 1.92, 8.48), triglycerides, and blood glucose	
Maranhao Neto et al. (2022)	Lit update	Serum lipids, blood pressure, adiposity, blood glucose	Inverse associations with blood glucose, adiposity, and blood pressure. No association with serum lipids	
Mitro et al. (2020a)	Lit update	Blood pressure	No association with blood pressure, BMI, waist circumference, mid-upper arm circumference, or skinfold thickness	
Sood et al. (2019)	Commenter (on PFDA)	Blood pressure	No association with blood pressure (beta 0.4, 95% CI −0.2, 1.1)	
Ma et al. (2019)	Commenter (on PFHxS)	Blood pressure	No association with blood pressure	

Reference	Source	Health outcome	Results summary	EPA disposition on incorporation and characterization of impact[a]
Ding et al. (2022)	Lit update	Hypertension	No association with hypertension (HR 1.00, 95% CI 0.83, 1.19 in T3 vs. T1)	
Lind et al. (2018)	Commenter (on PFDA)	Carotid artery intima-media thickness	Positive association with IMT thickness (beta 0.017, 95% CI 0.005, 0.0028)	No. These results support coherence with serum lipids but would not change the current draft synthesis judgment.
Li et al. (2023b)	Lit update	Cardiovascular disease	No association with acute coronary syndrome	No. Studies contribute to existing inconsistency and would not change the current draft synthesis judgment.
Feng et al. (2022a)	Lit update	Cardiovascular disease	Positive association with coronary heart disease (OR 1.10, 95% CI 1.01, 1.20), heart attack, and stroke in males but not females	
Hutcheson et al. (2020)	Commenter (on PFHxS)	Stroke	No association with stroke	
Yang et al. (2022a)	Lit update	Gestational hypertension	Lower odds of gestational hypertension (OR 0.70, 95% CI 0.45, 1.07) and lower continuous blood pressure	No. New studies contribute to existing inconsistency and would not change the current draft synthesis judgment.
Huo et al. (2020)	Lit update	Gestational hypertension	No association with gestational hypertension (OR 1.02, 95% CI 0.63, 1.67) or preeclampsia (OR 0.85, 95% CI 0.54, 1.33)	
Xu et al. (2022)	Lit update	Gestational diabetes	Positive association with gestational diabetes (OR 2.01, 95% CI 0.97, 4.16 in third tertile), no association with continuous blood glucose in oral glucose tolerance test	No. Existing studies are inconsistent and new studies would not change the current draft synthesis judgment.
Zhang et al. (2023a)	Lit update	Gestational diabetes	Positive association with gestational diabetes (OR 2.61, 95% CI 1.26, 5.40 in third tertile)	
Xu et al. (2020)	Lit update	Gestational diabetes	No association with gestational diabetes (OR 0.70, 95% CI 0.34, 1.67 in Q4 vs. Q3)	

Reference	Source	Health outcome	Results summary	EPA disposition on incorporation and characterization of impact[a]
Preston et al. (2020)	Lit update	Gestational diabetes	No association with gestational diabetes	
Liu et al. (2019)	Commenter (on PFHxS)	Gestational diabetes	No association with gestational diabetes in crude analysis	
Li et al. (2020b)	Commenter (on PFDA)	Gestational blood glucose	Positive association with blood glucose in oral glucose tolerance test (beta 0.13, 95% CI 0.01, 0.25)	
Dunder et al. (2023)	Lit update	Blood glucose	Inverse but small and not statistically significant association (−0.009, 95% CI −0.02, 0.007), stronger in women than men	No. Existing and new studies are primarily null and would not change the current draft synthesis judgment.
Christensen et al. (2016)	Commenter (on PFDA)	Diabetes	Positive but not statistically significant association with diabetes (OR 1.33, 95% CI 0.86, 1.96)	
Park et al. (2022)	Lit update	Diabetes	Positive association with incident diabetes (OR 1.34, 95% CI 0.95, 1.90 in T3 vs. T1)	
Cardenas et al. (2019)	Commenter (on PFHxS)	Diabetes	No association with incident diabetes in a cohort of participants from a diabetes prevention trial.	
Zong et al. (2016)	Commenter (on PFHxS)	Diabetes	No association with diabetes	
Donat-Vargas et al. (2019a)	Commenter (on PFDA)	Diabetes risk, insulin resistance	No increase in diabetes risk or HOMA-IR	
Kim et al. (2015)	Commenter (on PFDA)	Insulin resistance	No association with HOMA (beta −0.02, 95% CI −0.60, 0.55)	
Mehta et al. (2021)	Commenter (on PFDA)	Insulin resistance	Inverse but not statistically significant association with blood glucose (−2.06% difference, 95% CI −4.24, 0.17) and HOMA-IR (−7.34% difference, 95% CI −19.07, 6.09)	

Reference	Source	Health outcome	Results summary	EPA disposition on incorporation and characterization of impact[a]
Bassler et al. (2019)	Commenter (on PFHxS)	Insulin resistance	No association with insulin	
Brosset and Ngueta (2022)	Lit update	Glycemic control	Positive association with poor glycemic control (OR 2.30, 95 CI 1.25, 4.21 in third tertile)	
Ye et al. (2021)	Commenter (on PFDA)	Metabolic syndrome	Positive association with metabolic syndrome (OR 1.78, 95% CI 1.29, 2.45) as well as blood glucose, triglycerides, and waist circumference	No. Existing studies are inconsistent and new studies would not change the current draft judgment.
Leary et al. (2020)	Commenter (on PFHxS)	Metabolic syndrome	Inverse but not statistically significant association with metabolic syndrome in firefighters	
Schillemans et al. (2022)	Lit update	Adiposity	Inverse association with BMI z-score	No. Existing studies are inconsistent and would not change the current draft judgment. The majority of additional studies are intended to examine determinants of PFNA concentrations and/or are crude analyses without adjustment for potential confounders.
Zeng et al. (2023)	Lit update	Adiposity	Positive association ($p < 0.05$) with persistent increase for BMI z-score trajectory	
Harris et al. (2017)	Commenter (on PFDA)	Adiposity	No association between PFNA exposure and overweight/obese status	
Ji et al. (2012)	Commenter (on PFDA)	Adiposity	Higher PFNA concentrations in obese participants, but no statistical analysis	
Pirard et al. (2020)	Commenter (on PFDA)	Adiposity	No association with BMI (quantitative results not presented)	
Liu et al. (2020b)	Commenter (on PFDA)	Adiposity	No association with BMI	
Kim et al. (2020)	Commenter (on PFHxS)	Adiposity	Inverse association in crude analysis with PFNA modeled as outcome	
Bjerregaard-Olesen et al. (2016)	Commenter (on PFHxS)	Adiposity	No association with BMI in model predicting exposure	

Reference	Source	Health outcome	Results summary	EPA disposition on incorporation and characterization of impact[a]
Chang et al. (2020)	Commenter (on PFHxS)	Adiposity	No association with BMI in analysis with PFHxS modeled as outcome	
Cardenas et al. (2018)	Commenter (on PFHxS)	Adiposity	Positive association with some measures of adiposity including skinfold thickness ($p < 0.05$) and subcutaneous fat	
Colles et al. (2020)	Commenter (on PFHxS)	Adiposity	Inverse association with BMI in analysis with PFNA modeled as outcome	
Eick et al. (2021)	Commenter (on PFHxS)	Adiposity	No association with BMI in crude analysis	
Han et al. (2018)	Commenter (on PFHxS)	Adiposity	Positive association with maternal BMI in analysis with PFNA modeled as outcome	
Huang et al. (2019)	Commenter (on PFHxS)	Adiposity	No association with BMI in analysis with PFNA modeled as outcome	
Koponen et al. (2018)	Commenter (on PFHxS)	Adiposity	No association with BMI in crude correlation analysis (quantitative result not reported)	
Mehta et al. (2020)	Commenter (on PFHxS)	Adiposity	No association with BMI	
Nair et al. (2021)	Commenter (on PFHxS)	Adiposity	No association with BMI in crude analysis	
Ramli et al. (2020)	Commenter (on PFHxS)	Adiposity	No association with BMI in analysis with PFNA modeled as outcome	
Rylander et al. (2009)	Commenter (on PFHxS)	Adiposity	No association with BMI (quantitative result not reported)	
Tsai et al. (2018)	Commenter (on PFHxS)	Adiposity	No association with BMI (unadjusted means)	
Yang et al. (2019)	Commenter (on PFHxS)	Adiposity	No association with BMI (unadjusted means)	

Reference	Source	Health outcome	Results summary	EPA disposition on incorporation and characterization of impact[a]
Tian et al. (2019b)	Commenter (on PFHxS)	Adiposity	Positive association with BMI and waist circumference ($p < 0.05$)	
Brantsæter et al. (2013)	Commenter (on PFHxS)	Adiposity, gestational weight gain	No association with pre-pregnancy BMI or weight change in descriptive analysis	
Mitro et al. (2020b)	Commenter (on PFHxS)	Gestational weight gain	No association with gestational weight gain or postpartum weight retention	
Endocrine				
Jensen et al. (2022)	Lit update	Thyroid hormones	Positive association with free T4 (beta 1.70, 95% CI 0.48, 2.94) and inverse association with TSH (beta −2.88, 95% CI −10.17, 5.00)	No. Existing and new studies on thyroid hormones are inconsistent and new studies would not change the current draft synthesis judgment.
Derakhshan et al. (2022)	Lit update	Thyroid hormones	Positive association with free T4 (beta 0.21, 95% CI 0.05, 0.38) but no association with TSH or free T3	
Li et al. (2023a)	Lit update	Thyroid hormones	No association with TSH or free T4	
Tillaut et al. (2022)	Lit update	Thyroid hormones	No association with free T4, free T3, or TSH	
Jain and Ducatman (2019)	Commenter (on PFDA)	Thyroid hormones	Inverse association with TSH, statistically significant in participants at higher glomerular filtration stages.	
Dufour et al. (2020)	Commenter (on PFDA)	Thyroid disease	Inverse association with hypothyroidism (OR 0.19, 95% CI 0.05, 0.79) and hyperthyroidism (OR 0.10, 95% CI 0.02, 0.45)	
Christensen et al. (2016)	Commenter (on PFDA)	Thyroid disease	Inverse association with thyroid disease (OR 0.67, 95% CI 0.23, 1.30)	
Wang et al. (2023b)	Lit update	Thyroid hormones	Positive association with total T4, inverse association with total T3	
Other				

Reference	Source	Health outcome	Results summary	EPA disposition on incorporation and characterization of impact[a]
Højsager et al. (2022)	Lit update	Bone mineral density	Inverse association with bone mineral content and density ($p > 0.05$), stronger in boys	No. Current and newly identified studies are inconsistent; thus, the new evidence would not change the draft synthesis judgment of *indeterminate*.
Zhao et al. (2022)	Lit update	Bone mineral density	No association with femur bone mineral density	
Colicino et al. (2020)	Lit update	Bone mineral density	Positive association with femur density	
Xiong et al. (2022)	Lit update	Bone mineral density	Inverse association with femur and lumbar spine density in girls only	
Blomberg et al. (2022)	Lit update	Bone mineral density	Inverse association with bone mineral density at 5 yr	
Fan et al. (2023)	Lit update	Bone mineral density, osteoporosis	No association with osteoporosis (OR 0.99, 95% CI 0.75, 1.29) or bone mineral density	
Shiue (2015d)	Commenter (on PFDA)	Oral health	No association with teeth health, ache, tooth loss	
Liao et al. (2022a)	Lit update	Hematology	Positive but non-monotonic and not statistically significant association with gestational anemia in the first and third but not second trimesters. No association with hemoglobin concentration during pregnancy	No. The results in the new studies are inconsistent and would not change the current draft synthesis judgment of *indeterminate*.
Cui et al. (2022)	Lit update	Hematology	Positive association with hematocrit (3.51% change, 95% CI 1.82, 5.23) and hemoglobin (3.14% change, 95% CI 1.33, 4.98) during pregnancy	
Liu et al. (2022)	Lit update	Hematology	No association with white blood cells and lymphocytes	
Shiue (2015a)	Commenter (on PFDA)	Neurologic; Remembering condition	No association with difficulty remembering (RR 0.94, 95% CI 0.45–1.99 for >3 times per wk)	No. Lack of association in both existing and new studies for several isolated nervous system

Reference	Source	Health outcome	Results summary	EPA disposition on incorporation and characterization of impact[a]
Shiue (2015b)	Commenter (on PFDA)	Neurologic; Depression	No association with adult depression	outcomes; thus, the new evidence would not change the draft synthesis judgment of indeterminate human evidence.
Shiue (2015c)	Commenter (on PFDA)	Neurologic; Hearing disturbance	No association with trouble hearing	
Gaylord et al. (2019)	Commenter (on PFDA)	Pulmonary function	No association with FEV or FVC (FEV1 beta 0.01, 95% CI −0.12, 0.14, FVC beta 0.02, 95% CI −0.14, 0.17)	No. The lack of association in the newly identified studies does not justify development of a new hazard section.
Shi et al. (2023)	Lit update	Pulmonary function	No association with forced expiratory volume or forced volume capacity	
ADME/PBPK studies				
Chiu et al. (2022)	Lit update	One-compartment PK model fit to data from highly exposed communities (after intervention)	GM (95% CI) for $t_{1/2}$, Vd and CL are 8.30 (5.38–13.5) yr, 0.29 (0.17–0.45) L/kg and 0.068 (0.033–0.107) mL/kg-d. The CL is higher than our previous GM and health-protective lower bound, but in the range of other studies.	Yes. This study led to the incorporation of an updated clearance value into the calculation of overall average clearance. See Section 3.1 in main document
Jain and Ducatman (2022)	Lit update	PFNA serum levels in US females vs. males as a function of age (NHANES).	In males a slow, steady increase from age 12 to ≥75, but in females the levels decline from age 12 to 30, reaching ~70% of the levels in males, then begin to increase around age 37 to match males by late 40s.	Yes. Quantitative support for impact of sex and lifestage on clearance. See Section 3.1 in main document
Oh et al. (2022a)	Lit update	Change in maternal PFNA levels from conception to 2 yr post-partum	Geometric mean PFNA serum levels decline 21% during pregnancy, decline 9% from 0–6 mo post-partum, then 14% from 6–24 mo post-partum. The decline in each period is statistically significant.	Yes. Maternal concentrations at or below concentration at conception throughout perinatal period. See Section 3.1 in main document

[a]Public and peer reviewers are asked to commenter on this disposition and the impact/importance of fully integrating the individual studies prior to finalizing the assessment.

APPENDIX C. SUPPLEMENTAL APPROACHES AND DATA ANALYSIS

C.1. PFAS CO-EXPOSURE AND OTHER CONFOUNDING CONSIDERATIONS AND META-ANALYSIS OF PFNA EFFECTS ON BIRTH WEIGHT

As noted in the PFAS protocol, the potential for confounding by co-occurring PFAS to bias effect estimates are a concern in epidemiological studies despite a lack of scientific consensus on how best to address PFAS co-exposures (and other co-occurring contaminants). The potential for confounding across PFAS is incorporated in individual study evaluations and assessed across studies in evidence syntheses and in the characterizations of the strength of evidence. For other covariates like glomerular filtration rate, in general, more confidence was placed in studies that adjusted for pregnancy hemodynamics or that considered this potential source of confounding in the design phase by sampling PFAS levels earlier in pregnancy. More details on the considerations of the potential impact of PFAS co-exposures and pregnancy hemodynamics follow.

C.1.1. Confounding Directionality and PFAS Co-Exposure Statistical Approaches

A source of uncertainty in the epidemiological database was the potential for confounding by other PFAS (and other co-occurring contaminants) that co-occur and are actual confounders (i.e., associated with both the PFAS of interest and the outcome but not an intermediate in the causal pathway between the two). In this example, such PFAS are considered positive confounders if their effect estimate with the endpoint of interest is in the same direction as the primary PFAS of interest. If positive confounders are not accounted for in the epidemiological study design or analysis phase, the anticipation is that any resultant bias would be away from the null. Certain statistical approaches can help address the challenges of evaluating the effects of numerous (often correlated) PFAS that may be present in the environment and estimated via different biomarkers and other measures (i.e., those that adjust for at least one co-occurring exposure) can provide an estimate of the independent association for specific pollutants with the endpoint of interest. However, these models may not perform well when co-occurring exposures are highly correlated. Such correlation can lead to collinearity concerns and instability of modeling results. When exposures are highly correlated and additionally subject to different potential confounding factors (which may occur, e.g., when PFAS arise from different sources), co-exposure amplification bias may be a concern (Weisskopf et al., 2018). Under this scenario, estimated associations from multi-PFAS adjusted models would be subject to greater bias compared with results from single-PFAS models.

Other mixture approaches are employed in epidemiological studies to characterize overall mixture effects and, in some cases, to "screen" large groups of exposures and identify exposure

patterns and/or contributions, which may help to determine which exposure(s) are most important to retain in further analyses. These statistical methods using dimension-reduction (e.g., principal component analysis, penalized modeling based on elastic net regression) and mixture methods (e.g., Bayesian kernel machine regression) are increasingly being used for identifying patterns among large groups of chemical exposures and for helping prioritize specific components/chemicals that contribute the highest proportion to the mixture. However, as noted by Meng et al. (2018), these approaches might be better suited as "prediction models to screen for a wide range of chemicals from different sources, and the interpretation of results might become less straightforward due to the necessary standardization of exposure values." These regression model outputs also do not provide confidence intervals, thus precluding evaluations of precision. Given these interpretation difficulties and potential for co-exposure amplification bias, it is unclear which statistical approach best represents independent effects of specific pollutants within complex PFAS mixtures. An evaluation of single-pollutant (i.e., PFNA-only) models and other approaches are detailed below.

The objective herein is to assess whether there is any direct evidence for confounding in the studies comparing results from multi-pollutant (mutually adjusted for other PFAS) models and results from single pollutant (i.e., PFNA alone with other confounders adjusted for) models. Additional objectives were to compare relationships between co-occurring PFAS as well as evaluate the extent to which these PFAS may be associated with a primary endpoint of interest (e.g., birth weight-related measures).

C.1.2. PFAS Co-Exposure Correlations with PFNA

In general, the stronger the correlation or association that is observed between co-exposures and the larger the associations between the co-exposure and endpoints such as fetal growth restriction, the more concern there would be for potential confounding. Table C-1 shows correlations between PFAS co-exposures and PFNA reported from six studies with mutually adjusted PFAS data, including two medium confidence studies (Meng et al., 2018; Lenters et al., 2016), and four *high* confidence studies (Luo et al., 2021; Shoaff et al., 2018; Manzano-Salgado et al., 2017; Starling et al., 2017). As shown in Table C-1 and for a larger number of epidemiological studies in the PFAS Systematic Review Protocol (see Appendix A), PFNA and PFDA often co-occur in biomarker samples (as expected given some similar anticipated sources) with all studies showing a consistent correlation of 0.6 to 0.85. Although the magnitude was smaller than with PFDA, PFNA was also consistently moderately correlated with PFOS (range: 0.42 to 0.62). Other PFAS showed more variability in correlations (such as PFOA, range: 0.28 to 0.76) or were low to moderately correlated (such as PFHxS, range: −0.04 to 0.45). These results show that not all PFAS consistently co-occur with PFNA across this small subset of studies.

Table C-1. PFAS correlation coefficients in mutually adjusted studies

Reference	Study confidence	Correlations with PFNA			
		PFOS	PFOA	PFDA	PFHxS
Shoaff et al. (2018)[a]	*High*	~0.5	~0.4	~0.6	~0.3
Starling et al. (2017)	*High*	0.62	0.76	0.65	0.45
Manzano-Salgado et al. (2017)	*High*	0.56	0.71	N/A	0.36
Luo et al. (2021)	*High*	0.63	0.28	0.85	−0.04
Lenters et al. (2016)	*Medium*	0.42	0.30	0.60	0.22
Meng et al. (2018)	*Medium*	0.48	0.47	0.73	0.28
Robledo et al. (2015)	*Medium*	N/A	N/A	N/A	N/A

[a]Pearson correlation coefficient from Shoaff et al. (2018) ranged from 0.32 (PFNA and PFHxS) to 0.60 (PFOA and PFOS). The estimated correlation coefficients above are based on their sister publication (Woods et al., 2017); thus, this may slightly over-estimate the PFDA and PFNA correlation given the initial range provided by Shoaff et al. (2018).

C.1.3. PFNA and PFAS Co-Exposure Study Results

The results for the six studies based on continuous PFNA data (expressed as change in mean birth weight per unit change in exposure) are compared and summarized below in Table C-2. Robledo et al. (2015) did not report results from single-pollutant models (or correlations) and showed no evidence of deficits for either boys or girls following adjustment for other contaminant mixture groups, such as other PFAS, organochlorine pesticides, polybrominated diphenyl ethers, polychlorinated biphenyls (PCBs), or one polybrominated biphenyl.

Although two were not statistically significant, three of the five studies (Meng et al., 2018; Manzano-Salgado et al., 2017; Starling et al., 2017) that included multiple PFAS as predictors in ordinary least squares regression models showed larger birth weight deficits (range: −10 to −92 g) compared to single-pollutant models. Two of these studies (Starling et al., 2017; Lenters et al., 2016) also examined multiple PFAS using elastic net regression models. Elastic net regression is a modeling approach to select independent predictors (from an initial group of potentially correlated predictors) for inclusion in the model using penalized shrinkage methods (Lenters et al., 2016). In the Lenters et al. (2016) study, PFNA was not selected in the multi-pollutant elastic net model following adjustment for other contaminants (such as PFAS, phthalates, PCB-153, and p,p´-DDE). In the Starling et al. (2017) study, only PFNA (β = −33 g) and PFOA (β = −14 g) were selected as important contributors to birth weight deficits, albeit at a magnitude smaller than the ordinary least squares multi-PFAS models.

Given the moderate and strong correlations between PFNA and PFDA and other PFAS, the magnitude of any associations that may exist between these co-occurring PFAS and birth weight-related measures (and other developmental effects) may inform the potential for confounding of PFNA associations. As noted above, in Starling et al. (2017), birth weight deficits for both PFNA

(β = −92 g; 95% CI: −167, −18) and PFOA (β = −70 g; 95% CI: −148, −9) based on multi-pollutant ordinary least squares regression were larger compared to those based on a penalized elastic net regression model (βs = −33 g and −14 g, respectively). Meng et al. (2018) reported that adverse birth weight associations similar in magnitude were associated with increased exposure to PFNA (β = −54.2 g; 95% CI: −105.8, −2.7) and PFOS (β = −55.5 g; 95% CI: −145.6, 34.5) in their model containing mutually adjusted PFAS. Multi-pollutant modeling mean birth weight results (β = −18.5 g; 95% CI: −93.7, 51.9) from Luo et al. (2021) for PFNA were greatly reduced compared to single-pollutant findings (β = −123.6 g; 95% CI: −214.4, −32.7) based on the highest exposure quartile. Among the three PFAS showing some birth weight deficits (β's = PFNA: −44.7 g; 95% CI: −92.0, 2.7; PFOS: −68.8 g; 95% CI: −152.9, 15.2; PFOA: −78.5 g; 95% CI: −137.0, −20.0) in the single-pollutant models from the Lenters et al. (2016) study, only PFOA (β = −63.8 g; 95% CI: −122.8, −4.7) was retained in the elastic net regression model. In Shoaff et al. (2018), all of the four PFAS examined, including PFNA, were null for birth weight z-scores in single-pollutant or multi-pollutant modeling. Interestingly, two of the five individual studies that advanced for modeling a lifetime toxicity reference value (and two of three studies in total examined here) showed larger birth weight deficits in OLS models adjusting for other PFAS than when only PFNA was included (i.e., multi-PFAS compared to PFNA-only models).

As noted in Section 3.2.2 (Developmental Effects), 22 of 32 studies showed evidence of some association with PFNA and different birth weight-related measures either in the overall population or at least one of the sexes. As shown in Table C-2, most of the studies using mutually adjusted PFAS approaches to address co-exposures suggested that the PFNA results were robust to modeling approaches, and in three of five studies, these associations were stronger (as shown by the magnitude of association reflected in beta coefficients) upon additional adjustment. Despite consistently high correlations between PFNA and PFDA across all studies considered here, the results for PFNA were often the strongest or among the strongest PFAS-related results. Thus, there is not a lot of direct evidence that confounding by other PFAS is responsible for the birth weight deficits detected with increasing PFNA exposure across studies.

Table C-2. Impact of co-exposure adjustment on estimated change in mean birth weight per unit change in PFNA levels[a]

Reference	BWT measure	Exposure comparison[a]	Single-PFAS model results with 95% CIs	Multi-PFAS[b] results with 95% CIs	Elastic net model results	Effect of adjustment on PFNA birth weight results	PFAS adjustments
High confidence studies							
Shoaff et al. (2018)	BWT z-score[c]	Log_2unit (ng/mL) increase	−0.02 (−0.19, 0.26)	0.05 (−0.17, 0.26)		Remained null	PFOS, PFOA, PFHxS
Starling et al. (2017)	Mean BWT	ln-unit (ng/mL) increase	−57.6 (−104.1, −11.2)	−92.4 (−167.2, −17.6)	−32.7	Strengthened for Ordinary Least Squares but Diminished for Elastic Net	PFOS, PFOA, PFHxS, PFDeA
Manzano-Salgado et al. (2017)	Mean BWT	ln-unit (ng/mL) increase	−14.8 (−55.0, 25.4)	−20.3 (−79.2, 37.8)		Strengthened	PFOS, PFOA, PFHxS
Luo et al. (2021)	Mean BWT	ln-unit (ng/mL) increase	−123.6 (−214.4, −32.7)	−18.5 (−93.7, 51.9)		Diminished	PFBA, PFBS, PFDA, PFOA, PFOS, PFHxS, PFUnDA, PFDoDA, PFTrDA, 6:2 Cl-PFESA, 8:2 Cl-PFESA
Medium confidence studies							
Lenters et al. (2016)	Mean BWT	ln-unit (ng/mL) increase	−43.5 (−89.5, 2.6)	N/A	N/S	Diminished for Elastic Net	PFOS, PFOA, PFHxS, PFUnDA, PFDoDA, PFDA
Meng et al. (2018)	Mean BWT	ln-unit (ng/mL) increase	−52.4 (−101.9, −2.9)	−78.2 (−152.6, −3.9)		Strengthened	PFOS, PFOA, PFHxS, PFDA, PFHpS
Robledo et al. (2015)	Mean BWT	ln-unit (ng/mL) increase	N/A	Girls: −32.1 (−355.1, 290.8) Boys: 196.6 (−100.6, 493.8)		N/A	PFOA, PFOS, PFDA, PFOSA, Et-PFOSA-AcOH, Me-PFOSA-AcOH

Abbreviations: BWT = birth weight; N/A = not available; N/S = PFAS not selected in final elastic net regression model.

[a]Study results presented here are for each ln-unit increase based on original results from publication or EPA re-expressions.

[b]Models were based on ordinary least squares regression.

[c]The mean birth weight result for the single-pollutant model in Shoaff et al. (2018) was −8.00 g (95% CI: −159.49, 143.48) per each 1 ng/mL increase.

C.1.4. Pregnancy Hemodynamics Background

Hemodynamic changes that occur during pregnancy (e.g., increased blood plasma volume due to decreased mean arterial pressure, increased cardiac output, and systemic vasodilation (Sagiv et al., 2018; Sanghavi and Rutherford, 2014; Chapman et al., 1998)) are complex and can lead to challenges in data interpretability when timing of PFAS measurement differs within and across studies. These hemodynamic changes could lead to lower PFAS levels in plasma due to dilution and increased renal filtration as pregnancy progresses. A decrease in PFAS levels has been noted in serial measurements for most PFAS during pregnancy, namely PFOA, PFOS, and PFNA (Chen et al., 2021; Glynn et al., 2012). Hemodynamic changes have been proposed as a potential source of bias for associations between different PFAS measured in maternal samples and neonatal and early childhood growth measures. This is suggested by the association between glomerular filtration rate (GFR), a marker of renal function and, indirectly, of plasma volume expansion, and fetal growth that is independent of gestational age and other maternal covariates (Morken et al., 2014; Gibson, 1973). Because PFNA concentration in serum is expected to decrease during pregnancy due to the hemodynamic changes described above, as well as through transplacental transfer, PFNA measured earlier in pregnancy may represent the largest in utero dosage to PFNA. As noted earlier, given long half-lives, these early trimester windows are considered relevant for evaluating potential effects on the developing fetus. There is little demonstrated evidence of confounding in epidemiological studies to date related to pregnancy hemodynamics, but Steenland et al. (2018a) has proposed that reverse causality may be present if increased fetal growth leads to increased maternal blood expansion and GFR. The potential impact of any bias is unknown but is anticipated to be of greater concern when maternal serum PFAS samples are collected later in pregnancy. Therefore, as part of the study quality evaluations, more confidence was placed in studies that adjusted for pregnancy hemodynamics or that considered this potential source of bias by measuring PFAS levels earlier in pregnancy.

Only three (two *high* and one *medium* confidence) of the 21 PFNA studies examined in the developmental effects section collected and were able to analyze maternal hemodynamic data such as GFR and albumin (a marker of plasma volume expansion). All three of these PFNA studies of fetal growth showed no evidence of confounding following statistical adjustment for GFR (Gyllenhammar et al., 2018; Manzano-Salgado et al., 2017) and GFR and/or albumin (Sagiv et al., 2018) across all fetal growth measures examined. Although early pregnancy measures are preferred to limit these potential sources of bias, the first trimester sampling of plasma albumin and GFR in the two studies (Sagiv et al., 2018; Manzano-Salgado et al., 2017) may be occurring too early to fully reflect the extent of pregnancy-related hemodynamic changes. However, the study by Gyllenhammar et al. (2018) with post-partum samples, as well as another PFOA and PFOS study based on mid-pregnancy samples (Whitworth et al., 2012), have also shown no evidence of confounding by albumin or GFR. To the extent they are designed to evaluate this, these data do not provide evidence of confounding by measure of hemodynamics as suggested by larger birth weight

deficits for later trimester sampling (e.g., beyond the first trimester) in different meta-analyses for both PFOA (Steenland et al., 2018a) and PFOS (Dzierlenga et al., 2020).

C.1.5. Meta-Analysis Methods for Decreased Birthweight

Study Inclusion

Following a systematic review, EPA identified 41 observational epidemiological studies of PFNA that examined mean birth weight (BWT) changes. Among these 41, all but one (Hall et al., 2022) reported data on birth weight differences in relation to PFNA exposures based on maternal and/or infant blood serum or plasma. Four studies reporting only categorical data were not included in the meta-analysis (Gao et al., 2022; Hall et al., 2022; Eick et al., 2020; Cao et al., 2018). Two of these studies did not detect BWT deficits across PFNA tertiles (Eick et al., 2020; Cao et al., 2018), whereas two reported some deficits that varied across quartiles and sex (Gao et al., 2022; Hall et al., 2022). Given demonstrated heterogeneity in BWT results across sexes in the PFAS literature, we also excluded a study in boys only (Marks et al., 2019), which showed large deficits (β = −169.6 g; 95% CI: −448.3, 109.2) per each ng/mL increase in PFNA and evidence of an exposure-response relationship across categorical exposures. To avoid duplication, we restricted the meta-analysis to the larger study population wherein multiple publications reported results from the same birth cohorts (i.e., overlapping study populations were not double counted). For example, the Rokoff et al. (2018) study overlapped with the Project Viva study by Sagiv et al. (2018), as did the Bjerregaard-Olesen et al. (2019) study with the Aarhus birth cohort detailed in Bach et al. (2016). Similarly, the Woods et al. (2017) study overlapped with the Shoaff et al. (2018) study from the Health Outcomes and Measures of the Environment cohort. Three studies (Kobayashi et al., 2017; Minatoya et al., 2017; Kishi et al., 2015) were also not considered further because they had overlapping data from the Hokkaido Study on Environment and Children's Health birth cohort population detailed in Kashino et al. (2020).

After the few exclusions above and limiting the analyses of the same cohorts to these 6 primary studies, 30 non-overlapping studies that met the inclusion criteria and had mean BWT data in the overall population or sex-specific data for both sexes were part of the study evaluation phase of this systematic review. Three of the studies (Maekawa et al., 2017; Lee et al., 2016; Monroy et al., 2008) included in the study evaluation are not considered further in the meta-analysis as they were considered *uninformative* largely due to study quality deficiencies across multiple domains (most often due to deficiencies in the Participant Selection, Confounding, Analysis, and Study Sensitivity domains). For example, in the Maekawa et al. (2017) study, critical deficiencies were identified due to lack of consideration of confounding and insufficient information provided on the sampling frame to evaluate potential for different biases. This resulted in a total of 27 studies for inclusion in the meta-analysis.

Data Pre-Processing

Before performing the overall meta-analysis, estimates from studies reporting only sex-specific estimates for boys and girls were pooled using inverse-variance weighting. These studies included Lind et al. (2017), Robledo et al. (2015), and Wang et al. (2016b).

EPA converted the exposure-response functions quantifying the effects reported in the 27 studies based on different units into two common exposure metrics: natural units (i.e., per ng/mL) or natural log units (i.e., per ln(ng/mL)). For example, to standardize the units and reduce between-study heterogeneity due to the choice of unit, different units of effect changes such as $\log_2$, $\log_{10}$, and per SD- or IQR-unit changes were converted into a common logarithmic function (natural log). Three of the 27 included studies were based on natural scale PFNA data (Sagiv et al., 2018; Shoaff et al., 2018; Bach et al., 2016), and EPA used those data to estimate what the results would have been had they been based on a natural log unit transformation. This approach was developed by Dzierlenga et al. (2020) and involved plotting the reported linear function on the natural scale for the main effect using 25th – 75th percentiles at 10 percentile intervals of the exposure distribution in each study and then fitting a natural logarithmic function to those points. This process was repeated using the reported upper and lower confidence intervals to estimate the bounds of the natural log function and thus the estimated standard error of the natural log function (i.e., standard error = (upper confidence limit − lower confidence limit) / 3.92 (Higgins et al., 2022)).

This meta-analysis was carried out on the natural log scale since a majority (24 out of 27) of the studies reported results on the log scale. Transformations to the log scale are commonly employed in epidemiological studies (e.g., to satisfy regression assumptions). However, the re-scaling methods used by Dzierlenga et al. (2020) and Steenland et al. (2018a) can also be used to express the data on the natural scale, which may be useful for dose-response analysis. As shown in the sensitivity analysis section below, a sensitivity analysis was conducted to test the robustness of our meta-analysis to either the natural or natural log scale.

Statistical Analysis

The 27 developmental PFNA studies included here were evaluated using meta-analysis package *metafor* in R (Version 4.0.3). The meta-analysis was carried out using a random-effects model, following the assumption that each study produced an estimate of a study-specific true effect that varies across studies (Borenstein et al., 2009). Inverse-variance weighting was employed to minimize the influence of both sampling variance and between-study variance on the pooled effect estimate. The amount of variation due to study heterogeneity was captured by two metrics: the I^2 statistic and Cochran's Q Test. The I^2 statistic represents the percentage of variation in the pooled estimate due to between-study heterogeneity. Considering the range of values shown in Cochran's I^2 guidelines (Higgins et al., 2022), EPA considered I^2 statistics <40% to represent "low" potential heterogeneity, with values from 40% to 69% being "moderate" and values ≥70% representing "high" heterogeneity. Cochran's Q test evaluates whether the dispersion of study-

specific estimates about the pooled effect estimate is statistically significant via a *p*-value (p_Q), based on significance level (α) of 0.05. Both metrics may suffer from low statistical power when few studies are available, potentially complicating interpretation of the examinations of heterogeneity. Thus, consideration of both measures in conjunction is recommended to identify situations in which significant heterogeneity may be present (Huedo-Medina et al., 2006). Given the relatively large sample size (n = 27) in the overall analysis, this is less likely to be affected by low statistical power. However, this could be a concern for stratified analyses in which there are smaller numbers of studies per strata.

EPA conducted stratified analyses to evaluate whether the summary effect estimate varied by the study confidence rating or by the timing of maternal serum sampling. As detailed in Section 3.2.2, study confidence designations included 5 *low* confidence studies (Workman et al., 2019; Xu et al., 2019; Li et al., 2017; Shi et al., 2017; Callan et al., 2016), 10 *medium* confidence studies (Chang et al., 2022; Chen et al., 2021; Hjermitslev et al., 2020; Kashino et al., 2020; Gyllenhammar et al., 2018; Meng et al., 2018; Kwon et al., 2016; Lenters et al., 2016; Robledo et al., 2015; Chen et al., 2012), and 12 *high* confidence studies (Luo et al., 2021; Yao et al., 2021; Wikström et al., 2020; Buck Louis et al., 2018; Sagiv et al., 2018; Shoaff et al., 2018; Lind et al., 2017; Manzano-Salgado et al., 2017; Starling et al., 2017; Valvi et al., 2017; Bach et al., 2016; Wang et al., 2016b). Sample timing strata were defined according to two strategies based on reported gestational age (weeks) at time of biomarker collection. Strategy 1 was a three-strata approach with subgroups *early* (n = 11), *mid & late* (n = 10), and post (n = 6) pregnancy. Strategy 2 was a two-strata approach, using the same definition of *early* pregnancy as in Strategy 1 but combining *mid & late* and *post* pregnancy into a single stratum, *mid & late + post* (n = 16). Early pregnancy included studies reporting samples from preconception (0 days), the first trimester (0 days to 13 weeks and 6 days), or a mixture of the first and second trimesters (0 days to 27 weeks and 6 days); *late-pregnancy* studies sampled in the second trimester (14 weeks and 0 days to 27 weeks and 6 days), a mixture of the second and third trimester (14 weeks and 0 days to birth), or the third trimester only (28 weeks and 0 days to birth); postpregnancy studies sampled at or after birth (ACOG, 2020). Studies were assigned to sample timing strata based on reported sampling ranges when available or by measures of centrality otherwise (see Table C-3 below for details on sample timing distributions and strata assignments).

The two-strata sample timing approach was also used by two previous PFAS meta-analyses of birth weight (Dzierlenga et al., 2020; Steenland et al., 2018a). EPA separated studies in which PFNA was measured in pregnancy samples from those with post pregnancy samples to better understand differences in sampling matrices, i.e., maternal serum sampled during pregnancy versus umbilical cord samples or post-partum maternal serum samples (i.e., termed post-pregnancy here). Furthermore, the use of a larger number of subgroups increases the ability to examine between-study differences associated with differences in sample timing approaches. A sensitivity analysis was employed to assess the robustness of the meta-analysis results to using three strata instead of two.

All stratified meta-analyses were carried out using the *metafor* package in R (Version 4.0.3). EPA conducted separate random-effects modeling for each stratum, producing estimates that account for possible heterogeneity among studies. A subsequent fixed-effects model was used to test for statistically significant differences across the subgroups (Borenstein et al., 2009). A *p*-value less than 0.05 from this hypothesis test is indicative of no statistically significant differences between any of the strata. Strata-specific statistical tests conducted on subgroups with lower sample sizes are subject to lower power and susceptible to higher uncertainty and should therefore be interpreted with caution. For full details on the computations involved in both the stratified and overall meta-analyses, please refer to the R code developed by EPA (Larsen, 2022).

Table C-3. Details on reported sample timing distributions and sample timing strata assignments

Study, confidence	Exposure window	Central estimate of the sampling distribution	Spread of the sampling distribution	Sample timing strata	Notes
Bach et al. (2016), ***High***	Trimesters 1, 2	12 wk (mode)	9, 20 wk (min, max)	Early	
Buck Louis et al. (2018), ***High***	Trimester 1	N/R	10, 13.9 wk (min, max)	Early	Value of 11.9 wk was estimated as midpoint of the range (10 to 13.9 wk).
Callan et al. (2016), ***Low***	Trimester 3	N/R	33, 40 wk (min, max)	Late	Samples were taken 2wk before due date, with a mean of 39.7 (ranged: 35 to 42 wk); estimate measure of centrality used here of 37.7 wk.
Chang et al. (2022), ***Medium***	Trimesters 1, 2	11.4 wk (median)	8.1, 14.6 wk (min, max)	Early	Median and other measures of centrality and variability provided by authors (Liang, 2022)
Chen et al. (2012), ***Medium***	At birth	39 wk (median)	N/R	Post	
Chen et al. (2021), ***Medium***	Trimesters 1, 2	16.3 wk (median)	13.85, 20.43 (min, max)	Early	The authors Zhang (2022) provided additional data, which showed their serial measures included overlapping trimesters, e.g., their first trimester results encompassed the first and second trimester samples.
Gyllenhammar et al. (2018), ***Medium***	Post-birth	43 wk (mean)	37.9, 46.1 wk (min, max)	Post	Samples were taken 3 wk after delivery; mean (range) delivery date = 40 wk (34.9–43.1).
Hjermitslev et al. (2020), ***Medium***	Trimesters 1, 2, 3	N/R	7, 40 wk (min, max)	Early	This study was assigned to the early strata because sampling predominantly occurred earlier in pregnancy: study authors reported that the mean

Study, confidence	Exposure window	Central estimate of the sampling distribution	Spread of the sampling distribution	Sample timing strata	Notes
					gestational wk of sampling in 2010–2011 was wk 26.2, and in 2013–2015 all samples were collected before the end of wk 13. 38% of samples were taken in 2010–2011; 62% were collected in 2013–2015 (Bonefeld-Jørgensen, 2022).
Kashino et al. (2020), ***Medium***	Trimester 3	29 wk (median)	N/R	Late	
Kwon et al. (2016), ***Medium***	At Delivery	40 wk (exact)	N/R	Post	
Lenters et al. (2016), ***Medium***	Trimesters 2, 3	25.2 wk (Weighted mean of medians)	N/R	Late	Study authors reported country-specific medians: 33 wk (Poland, 18%), 25 wk (Greenland, 32%), 23 wk (Ukraine, 49%).
Li et al. (2017), ***Low***	At Delivery	39 wk (mean)	N/R	Post	
Lind et al. (2017), ***High***	Trimester 1	10 wk (median)	5, 12 wk (min, max)	Early	
Luo et al. (2021), ***High***	Trimester 3	39.3 wk (mean)	N/R	Late	
Manzano-Salgado et al. (2017), ***High***	Trimesters 1, 2, 3	12.3 wk (mean)	5.6 wk (SD)	Early	While sampling is reported to have taken place in the first trimester (Manzano-Salgado et al., 2017) supporting information clarifies that some sampling outside of the first trimester also occurred (Wright et al., 2023). However, first trimester sampling was predominant, so this study is designated as conducting "early" sample timing.

Study, confidence	Exposure window	Central estimate of the sampling distribution	Spread of the sampling distribution	Sample timing strata	Notes
Meng et al. (2018), ***Medium***	Trimesters 1, 2	8 wk (mean)	N/R	Early	The mean is reported in related publication (Liew et al., 2020).
Robledo et al. (2015), ***Medium***	Preconception	N/R	N/R	Early	Pre-conception samples, so a value of 0 was used for gestational wk analysis.
Sagiv et al. (2018), ***High***	Trimesters 1, 2	9 wk (median)	5, 19 wk (Min, max)	Early	
Shi et al. (2017), ***Low***	At delivery	39.8 wk (mean)	4.2 wk (SD)	Post	
Shoaff et al. (2018), ***High***	Trimesters 2, 3, At delivery	N/R	N/R	Late	This study was assigned to the late strata instead of post because only 5% of samples taken at delivery, and sensitivity analysis conducted by study authors found results robust to second trimester only.
Starling et al. (2017), ***High***	Trimesters 2, 3	27 wk (median)	20, 34 wk (Min, max)	Late	
Valvi et al. (2017), ***High***	Trimester 3	34 wk (exact)	N/R	Late	
Wang et al. (2016b), ***High***	Trimester 3	N/R	N/R	Late	
Wikström et al. (2020), ***High***	Trimesters 1, 2	10 wk (median)	N/R	Early	
Workman et al. (2019), ***Low***	Trimesters 2, 3	28.6 wk (median)	14.3, 39.6 wk (Min, max)	Late	Median and other measures of centrality and variability provided by author (U.S. EPA, 2022)
Xu et al. (2019), ***Low***	At delivery	39.4 wk (mean)	1.4 wk (SD)	Post	

Study, confidence	Exposure window	Central estimate of the sampling distribution	Spread of the sampling distribution	Sample timing strata	Notes
Yao et al. (2021), ***High***	Trimester 3	39.4 wk (mean)	N/R	Late	

Abbreviations: min = minimum; max = maximum; N/R = not reported; SD = standard deviation.

C.1.6. Meta-Analysis Results

As shown in the forest plot below (see Figure C-1), the overall pooled effect estimates from 27 studies based on the random-effects model was −32.9 g (95% CI: −47.0, −18.7) of birth weight per ln(ng/mL) increase in PFNA exposure. The I^2 test for heterogeneity showed that between-study variability is just below the demarcation between "low" and "moderate" levels, and the Cochran's Q test showed borderline statistically significant evidence for heterogeneity (I^2 = 35.9%, p_Q = 0.05).

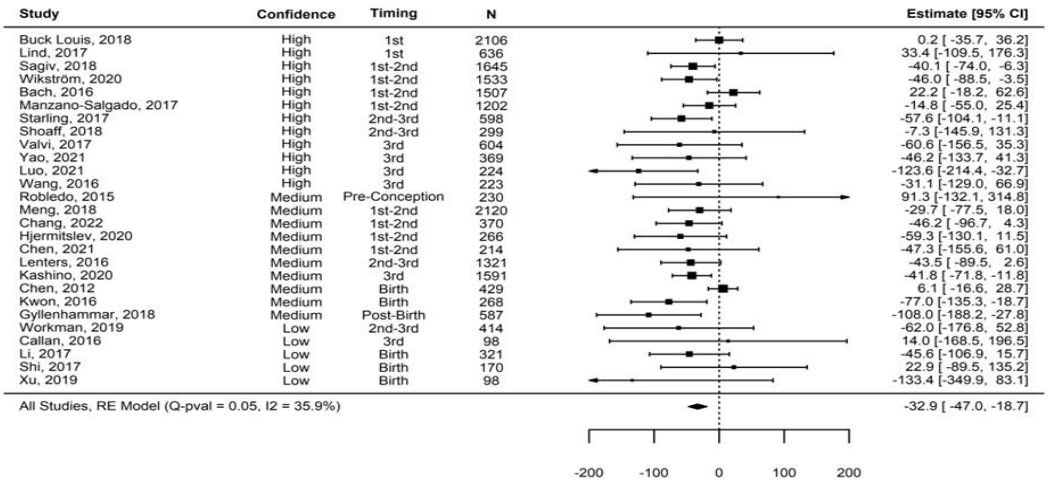

Figure C-1. Forest plot of 27 studies included for the meta-analysis on PFNA exposures and changes in birth weight.

Arrows indicate where 95% CIs are truncated.

The meta-analysis results stratified by study confidence are displayed in Table C-4. The 12 *high* confidence studies yield a smaller pooled effect estimate of decreased birthweight (β = −28.0 g; 95% CI: −49.0, −6.9) than the *medium* or *low* confidence studies; however, the differences between strata are not statistically significant (p = 0.77). There was "low" between-study heterogeneity for the *high* confidence studies (I^2 = 38.8%, p_Q = 0.11).

As expected, the pooled effect of the *high* + *medium* confidence studies were similar in magnitude to the overall pooled effect (β = −32.9 g; 95% CI: −48.0, −17.8) given that both groups shared 12 out of 22 studies. Roughly 42% of the variation in the *high* + *medium* confidence pooled effect was associated with between-study variation, and Cochran's Q test detected a statistically significant level of heterogeneity (I^2 = 45.2%, p_Q = 0.02). The difference between the *high* + *medium* and the *low* confidence groups was not statistically significant (p = 0.87).

Of the three levels, the *low* confidence subgroup showed the least amount of estimated heterogeneity (I^2 = 0%, p_Q = 0.66). Given the small sample size of the strata (n = 5), the *low* confidence effect estimates and heterogeneity statistics are subject to relatively more uncertainty and should be interpreted with caution.

Table C-4. Meta-analysis of the effect of PFNA on birth weight stratified by study confidence

Set of studies	n	β (g per ln(ng/mL))	95% Confidence interval	I^2 (%)	p_Q
All studies	27	−32.9	−47.0, − 18.7	35.9	0.05
High confidence	12	−28.0	−49.0, −6.9	38.8	0.11
Medium confidence	10	−39.0	−61.8, −16.3	48.1	0.03
Low confidence	5	−36.9	−82.9, 9.1	0.0	0.66
High + *medium* confidence	22	−32.9	−48.0, −17.8	42.2	0.02

Symbols and abbreviations: n = sample size; β = combined estimate of change in birth weight (g) per ln (ng/mL) PFNA exposure; I2 = % variation in the pooled effect due to study heterogeneity; p_Q = *p*-value for Cochran's Q test for heterogeneity.

The meta-analysis results stratified by sample timing are displayed in Table C-5. While not statistically significantly different for either the two- or three-strata approach (p = 0.12, 0.14, respectively), the pooled estimates from later sampling were approximately twice as large than those from earlier sampling regardless of the stratification strategy: The estimated birth weight deficit for *early* pregnancy was −22.0 g (95% CI: −40.0, −4.0) compared to −48.4 g (95% CI: −67.7, −29.0) for *mid- & late*-pregnancy, −42.9 g (95% CI: −88.0, 2.2) for *post* pregnancy, and −44.5 g (95% CI: −65.9, −23.0) for mid- & late- + post pregnancy.

Effect estimates from the *late* and the *late + post* groups were similar in magnitude (−48.4 g for *mid & late* versus −44.5 g for *mid & late + post*). Although no heterogeneity was detected among the *mid & late*-pregnancy studies (I^2 = 0%; p_Q = 0.91), "moderate" heterogeneity was observed for *post*-birth studies (I^2 = 63.1%, p_Q = 0.01) and *mid & late + post* pregnancy studies (I^2 = 40.0%, p_Q = 0.05). However, the *post* pregnancy stratum has a relatively small sample size (n = 6), so results from this heterogeneity test are expected to be more uncertain.

Table C-5. Meta-analysis of the effect of PFNA on birth weight stratified by sample timing

Set of studies	n	β (g per ln(ng/mL))	95% Confidence interval	I^2 (%)	p_Q
All studies	27	−32.9	−47.0, −18.7	35.9	0.05
Early pregnancy (note: all ***high*** or ***medium*** confidence)	11	−22.0	−40.1, −4.0	25.9	0.26
Mid- & late-pregnancy	10	−48.4	−67.7, −29.0	0.0	0.91
Post-pregnancy	6	−42.9	−88.0, 2.2	63.1	0.01
Late + post pregnancy	16	−44.5	−65.9, −23.0	40.0	0.05

Symbols and abbreviations: n = sample size; β = combined estimate of change in birth weight (g) per ln (ng/mL) PFNA exposure; I^2 = % variation in the pooled effect due to study heterogeneity; p_Q = *p*-value for the Cochran's Q test for heterogeneity.

C.1.7. Sensitivity Analysis Results

The sensitivity of the meta-analysis results to re-expression was tested by comparing results based on effect estimates re-expressed to the natural log scale to those converted to the natural scale. Table C-6 illustrates that the overall pattern of effect estimates remains the same for both the primary and stratified analyses. Larger effects and correspondingly larger standard errors are seen in the strata with lower sample sizes, i.e., *low* confidence and post-pregnancy.

Table C-6. Sensitivity of the overall and stratified meta-analyses to natural log scale or natural scale re-expression

Set of studies	n	β (95% CI) in g per ln(ng/mL)	β (95% CI) in g per ng/mL
All studies	27	−32.9 (−47.0, −18.7)	−37.0 (−56.9, −17.0)
Study confidence strata			
High	12	−28.0 (−49.0, −6.9)	−37.7 (−69.0, −6.5)
Medium	10	−39.0 (−61.8, −16.3)	−35.1 (−62.4, −7.9)
Low	5	−36.9 (−82.9, 9.1)	−163.5 (−367.8, 40.8)

Set of studies	n	β (95% CI) in g per ln(ng/mL)	β (95% CI) in g per ng/mL
High + medium	22	−32.9 (−48.0, −17.8)	−35.4 (−55.1, −15.7)
Sample timing strata			
Early Pregnancy	11	−22.0 (−40.1, −4.0)	−25.7 (−50.4, −1.1)
Mid & Late-Pregnancy	10	−48.4 (−67.7, −29.0)	−49.0 (−75.9, −22.1)
Post- Pregnancy	6	−42.9 (−88.0, 2.2)	−186.3 (−373.2, 0.6)
Late + Post	16	−44.5 (−65.9, −23.0)	−72.7 (−117.1, −28.3)

Symbols and abbreviations: n = sample size; β = pooled estimate of change in birth weight (g) per ln (ng/mL) or ng/mL PFNA exposure; CI = confidence interval.

C.1.8. Summary of Meta-Analysis of PFNA Effects on Birth Weight

The meta-analysis of the 27 epidemiological studies showed statistically significant decreases in mean birth weight of 33 g (β = −32.9 g; 95% CI: −47.0, −18.7) per ln-unit increase in maternal serum PFNA (see Table C-4; see Figure C-1). For all study confidence levels, decreases in mean birthweight were similar in magnitude and in excess of −28 g per ln(ng/mL) change in PFNA exposure when analyzed separately (i.e., *high*, *medium*, and *low* confidence) or grouped together (i.e., *medium* + *high* confidence). Stratified analyses by sampling timing show some difference in effect size, with the largest differences detected in studies with blood sampling late in pregnancy, at birth (i.e., umbilical cord samples), or post-partum. This pattern is consistent with findings in the developmental epidemiology literature on exposure to PFOS and PFOA that reported differences in birth weight deficits by sample timing windows (Dzierlenga et al., 2020; Steenland et al., 2018a). The key distinction between this current work and previous PFOS and PFOA meta-analyses is that the results for early sampled studies are not null. Although studies conducted earlier in pregnancy yielded smaller pooled effects compared to later sampling (β = −22.0 g; 95% CI: −40.1, −4.0), statistically significant birth weight deficits were still demonstrated in this analysis. Overall, the results show a consistent deficit in birth weight across all studies and across subgroups.

Similar to the hazard synthesis of the categorical and continuous results detailed in the main assessment, Section 3.2.2, the meta-analysis study results examined here also provide supportive evidence of an adverse effect on birth weight from maternal exposure to PFNA. The findings appear to be robust to considerations of both study confidence and sample timing, although, as expected, the findings for earlier-sampled studies were smaller in magnitude. Nonetheless, potential bias from pregnancy hemodynamics should continue to be examined as a source of uncertainty in epidemiological studies given potential differences by PFAS biomarker sample timing. The meta-analytical findings, along with this research, are indicative of complex

patterns of influence due to pregnancy hemodynamic differences that are not completely understood. And, while a 33 g deficit per each ln-unit increase may seem modest, these differences need to be extrapolated across the full exposure range reported across studies. For example, PFNA median exposure levels ranged from 0.2 to 2.3 ng/mL with maximum values of 0.81 to 22 ng/mL (median of the maximums = 4.5 ng/mL) in studies that reported the full exposure ranges.

C.2. ANALYSIS OF RELEVANT HIGH-THROUGHPUT SCREENING ASSAYS FROM EPA'S CHEMICALS DASHBOARD

The results of the ToxCast program's in vitro high-throughput screening (HTS) for PFNA are summarized below and are based on invitroDB version 3.5, queried on March 15, 2023, from EPA's Chemicals Dashboard, which was released in August 2022. Note that the ToxCast database of in vitro bioactivity data is updated approximately every 6–12 months.

C.2.1. ToxCast Methods

ToxCast targets numerous biological endpoints and employs both cell-based and biochemical models. Results are typically presented as positive (hitcall = 1) or negative (hitcall = 0), associated half-maximal activity (AC50) values, and efficacy values (cutoff and maximum responses) for active substances. To derive activity values, raw chemical-screening data in assay tests are processed and modeled through the ToxCast data analysis pipeline (ToxCast Manual). The model selected (i.e., Constant, Hill, Gain-Loss) is based on the best fit of the concentration-response data, and concentration-response curves for tested chemicals are considered active when: (1) Hill or Gain-Loss curve fit models are the selected models; (2) the modeled curve fit top exceeds the efficacy cutoff for at least one dose; and (3) the median response exceeds the efficacy cutoff.

C.2.2. Overall Results

For PFNA, 280 of 1,136 ToxCast in vitro HTS assays were identified as active, including active assays targeting more generalized pleiotropic gene pathways, multifunctional enzymes, and cell-signaling targets. The active hit assays with the lowest AC50 values (highest potency) included those targeting human farnesoid X receptor (FXR), interactions between thyroxine (T4) and the transthyretin receptor (TTR), and cytochrome P450 2C9 (CYP2C9). FXR is involved in regulating the synthesis of bile acids from cholesterol. CYP2C9 is expressed in the liver and intestine and catalyzes xenobiotic metabolism. TTR is a serum transporter protein that binds to and distributes thyroid hormone in circulation. A low AC50 was also identified for mERα in a reporter binding assay targeting PFNA binding the mouse estrogen receptor.

C.2.3. Hepatic System Pathway Results

Toxcast in vitro HTS assays targeting the liver are summarized in Table C-7.

Table C-7. Liver-related in vitro HTS assays identified as "active" hits with half-maximal activity concentration (AC50) values for PFNA in ToxCast and Tox21

Assay name	Gene target	Biological process target	Cell model	AC50 (µM)
NVS_NR_hFXR_Antagonist	*NR1H4*	Receptor binding, reporter	Human cell free	0.041
NVS_ADME_hCYP2C9	*CYP2C9*	Regulation of catalytic activity, enzyme reporter	Human cell free	0.601
LTEA_HepaRG_APOA5_up	*APOA5*	Regulation of TF activity, mRNA induction	Human, liver HepaRG	2.42
LTEA_HepaRG_CYP4A11_up	*CYP4A11*	Regulation of TF activity, mRNA induction	Human, liver HepaRG	2.91
LTEA_HepaRG_CYP2C19_up	*CYP2C19*	Regulation of TF activity, mRNA induction	Human, liver HepaRG	3.94
LTEA_HepaRG_HMGCS2_up	*HMGCS2*	Regulation of TF activity, mRNA induction	Human, liver HepaRG	6.2
LTEA_HepaRG_ACOX1_up	*ACOX1*	Regulation of TF activity, mRNA induction	Human, liver HepaRG	6.74
LTEA_HepaRG_CYP4A22_up	*CYP4A22*	Regulation of TF activity, mRNA induction	Human, liver HepaRG	7.15
LTEA_HepaRG_FABP1_up	*FABP1*	Regulation of TF activity, mRNA induction	Human, liver HepaRG	7.51
TOX21_RXR_BLA_Agonist_ratio	*RXRA*	Regulation of TF activity, inducible reporter	Human, kidney HEK293	9.49
LTEA_HepaRG_UGT1A1_up	*UGT1A1*	Regulation of TF activity, mRNA induction	Human, liver HepaRG	9.63
LTEA_HepaRG_CYP3A7_up	*CYP3A7*	Regulation of TF activity, mRNA induction	Human, liver HepaRG	9.86
ATG_PXRE_CIS_up	*NR1I2*	Regulation of TF activity, mRNA induction	Human, liver HepG2	10.2
ATG_PPARa_TRANS_up	*PPARA*	Regulation of TF activity, mRNA induction	Human, liver HepG2	14.3
ATG_RXRb_TRANS_up	*RXRB*	Regulation of TF activity, mRNA induction	Human, liver HepG2	16.1
ERFPL_NR_binding_hPPARG_up	*PPARG*	Receptor binding, reporter	Human, cell free	20.83
NVS_NR_hCAR_Antagonist	*NR1I3/CAR*	Receptor binding, reporter	Human, cell free	23.74
TOX21_PPARg_BLA_antagonist_ratio	*PPARG*	Regulation of TF activity, inducible reporter	Human, kidney HEK293	25.98
NVS_NR_hRAR_Antagonist	*RARA*	Receptor binding, reporter	Human cell free	32.7

Assay name	Gene target	Biological process target	Cell model	AC50 (µM)
ATG_PPRE_CIS_up	*PPARA, PPARD, PPARG*	Regulation of TF activity, mRNA induction	Human, liver HepG2	38.82
ATG_PPARg_TRANS_up	*PPARG*	Regulation of TF activity, mRNA induction	Human, liver HepG2	43.4
LTEA_HepaRG_CYP1A2_dn	*CYP1A2*	Regulation of TF activity, mRNA induction	Human, liver HepRG	43.8
LTEA_HepaRG_MIR122_dn	*MIR122*	Regulation of TF activity, mRNA induction	Human, liver HepRG	44.42
TOX21_PPARd_BLA_antagonist_ratio	*PPARD*	Regulation of TF activity, inducible reporter	Human, kidney HEK293	44.6
ATG_DR4_LXR_CIS_dn*	*NR1H3*	Regulation of TF activity, mRNA induction	Human, liver HepG2	47.3
ATG_PXR_TRANS_up	*NR1I2*	Regulation of TF activity, mRNA induction	Human, liver HepG2	47.7
LTEA_HepaRG_UGT1A6_dn	*UGT1A6*	Regulation of TF activity, mRNA induction	Human, liver HepRG	50.66
LTEA_HepaRG_UGT1A6_dn	*UGT1A6*	Regulation of TF activity, mRNA induction, phase II metabolism	Human, liver HepRG	50.7
LTEA_HepaRG_ABCB11_dn	*ABCB11*	Regulation of TF activity, mRNA induction	Human, liver HepRG	56.51
LTEA_HepaRG_SLCO1B1_dn	*SLCO1B1*	Regulation of TF activity, mRNA induction	Human, liver HepRG	59.69
LTEA_HepaRG_DDIT3_up	*DDIT3*	Regulation of TF activity, mRNA induction	Human, liver HepRG	63.0
LTEA_HepaRG_GSTA2_dn	*GSTA2*	Regulation of TF activity, mRNA induction	Human, liver HepRG	63.43
LTEA_HepaRG_IGFBP1_up	*IGFBP1*	Regulation of TF activity, mRNA induction	Human, liver HepRG	72.3
LTEA_HepaRG_CYP7A1_dn	*CYP7A1*	Regulation of TF activity, mRNA induction	Human, liver HepRG	73.1
LTEA_HepaRG_CYP1A1_up	*CYP1A1*	Regulation of TF activity, mRNA induction	Human, liver HepRG	81.5
LTEA_HepaRG_APOA5_dn	*APOA5*	Regulation of TF activity, mRNA induction	Human, liver HepRG	81.8
LTEA_HepaRG_CYP2E1_dn	*CYP2E1*	Regulation of TF activity, mRNA induction	Human, liver HepRG	82.8
LTEA_HepaRG_CYP4A22_dn	*CYP4A22*	Regulation of TF activity, mRNA induction	Human, liver HepRG	83.1
LTEA_HepaRG_FABP1_dn	*FABP1*	Regulation of TF activity, mRNA induction	Human, liver HepRG	84.3

Assay name	Gene target	Biological process target	Cell model	AC50 (µM)
LTEA_HepaRG_FASN_dn	*FASN*	Regulation of TF activity, mRNA induction	Human, liver HepRG	84.5
LTEA_HepaRG_CYP2B6_dn	*CYP2B6*	Regulation of TF activity, mRNA induction	Human, liver HepRG	85.7
LTEA_HepaRG_CYP3A4_dn	*CYP3A4*	Regulation of TF activity, mRNA induction	Human, liver HepRG	86.5
LTEA_HepaRG_CYP2C8_dn	*CYP2C8*	Regulation of TF activity, mRNA induction	Human, liver HepRG	87.6
LTEA_HepaRG_CYP4A11_dn	*CYP4A1*	Regulation of TF activity, mRNA induction	Human, liver HepRG	87.7
LTEA_HepaRG_UGT1A1_dn	*UGT1A1*	Regulation of TF activity, mRNA induction	Human, liver HepRG	88.9
LTEA_HepaRG_CYP2C19_dn	*CYP2C19*	Regulation of TF activity, mRNA induction	Human, liver HepRG	91,6
LTEA_HepaRG_CYP3A7_dn	*CYP3A7*	Regulation of TF activity, mRNA induction	Human, liver HepRG	93.2
LTEA_HepaRG_CYP2C9_dn	*CYP2C9*	Regulation of TF activity, mRNA induction	Human, liver HepRG	93.7
LTEA_HepaRG_ACOX1_dn	ACOX1	Regulation of TF activity, mRNA induction	Human, liver HepRG	95.3
ATG_RARa_TRANS_dn[a]	*RARa*	Regulation of TF activity, mRNA induction	Human, liver HepG2	109.3
ATG_FXR_TRANS_up	*NR1H4*	Regulation of TF activity, mRNA induction	Human, liver HepG2	125.8
ATG_LXRa_TRANS_up	*NR1H3*	Regulation of TF activity, mRNA induction	Human, liver HepG2	86.8
ATG_FXR_TRANS_up	*NR1H4*	Regulation of TF activity, mRNA induction	Human, liver HepG2	125.77

Many of the gene targets are pleiotropic and expressed in numerous tissues. Inactive null assays with PFNA can be found at: https://comptox.epa.gov/dashboard/dsstoxdb/results?search=DTXSID8031863#invitrodb-bioassays-ToxCast-data.

[a]ToxCast reports assay to be not optimized; results interpreted with caution.

C.2.4. Immune System Pathway Results

Eleven active assays examined genes associated with immune functioning (see Table C-8).

Table C-8. Immune system related in vitro HTS assays identified as "active" hits with half-maximal activity concentration (AC50) values for PFNA

Assay name	Gene target	Biological process target	Tissue and cell model	AC50 (µM)
BSK_KF3CT_IL1a_down	*IL1A*	Regulation of gene expression, reporter binding, cytokine/interleukin	Human, keratinocytes, and fibroblasts	2
BSK_KF3CT_MCP1_down	*CCL2*	Regulation of gene expression, reporter binding, cytokine/chemotactic	Human, keratinocytes, and fibroblasts	2
BSK_BE3C_HLADR_down	*HLADR*	Regulation of gene expression, reporter binding, cytokine/cell adhesion	Human, lung bronchial epithelial	7
BSK_BF4T_VCAM1_down	*VCAM1*	Regulation of gene expression, reporter binding, cytokine/cell adhesion	Human, vascular bronchial epithelial and fibroblasts	7
BSK_BE3C_IP10_down	*CXCL10*	Regulation of gene expression, reporter binding, cytokine/chemotactic	Human, lung bronchial epithelial	10
BSK_BE3C_IL8_down	*CXCL8*	Regulation of gene expression, reporter binding, cytokine/interleukin	Human, lung bronchial epithelial	20
BSK_BF4T_MCP1_down	*CCL2*	Regulation of gene expression, reporter binding, cytokine/chemotactic	Human, vascular bronchial epithelial and fibroblasts	20
BSK_BE3C_PAI1_down	*SERPINE1*	Regulation of gene expression, reporter binding, cytokine	Human, lung bronchial epithelial	20
BSK_IMphg_IL8_up	*CXCL8*	Regulation of gene expression, reporter binding, cytokine/interleukin	Human, vascular venular endothelial cells and macrophages	20
BSK_BF4T_Eotaxin3_down	*CCL26*	Regulation of gene expression, reporter binding, cytokine/chemotactic	Human, vascular bronchial epithelial and fibroblasts	20
BSK_hDFCGF_MIG_down	*CXCL9*	Regulation of gene expression, reporter binding, cytokine/chemotactic	Human, fibroblast	20
TOX21_ARE_BLA_agonist_ratio	*NFE2L2*	Regulation of gene expression, reporter binding, inflammation	Human, liver HepG2	24.4
ATG_TGFb_CIS_up	*TGFB1*	Regulation of TF activity, mRNA induction, inflammation	Human, liver HepG2	26.2
NVS_GPCR_gLTB4	*LTB4*	Receptor binding, inflammation	Guinea pig, spleen, tissue based	28.94
LTEA_HepaRG_FAS_up	*FAS*	Regulation of TF activity, mRNA induction, cytokine receptor	Human, liver HepaRG	38.06

Assay name	Gene target	Biological process target	Tissue and cell model	AC50 (µM)
BSK_BE3C_IL1a_down	*IL1A*	Regulation of gene expression, reporter binding, cytokine/interleukin	Human, lung bronchial epithelial	40
BSK_BE3C_TGFb1_down	*TGFB1*	Regulation of gene expression, reporter binding, inflammation	Human, lung bronchial epithelial	40
BSK_KF3CT_IP10_down	*CXCL10*	Regulation of gene expression, reporter binding, cytokine/chemotactic	Human keratinocytes, fibroblasts	40
LTEA_HepaRG_TGFB1_up	*TGFB1*	Regulation of TF activity, mRNA induction	Human, liver HepRG	41.73
LTEA_HepaRG_NFE2L2_up	*NFE2L2*	Regulation of gene expression, reporter binding, inflammation	Human, liver HepRG	44.12
ATG_Oct_MLP_CIS_up	*POU2F1*	Regulation of TF activity, mRNA induction	Human, liver HepG2	50.6
LTEA_HepaRG_NFE2L2_up	*NFE2L2*	Regulation of TF activity, mRNA induction, inflammation response	Human, liver HepRG	44.12
BSK_BE3C_MIG_down	*CXCL9*	Regulation of gene expression, reporter binding, cytokine/chemotactic	Human, lung bronchial epithelial	60
BSK_BE3C_ICAM1_down	*ICAM1*	Regulation of gene expression, reporter binding, cytokine	Human, lung bronchial epithelial	60
BSK_BE3C_ITAC_down	*CXCL11*	Regulation of gene expression, reporter binding, cytokine	Human, lung bronchial epithelial	60
BSK_BF4T_ICAM1_down	*ICAM1*	Regulation of gene expression, reporter binding, cell adhesion	Human, primary vascular bronchial epithelial cells, and dermal fibroblasts	60
BSK_BF4T_IL1a_down	*IL1A*	Regulation of gene expression, reporter binding, cell adhesion	Human, primary vascular bronchial epithelial cells, and dermal fibroblasts	60
BSK_BF4T_IL8_down	*IL8*	Regulation of gene expression, reporter binding, cell adhesion	Human, primary vascular bronchial epithelial cells, and dermal fibroblasts	60
BSK_hDFCGF_ICAM1_down	*ICAM1*	Regulation of gene expression, reporter binding, cell adhesion	Human, primary, foreskin fibroblast	60
BSK_4H_Eotaxin3_down	*CCL26*	Regulation of gene expression, reporter binding, inflammation	Human, primary vascular umbilical vein endothelium	60
BSK_3C_HLADR_down	*HLA-DRB1*	Regulation of gene expression, reporter binding, cytokine/cell adhesion	Human, primary vascular umbilical vein endothelium	60
BSK_3C_VCAM1_down	*VCAM1*	Regulation of gene expression, reporter binding, cytokine/cell adhesion	Human, primary vascular umbilical vein endothelium	60

Assay name	Gene target	Biological process target	Tissue and cell model	AC50 (µM)
BSK_MyoF_VCAM1_down	*VCAM1*	Regulation of gene expression, reporter binding, cytokine/cell adhesion	Human, primary vascular lung fibroblast	60
BSK_SAg_CD40_down	*CD40*	Regulation of gene expression, reporter binding, cytokine, inflammation	Human, primary vascular umbilical vein endothelium and peripheral blood mononuclear cells	60
BSK_SAg_CD69_down	*CD69*	Regulation of gene expression, reporter binding, cytokine	Human, primary vascular umbilical vein endothelium and peripheral blood mononuclear cells	60
BSK_SAg_IL8_down	*IL8*	Regulation of gene expression, reporter binding, cytokine	Human, primary vascular umbilical vein endothelium and peripheral blood mononuclear cells	60
BSK_BF4T_CD90_down	*CD90*	Regulation of gene expression, reporter binding, cytokine	Human, primary vascular bronchial epithelial cells, and dermal fibroblasts	60
BSK_IMphg_IL10_down	*IL10*	Regulation of gene expression, reporter binding, cytokine	Human, primary, venular endothelial cells and macrophages	60
BSK_IMphg_MCP1_down	*CCL2*	Regulation of gene expression, reporter binding, cytokine	Human, primary, venular endothelial cells and macrophages	60
BSK_KF3CT_MIG_down	*CXCL9*	Regulation of gene expression, reporter binding, cytokine	Human keratinocytes, fibroblasts	60
BSK_BT_xTNFa_up	*TNFa*	Regulation of gene expression, cytokine quantitation reporter, cytokine	Human, primary, B and peripheral blood mononuclear cells	60
BSK_hDFCGF_IP10_down	*CXCL10*	Regulation of gene expression, reporter binding, cytokine	Human, primary, foreskin fibroblast	60
BSK_hDFCGF_ITAC_down	*CXCL11*	Regulation of gene expression, reporter binding, cytokine	Human, primary, foreskin fibroblast	60
BSK_LPS_CD40_down	*CD40*	Regulation of gene expression, reporter binding, cytokine	Human, primary vascular umbilical vein endothelium and peripheral blood mononuclear cells	60
BSK_LPS_CD69_down	*CD69*	Regulation of gene expression, reporter binding, cytokine	Human, primary vascular umbilical vein endothelium and peripheral blood mononuclear cells	60

Assay name	Gene target	Biological process target	Tissue and cell model	AC50 (µM)
BSK_LPS_IL1a_down	*IL1a*	Regulation of gene expression, reporter binding, cytokine	Human, primary vascular umbilical vein endothelium and peripheral blood mononuclear cells	60
BSK_LPS_MCP1_down	*CCL2*	Regulation of gene expression, reporter binding, cytokine	Human, primary vascular umbilical vein endothelium and peripheral blood mononuclear cells	60
BSK_MyoF_IL8_up	*IL8*	Regulation of gene expression, reporter binding, cytokine	Human, primary vascular lung fibroblast	60
LTEA_HepaRG_IL6_up	*IL6*	Regulation of TF activity, mRNA induction	Human, liver HepRG	85.8
LTEA_HepaRG_LIPC_dn	*LIPC*	Regulation of TF activity, mRNA induction	Human, liver HepRG	86.1
LTEA_HepaRG_NFKB1_up	*NFKB1*	Regulation of TF activity, mRNA induction	Human, liver HepRG	90.8

Many of the gene targets are pleiotropic and expressed in numerous tissues. Inactive null assays with PFNA can be found at: https://comptox.epa.gov/dashboard/dsstoxdb/results?search=DTXSID8031863#invitrodb-bioassays-toxcast-data.

C.2.5. Reproductive, Thyroid, and Developmental Pathway Results

In vitro HTS assays for the ER and AR pathways are intended to target the receptor at multiple points, including receptor binding, coactivator recruitment, gene transcription, and protein production. Assays found to be active for PFNA targeting the ER and AR pathways included those targeting effects on mRNA transcript levels and antagonist transactivation assays measuring suppressed protein production (see Table C-9). Antagonist assays that measured suppression of protein production also included viability readouts measuring nonspecific interference and cytotoxicity. As described in Noyes et al. (2019), in vitro HTS assays for the thyroid pathway are aimed at multiple molecular targets in the thyroid system. Endpoints with positive hits involved PFNA competitive binding with transthyretin (TTR), weak interference with thyroid peroxidase (TPO) activity, and antagonism of the thyroid hormone receptor (TR) as measured by suppressed protein production. There were also a limited number of active hit assays for developmental toxicity using zebrafish, rat cortical tissue, and human HepG2 cells.

Table C-9. ToxCast in vitro HTS assays aimed at endocrine and developmental targets that were identified as "active" hits for PFNA with associated half-maximal activity concentration (AC50) values

Assay name	Gene target	Biological process target	Tissue and cell model	AC50 (µM)
Estrogen receptor pathway				
NVS_NR_mERa	*Esr1*	Receptor binding	Mouse, cell-free	0.707
ATG_ERE_CIS_up	*Esr1*	Regulation of TF activity, mRNA induction	Human, liver HepG2	11.71
ATG_ERa_TRANS_up	*ESR1*	Regulation of TF activity, mRNA induction	Human, liver HepG2	21.4
Tox21_ERa_BLA_Antagonist_ratio	*ESR1*	Regulation of TF activity, inducible reporter	Human, kidney HEK293T	23.5
Tox21_ERb_BLA_Antagonist_ratio	*ESR2*	Regulation of TF activity, inducible reporter	Human, kidney HEK293T	26.7
Tox21_ERR_antagonist	*ESRRA*	Regulation of TF activity, inducible reporter	Human, kidney ERR-HEK293T	31.4
CCTE_Deisenroth_AIME_384WELL_CTox_Active_dn	N/A	regulation or estrogen receptor activity, inducible reporter (also loss of viability)	Human, mammary, VM7Luc4E2	105.7
CCTE_Deisenroth_AIME_384WELL_CTox_Inactive_dn	N/A	regulation or estrogen receptor activity, inducible reporter (also loss of viability)	Human, mammary, VM7Luc4E2	112.2
Androgen receptor pathway				
NVS_NR_hAR	AR	Receptor binding	Human, cell-free	7.73
NVS_NR_rAR	AR	Receptor binding	Rat, cell-free	27.4
ACEA_AR_antagonist_80hr	AR	Cell proliferation, growth reporter	Human, prostate 22Rv1	35.8
Thyroid pathway				
CCTE_GLTED_hTTR_dn	*TTR*	Receptor binding, T4 and transthyretin	Human, cell free	0.46
CCTE_Simmons_AUR_TPO_dn	Tpo	Regulation of catalytic activity, enzyme reporter, thyroperoxidase	Rat thyroid, tissue-based	41.2
CCTE_GLTED_hDIO2_dn	*Dio2*	Regulation of catalytic activity, enzyme reporter,	Human, cell free HEK293	63.2
TOX21_TR_LUC_GH3_Antagonist[a]	Thrb	Regulation of TF activity, inducible reporter	Rat, pituitary GH3	71.7
CCTE_GLTED_hIYD_dn	*hIYD*	Regulation of catalytic activity, enzyme reporter	Human, cell free	86.4
CCTE_GLTED_xIYD_dn	*xIYD*	Regulation of catalytic activity, enzyme reporter	Human, cell free	96.6

Assay name	Gene target	Biological process target	Tissue and cell model	AC50 (µM)
CCTE_GLTED_hTBG_dn	*hTBG*	Regulation of catalytic activity, enzyme reporter	Human, cell free	98.2
CCTE_GLTED_hTPO_dn	*hTPO*	Regulation of catalytic activity, enzyme reporter	Human, cell free	204.4
LTEA_HepaRG_THRSP_dn	*THRSP*	Regulation of TF activity, mRNA induction	Human, liver, HepRG	209.6
Developmental toxicity				
CCTE_Shafer_MEA_dev_network_spike_number_up	N/A	Neuronal transmission	Rat, cortical	7.99
ATG_Pax6_CIS_up	*PAX6*	Pleiotropic regulator of TF activity, including tissue development and neurogenesis (ocular, olfactory, endocrine glands)	Human, liver, HepG2	54.22
CCTE_Padilla_ZF_144hpf_TERATOSCORE	N/A	Embryonic development; morphometry	Zebrafish embryo	62.67

Inactive null assays with PFNA can be found at:
https://comptox.epa.gov/dashboard/chemical/details/DTXSID8031863.
[a]ToxCast reports assay to be not optimized; results interpreted with caution.

C.2.6. Active Hits for Putative Cell Signaling Pathways and Assay Performance

In vitro HTS assays targeting putative cell signaling pathways and designed for evaluating in vitro assay performance are summarized in Tables C-10 and C-11, respectively.

Table C-10. Putative cell signaling in vitro HTS assays identified as "active" hits with half-maximal activity concentration (AC50) values for PFNA

HTS assay	Intended target family	AC50 (µM)
NVS_ENZ_hPTPN1_Activator[a]	Phosphatase	0.88
BSK_KF3CT_MMP9_down	Protease	7
NVS_ENZ_hTie2	Kinase	7.24
NVS_GPCR_hTXA2	GPCR	8.31
NVS_ENZ_hBACE	Protease	11.04
ATG_NRF2_ARE_CIS_up	DNA binding	12.12
NVS_GPCR_hAdoRA2a	GPCR	13.43
ATG_AP_1_CIS_up	DNA binding	13.50
NVS_ENZ_hAurA	Kinase	15.55
NVS_GPCR_h5HT5A	GPCR	18.36
BSK_BE3C_tPA_down	Protease	20
BSK_BF4T_tPA_down	Protease	20

HTS assay	Intended target family	AC50 (µM)
BSK_LPS_PGE2_down	GPCR	20
BSK_MyoF_CollagenI_down	Cell adhesion molecule	20
BSK_MyoF_CollagenIV_up	Cell adhesion molecule	20
NVS_ENZ_hPTPRB	Phosphatase	21.30
TOX21_ARE_BLA_agonist_ratio	DNA binding	24.4
ATG_TGFb_CIS_up	Growth factor	26.20
NVS_ENZ_hAMPKa1	Kinase	26.45
NVS_ENZ_hTrkA	Kinase	28.16
NVS_GPCR_gLTB4	GPCR	28.94
ATG_TCF_b_cat_CIS_dn[a]	DNA binding	31.53
NVS_GPCR_hAdra2C	GPCR	32.41
NVS_ENZ_hPTPN9	Phosphatase	32.74
LTEA_HepaRG_PDK4_up	Kinase	32.97
LTEA_HepaRG_BID_up	Cell cycle	34.60
ATG_NURR1_TRANS_up	Regulation of TF activity, inducible reporter	35.52
ATG_p53_CIS_dn[a]	DNA binding	35.52
LTEA_HepaRG_KRT19_up	Filaments	36.72
ATG_RORE_CIS_up	Nuclear receptor	36.96
ATG_ISRE_CIS_dn[a]	DNA binding	39.64
BSK_BE3C_uPA_down	Protease	40
NVS_ENZ_hNEK2	Kinase	40.91
LTEA_HepaRG_TGFB1_up	Growth factor	41.73
LTEA_HepaRG_BCL2_up	Cell cycle	41.84
ATG_HIF1a_CIS_up	DNA binding	42.61
LTEA_HepaRG_ABCB1_up	Transporter	43.13
LTEA_HepaRG_MIR122_dn	microRNA	44.42
LTEA_HepaRG_GADD45A_up	Cell cycle	44.43
LTEA_HepaRG_GCLC_up	Ligase	46.10
ATG_VDRE_CIS_up	Nuclear receptor	47.16
LTEA_HepaRG_GADD45B_up	Mutagenicity response	47.56
LTEA_HepaRG_BAX_up	Cell cycle	50.85
LTEA_HepaRG_ABCG2_up	Transporter	51.31
ATG_EGR_CIS_up	DNA binding	54.01
ATG_MRE_CIS_up	DNA binding	54.07
ATG_Pax6_CIS_up	Regulation of TF activity, mRNA induction	54.22

HTS assay	Intended target family	AC50 (µM)
LTEA_HepaRG_CCND1_up	Cell cycle	56.53
LTEA_HepaRG_XBP1_up	DNA binding	58.83
BSK_BE3C_Keratin818_down	Cell adhesion molecules	60
BSK_BE3C_MMP9_down	Protease	60
BSK_BF4T_Keratin818_down	Cell adhesion molecules	60
BSK_BF4T_MMP1_down	Protease	60
BSK_BF4T_uPA_down	Protease	60
BSK_3C_MCP1_down	Cytokine/chemokine	60
BSK_3C_TissueFactor_down	Cytokine	60
BSK_SAg_MCP1_down	Cytokine/chemokine	60
BSK_IMphg_ESelectin_down	Cell adhesion molecules	60
BSK_IMphg_SRB_down	Cell cycle	60
BSK_IMphg_VCAM1_down	Cell adhesion molecules	60
BSK_KF3CT_PAI1_down	Cytokine	60
BSK_BE3C_MMP1_down	Protease	60
BSK_LPS_SRB_down	Cell cycle	60
BSK_LPS_VCAM1_down	Cell adhesion molecules	60
BSK_MyoF_ACTA1_down	Cell adhesion molecules	60
BSK_MyoF_CollagenIII_down	Cell adhesion molecules	60
BSK_3C_uPAR_down	Cytokine	60
BSK_BF4T_MMP3_down	Protease	60
BSK_BF4T_MMP9_down	Protease	60
BSK_BF4T_PAI1_down	Cytokine	60
LTEA_HepaRG_JUN_up	DNA binding	60.98
LTEA_HepaRG_HGF_dn	Growth factor	62.76
LTEA_HepaRG_KCNK1_up	Ion channel	62.88
LTEA_HepaRG_HSPA1A_up	DNA binding	
LTEA_HepaRG_FOXO3_up	DNA binding	64.43
LTEA_HepaRG_LPL_up	Esterase	65.84
LTEA_HepaRG_TGFA_up	Growth factor	69.98
LTEA_HepaRG_EZR_up	Membrane protein	71.43
ATG_HSE_CIS_up	DNA binding	71.44
TOX21_p53_BLA_p5_ratio	DNA binding	71.54
LTEA_HepaRG_SLC22A1_dn	Transporter	71.65
LTEA_HepaRG_ALPP_dn	Phosphatase	74.75

HTS assay	Intended target family	AC50 (µM)
LTEA_HepaRG_GADD45G_up	Mutagenicity response	75.09
LTEA_HepaRG_MMP10_up	Protease	81.36
LTEA_HepaRG_MYC_up	DNA binding	82.92
LTEA_HepaRG_HMGCS2_dn	Lyase	84.67
LTEA_HepaRG_IGF1_dn	Growth factor	84.72
LTEA_HepaRG_ICAM1_up	Cell adhesion molecules	85.12
LTEA_HepaRG_EGR1_up	DNA binding	85.37
LTEA_HepaRG_FMO3_dn	Oxidoreductase	85.41
LTEA_HepaRG_TP53_up	DNA binding	85.72
LTEA_HepaRG_CAT_dn	Catalase	87.25
LTEA_HepaRG_SULT2A1_dn	Transferase	88.18
TOX21_p53_BLA_p1_ratio	DNA binding	88.46
LTEA_HepaRG_CDKN1A_up	Cell cycle	89.12
LTEA_HepaRG_ABCC2_dn	Transporter	91.75
LTEA_HepaRG_NQO1_dn	Oxidoreductase	95.69
LTEA_HepaRG_BCL2L11_up	Cell cycle	100.28
APR_HepG2_p53Act_72h_up	DNA binding	107.82
APR_HepG2_P-H2AX_72h_up	DNA binding	109.56
APR_HepG2_CellCycleArrest_24h_dn	Cell cycle	110.39
APR_HepG2_CellCycleArrest_72h_dn	Cell cycle	110.71
ATG_Xbp1_CIS_up	DNA binding	111.02
APR_HepG2_MitoticArrest_72h_up	Cell cycle	111.69
APR_HepG2_MitoticArrest_24h_up	Cell cycle	112.91
APR_HepG2_CellLoss_72h_dn	Cell cycle	113.79
APR_HepG2_MitoMass_24h_dn	Cell morphology	115.35
APR_HepG2_p53Act_24h_up	DNA binding	124

Inactive null assays with PFNA can be found at:
https://comptox.epa.gov/dashboard/chemical/details/DTXSID8031863.
[a]ToxCast reports assay to be not optimized; results interpreted with caution.

C.2.7. Active Hits for Assay Performance (e.g., Cell Viability, Artifacts)

Table C-11. In vitro HTS assays identified as "active" hits for performance with half-maximal activity concentration (AC50) values for PFNA

HTS assay	Intended target family	AC50 (µM)
TOX21_RT_HEK293_FLO_32hr_viability	Viability reporter	0.41
TOX21_RXR_BLA_Agonist_ch2	Regulation of TF activity, artifact detection	4.96
TOX21_ERb_BLA_Agonist_viability	Viability reporter	13.26
TOX21_HRE_BLA_Agonist_viability	Viability reporter	14.24
TOX21_ARE_BLA_Agonist_ch2	Regulation of TF activity, artifact detection	19.13
TOX21_ERb_BLA_Antagonist_viability	Viability reporter	19.73
BSK_hDFCGF_Proliferation_down	Viability reporter	20
BSK_IMphg_SRB.Mphg_down	Viability reporter	20
TOX21_ERa_BLA_Antagonist_ch2	Regulation of TF activity, artifact detection	22.85
TOX21_RT_HEPG2_GLO_16hr_ctrl_viability	Viability reporter	24.71
TOX21_RT_HEPG2_GLO_08hr_ctrl_viability	Viability reporter	24.71
TOX21_RT_HEPG2_GLO_00hr_ctrl_viability	Viability reporter	24.87
TOX21_RT_HEPG2_GLO_24hr_ctrl_viability	Viability reporter	24.92
TOX21_RT_HEPG2_GLO_32hr_ctrl_viability	Viability reporter	25.14
ACEA_AR_antagonist_AUC_viability	Viability reporter	28.78
ACEA_AR_agonist_AUC_viability	Viability reporter	32.22
TOX21_ERb_BLA_Antagonist_ch1	Regulation of TF activity, artifact detection	38.90
TOX21_p53_BLA_p4_ch1	Regulation of TF activity, artifact detection	43.58
TOX21_p53_BLA_p3_viability	Viability reporter	45.35
TOX21_p53_BLA_p4_viability	Viability reporter	45.45
TOX21_p53_BLA_p2_ch1	Regulation of TF activity, artifact detection	47.15
TOX21_p53_BLA_p3_viability	Viability reporter	45.35
TOX21_p53_BLA_p4_viability	Viability reporter	45.45
TOX21_p53_BLA_p2_ch1	Regulation of TF activity, artifact detection	47.15
LTEA_HepaRG_GADD45B_up	Regulation of TF activity, artifact detection, cell cycle	47.56
TOX21_p53_BLA_p3_ch1	Regulation of TF activity, artifact detection	48.90
TOX21_p53_BLA_p1_viability	Cell viability	58.81
TOX21_ERb_BLA_Antagonist_ch2	Regulation of TF activity, artifact detection	61.30
TOX21_p53_BLA_p1_ch1	Regulation of TF activity, artifact detection	64.07
TOX21_ARE_BLA_agonist_viability	Cell viability	66.69
TOX21_p53_BLA_p5_ch2	Regulation of TF activity, artifact detection	73.65

HTS assay	Intended target family	AC50 (µM)
TOX21_p53_BLA_p2_viability	Viability reporter	73.68
CCTE_Simmons_CellTiterGLO_HEK293T	Viability reporter	73.74
TOX21_p53_BLA_p1_ch2	Regulation of TF activity, artifact detection	84.63
LTEA_HepaRG_LDH_cytotoxicity	Viability reporter	87.44
APR_HepG2_CellLoss_24h_dn	Viability reporter	105.85
ACEA_ER_AUC_viability	Viability reporter	199

Inactive null assays with PFNA can be found at:
https://comptox.epa.gov/dashboard/chemical/details/DTXSID8031863.

APPENDIX D. BENCHMARK DOSE MODELING RESULTS

This appendix provides technical detail on dose-response evaluation and determination of PODs for relevant toxicological endpoints. The endpoints are modeled using EPA's Benchmark Dose Software (BMDS, Version 3.2). Sections D.1 (human data modeling) and Section D.2 (animal data modeling) describe the common practices used in evaluating the model fit and selecting the appropriate model for determining the POD, as outlined in the *Benchmark Dose Technical Guidance* (U.S. EPA, 2012). The files related to these analyses are available in HERO (Ru and White, 2024).

D.1. BENCHMARK DOSE MODELING SUMMARY OF HUMAN STUDIES EVALUATING DECREASED ANTIBODY CONCENTRATIONS, BIRTH WEIGHT, AND LIVER ENZYMES

D.1.1. Benchmark Dose Modeling Approaches

The endpoints selected for benchmark dose (BMD) modeling include decreased serum antibody concentrations for tetanus and diphtheria (Budtz-Jørgensen and Grandjean, 2018a; Grandjean et al., 2012), decreased birth weight (Sagiv et al., 2018; Manzano-Salgado et al., 2017; Starling et al., 2017; Valvi et al., 2017), and increased serum ALT (Kim et al., 2023b; Nian et al., 2019). The internal doses reported in the human studies were used in the BMD modeling and then, as appropriate, converted to human equivalent doses (HEDs; see Section 5.2.1).

D.1.2. Results for Childhood PFNA Concentrations and Subsequent Childhood Antibody Concentrations

As noted in Section 5.1, the available evidence ***suggests***, but is not sufficient to infer, that PFNA exposure may cause immune effects in humans given sufficient exposure conditions. However, while a dose-response assessment is typically not conducted for health effect judgments of "***evidence suggests***," when the evidence base includes at least one well-conducted study, quantitative analysis may still be useful for some purposes such as providing a sense of the magnitude and uncertainty of estimates for health effects of concern, informing responses in potentially susceptible populations, or setting research priorities (U.S. EPA, 2020, 2005). For this assessment, the ***suggestive evidence*** of immunosuppression in children was modeled by EPA to compare with other PFNA PODs and to inform the UF given that this effect is observed with other PFAS (e.g., PFDA, PFHxS, PFOA, PFOS).

Overall, due to the poor fits for all the modeling approaches that were attempted for immune effects, the BMDs and BMDLs presented below were not interpreted as reliable and thus

were not represented as PODs in the Toxicological Review. This is consistent with the weaker pattern of effects on antibody levels for PFNA that has been observed for other PFAS (see Section 3.2.3). Thus, the immune effects data did not ultimately inform any other dose-response decisions, including UF selection, but are presented for completeness. However, the absence of an observed effect of PFNA in these data does provide an important piece of information as it effectively rules out PFNA as a potential confounder of the observed immune effects of other PFAS; this is especially relevant to the interpretation of the observed immune effects of PFDA, which was found to be highly correlated with PFNA ($\rho = 0.78$; (Grandjean et al., 2012)). The BMD modeling results from epidemiological studies of decreased anti-tetanus and anti-diphtheria antibody concentrations and birth weight are presented as follows.

Modeling Results for Decreased Tetanus Antibody Concentrations at 7 Years of Age and PFNA Measured at 5 Years of Age

Budtz-Jørgensen and Grandjean (2018a) fit multivariate models of PFNA measured at age 5 years against $\log_2$-transformed anti-tetanus antibody concentrations measured at the 7-year-old examination, controlling for sex, exact age at the 7-year-old examination, and booster type at age 5 years. Models were evaluated with additional control for PFOS (as $\log_2$[PFOS]) and PFOA (as $\log_2$[PFOA]) and without PFOS and PFOA. Three model shapes were evaluated by Budtz-Jørgensen and Grandjean (2018a) using likelihood ratio tests: a linear model, a piecewise-linear model with a knot at the median PFNA concentration, and a logarithmic function. The logarithmic functions did not fit better than the piecewise-linear functions (Budtz-Jørgensen and Grandjean, 2018a). The piecewise-linear model did not fit better than the linear model for the PFNA exposure without adjustment for PFOS and PFOA using a likelihood ratio test ($p = 0.27$; see Budtz-Jørgensen and Grandjean (2018a) Table 3) or for the model that did adjust for PFOS and PFOA ($\log_2$[PFOS] and $\log_2$[PFOA]) ($p = 0.46$).

Table D-1 summarizes the results from Budtz-Jørgensen and Grandjean (2018a) for PFNA at age 5 years and tetanus antibodies at age 7 years. These regression coefficients (β), their standard errors (SE), *p*-values, and the 90% lower confidence bounds were provided by Budtz-Jørgensen and Grandjean (2018b).

Table D-1. Results specific to the slope from the linear analyses of PFNA measured in serum at age 5 years and $\log_2$(tetanus antibody concentrations) measured at age 7 years in a single-PFAS model and in a multi-PFAS model from Budtz-Jørgensen and Grandjean (2018b)

Exposure	Model shape	PFOS and PFOA adjusted	Slope (β) per ng/mL in serum	SE(β) ng/mL in serum	Slope (β) fit	Lower bound slope (β_{LB}) per ng/mL in serum
PFNA at age 5	Linear	No	−0.227	0.161	p = 0.16	−0.493
PFNA at age 5	Linear	Yes	0.093	0.201	p = 0.64	−0.238

Interpretation of results in Table D-1

- PFNA is a non-significant predictor in the single-PFAS model (β = −0.227; p = 0.16).
- Effects of PFNA in the single-PFAS model change sign when $\log_2$[PFOS] and $\log_2$[PFOA] are included in the model (β = 0.093; p = 0.64).
- The large change in slopes for PFNA between the single-PFAS models compared to the multi-PFAS models may reflect poor model fit for PFNA, model instability due to correlated co-exposures, or potential confounding.
- Nevertheless, these data can be used to estimate a BMDL for completeness and to allow comparisons across PFAS. Given the poor fit, PODs based on the BMDLs were not advanced.

Selection of the benchmark response

The benchmark dose (BMD) approach involves dose-response modeling to obtain BMDs, i.e., dose levels corresponding to specific response levels near the low end of the observable range of the data and the lower limit of the BMD (BMDLs) to serve as potential PODs for deriving quantitative estimates below the range of observation (U.S. EPA, 2012). Selecting a BMR to estimate the BMDs and BMDLs involves making judgments about the statistical and biological characteristics of the dataset and about the applications for which the resulting BMDs and BMDLs will be used. An extra risk of 10% is recommended as a standard reporting level for quantal data for toxicological data. Biological considerations may warrant the use of a BMR of 5% or lower for some types of effects as the basis of the POD for a reference value. However, a BMR of 1% has typically been used for quantal human data from epidemiology studies (U.S. EPA, 2012), although this is more typically used for epidemiological studies of cancer mortality within large cohorts of workers that can support the statistical estimation of small BMRs.

A blood concentration for tetanus antibodies of 0.1 IU/mL is sometimes cited in the tetanus literature as a "protective level," and Grandjean et al. (2017) noted that the Danish vaccine producer Statens Serum Institut recommended the 0.1 IU/mL "cutoff" level "to determine whether

antibody concentrations could be considered protective"; Tailleur (2008) mentions the same concentration, but Galazka et al. (1993) argues:

> "The amount of circulating antitoxin needed to ensure complete immunity against tetanus is not known for certain. Establishment of a fixed level of tetanus antitoxin does not take into consideration variable conditions of production and adsorption of tetanus toxin in the anaerobic area of a wound or a necrotic umbilical stump. A given serum level could be overwhelmed by a sufficiently large dose of toxin. Therefore, there is no absolute protective level of antitoxin and protection results when there is sufficient toxin-neutralizing antibody in relation to the toxin load" (Passen and Andersen, 1986).

In the absence of a clear definition of an adverse effect for a continuous endpoint like antibody concentrations, a default BMR of 1 SD change from the control mean may be selected, as suggested in EPA's Benchmark Dose Technical Guidance (U.S. EPA, 2012). As noted above, a lower BMR can also be used if it can be justified on a biological and/or statistical basis. Figure D-1 replicates a figure in the guideline (page 23; (U.S. EPA, 2012) to show that in a control population in which 1.4% are considered to be at risk of having an adverse effect, a downward shift in the control means of 1 SD results in a ~10% extra risk of being at risk of having an adverse effect.

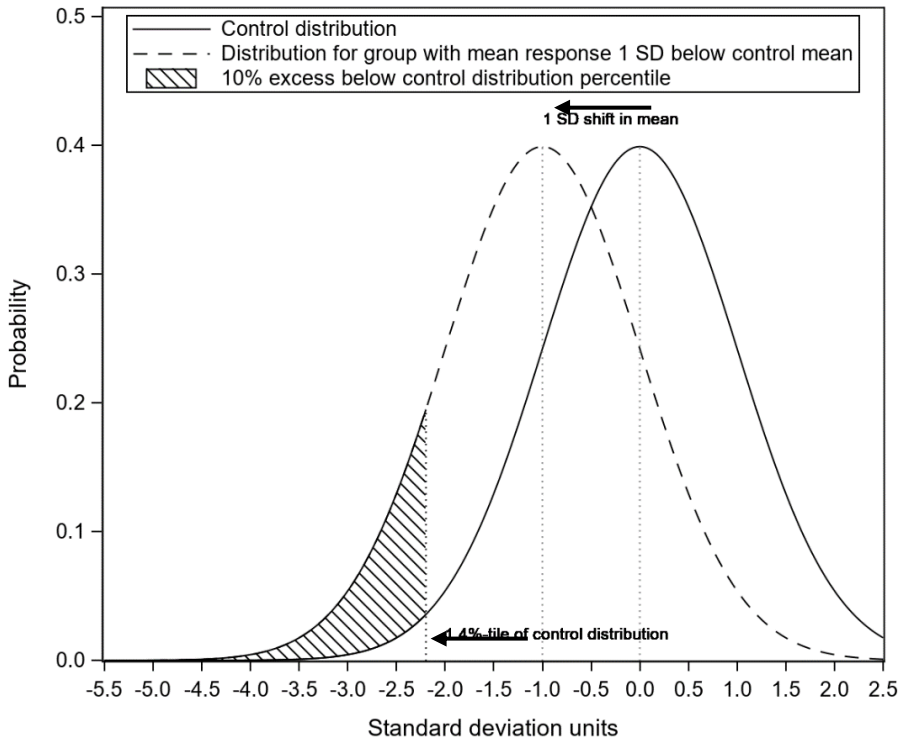

Figure D-1. Difference in population tail probabilities resulting from a one standard deviation shift in the mean from a standard normal distribution, illustrating the theoretical basis for a baseline BMR of 1 SD.

Statistically, the technical guideline additionally suggests that studies of developmental effects can support lower BMRs. Biologically, a BMR of ½ SD is a reasonable choice as anti-tetanus antibody concentrations prevent against tetanus, which is a rare but severe and sometimes fatal infection, with a case-fatality rate in the U.S. of 13% during 2001–2008 (Liang et al., 2018). The case-fatality rate can be more than 80% for early lifestage cases (Patel and Mehta, 1999). Selgrade (2007) suggests that specific immuno-toxic effects observed in children may be broadly indicative of developmental immunosuppression impacting these children's ability to protect against a range of immune hazards—which has the potential to be a more adverse effect than just a single immuno-toxic effect. Thus, decrements in the ability to maintain effective levels of tetanus antitoxins following immunization may be indicative of wider immunosuppression in these children exposed to PFNA. By contrast, a BMR of 1 SD may be more appropriate for an effect that would be considered "minimally adverse." A BMR smaller than ½ SD is generally selected for severe effects (e.g., 1% extra risk of cancer mortality); decreased antibody concentrations offer diminished protection from severe effects but are not themselves severe effects.

Following the guideline (U.S. EPA, 2012), EPA derived BMDs and BMDLs associated with a 1 SD change in the distribution of $\log_2$ (tetanus antibody concentrations), and ½ SD change in the distribution of $\log_2$(tetanus antibody concentrations). The SD of the $\log_2$(tetanus antibody concentrations) at age 7 years was estimated from the distributional data presented in Grandjean et al. (2012) as follows: the interquartile range (IQR) of the tetanus antibody concentrations at age 7 years in IU/mL was (0.65, 4.6). Log_2-tranforming these values provides the IQR in $\log_2$(IU/mL) as (−0.62, 2.20). Assuming that these $\log_2$-transformed values are reasonably represented by a normal distribution, the width of the IQR is approximately 1.35 SDs. Thus, SD = IQR/1.35, and the SD of tetanus antibodies in $\log_2$(IU/mL) is (2.20 – (−0.62))/1.35 = 2.09 $\log_2$(IU/mL). To show the impact of the BMR on these results, Table D-2 presents the BMDs and BMDLs at BMRs of ½ SD and 1 SD.

While there was not a clear definition of the size of an adverse effect for a continuous endpoint like antibody concentrations, the value of 0.1 IU/mL is sometimes cited. As a check, EPA evaluated how much extra risk would have been associated with a BMR set at a cutoff value of 0.1 IU/mL. Using the observed distribution of tetanus antibodies at age 7 years in $\log_2$(IU/mL), EPA calculated that 2.8% of those values would be below the cutoff value of 0.1 IU/mL, which is −3.32 $\log_2$(IU/mL). A BMR of ½ SD resulted in 7.9% of the values being below that cutoff, which is 5.1% extra risk, and shows that the generic guideline that a BMR of ½ SD can provide a reasonably good estimate of 5% extra risk. Figure D-2 shows an example of this.

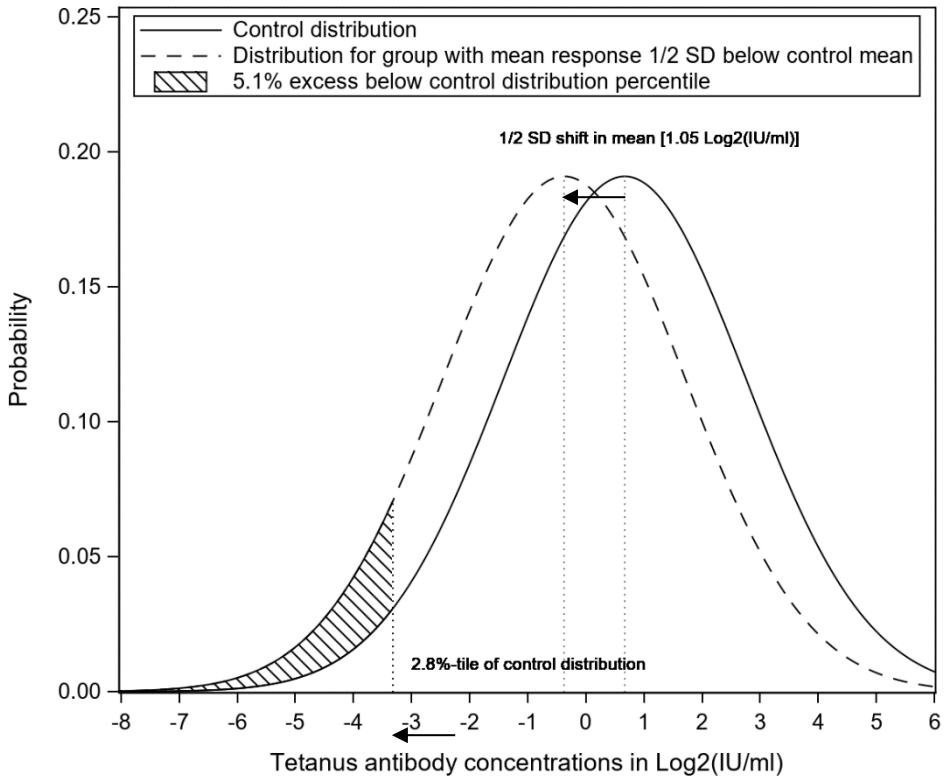

Figure D-2. Difference in population tail probabilities resulting from a ½ standard deviation shift in the mean from an estimation of the distribution of $\log_2$(tetanus antibody concentrations at age 7 years).

Table D-2. BMDs and BMDLs for effect of PFNA at age 5 years on anti-tetanus antibody concentrations at age 7 years using a BMR of ½ SD change in $\log_2$(tetanus antibodies concentration) and a BMR of 1 SD change in $\log_2$(tetanus antibodies concentration)

	Estimated without control of PFOS and PFOA		Estimated with control of PFOS and PFOA	
BMR	**BMD (ng/mL in serum) β = −0.227 per ng/mL**	**BMDL (ng/mL in serum) β_{LB} = −0.493 per ng/mL**	**BMD (ng/mL in serum) β = 0.093 per ng/mL**	**BMDL (ng/mL in serum) β_{LB} = −0.238 per ng/mL**
½ SD	4.60	2.12	–	4.40
1 SD	9.21	4.24	–	8.80

– = values cannot be determined.

BMDs and BMDLs were estimated for completeness and to allow comparisons across PFAS. Given the poor fit, PODs based on the BMDLs were not advanced.

Modeling Results for Decreased Diphtheria Antibody Concentrations at 7 Years of Age and PFNA Measured at 5 Years of Age

Budtz-Jørgensen and Grandjean (2018a) fit multivariate models of PFNA measured at age 5 years against $\log_2$-transformed anti-diphtheria antibody concentrations measured at the 7-year-old examination controlling for sex, exact age at the 7-year-old examination, and booster type at age 5 years. Models were evaluated with additional control for PFOS (as $\log_2$[PFOS]) and PFOA (as $\log_2$[PFOA]) and without PFOS and PFOA. Three model shapes were evaluated by Budtz-Jørgensen and Grandjean (2018a) using likelihood ratio tests: a linear model of PFNA, a piecewise-linear model with a knot at the median, and a logarithmic function. The logarithmic functions did not fit better than the piecewise-linear functions (Budtz-Jørgensen and Grandjean, 2018a). The piecewise-linear model did not fit better than the linear model for the PFNA exposure without adjustment for PFOS and PFOA using a likelihood ratio test (p = 0.12; see Budtz-Jørgensen and Grandjean (2018a) Table 3) or for the model that did adjust for PFOS and PFOA ($\log_2$[PFOS] and $\log_2$[PFOA]) (p = 0.40). Table D-3 summarizes the results from Budtz-Jørgensen and Grandjean (2018a) for diphtheria in this exposure window. These regression coefficients (β), their standard errors (SE), p-values, and the 90% lower confidence bounds were provided by Budtz-Jørgensen and Grandjean (2018b).

Table D-3. Results specific to the slope from the linear analyses of PFNA measured in serum at age 5 years and $\log_2$(diphtheria antibodies concentrations) measured at age 7 years in a single-PFAS model and in a multi-PFAS model from Budtz-Jørgensen and Grandjean (2018b)

Exposure	Model shape	PFOS and PFOA adjusted	Slope (β) per ng/mL in serum	SE(β) ng/mL in serum	Slope (β) fit	Lower bound slope (β_{LB}) per ng/mL in serum
PFNA at age 5	Linear	No	−0.138	0.150	p = 0.36	−0.385
PFNA at age 5	Linear	Yes	0.124	0.187	p = 0.51	−0.183

Interpretation of results in Table D-3

- PFNA is a non-significant predictor in the single-PFAS model (β = −0.138; p = 0.26).
- Effects of PFNA in the single-PFAS model change sign when $\log_2$[PFOS] and $\log_2$[PFOA] are included in the model (β = 0.124; p = 0.51).
- The large change in slopes for PFNA between the single-PFAS models compared to the multi-PFAS models may reflect poor model fit for PFNA, model instability due to correlated co-exposures, or potential confounding.

- Nevertheless, these data can be used to estimate a BMDL for completeness and to allow comparisons across PFAS. Given the poor fit, PODs based on the BMDLs were not advanced.

Selection of the benchmark response

Following the technical guideline (U.S. EPA, 2012), EPA derived BMDs and BMDLs associated with a 1 SD change in the distribution of $\log_2$(diphtheria antibody concentrations), and ½ SD change in the distribution of $\log_2$(diphtheria antibody concentrations). A blood concentration for diphtheria antibodies of 0.1 IU/mL is sometimes cited in the diphtheria literature as a "protective level," and Grandjean et al. (2017) noted that the Danish vaccine producer Statens Serum Institut recommended the 0.1 IU/mL "cutoff" level; Galazka et al. (1993) mentions the same concentration, but Galazka et al. (1993) argues:

> "However, it has also been shown that there is no sharply defined level of antitoxin that gives complete protection from diphtheria (Ipsen, 1946). A certain range of variation must be accepted; the same degree of antitoxin may give an unequal degree of protection in different persons. Other factors may influence the vulnerability to diphtheria including the dose and virulence of the diphtheria bacilli and the general immune status of the person infected (Christenson and Böttiger, 1986). Thus, an antibody concentration between 0.01 and 0.09 IU/mL may be regarded as giving basic immunity, whereas a higher titer may be needed for full protection. In some studies that used in vitro techniques, a level of 0.1 IU/mL was considered protective" *(*Cellesi et al., 1989*;* Galazka and Kardymowicz, 1989*)*.

Statistically, the technical guideline suggests that studies of developmental effects can support lower BMRs. Biologically, a BMR of ½ SD is a reasonable choice as anti-diphtheria antibody concentrations prevent against diphtheria, which is very rare in the U.S. but can cause life-threatening airway obstruction or cardiac failure (Collier, 1975). Among 13 cases reported in the U.S. during 1996–2016, no deaths were mentioned (Liang et al., 2018). However, diphtheria remains a potentially fatal disease in other parts of the world (Galazka et al. (1993) mentions a case-fatality rate of 5%–10%), and PFNA-related changes in anti-diphtheria antibody concentrations cannot be considered "minimally adverse" given the historic lethality of diphtheria in the absence of vaccination. Selgrade (2007) suggests that specific immuno-toxic effects observed in children may be broadly indicative of developmental immunosuppression impacting these children's ability to protect against a range of immune hazards—which has the potential to be a more adverse effect that just a single immuno-toxic effect.

Following the technical guideline (U.S. EPA, 2012), EPA derived BMDs and BMDLs associated with a 1 SD change in the distribution of $\log_2$(diphtheria antibody concentrations) as a standard reporting level and ½ SD change in the distribution of $\log_2$(diphtheria antibody concentrations). The SD of the $\log_2$(diphtheria antibody concentrations) at age 7 years was estimated from the distributional data presented in Grandjean et al. (2012) as follows: the interquartile range (IQR) of the diphtheria antibody concentrations at age 7 years in IU/mL was

(0.4, 1.6). Log_2-tranforming these values provides the IQR in log_2(IU/mL) as (−1.32, 0.68). Assuming that these log_2-transformed values are similar to the normal distribution, the width of the IQR is approximately 1.35 SDs; thus, SD = IQR/1.35, and the SD of diphtheria antibodies in log_2(IU/mL) is (0.68 – (−1.32))/1.35 = 1.48 log_2(IU/mL). To show the impact of the BMR on these results, Table D-4 presents the BMDs and BMDLs at BMRs of ½ SD and 1 SD.

Table D-4. BMDs and BMDLs for effect of PFNA at age 5 years on anti-diphtheria antibody concentrations at age 7 years using a BMR of ½ SD change in log_2(diphtheria antibodies concentration) and a BMR of 1 SD change in log_2(diphtheria antibodies concentration)

	Estimated without control of PFOS and PFOA		Estimated with control of PFOS and PFOA	
BMR	BMD (ng/mL in serum) β = −0.138 per ng/mL	BMDL (ng/mL in serum) β_{LB} = −0.385 per ng/mL	BMD (ng/mL in serum) β = 0.124 per ng/mL	BMDL (ng/mL in serum) β_{LB} = −0.183 per ng/mL
½ SD	5.36	1.92	–	4.03
1 SD	10.7	3.85	–	8.07

– = values cannot be determined.

BMDs and BMDLs were estimated for completeness and to allow comparisons across PFAS. Given the poor fit, PODs based on the BMDLs were not advanced.

Modeling Results for Decreased Tetanus Antibody Concentrations at 5 Years of Age and Perinatal PFNA

Budtz-Jørgensen and Grandjean (2018a) fit multivariate models of PFNA measured perinatally in maternal serum against log_2-transformed anti-tetanus antibody concentrations measured at the 5-year-old examination, controlling for sex, exact age at the 5-year-old examination, cohort, and interaction terms between cohort and sex and between cohort and age. Models were evaluated with additional control for PFOS (as log_2[PFOS]) and PFOA (as log_2[PFOA]) and without PFOS and PFOA. Three model shapes of PFNA were evaluated by Budtz-Jørgensen and Grandjean (2018a) using likelihood ratio tests: a linear model, a piecewise-linear model with a knot at the median, and a logarithmic function. The logarithmic functions did not fit better than the piecewise-linear functions Budtz-Jørgensen and Grandjean (2018a). Compared to the linear model, the piecewise-linear model did not fit better than the linear model for either the PFNA exposure without adjustment for PFOS and PFOA using a likelihood ratio test (p = 0.37; see Budtz-Jørgensen and Grandjean (2018a) Table 3) or for the model that did adjust for PFOS and PFOA (log_2[PFOS] and log_2[PFOA]) (p = 0.12).

Table D-5 summarizes the results from Budtz-Jørgensen and Grandjean (2018a) for tetanus in this exposure window. These regression coefficients (β), their standard errors (SE), p-values, and the 90% lower confidence bounds were provided by Budtz-Jørgensen and Grandjean (2018b).

Table D-5. Results of the linear analyses of PFNA measured perinatally in maternal serum and tetanus antibodies measured at age 5 years in a single-PFAS model and in a multi-PFAS model from Budtz-Jørgensen and Grandjean (2018b)

Exposure	Model shape	PFOS and PFOA adjusted	Slope (β) per ng/mL in serum	SE(β) ng/mL in serum	Slope (β) fit	Lower bound slope (β_{LB}) per ng/mL in serum
Perinatal PFNA	Linear	No	0.00676	0.204	$p = 0.97$	−0.329
Perinatal PFNA	Linear	Yes	0.293	0.245	$p = 0.23$	−0.111

Interpretation of results in Table D-5

- PFNA is a non-significant predictor in the single-PFAS model (β = 0.00676; $p = 0.97$).
- Effects are increased when $\log_2$[PFOS] and $\log_2$[PFOA] are included in the model (β = 0.293; $p = 0.23$).
- The large change in slopes for PFNA between the single-PFAS models compared to the multi-PFAS models may reflect poor model fit for PFNA, model instability due to correlated co-exposures, or potential confounding.
- Nevertheless, these data can be used to estimate a BMDL for completeness and to allow comparisons across PFAS. Given the poor fit, PODs based on the BMDLs were not advanced.

Selection of the benchmark response

Following the technical guideline (U.S. EPA, 2012), EPA derived BMDs and BMDLs associated with a 1 SD change in the distribution of $\log_2$(tetanus antibody concentrations) and ½ SD change in the distribution of $\log_2$(tetanus antibody concentrations). The SD of the $\log_2$(tetanus antibody concentrations) at age 5 years was estimated from two sets of distributional data presented from two different cohorts of 5-year-olds that were pooled in Budtz-Jørgensen and Grandjean (2018a). Grandjean et al. (2012) reported on 587 5-year-olds from the cohort of children born during 1997–2000 and in Grandjean et al. (2017) reported on 349 5-year-olds from the cohort of children born during 2007–2009. The means and SDs were computed separately and then pooled to describe the common SD. The IQR of the tetanus antibody concentrations in the earlier birth cohort at age 5 years in IU/mL was (0.1, 0.51). Log_2-tranforming these values provides the IQR in $\log_2$(IU/mL) as (−3.32, −0.97). Assuming that these $\log_2$-transformed values are similar to the normal distribution, the width of the IQR is approximately 1.35 SDs; thus, SD = IQR/1.35, and the SD of tetanus antibodies in $\log_2$(IU/mL) is (−0.97 – (−3.32))/1.35 = 1.74 $\log_2$(IU/mL). The IQR of the

tetanus antibody concentrations in the later birth cohort at age 5 years in IU/mL was (0.1, 0.3). Log_2-tranforming these values provides the IQR in log_2(IU/mL) as (−3.32, −1.74), and the SD of tetanus antibodies in log_2(IU/mL) is (−1.74 – (−3.32))/1.35 = 1.17 log_2(IU/mL). The pooled variance is a weighted sum of the independent SDs, and the pooled SD was estimated as 1.55 log_2(IU/mL).[1] To show the impact of the BMR on these results, Table D-6 presents the BMDs and BMDLs at BMRs of ½ SD and 1 SD.

Table D-6. BMDs and BMDLs for effect of PFNA measured perinatally and anti-tetanus antibody concentrations at age 5 years

	Estimated without control of PFOS and PFOA		Estimated with control of PFOS and PFOA	
BMR	BMD (ng/mL in serum) β = 0.00676 per ng/mL	BMDL (ng/mL in serum) β_{LB} = −0.329 per ng/mL	BMD (ng/mL in serum) β = 0.293 per ng/mL	BMDL (ng/mL in serum) β_{LB} = 0.111 per ng/mL
½ SD	–	2.36	–	6.95
1 SD	–	4.71	–	13.9

– = values cannot be determined.

BMDs and BMDLs were estimated for completeness and to allow comparisons across PFAS. Given the poor fit, PODs based on the BMDLs were not advanced.

Modeling Results for Decreased Diphtheria Antibody Concentrations at 5 Years of Age and Perinatal PFNA

Budtz-Jørgensen and Grandjean (2018a) fit multivariate models of PFNA measured perinatally against log_2-transformed anti-diphtheria antibody concentrations measured at the 5-year-old examination, controlling for sex and age. Models were evaluated with additional control for PFOS (as log_2[PFOS]) and PFOA (as log_2[PFOA]) and without PFOS and PFOA. Three model shapes were evaluated by Budtz-Jørgensen and Grandjean (2018a) using likelihood ratio tests: a linear model of PFNA, a piecewise-linear model with a knot at the median, and a logarithmic function. The logarithmic functions did not fit better than the piecewise-linear functions Budtz-Jørgensen and Grandjean (2018a). Compared to the linear model, the piecewise-linear model did not fit better than the linear model for either the PFNA exposure without adjustment for PFOS and PFOA using a likelihood ratio test (p = 0.06; see Budtz-Jørgensen and Grandjean (2018a) Table 3) or for the model that did adjust for PFOS and PFOA (log_2[PFOS] and log_2[PFOA]) (p = 0.37). Table D-7 summarizes the results from Budtz-Jørgensen and Grandjean (2018a) for diphtheria in this exposure window. These regression coefficients (β), their standard errors (SE), p-values, and the 90% lower confidence bounds were provided by Budtz-Jørgensen and Grandjean (2018b).

[1]Pooled variance for tetanus in 5-year-olds = [(502−1)(1.74)^2+ (298−1)(1.17)^2]/[502+298−2] = 2.41. The pooled SD is the square root of 2.41 which is 1.55 log2(IU/mL).

Table D-7. Results of the analyses of PFNA measured perinatally in maternal serum and diphtheria antibodies measured at age 5 years in a single-PFAS model and in a multi-PFAS model from Budtz-Jørgensen and Grandjean (2018b)

Exposure	Model shape	PFOS and PFOA adjusted	Slope (β) per ng/mL in serum	SE(β)	Slope (β) fit	Lower bound slope (β_{LB}) per ng/mL in serum
Perinatal PFNA	Linear	No	−0.0522	0.215	p = 0.81	−0.406
Perinatal PFNA	Linear	Yes	0.486	0.257	p = 0.06	0.0622

Interpretation of results in Table D-7

- PFNA is a non-significant predictor in the single-PFAS model (β = −0.0522; p = 0.81).
- Effects of PFNA in the single-PFAS model change sign when $\log_2$[PFOS] and $\log_2$[PFOA] are included in the model (β = 0.486; p = 0.06).
- The large change in slopes for PFNA between the single-PFAS models compared to the multi-PFAS models may reflect poor model fit for PFNA, model instability due to correlated co-exposures, or potential confounding.
- Nevertheless, these data can be used to estimate a BMDL for completeness and to allow comparisons across PFAS. Given the poor fit, PODs based on the BMDLs were not advanced.

Selection of the benchmark response

Following the technical guideline (U.S. EPA, 2012), EPA derived BMDs and BMDLs associated with a 1 SD change in the distribution of $\log_2$(diphtheria antibody concentrations) as a standard reporting level and ½ SD change in the distribution of $\log_2$(diphtheria antibody concentrations). The SD of the $\log_2$(diphtheria antibody concentrations) at age 5 years was estimated from two sets of distributional data presented from two different birth cohorts of 5-year-olds that were pooled in Budtz-Jørgensen and Grandjean (2018a). Grandjean et al. (2012) reported on 587 5-year-olds from the cohort of children born during 1997–2000, and Grandjean et al. (2017) reported on 349 5-year-olds from the cohort of children born during 2007–2009. The means and SDs were computed separately and then pooled to describe the common SD. The IQR of the diphtheria antibody concentrations in the earlier birth cohort at age 5 years in IU/mL was (0.05, 0.4). Log_2-tranforming these values provides the IQR in $\log_2$(IU/mL) as (−4.32, −1.32). Assuming these $\log_2$-transformed values are similar to the normal distribution, the width of the IQR is approximately 1.35 SDs; thus, SD = IQR/1.35, and the SD of diphtheria antibodies in $\log_2$(IU/mL) is (−1.32 – (−4.32))/1.35 = 2.22 $\log_2$(IU/mL). The IQR of the diphtheria antibody concentrations in the

later birth cohort at age 5 years in IU/mL was (0.1, 0.3). Log_2-tranforming these values provides the IQR in log_2(IU/mL) as (−3.32, −1.74), and the SD of diphtheria antibodies in log_2(IU/mL) is (−1.74 – (−3.32))/1.35 = 1.17 log_2(IU/mL). The pooled variance is a weighted sum of the independent SDs, and the pooled SD was estimated as 1.90 log_2(IU/mL).[2] To show the impact of the BMR on these results, Table D-8 presents the BMDs and BMDLs at BMRs of ½ SD and 1 SD.

Table D-8. BMDs and BMDLs for effect of PFNA measured perinatally and anti-diphtheria antibody concentrations at age 5 years

	Estimated without control of PFOS and PFOA		Estimated with control of PFOS and PFOA	
BMR	BMD (ng/mL in serum) β = −0.0522 per ng/mL	BMDL (ng/mL in serum) β_{LB} = −0.406 per ng/mL	BMD (ng/mL in serum) β = 0.486 per ng/mL	BMDL (ng/mL in serum) β_{LB} = 0.0622 per ng/mL
½ SD	18.2	2.34	–	-
1 SD	36.4	4.68	–	-

– = values cannot be determined.

BMDs and BMDLs were estimated for completeness and to allow comparisons across PFAS. Given the poor fit, PODs based on the BMDLs were not advanced.

D.1.3. Mean Decreased Birth Weight Using Individual Study Results

Five high confidence studies report decreased birth weight in infants whose mothers were exposed to PFNA (Wikström et al., 2020; Sagiv et al., 2018; Manzano-Salgado et al., 2017; Starling et al., 2017; Valvi et al., 2017), providing regression (β) coefficients as the measure of effect. Essentially, these studies have already performed a dose-response analysis (i.e., the regression analysis) and have accounted for relevant confounding factors in that analysis. Further, EPA does not have access to the individual-level data that would be necessary to model the data from these studies with standard BMDS-based approaches. Therefore, the regression coefficients reported in these studies were used to calculate BMD and BMDL values.

All five studies report their exposure metric in units of ng/mL. Two studies report the β coefficients per log_2(ng/mL), two studies report the β coefficient per ln(ng/mL), and one study reports the β coefficients per interquartile range (IQR) increase in ng/mL, along with 95% CIs estimated from linear regression models. The logarithmic transformation of exposure yields a negative value for low numbers, which can result in implausible results from dose-response modeling (i.e., estimated risks are negative and unable to determine the responses at zero exposure). This analysis first re-expresses the reported β coefficients in terms of per ng/mL, if necessary, according to Dzierlenga et al. (2020). Then, it uses the re-expressed β and lower limit on

[2]Pooled variance for diphtheria in 5-year-olds = [(502−1)(2.22)^2+ (298−1)(1.17)^2]/[502+2,982] = 3.60. The pooled SD is the square root of 2.41, which is 1.90 log_2(IU/mL).

the confidence interval to estimate BMD and BMDL values using the general equation $y = mx + b$, where y is birth weight and x is exposure, substituting the re-expressed β values from these studies for m. The intercept b represents the baseline value of birth weight in an unexposed population and it can be estimated through $\overline{y} = m\overline{x} + b$ using an average birth weight from an external population as $\overline{y}$, an average exposure as $\overline{x}$, and re-expressed β from the studies as m.

The CDC WONDER site (https://wonder.cdc.gov/natality.html) provides vital statistics for babies born in the United States. There were 3,791,712 all live births in the United States in 2018, according to final natality data. The mean and standard deviation of birth weight was 3,261.6 ± 590.7 g (7.19 ± 1.30 lb), with 8.27% of live births falling below the public health definition of low birth weight (i.e., 2,500 g or 5.5 lb). The full natality data for the U.S. data on birth weight were used as they are more relevant for deriving toxicity values for the U.S. general population than the study-specific birth weight data. In addition, the CDC WONDER database may be queried to find the exact percentage of the population falling below the cutoff value for clinical adversity. America's Children and the Environment (ACE) Biomonitoring on Perfluorochemicals (https://www.epa.gov/americaschildrenenvironment/ace-biomonitoring-perfluorochemicals-pfcs#B6) provides the median blood serum levels of PFNA of 0.4 ng/mL in 2015–2016 in women ages 16 to 49, using National Health and Nutrition Examination Survey (NHANES) as a data source. These values are assumed to be representative of women of reproductive age and are subsequently used in the estimation of BMD and BMDL values from the available five epidemiological studies.

Valvi et al. (2017) reported a β coefficient of −42.0 g (95% CI: −108.0, 25.0) per $\log_2$ (ng/mL) increase for the association between birth weight and maternal PFNA serum concentrations (collected during 34 weeks of pregnancy) in a Denmark cohort, based on multiple linear regression analysis. The reported β coefficient was re-expressed in terms of per ng/mL according to Dzierlenga et al. (2020). Given the reported study-specific median (0.59 ng/mL) and IQR (0.46–0.79 ng/mL) of the exposure from Valvi et al. (2017), EPA estimated the distribution of exposure by assuming the exposure follows a log-normal distribution with mean and standard deviation as:

$$\mu = ln(q_{50}) = ln(0.59) = -0.53 \quad \text{(D-1)}$$

$$\sigma = ln(q_{75}/q_{25})/1.349 = ln(0.79/0.46)/1.349 = 0.40 \quad \text{(D-2)}$$

Then, EPA estimated the 25th–75th percentiles at 10 percentile intervals of the exposure distribution and corresponding responses of reported β coefficient. The re-expressed β coefficient is determined by minimizing the sum of squared differences between the curves generated by the re-expressed β and the reported β. Doing so results in a re-expressed β coefficient of −101.0 g (95% CI: −259.8, 60.1) per ng/mL PFNA.

Typically, for continuous data, the preferred definition of the BMR will have a basis for what constitutes a minimal level of change in the endpoint that is biologically significant. For birth weight, there is no accepted percent change that is considered adverse. However, there is a clinical

measure for what constitutes an adverse response: Babies born weighing less than 2,500 g (5.5 lb) are considered to have low birth weight; further, low birth weight is associated with a wide range of health conditions throughout life (Tian et al., 2019a; Reyes and Mañalich, 2005; Hack et al., 1995). Given this clinical cutoff for adversity and the fact that 8.27% of all live births in the United States in 2018 fell below this value, the hybrid approach can be used to define the BMR. The hybrid approach is advantageous in that it harmonizes the definition of the BMR for continuous data with that for dichotomous data.[3] Essentially, the hybrid approach involves the estimation of the dose that increases the percentage of responses falling below (or above) some cutoff for adversity in the tail of the response distribution. Application of the hybrid approach requires the selection of an extra risk value for BMD estimation. In the case of birth weight, an extra risk of 5% is selected given that this level of response is typically used when modeling developmental responses from toxicology studies and given that low birthweight confers increased risk for adverse health effects throughout life, thus supporting a BMR lower than the standard BMR of 10% extra risk.

Therefore, given a background response and a BMR = 5% extra risk, the BMD would be the dose that results in 12.86% of the responses falling below the 2,500 g cutoff value:

$$Extra\ Risk(ER) = (P(d) - P(0)) \,/\, (1 - P(0)) \quad \text{(D-3)}$$

$$P(d) = ER(1 - P(0)) + P(0) = 0.05(1 - 0.0827) + 0.0827 = 0.1286 \quad \text{(D-4)}$$

Using the mean birth weight for all births in the United States of 3,261.6 g with a standard deviation of 590.7 g, the analysis calculates the mean response that would be associated with the 12.86th percentile of the distribution falling below 2,500 g. In this case, the mean birth weight would be 3,169.2 g. Given the median exposure of 0.40 ng/mL from ACE Biomonitoring on Perfluorochemicals as $\overline{x}$, the mean birth weight in the U.S. as $\overline{y}$, and the re-expressed β as the m term, the intercept b can be estimated as:

$$b = \overline{y} - m\overline{x} = 3{,}261.6\ g - \left(-101\ g\left(\frac{ng}{mL}\right)^{-1}\right) 0.40\frac{ng}{mL} = 3{,}302.1\ g \quad \text{(D-5)}$$

The BMD was calculated by rearranging the equation $y = mx + b$ and solving for x, using 3,302.1 g for the b term and −101.0 for the m term. Doing so results in a value of 1.31 ng/mL:

$$x = (y - b)/m = (3{,}169.2\ g - 3{,}302.1\ g)/(-101\ g\left(\frac{ng}{mL}\right)^{-1}) = 1.31\ ng/mL \quad \text{(D-6)}$$

To calculate the BMDL, the method is essentially the same except that the lower limit (LL) on the β coefficient (−259.8) is used for the m term. However, Valvi et al. (2017) reports a two-

[3]While the explicit application of the hybrid approach is not commonly used in IRIS dose/concentration/exposure-response analyses, the more commonly used SD-definition of the BMR for continuous data is simply one specific application of the hybrid approach. The SD-definition of the BMR assumes that the cutoff for adversity is the 1.4th percentile of a normally distributed response and that shifting the mean of that distribution by one standard deviation approximates an extra risk of 10%.

sided 95% confidence interval for the β coefficient, meaning that the lower limit of that confidence interval corresponds to a 97.5% one-sided lower limit. The BMDL is defined as the 95% lower limit of the BMD (i.e., corresponds to a two-sided 90% confidence interval), so the corresponding lower limit on the β coefficient needs to be calculated before calculating the BMDL. First, the standard error of the β coefficient can be calculated as:

$$SE = \frac{Upper\ Limit - Lower\ Limit}{3.92} = \frac{60.1\ g(\frac{ng}{mL})^{-1} - \left(-259.8\ g(\frac{ng}{mL})^{-1}\right)}{3.92} = 81.6\ g(\frac{ng}{mL})^{-1} \quad \text{(D-7)}$$

Then the corresponding 95% one-sided lower bound on the β coefficient can be calculated as:

$$95\%\ one\ sided\ LL = \beta - 1.645\big(SE(\beta)\big) = -101\ g(\frac{ng}{mL})^{-1} - 1.645\left(81.6\ g(\frac{ng}{mL})^{-1}\right) = -235.3 g(\frac{ng}{mL})^{-1} \quad \text{(D-8)}$$

Using this value for the m term results in a BMDL value of 0.56 ng/mL maternal serum concentration.

Sagiv et al. (2018) reported a β coefficient of −28.2 g (95% CI: −52.0, −4.4) per IQR increase in PFNA (ng/mL), corresponding to a β coefficient of −56.4 g (95% CI: −104.0, −8.8) per ng/mL increase, for the association between birth weight and maternal PFNA serum concentrations (collected during 5 to 19 weeks of pregnancy with a median of 9 weeks) in a U.S. cohort. The intercept b is 3,284.2 g based on the β coefficient of −56.4 g per ng/mL. A BMD of 2.04 ng/mL was calculated from Sagiv et al. (2018) using the same approach as above with the same values for the mean birth weight in the U.S. general population. To calculate the BMDL, the same procedure as above is used to calculate the corresponding 95% one-sided lower limit for the β coefficient from the lower limit on the 95% two-sided confidence interval of −104.0 g per ng/mL. Using the corresponding lower limit (−96.4 g per ng/mL), a BMDL of 1.19 ng/mL is calculated.

Manzano-Salgado et al. (2017) reported a β coefficient of −10.3 g (95% CI: −38.1, 17.6) per $\log_2$ (ng/mL) for the association between birth weight and maternal PFNA serum concentrations (collected during the first trimester of pregnancy with a mean of 12.3 weeks) in a Spanish cohort. Given the median (0.66 ng/mL) and SD (0.36 ng/mL) of the exposure, EPA estimated the mean (−0.55) and standard deviation (0.51) of the natural logarithm of exposure. The re-expressed β coefficient is −24.9 g (95% CI: −92.5, 42.7) per ng/mL, and the intercept is 3,271.6 g. The 95% one-sided lower limits for the re-expressed β coefficient are −81.6 g per ng/mL. The values of the BMD and BMDL are 4.11 ng/mL and 1.25 ng/mL, respectively.

Starling et al. (2017) reported a β coefficient of −57.6 g (95% CI: −104.1, −11.2) per ln (ng/mL) for the association between birth weight and maternal PFNA serum concentrations (collected during 20 to 34 weeks of pregnancy with a median of 27 weeks) in a U.S. cohort. Given the reported study-specific median (0.4 ng/mL) and IQR (0.3–0.6 ng/mL) of the exposure, EPA estimated the mean (−0.92) and standard deviation (0.51) of the natural logarithm of exposure. The

re-expressed β coefficient is −140.2 g (95% CI: −253.2, −27.3) per ng/mL, and the intercept is 3,317.7 g. The 95% one-sided lower limits for the re-expressed β coefficient are −235.0 g per ng/mL. The values of the BMD and BMDL are 1.06 ng/mL and 0.63 ng/mL, respectively.

Wikström et al. (2020) reported a β coefficient of −46.0 g (95% CI: −89.0, −4.0) per ln (ng/mL) for the association between birth weight and maternal PFNA serum concentrations (collected during 3 to 27 weeks of pregnancy with a median of 10 weeks) in a Swedish cohort. Given the reported study-specific median (0.53 ng/mL) and IQR (0.39–0.73 ng/mL) of the exposure, EPA estimated the mean (−0.63) and standard deviation (0.46) of the natural logarithm of exposure. The re-expressed β coefficient is −84.9 g (95% CI: −164.3, −7.4) per ng/mL, and the intercept is 3,295.6 g. The 95% one-sided lower limits for the re-expressed β coefficient are −150.7 g per ng/mL. The values of the BMD and BMDL are 1.49 ng/mL and 0.84 ng/mL, respectively.

For all of the above calculations, EPA used the exact percentage (8.27%) of live births in the United States in 2018 that fell below the cutoff of 2,500 g as the tail probability to represent the probability of extreme ("adverse") response at zero dose ($P(0)$). However, this exact percentage of 8.27% was calculated without accounting for the existence of background PFNA exposure in the U.S. population (i.e., 8.27% was not the tail probability of extreme response at zero dose). Thus, EPA considered an alternative control-group response distribution ($N(\mu_c, \sigma_c)$), using the study-specific intercept b obtained through equation (D-5) (representing the baseline value of birth weight in an unexposed population) as μ_c and the standard deviation of U.S. population as σ_c to estimate the tail probability falling below the cutoff of 2,500 g. EPA estimated the study-specific tail probability of live births falling below the public health definition of low birth weight (2,500 g) as:

$$P(0) = \frac{1}{\sigma_c\sqrt{2\pi}}\int_{-\infty}^{2{,}500} e^{\left(-\frac{(x-b)^2}{2\sigma_c^2}\right)}\,dx = \frac{1}{590.7\sqrt{2\pi}}\int_{-\infty}^{2{,}500} e^{\left(-\frac{(x-b)^2}{2*590.7^2}\right)}\,dx$$

$$b = \overline{y} - m\overline{x} = 3{,}261.6 - \left(\beta_{re-expressed} * 0.40\frac{ng}{mL}\right) \qquad \text{(D-9)}$$

In this alternative approach, $P(0)$ is 9.86% if there is no background exposure ($\overline{x} = 0$). By using the median of serum PFNA concentrations (0.40 ng/mL) from ACE Biomonitoring on Perfluorochemicals as background exposure ($\overline{x}$), the tail probabilities using this alternative approach are study specific and range from 8.31% to 9.57%. As such, the results from this alternative approach, presented under the column of "Alternative Tail Probability" in Table D-9, are very similar to the main results, presented under the column of "Exact Percentage" in the same table, when background exposure was not accounted for while estimating the tail probability.

Table D-9 presents the BMDs and BMDLs for all studies considered for POD derivation, with and without accounting for background exposure while estimating the percentage of the population falling below the cutoff value. The BMDLs for the studies ranged from 0.56 ng/mL to 1.67 ng/mL.

Table D-9. BMDs and BMDLs for effect of PFNA on decreased birth weight, by using percentage (8.27%) of live births falling below the public health definition of low birth weight, or alternative study-specific tail probability

Study	Exposure median (IQR)	Exposure distribution (μ, σ)	Reported β (95% CI)	Re-expressed β (95% CI)	Intercept b	SE of β	95% one-sided LL of β	Exact percentage ($P(0)$=8.27%)		Alternative tail probability[a]		
								BMD (ng/mL)	BMDL (ng/mL)	$P(0)$	BMD (ng/mL)	BMDL (ng/mL)
Sagiv et al. (2018)	0.7 (0.5–1.0)	(−0.36, 0.51)	−28.2 (−52.0, −4.4) g/IQR (ng/mL)	−56.4 (−104.0, −8.8) g/ng/mL	3,284.2	24.3	−96.4	2.04	1.19	9.21%	2.47	1.45
Valvi et al. (2017)	0.59 (0.46–0.79)	(−0.53, 0.40)	−42.0 (−108.0, 25.0) g/$\log_2$(ng/mL)	−101.0 (−259.8, 60.1) g/ng/mL	3,302.1	81.6	−235.3	1.31	0.56	8.72%	1.43	0.62
Manzano-Salgado et al. (2017)	0.66 (0.36)	(−0.55, 0.51)	−10.3 (−38.1, 17.6) g/$\log_2$(ng/mL)	−24.9 (−92.5, 42.7) g/ng/mL	3,271.6	34.5	−81.6	4.11	1.25	9.57%	5.46	1.67
Starling et al. (2017)	0.4 (0.3–0.6)	(−0.92, 0.51)	−57.6 (−104.1, −11.2) g/ln(ng/mL)	−140.2 (−253.3, −27.3) g/ng/mL	3,317.7	57.7	−235.0	1.06	0.63	8.31%	1.07	0.64
Wikström et al. (2020)	0.53 (0.39–0.73)	(−0.63, 0.46)	−46.0 (−89.0, −4.0) g/ln(ng/mL)	−84.9 (−164.3, −7.4) g/ng/mL	3,295.6	40.02	−150.7	1.49	0.84	8.90%	1.68	0.95

Abbreviations: CI = confidence interval; IQR = Interquartile range; SE = standard error.

[a]The alternative study-specific tail probability of live births falling below the public health definition of low birth weight based on Normal distribution with intercept b as mean and standard deviation of 590.7 based on U.S. population.

ACE Biomonitoring on Perfluorochemicals also provides the median blood serum levels of PFNA in women ages 16 to 49; these values were 0.5 ng/mL in 1999–2000, and 1.0 ng/mL in 2009–2010. A sensitivity analysis was performed (see Appendix C.1.7) by estimating BMD and BMDL using these values as background exposures. The results for Sagiv et al. (2018), presented in Table D-10, demonstrate the robustness of EPA's approaches with alternative assumptions on background exposures.

Table D-10. BMDs and BMDLs for effect of PFNA on decreased birth weight by background exposure, using percentage (8.27%) of live births falling below the public health definition of low birth weight, or alternative tail probability

Study	Background exposure[a]	Intercept *b*	Exact percentage (*P(0)* = 8.27%)		Alternative tail probability[b]		
			BMD (ng/mL)	BMDL (ng/mL)	*P(0)*	BMD (ng/mL)	BMDL (ng/mL)
Sagiv et al. (2018)	0.40	3,284.2	2.04	1.19	9.21%	2.47	1.45
	0.50	3,289.8	2.14	1.25	9.06%	2.50	1.46
	1.00	3,318.0	2.64	1.54	8.30%	2.65	1.55

[a]Assumptions on background exposure for the estimation of intercept using Equation (D-3).
[b]The tail probability of live births falling below the public health definition of low birth weight based on Normal distribution.

D.1.4. Mean Decreased Birth Weight Using Meta-Analysis Results

In addition to the above five studies, epidemiological data were also available on another 22 studies with β coefficients for the association between birth weight and PFNA concentrations reported using different units, as discussed in the meta-analysis methods section (see Appendix C.1.5). As noted in Appendix C.1.5, the exposure-response functions quantifying the effects for these studies based on different units were converted into natural log units (i.e., per ng/mL) according to Dzierlenga et al. (2020). Three studies, Lind et al. (2017), Robledo et al. (2015), and Wang et al. (2016b), only reported separate estimates for boys and girls; before performing the overall meta-analysis, these estimates were pooled using inverse-variance weighting. Meta-analyses were performed using β coefficient per ln(ng/mL) of all 27 studies since the majority of the studies reported results on log scale (see Appendix C.1.6). Additionally, analyses were performed using subsets of the studies to evaluate whether the summary effect estimate varied by study confidence or by the timing of maternal serum sampling. The results are presented in Table D-11.

Using a random-effects model with inverse-variance weights, the meta-analysis conducted using β coefficient per ln(ng/mL) for all studies (n = 27) resulted in a β coefficient of −32.9 g (95% CI: −47.0, −18.7) per ln(ng/mL) increase for the association between birth weight and PFNA concentrations. This β coefficient can be re-expressed in terms of per ng/mL according to Dzierlenga et al. (2020). First, the distribution of exposure for each individual study was estimated

by assuming the exposure followed a log-normal distribution. Then, 100 replicates of random samples (sample size was the same as the reported sample size in each study) were simulated from the exposure distributions for each study included in the meta-analysis, and random samples from all studies were pooled for each replicate to get quantiles from the pooled random samples for each replicate. Lastly, the mean quantiles (median and IQR) from the 100 replicates were used to obtain the exposure distribution for all studies using Equations (D-1) and (D-2) since the joint distribution of the exposures are also log normally distributed. The re-expressed summary estimate is −48.9 g (95% CI: −69.9, −27.8) per ng/mL.

The BMD of 2.29 ng/mL from all studies can be calculated using the same approach as above with the same values for the mean birth weight in the United States. To calculate the BMDL, the same procedure as above was used to calculate the corresponding 95% one-sided lower limit for the re-expressed β coefficient from the re-expressed lower limit on the two-sided 95% CI. Using the corresponding lower limit, a BMDL of 1.68 ng/mL is calculated.

The BMD and BMDL for the effect of PFNA on decreased birth weight using meta-analysis results, conducted in log scale, and stratified by study confidence and by sample timing, are presented in Table D-11 below. The overall combined β coefficient of −32.9 g (95% CI: −47.0, −18.7) per ln(ng/mL) increase was robust and very comparable to that seen for only the 12 *high* studies (−28.0 g; 95% CI: −49.0, −6.9) or the 22 *medium* and *high* studies combined (−32.9 g; 95% CI: −48.0, −17.8). Similarly, the BMDLs for the 11 earlier sampled study subsets (1.87 ng/mL) were very comparable to the earlier sampled study subset excluding one study (Robledo et al., 2015) with samples collected in the preconception period (1.81 ng/mL), and the overall full set of studies (1.68 ng/mL). EPA also conducted the analysis with the alternative approach discussed above by considering an alternative control-group response distribution ($N(\mu_c, \sigma_c)$). The results from this alternative approach, presented in Table D-12 below, are very similar to the previous results.

Table D-11. BMDs and BMDLs for effect of PFNA on decreased birth weight using meta-analysis results conducted in log scale overall, by study confidence and by sample timing, using the percentage (8.27%) of live births falling below the public health definition of low birth weight

Set of studies	Meta-analysis in log scale				
	Exposure distribution (μ, σ)	β per ln(ng/mL) (95% CI)	Re-expressed β per ng/mL (95% CI)	BMD (ng/mL)	BMDL (ng/mL)
All studies (n = 27)	(−0.44, 0.62)	−32.9 (−47.0, −18.7)	−48.9 (−69.9, −27.8)	2.29	1.68
Study confidence					
High confidence (n = 12)	(−0.40, 0.53)	−28.0 (−49.0, −6.9)	−40.8 (−71.3, −10.0)	2.67	1.64
Medium confidence (n = 10)	(−0.39, 0.74)	−39.0 (−61.8, −16.3)	−54.7 (−86.7, −22.9)	2.09	1.40
Low confidence (n = 5)	(−1.53, 0.64)	−36.9 (−82.9, 9.1)	−164.1 (−368.7, 40.5)	0.96	0.47
High + Medium confidence (n = 22)	(−0.40, 0.60)	−32.9 (−48.0, −17.8)	−47.3 (−69.1, −25.6)	2.35	1.70
Sample timing[a]					
Early Pregnancy (n = 11)	(−0.45, 0.53)	−22.0 (−40.1, −4.0)	−33.5 (−61.0, −6.1)	3.16	1.87
Early Pregnancy[b] (n = 10)	(−0.45, 0.52)	−22.8 (−41.0, −4.6)	−35.2 (−63.3, −7.1)	3.03	1.81
Late Pregnancy (n = 10)	(−0.27, 0.67)	−48.4 (−67.7, −29.0)	−60.7 (−84.8, −36.3)	1.92	1.44
Post Pregnancy (n = 6)	(−1.07, 0.91)	−42.9 (−88.0, 2.2)	−114.8 (−235.5, 5.9)	1.21	0.64
Late + Post Pregnancy (n = 16)	(−0.41, 0.80)	−44.5 (−65.9, −23.0)	−62.6 (−92.8, −32.4)	1.88	1.34

[a]Sample time periods include early pregnancy (the first trimester, first or second trimester), late pregnancy (second trimester, second or third trimester), post pregnancy (birth and post-birth); CI = confidence interval; n = number of studies; effect estimates, β, represent change in birthweight (grams) per unit change in ln (ng/mL) or ng/mL PFNA exposure.

[b]Sample time periods in early pregnancy excluding one study, Robledo et al. (2015), with samples collected in the preconception period.

Table D-12. BMDs and BMDLs for effect of PFNA on decreased birth weight using meta-analysis results conducted in log scale overall, by study confidence and by sample timing, using the alternative study-specific tail probability of live births falling below the public health definition of low birth weight

Set of studies	Meta-analysis in log scale				
	Exposure distribution (μ, σ)	β per ln(ng/mL) (95% CI)	Re-expressed β per ng/mL (95% CI)	BMD (ng/mL)	BMDL (ng/mL)
All studies (n = 27)	(−0.44, 0.62)	−32.9 (−47.0, −18.7)	−48.9 (−69.9, −27.8)	2.83	2.08
Study confidence					
High confidence (n = 12)	(−0.40, 0.53)	−28.0 (−49.0, −6.9)	−40.8 (−71.3, −10.0)	3.38	2.07
Medium confidence (n = 10)	(−0.39, 0.74)	−39.0 (−61.8, −16.3)	−54.7 (−86.7, −22.9)	2.55	1.71
Low confidence (n = 5)	(−1.53, 0.64)	−36.9 (−82.9, 9.1)	−164.1 (−368.7, 40.5)	0.93	0.45
High + Medium confidence (n = 22)	(−0.40, 0.60)	−32.9 (−48.0, −17.8)	−47.3 (−69.1, −25.6)	2.93	2.11
Sample timing[a]					
Early Pregnancy (n = 11)	(−0.45, 0.53)	−22.0 (−40.1, −4.0)	−33.5 (−61.0, −6.1)	4.09	2.42
Early Pregnancy[b] (n = 10)	(−0.45, 0.52)	−22.8 (−41.0, −4.6)	−35.2 (−63.3, −7.1)	3.90	2.33
Late Pregnancy (n = 10)	(−0.27, 0.67)	−48.4 (−67.7, −29.0)	−60.7 (−84.8, −36.3)	2.31	1.73
Post Pregnancy (n = 6)	(−1.07, 0.91)	−42.9 (−88.0, 2.2)	−114.8 (−235.5, 5.9)	1.27	0.68
Late + Post Pregnancy (n = 16)	(−0.41, 0.80)	−44.5 (−65.9, −23.0)	−62.6 (−92.8, −32.4)	2.24	1.59

[a]Sample time periods include early pregnancy (the first trimester, first or second trimester), late pregnancy (second trimester, second or third trimester), post pregnancy (birth and post-birth); CI = confidence interval; n = number of studies; effect estimates, β, represent change in birthweight (grams) per unit change in ln (ng/mL) or ng/mL PFNA exposure.

[b]Sample time periods in early pregnancy excluding one study, Robledo et al. (2015), with samples collected in the preconception period.

For decreased birth weight associated with PFNA exposure, the POD selected from individual studies in the available epidemiological literature is 1.19 ng/mL maternal serum concentration based on birth weight data from Sagiv et al. (2018). Of the five individual studies, Sagiv et al. (2018), Manzano-Salgado et al. (2017), and Wikström et al. (2020) assessed maternal PFNA serum concentrations primarily in the first trimester, minimizing concerns surrounding bias due to pregnancy-related hemodynamic effects. Additionally, use of the Sagiv et al. (2018) results also remove any uncertainty associated with the re-expression of regression coefficients from transformed basis to untransformed basis.

The PODs from the meta-analyses of *high* and *medium* confidence studies or those with early sampling time studies were consistent in relative magnitude to the PODs from individual studies. The POD from the meta-analysis of 10 early sampling time studies assessed maternal PFNA

serum concentrations predominately in early pregnancy, minimizing concerns surrounding bias due to pregnancy-related hemodynamic effects. To carry out this meta-analysis, re-expression of 2 of the 10 effect estimates (β) from the natural scale to the log scale of exposure was performed, and re-expression from the log scale to the natural scale of exposure was performed while conducting BMD modeling. A recent study examined the uncertainty introduced by the re-expression method and found a systemic bias in the direction of a larger effect estimate, i.e., an overestimation of the true effect estimate, when converting from the log scale to the natural scale (Linakis et al., 2021). Specifically, with the results using simulated data from that study, EPA estimated that the average systemic bias from re-expression for an exposure distribution similar to that used in the POD derivation (sigma = 0.52) would be approximately 30%.

EPA evaluated the choice of using a POD based on the meta-analysis or based on a single study, weighing the benefit of the additional studies' evidence against the additional uncertainty and potential bias introduced by the re-expression. Given that these PODs are relatively close together, EPA has more confidence that either choice is suitable to inform the RfD for this endpoint. The large amount of additional data supporting the meta-analysis of 10 high quality early sampling time studies was judged to outweigh the potential bias introduced by the re-expression method. Therefore, the POD from the meta-analyses of 10 early sampling time studies was ultimately selected.

For details on the meta-analysis methods for decreased birthweight, including study inclusion criteria, data scaling, and statistical and sensitivity analysis, see Appendix C.1.5.

D.1.5. Results for Increased Serum ALT

PFNA is associated with increases in the liver enzyme alanine aminotransferase (ALT) (see Section 3.2.4). Two *medium* confidence epidemiology studies, Nian et al. (2019) and Kim et al. (2023b), were selected for the POD derivation. EPA derived multiple estimates of the POD from these two studies, for men and women, using different benchmark responses (BMRs) and different approaches to define adverse changes. EPA used three different approaches from the EPA Benchmark Technical Guidance (U.S. EPA, 2012) to estimate PODs: the hybrid approach, which uses a biologically based cutoff in the distribution of ALT concentrations to define a level above which ALT may be interpreted as abnormal—or uses a percentile-based approach to define such a level—and a BMR of 10% (or 5%) extra risk beyond that cutoff to estimate a magnitude of exceedance above this cutoff that is (minimally) adverse; the standard deviation approach, which defines the BMR as a change in the mean of one standard deviation (SD) (or ½ SD); and the NOAEL approach.

Both studies reported percentage change in ln-ALT per ln-unit increase or per $\log_2$-unit increase in PFNA defined as a function of the reported regression coefficient (i.e., $(e^{\beta}-1)*100$). EPA calculated the regression coefficients, and the 95% confidence intervals from the reported percent changes for both studies. The regression coefficients in one study (Kim et al., 2023b) were scaled in "per $\log_2$" units, and EPA re-scaled those as slopes of change in ln-ALT(U/L) per ln (ng/mL) PFNA. Essentially, these studies have already performed a dose-response analysis (i.e., the regression

analysis), and both studies were interpreted to have adequately accounted for relevant confounding factors in that analysis. EPA did not have access to the individual-level data that would be necessary to model the data from these studies with standard BMDS-based approaches. Therefore, EPA relied on the regression coefficients β from the linear regression models of ln-transformed ALT and ln-transformed PFNA concentrations in Kim et al. (2023b) and Nian et al. (2019) as described below to calculate BMD and BMDL values by using the general equation $y = \beta x + b$, where y is ln-ALT and x is ln-PFNA. The unknown intercept b can be estimated using $\overline{y} = \beta\overline{x} + b$ using an average ln-ALT from an external population as $\overline{y}$ and average ln-PFNA as $\overline{x}$.

The National Health and Nutrition Examination Survey (NHANES, https://wwwn.cdc.gov/Nchs/Nhanes/) provides ALT and PFNA concentrations for the periods of 1999–2018,[4] for adults age 18 years and over, which can be used to obtain an average ln-ALT as $\overline{y}$ and ln-PFNA as $\overline{x}$ to estimate the intercept b though the equation:

$$b = \bar{y} - \beta\bar{x} \quad \text{(D-10)}$$

EPA obtained the summary statistics (e.g., mean and SD of ln-ALT and mean of ln-PFNA) for the period of 1999–2018, separately for men and women ages 18 and over, while using the NHANES survey weights. These analyses used the NHANES-recommended regression model adjustment to correct the 2017–2018 ALT data to match the earlier laboratory method. The mean and SD of ln-ALT and mean of ln-PFNA for the period of 1999–2018 are reported in Table D-13 by gender.

Hybrid Approach

With a regression coefficient β and an estimated intercept b, a BMD can be estimated through the hybrid approach by defining the BMD as the dose yielding the specified extra risk (i.e., the dose that increases the percentage of responses falling below (or above) a cutoff level in the tail of the response distribution (EPA's Benchmark Dose Technical Guidance (U.S. EPA, 2012)). The hybrid approach is advantageous in that it harmonizes the definition of the BMR for continuous data with that for dichotomous data.

Elevated serum ALT is a biomarker of liver injury and has been associated with a variety of liver diseases. It is commonly used to help diagnose and monitor liver disease, and elevations are common in primary care medicine. ALT is highly abundant in liver, and injury to the organ leads to increased ALT levels, although it should be acknowledged that severe muscle injury may also increase ALT levels in the blood (i.e., it is sensitive but not specific to liver injury) (Thulin et al., 2014). There is a range of "baseline" serum ALT levels across individuals, e.g., Gowda et al. (2009)

[4]This date range was selected to utilize all available NHANES data that cover the sampling periods of both Kim et al. (2023b) and Nian et al. (2019). The study population of Kim et al. (2023b) was a sub-population of the KoNEHS cycle 3, 2015–2017. The study population of Nian et al. (2019) was part of the Isomers of C8 Health Project in China, 2015–2016.

reference a range of 7–56 U/L across individuals, and elevations of a small magnitude are typically considered nonspecific in relation to liver disease or disease progression. Since ALT concentrations are related to individuals' age, sex, alcohol consumption, and BMI, different populations will have different sets of baseline risk factors for higher ALT as well as having different anthropometric characteristics like metabolism and genetics (Pacifico et al., 2013).

Valenti (2021) analyzed ALT levels in 21,296 apparently healthy adults (the "whole cohort") and on a subset of 9,195 who were screened for viral hepatitis, with normal body mass index, cholesterol, triglycerides, and glucose, and without regular alcohol intake or drug use (the "healthy cohort"). Based on the healthy cohort, Valenti (2021) recommended updated ALT upper reference limits, also called the upper limit of normal (ULN), for the International Federation of Clinical Chemistry and Laboratory Medicine (IFCC) of 42 and 30 U/L for males and females, respectively. To test the ability of these cutoffs to predict liver pathology, analysis of a subset of the cohort with dysmetabolism indicated that people with ALT concentrations above the ULNs were at increased risk of steatosis. Park et al. (2019) followed the health of 338,216 people from their baseline visits in 2003–2004 until 2013 (mean follow-up of 9.83 years) and identified 1,048 decompensated liver events (cirrhosis) during that time period. Park et al. (2019) found that people with higher baseline ALT concentrations were at significantly increased risk for decompensated liver events with hazard ratios of 4.43 for men with ALT > 40 U/L (95% CI: 3.80, 5.17) and 4.29 for women with ALT > 40 U/L (95% CI: 3.17, 5.78).

One option for defining a biologically based cutoff in the ALT distribution is to use a definition of the ULN that is typically set at the 95th percentile of ALT in a population of healthy adults and is calculated by individual clinical laboratories or testing sites. The challenge is to define the ULN to detect small but biologically meaningful (adverse) changes. However, EPA is aware that there may be uncertainties in the data underlying published ULNs due to the variability of multiple aspects of measuring ALT in healthy populations. Historically, the measurement of ALT has included many sources of variability in interlaboratory practices (Valenti, 2021), as well as in the demographic and anthropometric characteristics of the studied population (Pacifico et al., 2013). Although the IFCC has published reference methods and materials for determining ALT in serum (Schumann et al., 2002), persistent challenges remain due to variations in assay conditions and differences in analyzer instruments across laboratory and clinical settings (Beste et al., 2020; Infusino I, 2009). For example, in 2002, Schumann et al. (2002) recommended that the reference temperature for measuring enzyme catalytic concentrations be changed from 30 to 37°C and Schumann and Klauke (2003) proposed new preliminary ALT cutoffs of 45 U/L for men and 34 U/L for women. Thus, many ULNs exist, and they vary considerably depending on features such as when the ULN was developed and the clinical features of patient cohorts upon which it is based.

Similarly, defining the quantitative limit of ULN for ALT is affected by many sources of variability including the definition of the "healthy" reference population, which may not always have excluded blood donors with hepatitis C or could not differentiate people with non-alcoholic

fatty liver disease (NAFLD) (Pacifico et al., 2013). Unintentional inclusion of unhealthy people in the reference population can skew ULN results toward higher values. For these reasons, there is no standardized ULN for ALT, including in the United States, and ULNs across laboratories range from <20 U/L to >50 U/L.

Owing to the large size of the study population and the careful attention to standardization of the methods (Valenti, 2021), EPA used the recently updated IFCC ULNs to define the cutoff in the ALT distribution used in the hybrid approach. Valenti (2021) reported ULNs for men and women as the upper 95th percentile of ALT in a population of apparently healthy blood donors, with robust exclusion criteria that included (among other factors) endemic infectious diseases and alcohol intake. The ULNs established for the healthy group in this study provide a strong foundation for comparison (and are routinely those used in practice) to set ULNs for clinical screening to avoid including conditions that may be causing elevated ALT concentration. However, for the purposes of applying cutoffs in the distribution of ALT to the U.S. population, the cutoffs reported for the larger whole cohort were also considered by EPA as they have the potential to be more generalizable to the U.S. general population, which includes susceptible populations with risk factors for liver disease.

While the ULNs reported by Valenti (2021) were developed for use in identifying patients for additional diagnostic screening, thus introducing some uncertainty regarding their precision in representing a definitive cutoff for increased disease on their own, they can serve to represent a reasonable boundary for detecting liver injury for the purposes of contextualizing a POD. Notably, there is clear evidence that liver injury (and particularly liver disease) is associated with increased ALT concentration in the blood. A further justification for the use of the 95th percentiles of ALT in Valenti (2021), beyond a strictly biological demarcation, is that the Valenti approach to derive the ULN is aligned with the BMD Technical Guidance that suggests the use of a percentile-based approach (U.S. EPA, 2012; Kavlock et al., 1995); given this background, use of the 95th percentile of ALT to define the ULN appears to be reasonable.

The ULN of ALT for liver disease was chosen to be C = 42 U/L for men and C = 30 U/L for women, based on the sex-specific ULNs found for the healthy population (i.e., people without risk factors for liver disease) in Table 2 of Valenti (2021). EPA also considered the alternative cutoffs based on the whole cohort of Valenti (2021) (i.e., C = 48 U/L for men and C = 33 U/L for women).

Given these clinical limits, the percentages above these cutoffs C U/L were obtained as $P(0)$, separately for men and women ages 18 and over for the period of 1999–2018 in the NHANES, while assuming that ALT is lognormally distributed using the equation:

$$P(0) = 1 - \Phi\left\{\frac{ln(C) - mean(ln\ ALT)}{SD(ln\ ALT)}\right\} \quad \text{(D-11)}$$

where Φ is the normal cumulative distribution function.[5]

In addition, application of the hybrid approach requires the selection of an extra risk value for BMD estimation. In the case of ALT, EPA considered both extra risks of 5% and 10% in the BMD estimation. A BMR of less than 10% (or less than 1 SD, see below) can be supported for severe or debilitating health outcomes; given the findings of associations between elevated ALT and severe liver disease in Park et al. (2019), a BMR of 5% was considered. However, modest elevations in ALT are more likely to be associated with mild forms of injury, including steatosis and NAFLD. Due to the uncertainties in measuring ALT, in selecting the most appropriate ULN (and the difficulty in interpreting specific elevations above the ULN as adverse), and in selecting the reference population described above, a BMR of 10% extra risk was selected as a (minimally) adverse effect and as a standard reporting level per the Benchmark Dose Technical Guidance (U.S. EPA, 2012).

The extra risk of adverse effects associated with increased ALT is given by the equation:

$$Extra\ Risk = \frac{P(d)-P(0)}{1-P(0)} \quad \text{(D-12)}$$

where $P(d)$ is the probability of ALT greater than or equal to C (U/L) for a given PFNA dose d. Thus, $P(d)$ can be solved using the above equation as

$$P(d) = \{1 - P(0)\} \times Extra\ Risk + P(0) \quad \text{(D-13)}$$

For a given group and dose, the probability of ALT greater than or equal to C can also be written as

$$P(d) = P(ALT\ \geq C) = P(ln\ ALT\ \geq ln\ C) = 1 - \Phi\left(\frac{ln\ C - y}{S}\right) \quad \text{(D-14)}$$

where Φ is the normal cumulative distribution function. Thus, with the $P(d)$ derived from equation D-12, the target mean ln ALT that would be associated with the $P(d)$th percentile of the target distribution falling above C (U/L), denoted as y, is the solution of the last equation, i.e., $y = \ln C - S \times \Phi^{-1}\{1 - P(d)\}$, where Φ^{-1} is the inverse of the normal cumulative distribution function and S is the standard deviation of y and assumed to be the same as SD of ln-ALT in NHANES.

The ln-PFNA benchmark dose (ln BMD) is the corresponding dose x such that $y = \beta x + b$. Thus

$$ln\ BMD = \frac{y-b}{\beta} \quad \text{(D-15)}$$

This gives the PFNA benchmark dose (BMD) as exp(ln BMD).

To calculate the BMDL, the method is essentially the same except that the upper limit (UL) on the β coefficient is used. However, both Nian et al. (2019) and Kim et al. (2023b) reported two-sided 95% confidence intervals for the β coefficients, meaning that the upper limits of those

[5]Concentration data are generally assumed to be log-normally distributed, and both Kim et al. (2023b) and Nian et al. (2019) applied natural log transformations of ALT prior to deriving the dose-response functions.

confidence intervals correspond to 97.5% one-sided upper limits. The BMDL is defined as the 95% lower limit of the BMD (i.e., corresponds to a two-sided 90% confidence interval), so the corresponding upper limit on the β coefficient needs to be calculated before calculating the BMDL. First, the standard error of the β coefficient can be calculated as:

$$se(\beta) = \frac{Upper\ Limit - Lower\ Limit}{3.92} \quad \text{(D-16)}$$

Then the corresponding 95% one-sided upper bound on the β coefficient can be calculated as:

$$\beta 95 = 95th\ one-sided\ Upper\ limit\ for\ \beta = \beta + 1.645 \times se(\beta) \quad \text{(D-17)}$$

Thus

$$ln\ BMDL = \frac{y-b}{\beta 95} \quad \text{(D-18)}$$

This gives the PFNA benchmark dose lower bound (BMDL) as exp(ln BMDL).

Kim et al. (2023b)[6] examined a sub-population of the Korean National Environmental Health Survey (KoNEHS)[7] and reported significant percentage changes in ln-ALT for log_2-unit increase in PFNA of 7.5% (95% CI: 2.3, 12.8) for men and 7.0% (95% CI: 2.2, 11.9) for women using multiple linear regression adjusted for age, sex, education, income, smoking, heavy drinking, exercise, and body mass index (BMI). The regression coefficients β were calculated as 0.0723 (95% CI: 0.0227, 0.1204) ln ALT(U/L) per log_2 (ng/mL) PFNA for men and 0.0677 (95% CI: 0.0218, 0.1124) ln ALT(U/L) per log_2 (ng/mL) PFNA for women.[8] These regression coefficients β can be rescaled to 0.1043 (95% CI: 0.0328, 0.1738) ln ALT(U/L) per ln (ng/mL) PFNA for men and 0.0976 (95% CI: 0.0314, 0.1622) ln ALT(U/L) per ln (ng/mL) PFNA for women by dividing each value by ln(2). Using the mean (2.96 ln(U/L) for women) and SD of ln-ALT (0.41 for women) as $\overline{y}$ and SD($\overline{y}$), the mean of ln-PFNA (−0.29 ln(ng/mL) for women) as $\overline{x}$, and the percentages falling above the cutoff $P(0)$ (14.0% for women) for the period of 1999–2018 in NHANES, $P(d)$ (22.6% for women) was calculated using equation D-12 with an extra risk of 10%, the intercept b (2.98) was estimated using equation D-9, and the target mean y (3.09 for women) was derived using equation D-13. Similarly, the target mean y was 3.42 for men. EPA estimated that the values of the BMDs for 10% extra risk with the cutoffs of the whole cohort of Valenti (2021) were 3.45 ng/mL for men and 2.99 ng/mL for women using equation D-14. The values of the BMDLs using the same extra risk and cutoffs were 2.20 ng/mL for men and 2.02 ng/mL for women, estimated using equation D-9. The

[6]Sex-specific results are in the Kim et al. (2023b) Supplemental.
[7]The study population of (Kim et al., 2023b) was a sub-population of the KoNEHS, the biomonitoring program in South Korea adult (age ≥ 19) population. Participants with self-reported history of liver diseases including hepatitis B, hepatitis C, liver cirrhosis, and liver cancer were excluded. The median (IQR) of PFNA exposure of the study population is 2.02 ng/mL (IQR: 1.38–2.94 ng/mL).
[8]Percentage increase = (e^{β}−1)*100) see Kim et al. (2023b).

8.6% upward shift (above the 14% of women above the cutoff at baseline) in the distribution of ln(ALT) using the hybrid method resulting from an extra risk of 10% is illustrated using Figure D-3 below for women using the period of 1999–2018 in NHANES. Note that the 8.6% shift results in 10% extra risk as (P(d)-P(0))/(1-P(0)) = (0.226–0.14)/(1–0.14) = 0.10.

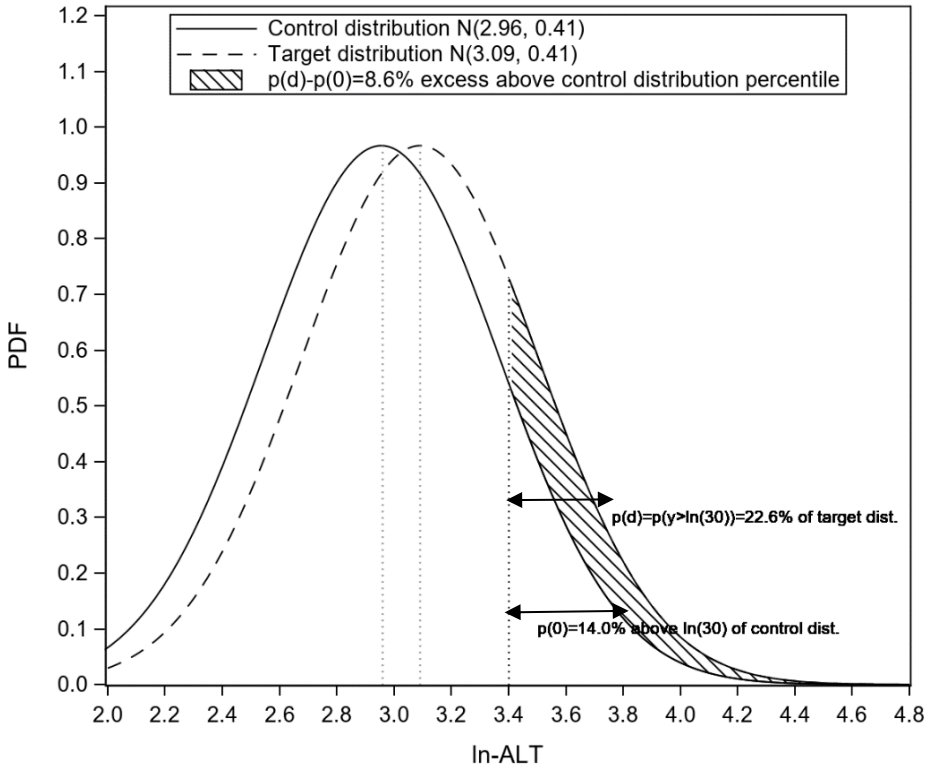

Figure D-3. The shift in the distribution using hybrid method resulting from an extra risk of 10% for Women of Kim et al. (2023b) using the ULN cutoff for the healthy population of Valenti (2021).

Nian et al. (2019) examined a large population of adults in Shenyang (one of the largest fluoropolymer manufacturing centers in China), part of the Isomers of C8 Health Project,[9] and reported a significant percentage change in ln-ALT for ln-unit increase in PFNA of 6.2 (95% CI: 3.1, 9.4) using multiple linear regression adjusted for age, sex, career, income, education, alcohol consumption, smoking, giblet and seafood consumption, exercise, and BMI. The regression coefficient β (for men and women combined) was calculated as 0.0602 (95% CI: 0.0305, 0.0898) ln-ALT(U/L) per ln-PFNA (ng/mL). Using the mean (3.28 ln(U/L) for men) and SD (0.46 for men) of ln-ALT, the mean of ln-PFNA (−0.10 ln(ng/mL) for men), and $P(0)$ (16.1% for men), EPA estimated

[9]The study population of Nian et al. (2019) was part of the Isomers of C8 Health Project in China adult (age ≥ 22) population. The program investigates the associations between PFAA exposures and health outcomes. The median (IQR) of PFNA exposure of the study population is 1.96 ng/mL (IQR: 1.11–3.07 ng/mL).

that the value of the BMD for 10% extra risk with the cutoffs for the healthy population of Valenti (2021) was 9.20 ng/mL for men. Similarly, the BMD was 7.09 ng/mL for women. The values of the BMDLs using the same extra risk and cutoffs were 4.81 ng/mL for men and 4.00 ng/mL for women.

Given potential concerns regarding the generalizability of ULN cutoffs based on a different demographic (an Italian cohort) to those populations in which ALT was measured in the selected studies of PFNA, EPA compared the distribution of ALT in the adult study populations of Kim et al. (2023b) and Nian et al. (2019) with the distribution of ALT in in the adult population in Valenti (2021). Table D-13 shows the distribution of ALT in Kim et al. (2023b), Nian et al. (2019), and Valenti (2021) to be close to each other with Kim et al. (2023b) slightly higher than Valenti (2021), which was higher than Nian et al. (2019).

Table D-13. Distribution of ALT by study and gender

Study	ALT (U/L)		ln-ALT (μ, σ)[a]
Kim 2023 All	24.7 (1.36)	GM (GSD)	(3.21, 0.31)
Kim 2023 Men	26.6 (1.38)	GM (GSD)	(3.28, 0.32)
Kim 2023 Women	23.2 (1.32)	GM (GSD)	(3.14, 0.28)
Nian 2019 All	20.0 (14.0–28.0)	Median (IQR)	(3.00, 0.51)
Nian 2019 Men	21.0 (16.0–30.0)	Median (IQR)	(3.04, 0.47)
Nian 2019 Women	15.0 (11.0–22.0)	Median (IQR)	(2.71, 0.51)
Valenti 2021 Whole Cohort Men	26.2 (13.3)	Mean (SD)	(3.15, 0.48)
Valenti 2021 Whole Cohort Women	18.9 (13.5)	Mean (SD)	(2.73, 0.64)
Valenti 2021 Healthy Population Men	23.7 (12.8)	Mean (SD)	(3.04, 0.51)
Valenti 2021 Healthy Population Women	18.0 (8.4)	Mean (SD)	(2.79, 0.44)

[a]When the median and interquartile range (IQR) were reported, EPA used $ln(median)$ to estimate μ and $ln(75\text{th percentile}/25\text{th percentile})/1.349$ to estimate σ; when the mean and standard deviation were presented, EPA estimated μ and σ using $\mu = ln(Mean/\sqrt{\omega})$ and $\sigma = \sqrt{ln(\omega)}$, where $\omega = 1 + (SD/Mean)^2$ (Limpert et al., 2001).

EPA also derived BMDs and BMDLs using the non-preferred alternative cutoffs based on the whole cohort of Valenti (2021). The parameter choices (e.g., ULN cutoff (C), the reported percent change, the regression coefficient β converted from the reported percent change, the mean and SD of ln-ALT ($\bar{y}$), the mean of ln-PFNA ($\bar{x}$), $P(0)$, $P(d)$, the intercept b, and the target mean y) and results of BMD and BMDL are presented by extra risk (e.g., 5% or 10%), study, and gender in Table D-14, representing the cutoff for the healthy population in Valenti (2021) and Table D-15 for the cutoff for the whole cohort in Valenti (2021). Unrounded values of summary statistics from NHANES were used in the derivation of BMD and BMDL reported in Tables D-14 and D-15.

Between the two *medium* confidence studies by Kim et al. (2023b) and Nian et al. (2019), the study by Kim et al. (2023b) was determined to be the better choice for deriving a POD for adverse liver effects because this study was judged to have a "*good*" rating in the confounding domain during study review (see the heat map in Figure 3-40 in the main document and double click on the "++" under confounding for this study). Kim et al. (2023b) used directed acyclic graphs (DAGs) to select potential confounders, and all models included age, sex, education level, household income, smoking status, BMI, heavy drinking, and regular exercise. Mixture modeling using multiple methods shows that PFNA is the strongest driver of the positive association with ALT and GGT, the latter of which provides additional support for a hepatic origin of elevated serum enzymes than ALT alone (Newsome et al., 2018; van Beek et al., 2013; Dufour et al., 2000). The exposure distribution of PFNA was largely overlapping between Kim et al. (2023b) and Nian et al. (2019), although Nian et al. (2019) has a wider distribution with a lower 25th-percentile.

Table D-14 shows the BMDLs based on the hybrid approach for both Kim et al. (2023b) and Nian et al. (2019) for BMRs of 10% and 5% using the healthier subset in Valenti (2021). The BMDLs were lower for women than for men, lower for Kim et al. (2023b) than for Nian et al. (2019), and lower for a BMR of 5% than for 10%. The range across the eight combinations was 1.34 ng/mL (Kim et al. (2023b), women, 5%) to 4.81 ng/mL (Nian et al. (2019), men, 10%). Table D-15 shows the BMDLs based on the hybrid approach for both Kim et al. (2023b) and Nian et al. (2019) for BMRs of 10% and 5% using the whole cohort. The BMDLs were also lower for women than for men, lower for Kim et al. (2023b) than for Nian et al. (2019), and lower for a BMR of 5% than for 10%. The range across the eight combinations was 1.55 ng/mL (Kim et al. (2023b), women, 5%) to 8.41 ng/mL (Nian et al. (2019), men, 10%).

Standard Deviation Approach

In circumstances in which there is no standardized, generally accepted, or well-supported adverse effect level upon which to base the BMR, a standard deviation approach can be useful. For ALT, EPA also estimated a BMD through the standard deviation approach by defining the BMD as the dose yielding the increases of log responses in specified multiples of the standard deviation (SD) of a control group. In contrast to the hybrid approach, which utilizes a cutoff to define a target mean that corresponds to a BMD using equations D-10 through D-13, the target mean ln ALT in the standard deviation approach that would be associated with the increases of log responses, denoted as y, is $y = y(0) + S(0) \times BMR$, where $y(0)$ is the mean of ln-ALT in a control group and $S(0)$ is the standard deviation of $y(0)$. EPA assumed the mean and SD of ln-ALT for the period of 1999–2018 in NHANES as $y(0)$ and $S(0)$ and derived BMDs and BMDLs using equations D-14 through D-17, similar to the hybrid approach in which the intercept b was estimated though the equation D-9.

The parameter choices (e.g., the reported percent change, the regression coefficient β converted from the reported percent change, the mean and SD of ln-ALT ($\bar{y}$), the mean of ln-PFNA ($\bar{x}$), the intercept b, and the target mean y) and results of BMD and BMDL are presented by BMR

(e.g., ½ SD or 1 SD), study, and gender in Table D-16. Unrounded values of summary statistics from NHANES were used in the derivation of BMD and BMDL reported in Table D-16.

Table D-14. BMDs and BMDLs for effect of PFNA (ng/mL) on elevated ALT using hybrid approach with cutoff for healthy population in Valenti (2021).

BMR extra risk	Study	Gender	Cutoff C (U/L)	Percent change (95% CI)	β (95% CI) ln-ALT(U/L) per ln (ng/mL)	Mean ln-ALT(U/L) $\bar{y}$	Standard deviation ln-ALT	Mean ln-PFNA (ng/mL) $\bar{x}$	$P(0)$	$P(d)$	$b = \bar{y} - \beta\bar{x}$	Target mean ln-ALT(U/L) y	BMD (ng/mL)	BMDL (ng/mL)
5%	Kim et al. (2023b)	Men	42	7.5 (2.3, 12.8)	0.1043 (0.0328, 0.1738)	3.28	0.46	−0.10	16.1%	20.3%	3.29	3.35	1.85	1.48
	Kim et al. (2023b)	Women	30	7.0 (2.2, 11.9)	0.0976 (0.0314, 0.1622)	2.96	0.41	−0.29	14.0%	18.3%	2.98	3.03	1.57	1.34
	Nian et al. (2019)	Men	42	6.2 (3.1, 9.4)	0.0602 (0.0305, 0.0898)	3.28	0.46	−0.10	16.1%	20.3%	3.28	3.35	3.11	2.23
	Nian et al. (2019)	Women	30	6.2 (3.1, 9.4)	0.0602 (0.0305, 0.0898)	2.96	0.41	−0.29	14.0%	18.3%	2.97	3.03	2.50	1.91
10%	Kim et al. (2023b)	Men	42	7.5 (2.3, 12.8)	0.1043 (0.0328, 0.1738)	3.28	0.46	−0.10	16.1%	24.5%	3.29	3.42	3.45	2.20
	Kim et al. (2023b)	Women	30	7.0 (2.2, 11.9)	0.0976 (0.0314, 0.1622)	2.96	0.41	−0.29	14.0%	22.6%	2.98	3.09	2.99	2.02
	Nian et al. (2019)	Men	42	6.2 (3.1, 9.4)	0.0602 (0.0305, 0.0898)	3.28	0.46	−0.10	16.1%	24.5%	3.28	3.42	9.20	4.81
	Nian et al. (2019)	Women	30	6.2 (3.1, 9.4)	0.0602 (0.0305, 0.0898)	2.96	0.41	−0.29	14.0%	22.6%	2.97	3.09	7.09	4.00

Table D-15. BMDs and BMDLs for effect of PFNA (ng/mL) on elevated ALT using hybrid approach with cutoff for whole cohort in Valenti (2021)

BMR extra risk	Study	Gender	Cutoff C (U/L)	Percent change (95% CI)	β (95% CI) ln-ALT(U/L) per ln (ng/mL)	Mean ln-ALT(U/L) $\bar{y}$	Standard deviation ln-ALT	Mean ln-PFNA (ng/mL) $\bar{x}$	$P(0)$	$P(d)$	$b = \bar{y} - \beta\bar{x}$	Target mean ln-ALT(U/L) y	BMD (ng/mL)	BMDL (ng/mL)
5%	Kim et al. (2023b)	Men	48	7.5 (2.3, 12.8)	0.1043 (0.0328, 0.1738)	3.28	0.46	−0.10	10.1%	14.6%	3.29	3.38	2.45	1.77
	Kim et al. (2023b)	Women	33	7.0 (2.2, 11.9)	0.0976 (0.0314, 0.1622)	2.96	0.41	−0.29	9.5%	14.0%	2.98	3.05	1.99	1.55
	Nian et al. (2019)	Men	48	6.2 (3.1, 9.4)	0.0602 (0.0305, 0.0898)	3.28	0.46	−0.10	10.1%	14.6%	3.28	3.38	5.06	3.15
	Nian et al. (2019)	Women	33	6.2 (3.1, 9.4)	0.0602 (0.0305, 0.0898)	2.96	0.41	−0.29	9.5%	14.0%	2.97	3.05	3.65	2.50
10%	Kim et al. (2023b)	Men	48	7.5 (2.3, 12.8)	0.1043 (0.0328, 0.1738)	3.28	0.46	−0.10	10.1%	19.1%	3.29	3.46	5.44	2.95
	Kim et al. (2023b)	Women	33	7.0 (2.2, 11.9)	0.0976 (0.0314, 0.1622)	2.96	0.41	−0.29	9.5%	18.5%	2.98	3.13	4.34	2.56
	Nian et al. (2019)	Men	48	6.2 (3.1, 9.4)	0.0602 (0.0305, 0.0898)	3.28	0.46	−0.10	10.1%	19.1%	3.28	3.46	20.29	8.41
	Nian et al. (2019)	Women	33	6.2 (3.1, 9.4)	0.0602 (0.0305, 0.0898)	2.96	0.41	−0.29	9.5%	18.5%	2.97	3.13	12.97	6.13

Table D-16. BMDs and BMDLs for effect of PFNA (ng/mL) on elevated ALT using BMR of half standard deviation (SD) or 1 SD

BMR standard deviation	Study	Gender	Percent change (95% CI)	β (95% CI) ln-ALT(U/L) per ln (ng/mL)	Mean ln-ALT(U/L) $\overline{y}$	Standard deviation ln-ALT	Mean ln-PFNA (ng/mL) $\overline{x}$	$b = \overline{y} - \beta\overline{x}$	Target mean ln-ALT(U/L) y	BMD (ng/mL)	BMDL (ng/mL)
½ SD	Kim et al. (2023b)	Men	7.5 (2.3, 12.8)	0.1043 (0.0328, 0.1738)	3.28	0.46	−0.10	3.29	3.51	8.41	3.89
	Kim et al. (2023b)	Women	7.0 (2.2, 11.9)	0.0976 (0.0314, 0.1622)	2.96	0.41	−0.29	2.98	3.16	6.18	3.21
	Nian et al. (2019)	Men	6.2 (3.1, 9.4)	0.0602 (0.0305, 0.0898)	3.28	0.46	−0.10	3.28	3.51	43.16	14.34
	Nian et al. (2019)	Women	6.2 (3.1, 9.4)	0.0602 (0.0305, 0.0898)	2.96	0.41	−0.29	2.97	3.16	23.05	9.20
1 SD	Kim et al. (2023b)	Men	7.5 (2.3, 12.8)	0.1043 (0.0328, 0.1738)	3.28	0.46	−0.10	3.29	3.74	77.95	16.12
	Kim et al. (2023b)	Women	7.0 (2.2, 11.9)	0.0976 (0.0314, 0.1622)	2.96	0.41	−0.29	2.98	3.37	51.17	12.41
	Nian et al. (2019)	Men	6.2 (3.1, 9.4)	0.0602 (0.0305, 0.0898)	3.28	0.46	−0.10	3.28	3.74	2,051.4	220.17
	Nian et al. (2019)	Women	6.2 (3.1, 9.4)	0.0602 (0.0305, 0.0898)	2.96	0.41	−0.29	2.97	3.37	711.65	104.12

For Kim et al. (2023b), the values of BMDLs using BMR of 1 SD were 16.12 ng/mL for men and 12.41 ng/mL for women. With this approach to deriving a POD, there is substantially more variability across PODs (as compared to the narrow range of BMDs and BMDLs across studies, sexes, and BMR levels using the hybrid approach), which appears to be driven by the use of a much larger BMR than in the hybrid approach. The 1 SD shift in the distribution of ln-ALT using the standard deviation approach is illustrated using Figure D-4 below for women of Kim et al. (2023b), using the period of 1999–2018 in NHANES. Note that the 1 SD shift is equivalent to a 38% extra risk if using the hybrid approach with the cutoff for the healthy population of Valenti (2021) and ½ SD shift is equivalent to 16% extra risk.

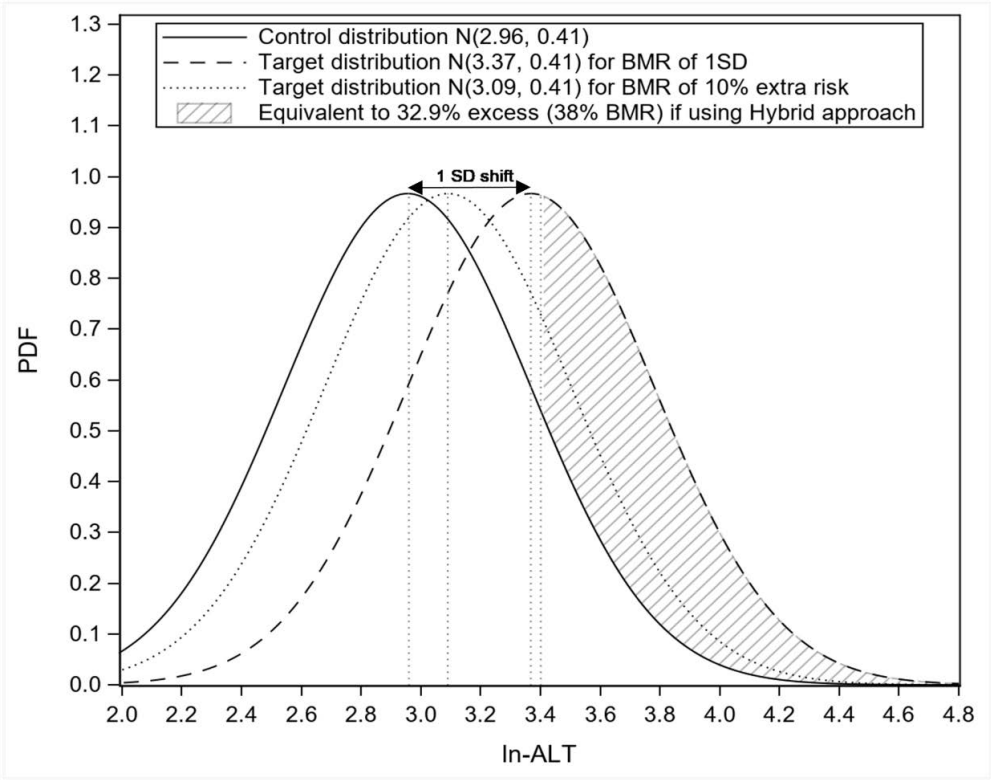

Figure D-4. The shift in the distribution using BMR of 1 SD for women of Kim et al. (2023b) compared to the shift using hybrid approach.

NOAEL Approach

Although both the measurements of ALT and standards for "unhealthy" ALT vary considerably across locations and years and although it is difficult to pinpoint exactly how exceedances of a selected ULN should be interpreted, from a BMD modeling perspective, these ULN cutoffs can inform the selection of a NOAEL. The simplest option is to look at the distributions of ALT and PFNA in the selected studies. In Kim et al. (2023b) and Nian et al. (2019), there was a significant linear relationship between $\log_2$-PFNA/ln-PFNA and ln-ALT; thus, there is a basic correspondence between the distribution of PFNA and the distribution of ALT in this population.

Acknowledging that there are likely to be many other predictors of ALT in this population and that the correspondence is likely to be more complex than a simple one-to-one relationship, there still may be some information that can provide context as a NOAEL for comparison purposes with the other PODs.

Building on the argument that the 95th percentile of ALT in a population represents the cutoff for abnormal levels, then the 95%-percentile can represent the LOAEL and a lower percentile of ALT can represent a NOAEL. In Kim et al. (2023b), the 75th-percentile ALT values are below, but still near to, the selected (Valenti, 2021) ULN cutoffs of 42 U/L in men and 30 U/L in women and thus, may be reasonably interpreted as a no effect level. The presented 95th percentile ALT values are far above the selected NOAEL, and the 50th percentile ALT values are well below the selected ULNs. The 75th percentile of ALT in Kim et al. (2023b) (see Table 2) was 33 U/L in men and 28 U/L in women. The 75th percentile of PFNA in Kim et al. (2023b) (see Table 2) was 3.28 ng/mL in men and 2.66 ng/mL in women. For elevated ALT associated with PFNA exposure, the NOAEL selected from the available epidemiological literature is 3.28 ng/mL in men and 2.66 ng/mL in women based on ALT data from Kim et al. (2023b).

The 75th percentile of ALT in Nian et al. (2019) (see Supplemental Table S4) was 30 U/L in men and 22 U/L in women. The 75th percentile of PFNA in Nian et al. (2019) (see Supplemental Table S4) was 3.24 ng/mL in men and 2.23 ng/mL in women. For elevated ALT associated with PFNA exposure, the NOAEL selected from the available epidemiological literature is 3.24 ng/mL in men and 2.23 ng/mL in women based on ALT data from Nian et al. (2019).

Summary and Selection of the POD

In each of the three approaches, women were found to have lower PODs, and the final PODs for Human Equivalent Doses (HEDs) were computed just for women as the more sensitive sex. EPA selected the PODs based on the *medium* confidence Kim et al. (2023b) study over those derived from the *medium* confidence Nian et al. (2019) study because the dose-response function from Kim et al. (2023b) was based on mixture modeling using multiple methods showing that PFNA is the strongest driver of the positive association with ALT. Therefore, it is unlikely that this association is confounded by other PFAS.

Table D-17 shows the PODs for internal dose (mg/L) and the POD_{HED} (mg/kg-day) for men and women based on Kim et al. (2023b). The range of values is 1.21×10^{-7} (mg/kg-day) to 1.46×10^{-6} (mg/kg-day), wherein the lower limit is based on a BMR of 5% and the upper limit is based on the BMR of 1 SD, the latter of which was equivalent to an extra risk of 38% using the hybrid approach. Even with a wide range of different methods to derive a POD_{HED}, there is only a one order of magnitude difference across three BMD methodologies within one sex and one study including the NOAEL/LOAEL approach.

EPA selected a BMR of 10% extra risk for ALT concentrations greater than the 95th percentile in the healthy subset in Valenti (2021) among women, based on the dose-response

function from Kim et al. (2023b), highlighted in Table D-17; the corresponding POD_{HED} is 1.82×10^{-7} (mg/kg-day).

Table D-17. PODs from the preferred epidemiological study of hepatic effects considered for the derivation of PFNA candidate toxicity values

Endpoint/Study/ Confidence	Species/sex	POD type/model	POD internal dose (mg/L)[a]	POD_{HED} (mg/kg-d)[b]
Elevated ALT representing increased risk of liver effects Kim et al. (2023b), *Medium* confidence	Human, female	$BMDL_{ER5}$, Hybrid with cutoff 30	1.34×10^{-3}	1.21×10^{-7}
	Human, female	$BMDL_{ER10}$, Hybrid with cutoff 30	2.02×10^{-3}	1.82×10^{-7}
	Human, female	$BMDL_{ER5}$, Hybrid with cutoff 33	1.55×10^{-3}	1.40×10^{-7}
	Human, female	$BMDL_{ER10}$, Hybrid with cutoff 33	2.56×10^{-3}	2.30×10^{-7}
	Human, female	$BMDL_{1/2SD}$, Standard Deviation	3.21×10^{-3}	2.89×10^{-7}
	Human, female	$BMDL_{1SD}$, Standard Deviation	12.41×10^{-3}	1.12×10^{-6}
	Human, female	BMDL, NOAEL	2.66×10^{-3}	2.39×10^{-7}
	Human, male	$BMDL_{ER5}$, Hybrid with cutoff 30	1.48×10^{-3}	1.33×10^{-7}
	Human, male	$BMDL_{ER10}$, Hybrid with cutoff 30	2.20×10^{-3}	1.98×10^{-7}
	Human, male	$BMDL_{ER5}$, Hybrid with cutoff 33	1.77×10^{-3}	1.53×10^{-7}
	Human, male	$BMDL_{ER10}$, Hybrid with cutoff 33	2.95×10^{-3}	2.66×10^{-7}
	Human, male	$BMDL_{1/2SD}$, Standard Deviation	3.89×10^{-3}	3.50×10^{-7}
	Human, male	$BMDL_{1SD}$, Standard Deviation	16.21×10^{-3}	1.46×10^{-6}
	Human, male	BMDL, NOAEL	3.28×10^{-3}	2.95×10^{-7}

[a] Units for the POD internal dose have changed from Tables D-14, D-15, and D-16 where they are ng/mL (to match the concentrations reported in the studies) to mg/L because EPA uses units of mg/kg-d for POD_{HEDS}. The conversion factor is (ng/mL)*(mg/10^6 ng)*(1,000 mL/L).

[b] POD_{HED} = POD internal dose (mg/L) × 0.090 mL/kg-d × 10^{-3} L/mL, using the estimated clearance for men and women above age 40.

Between the two hybrid approaches, EPA chose the Valenti (2021) 95th percentiles by the International Federation of Clinical Chemistry and Laboratory Medicine from the sub-cohort of healthy people screened for absence of viral hepatitis and metabolic syndrome. The use of these 95th percentile cutoffs is based on both a biological and statistical basis, per the Benchmark Dose Technical Guidance (U.S. EPA, 2012; Kavlock et al., 1995). EPA considered the BMR of 10% extra

risk to be the most appropriate as ALT concentrations above the 95th percentile would predominantly be considered to be (minimally) adverse. EPA selected the POD_{HED} value of **1.82×10^{-7} (mg/kg-day)** for elevated ALT as the candidate POD_{HED} for liver effects defined as increased risk of liver disease. Despite some uncertainties in the approach used to derive this value, the selected POD_{HED} is not substantially different from that derived using a NOAEL-based approach (i.e., 2.39×10^{-7} mg/kg-day), which mitigates concern about the uncertainties.

For comparison, the POD_{HED} based on women using Kim et al. (2023b) and a 5% BMR would be 1.21×10^{-7} (mg/kg-day); the POD_{HED} using the standard deviation approach for women using Kim et al. (2023b) and a BMR of 1 SD would be 1.12×10^{-6} (mg/kg-day); and the POD_{HED} using the NOAEL approach for women using Kim et al. (2023b) would be 2.39×10^{-7} (mg/kg-day). If the adversity of elevated ALT were judged to be more severe than (minimally) adverse based on the results of a 10-year longitudinal follow-up of Park et al. (2019) that found people with higher baseline ALT concentrations were at significantly increased risk for decompensated liver effects (cirrhosis), then the preferred POD_{HED} based on women using Kim et al. (2023b) and a 5% BMR would be 1.21×10^{-7}.

Confidence in the candidate toxicity value (i.e., the selected osRfD for hepatic effects) based on the POD_{HED} of **1.82×10^{-7} (mg/kg-day)** for ALT is described in Table D-18. The osRfD for hepatic effects, including UFs, is compared with the osRfD for developmental effects in Table D-19 below.

Table D-18. Confidence in the Hepatic osRfD

Confidence in study[a] used to derive osRfD	*Medium*	Confidence in the Kim et al. (2023b) study is rated as *medium*. The study was selected for deriving a POD for adverse liver effects because it was judged to have a "good" rating in the confounding domain during study review (see the heat map in Figure 3-40). Kim et al. (2023b) used directed acyclic graphs (DAGs) to select potential confounders, and all models included age, sex, education level, household income, smoking status, BMI, heavy drinking, and exercise. Mixture modeling using multiple methods showed that PFNA from among all the examined PFAS was the strongest driver of the positive association with ALT and GGT, the latter of which provides additional support for a hepatic origin of increased serum enzymes than ALT alone (Newsome et al., 2018; van Beek et al., 2013; Dufour et al., 2000). Additionally, the exposure distribution of PFNA was largely overlapping between Kim et al. (2023b) and a second study advanced for modeling by Nian et al. (2019). However, some residual uncertainty remains due to the cross-sectional design of the study and other minor limitations that are not expected to have resulted in selection bias.

Confidence in evidence base supporting this hazard	*Medium*	Confidence in the evidence base is *medium*. There was *moderate* evidence of consistent positive associations between increased serum enzymes (ALT, GGT, AST) and PFNA exposures in multiple medium confidence human studies. The available evidence further suggests that the associations are unlikely due to confounding by other PFAS based on mixture modeling in a subset of studies. However, some residual uncertainty remains regarding potential bias in epidemiological studies due to some general potential confounding by exposure to other co-occurring PFAS that cannot be entirely ruled out. It is unlikely that PFAS co-exposures would explain the observed associations given that PFNA was a top contributor across several PFAS based on multipollutant modeling in three of five studies. In further evidence of liver effects, there was additional cross-stream coherence from animal and mechanistic studies, including *robust* evidence of liver effects based on consistent and coherent treatment-related increases in liver weight, histopathology, hepatobiliary cholestasis, and some clinical chemistry markers (e.g., increased ALT that was modest in rats but pronounced in mice) across multiple studies, species, rodent strains, sexes, and lifestages. Although uncertainties remain (e.g., lack of longer duration exposures), the animal and mechanistic findings were found in this assessment to meet the criteria set forth by Hall et al. (2012) for adversity (see Section 3.2.4. Hepatic Effects, Consideration for potential adaptive versus adverse responses). Overall, however, uncertainties in the available evidence base, particularly the studies on serum enzymes ultimately used to derive the selected quantitative estimate, best support a confidence level of *medium*.
Confidence in quantification of the POD_{HED}	*Medium*	Confidence in the quantification of the POD and osRfD is *medium*. The POD was based on a BMD hybrid approach within the range of the observed data. Uncertainty remains regarding the use and selection of the cutoff applied in the hybrid approach as well as the lack of a clear basis for BMR selection. However, this concern is reduced because three different methods, each examining multiple BMRs, all yielded PODs within a narrow range, and the PODs from the critical study (Kim et al., 2023b) were similar to those identified from another human study by Nian et al. (2019). Dosimetric calculation of the HED using the PFNA-specific clearance also introduces some uncertainty, however the clearance used is expected to provide appropriate coverage for the majority of adults when used in combination with UF_A = 3 (see discussion of "Analysis of uncertainty in the pharmacokinetic modeling of PFNA," in Section 5.2.1 of main document).
Overall confidence in the osRfD	*Medium*	The overall confidence in the osRfD is *medium* driven by *medium* confidence in the study, evidence base, and quantification of the POD_{HED}.

[a]Study evaluation details can be found in HAWC.

For comparison with the selected POD_{HED} and draft osRfD:

Table D-19. PODs from epidemiological evidence considered for the derivation of PFNA candidate toxicity values

Endpoint	Study/ confidence	Strain/ species/sex	POD type/model	POD internal dose (mg/L)	POD_{HED} (mg/kg-d)	UF_C	osRfD (mg/kg-d)	Confidence
Decreased birth weight	Sagiv et al. (2018), *High* confidence	Human, male and female	$BMDL_{ER5}$, Hybrid	1.19×10^{-3}	1.48×10^{-7} [a]	30[c]	5×10^{-9}	*Medium-high*[d]
Increased risk of liver effects	Kim et al. (2023b), *Medium* confidence	Human, female	$BMDL_{ER10}$, Hybrid	2.02×10^{-3}	1.82×10^{-7} [b]	30[c]	6×10^{-9}	*Medium*[e]

[a]POD_{HED} = POD internal dose (mg/L) × 0.124 mL/kg-d × 10^{-3} L/mL, based on estimated clearance in women of reproductive age.
[b]POD_{HED} = POD internal dose (mg/L) × 0.09 mL/kg-d × 10^{-3} L/mL, based on estimated clearance in men and women above age 40.
[c]UF_C = 30; UF_A = 1, UF_H = 10; UF_S = 1, UF_L = 1, UF_D = 3.
[d]Based on high confidence in the principal study, medium-high confidence in the evidence base, and medium confidence in the derivation of the POD_{HED} (see Step 2 draft).
[e]Based on medium confidence in the principal study, medium confidence in the evidence base, and medium confidence in the derivation of the POD_{HED} (see Table D-18).

The selected POD_{HED} for increased risk of liver effects in humans is approximately the same as the POD_{HED} for decreased birthweight in humans used to derive the RfD in the drafts previously reviewed by EPA and interagency partners. Given the similarities between the two osRfDs, the hepatic osRfD is considered supportive of the selected overall RfD based on developmental effects in the current draft being prepared for Step 4 release. The following language is used in the updated draft to describe RfD selection: "The organ-/system-specific RfD value for PFNA selected in the previous section is summarized in Table 5-20. From the identified human health effects of PFNA and the derived osRfD for developmental effects, an overall RfD of 7×10^{-9} mg/kg-day based on decreased birth weights in humans was selected. As described in Table 5-19, confidence in the RfD is medium-high, based on medium-high confidence in the developmental osRfD. The developmental osRfD is based on a meta-analysis of 10 studies. The developmental osRfD is expected to be protective across all lifestages and is based on effects observed in males and females indicating that the overall RfD would be protective for both sexes. Additional support for the developmental osRfD comes from the nearly identical *medium* confidence hepatic osRfD of 6×10^{-9} mg/kg-day based on increased ALT in adult females from a *medium* confidence epidemiological study. The negligibly higher developmental osRfD was selected over the hepatic osRfD due to greater overall confidence in the value, including higher confidence in the precision of the POD (see Table 5-19).

D.2. BENCHMARK DOSE MODELING SUMMARY OF ANIMAL STUDIES

The endpoints selected for benchmark dose (BMD) modeling are listed in Table D-20. The animal doses in the study were used in the BMD modeling and then converted to human equivalent doses (HEDs) using the PK model described in Section 3.1 of the main document to derive potential points of departure (PODs) relevant to human health; the BMD modeling results are presented in this appendix.

D.2.1. Modeling Procedures for Dichotomous and Continuous Noncancer Data

BMD modeling of dichotomous noncancer data was conducted using EPA's Benchmark Dose Software (BMDS, version 3.2). For these data, the Gamma, Logistic, Log-Logistic, Log-Probit, Multistage, Probit, Weibull, and Dichotomous Hill models available within the software were fit using a benchmark response (BMR) of 10% extra risk. The Multistage model is run for all polynomial degrees up to $n - 2$, where n is the number of dose groups including control. Adequacy of model fit was judged on the basis of χ^2 goodness-of-fit p-value ($p > 0.1$), scaled residuals at the data point (except the control) closest to the predefined benchmark response (absolute value < 2.0), and visual inspection of the model fit. Among all models providing adequate fit, the benchmark dose lower confidence limit (BMDL) from the model with the lowest Akaike's information criterion (AIC) was selected as a potential POD when BMDL values were sufficiently close (within threefold). Otherwise, the lowest BMDL was selected as a potential POD unless otherwise specified in results table footnotes.

BMD modeling of continuous noncancer data was conducted using EPA's Benchmark Dose Software (BMDS, version 3.2). For these data, the Exponential, Hill, Polynomial, and Power models available within the software are fit using a BMR of 1 standard deviation (SD) when no toxicological information was available to determine an adverse level of response. When toxicological information was available, the BMR was based on relative deviation, as outlined in the *Benchmark Dose Technical Guidance* (U.S. EPA, 2012). An adequate fit is judged on the basis of χ^2 goodness-of-fit p-value ($p > 0.1$), scaled residuals at the data point (except the control) closest to the predefined benchmark response (absolute value < 2.0), and visual inspection of the model fit. In addition to these three criteria for judging adequacy of individual model fit, a determination is made on whether the variance across dose groups can be modeled under one of two assumptions; failure to do so suggests an unreliable or biologically uninformative set of data. If a homogeneous variance model, also referred to as a "constant variance" (CV) model, is deemed appropriate based on the statistical test provided by BMDS (Test 2 for homogeneity of variance), the final BMD results are presented for the CV model. If the Test 2 p-value is significant ($p < 0.05$), the model is run again while modeling the variance as a power function of the mean to account for this nonhomogeneous variance, also referred to as "non-constant variance" (NCV). If the NCV model provides adequate fit to the variance of the data (i.e., Test 3 p-value > 0.05), the final BMD results are presented for the NCV model. If the variance data cannot be modeled by either CV or NCV models, the results of the NCV model will be presented and PODs will be determined by other methods (either a LOAEL/NOAEL approach or a removal of the high dose group as discussed below). After choosing the appropriate variance model, among all models providing adequate fit, the BMDL from the model with the lowest AIC was selected as a potential POD when BMDL estimates differed by less than threefold. Models with BMDLs that were 10-fold or lower than the lowest non-zero dose are excluded from further consideration to avoid substantial extrapolation beyond the observed dose range. When BMDL estimates differed by greater than threefold, the model with the lowest BMDL was selected to account for model uncertainty.

In cases where no best model was judged adequate based on model fit for a given non-cancer continuous or dichotomous endpoint and the corresponding experiment included three or more non-zero dose groups, BMD modeling was attempted on a reduced dataset with one [or more] high dose group[s] removed. If removal of the high dose group[s] resulted in adequate model fit and/or improved fit in the low dose range, these results were considered for POD derivation. Similarly, for non-cancer continuous endpoints meeting the same dataset criteria (at least three non-zero dose groups), in the case where both CV and NCV models fail to model the variance of the full dataset despite an adequate model fit, POD derivation with a reduced dataset is considered appropriate if removal of the high dose group[s] results in adequate variance modeled by either CV or NCV models. If the final POD is based on a reduced dataset, the full dataset will be provided, and results of the reduced dataset will be presented in the results summary; the title of the table for the BMD results will indicate which groups were used in the final model. If the BMDS fails to

recommend a viable model after taking the above considerations into account, final POD derivation is based on a NOAEL/LOAEL approach. The NOAEL/LOAEL approach for POD derivation may also be employed for endpoints with viable BMD values under special consideration as noted in the footnotes of the table results.

D.2.2. Data Used for Modeling

The source of the data used for modeling endpoints from animal studies is provided in Table D-20. These data also are included in full in the tables below.

Table D-20. Sources of data used in benchmark dose modeling of PFNA endpoints from animal studies

Endpoint/reference	Reference	HAWC link
Male reproductive		
Cauda epididymis weight (absolute)	NTP (2018) RAT	https://hawcprd.epa.gov/ani/endpoint/100505669/
↓ Epididymis weight (absolute)	NTP (2018) RAT	https://hawcprd.epa.gov/ani/endpoint/100505668/
↓ Testis weight – Right	NTP (2018) RAT	https://hawcprd.epa.gov/ani/endpoint/100505667/
↓ Testis weight – Left	NTP (2018) RAT	https://hawcprd.epa.gov/ani/endpoint/100505723/
↑ Testis – interstitial (Leydig) cell atrophy	NTP (2018) RAT	https://hawcprd.epa.gov/ani/endpoint/100505676/
↑ Testis – germinal epithelium degeneration	NTP (2018) RAT	https://hawcprd.epa.gov/ani/endpoint/100509299/
↑ Testis – seminiferous tubule spermatid retention	NTP (2018) RAT	https://hawcprd.epa.gov/ani/endpoint/100505681/
↑ Epididymis – duct exfoliated germ cell	NTP (2018) RAT	https://hawcprd.epa.gov/ani/endpoint/100505706/
↑ Epididymis – epithelium apoptosis	NTP (2018) RAT	https://hawcprd.epa.gov/ani/endpoint/100505707/
↑ Epididymis – hypospermia	NTP (2018) RAT	https://hawcprd.epa.gov/ani/endpoint/100505705/
↓ Serum testosterone	NTP (2018) RAT	https://hawcprd.epa.gov/ani/endpoint/100505670/
↓ Sperm Count – Cauda epididymis, Absolute	NTP (2018) RAT	https://hawcprd.epa.gov/ani/endpoint/100505677/
Hepatic		
↑ Liver weight, relative male	NTP (2018) RAT	https://hawcprd.epa.gov/ani/endpoint/100505638/

Endpoint/reference	Reference	HAWC link
↑ Liver weight, relative female	NTP (2018) RAT	https://hawcprd.epa.gov/ani/endpoint/100505741/
↑ Liver weight, relative male	Wang (2015) MOUSE	https://hawcprd.epa.gov/ani/endpoint/100505359/
↑ Liver weight, relative female (nonpregnant)	Das 2015 MOUSE	https://hawcprd.epa.gov/ani/endpoint/100505385/
↑ Liver weight, relative female (nonpregnant)	Wolf 2010 MOUSE (WT)	https://hawcprd.epa.gov/ani/endpoint/100505613/
↑ Liver weight, relative mixed (pups PND 1)	Das 2015 MOUSE	https://hawcprd.epa.gov/ani/endpoint/100505405/
↑ Liver weight, relative mixed (pups PND 24)	Das 2015 MOUSE	https://hawcprd.epa.gov/ani/endpoint/100505407/
↑ Liver weight, relative mixed (pups PND 70)	Das 2015 MOUSE	https://hawcprd.epa.gov/ani/endpoint/100505409/
↑ Liver weight, relative mixed (pups PND 21)	Wolf 2010 MOUSE (WT)	https://hawcprd.epa.gov/ani/endpoint/100505517/
↑ Hepatic hypertrophy male	NTP (2018) RAT	https://hawcprd.epa.gov/ani/endpoint/100505639/
↑ Hepatic hypertrophy female	NTP (2018) RAT	https://hawcprd.epa.gov/ani/endpoint/100505742/
Endocrine (thyroid)		
↓Thyroxine total T4 female	NTP (2018) RAT	https://hawcprd.epa.gov/ani/endpoint/100505787/
↓Thyroxine free T4 female	NTP (2018) RAT	https://hawcprd.epa.gov/ani/endpoint/100505673/
Developmental		
↓ Survival mixed (pups PND 21)	Das 2015 MOUSE	https://hawcprd.epa.gov/ani/endpoint/100505438/
↓ Survival mixed (pups PND 21)	Wolf 2010 MOUSE (WT)	https://hawcprd.epa.gov/ani/endpoint/100505514/
↓ Offspring body weight mixed (pups PND 7)	Das 2015 MOUSE	https://hawcprd.epa.gov/ani/endpoint/100505419/
↓ Offspring body weight male (pups PND 7)	Wolf 2010 MOUSE (WT)	https://hawc.epa.gov/ani/endpoint/100505564/
↓ Offspring body weight Female (pups PND 7)	Wolf 2010 MOUSE (WT)	https://hawc.epa.gov/ani/endpoint/100505556/
↓ offspring body weight mixed (pups PND 21)	Das 2015 MOUSE	https://hawcprd.epa.gov/ani/endpoint/100505423/
↓ offspring body weight	Wolf 2010	https://hawc.epa.gov/ani/endpoint/100505567/

Endpoint/reference	Reference	HAWC link
male (pups PND 21)	MOUSE (WT)	
↓ offspring body weight female (pups PND 21)	Wolf 2010 MOUSE (WT)	https://hawc.epa.gov/ani/endpoint/100505550/
↓ offspring body weight, post-weaning male (pups PND 24)	Das 2015 MOUSE	https://hawcprd.epa.gov/ani/endpoint/100505395/
↓ offspring body weight, post-weaning female (pups PND 24)	Das 2015 MOUSE	https://hawcprd.epa.gov/ani/endpoint/100505392/
↓ offspring body weight, post-weaning female (pups PND 42)	Das 2015 MOUSE	https://hawcprd.epa.gov/ani/endpoint/100532128/
↓ offspring body weight, post-weaning male (pups PND 287)	Das 2015 MOUSE	https://hawcprd.epa.gov/ani/endpoint/100505400/
Delayed eye opening	Das 2015 MOUSE	https://hawcprd.epa.gov/ani/endpoint/100505404/
Delayed preputial separation	Das 2015 MOUSE	https://hawcprd.epa.gov/ani/endpoint/100505394/

D.2.3. Individual Endpoint Modeling Results

Decreased Cauda Epididymis Weight (Absolute) in Rats (NTP, 2018)

Table D-21. Dose-response data for absolute decreased cauda epididymis weight in rats (NTP, 2018)

Dose (mg/kg-d)	n	Mean (g)	SD
0	10	0.195	0.01581
0.625	10	0.189	0.01581
1.25	10	0.173	0.01265
2.5	10	0.13	0.02530

Table D-22. Benchmark dose results for absolute decreased cauda epididymis weight in male rats — constant variance, BMR = 1 standard deviation (NTP, 2018)

Models	Test 2 (*p*-value)	1 standard deviation		Goodness of fit (*p*-value)	AIC	BMDS classification[a]	BMDS notes
		BMD	BMDL				
Exponential 2 (CV—normal)	0.1352	0.6050	0.4618	0.0627	−200.4286	Questionable	Goodness-of-fit *p*-value < 0.1
Exponential 3 (CV—normal)	**0.1352**	**1.0783**	**0.6865**	**0.9118**	**−203.9545**	**Viable – Recommended**	**Lowest AIC**
Exponential 4 (CV—normal)	0.1352	0.6050	0.4618	0.0627	−200.4286	Questionable	Goodness-of-fit *p*-value < 0.1
Exponential 5 (CV—normal)	0.1352	1.0785	0.6868	NA	−201.9561	Questionable	d.f. = 0, saturated model (Goodness-of-fit test cannot be calculated)
Hill (CV—normal)	0.1352	1.2404	0.6330	NA	−201.3561	Questionable	d.f. = 0, saturated model (Goodness-of-fit test cannot be calculated)
Polynomial (3 degree) (CV—normal)	0.1352	1.0759	0.6408	0.7378	−203.8547	Viable – Alternate	
Polynomial (2 degree) (CV—normal)	0.1352	1.0759	0.6488	0.7378	−203.8547	Viable – Alternate	
Power (CV—normal)	0.1352	1.0728	0.6635	0.8355	−203.9237	Viable – Alternate	
Linear (CV—normal)	0.1352	0.6630	0.5242	0.1800	−202.5371	Viable – Alternate	

[a]"Classification" column denotes whether a model can be considered for model selection purposes. See BMDS User Guide: https://www.epa.gov/bmds.

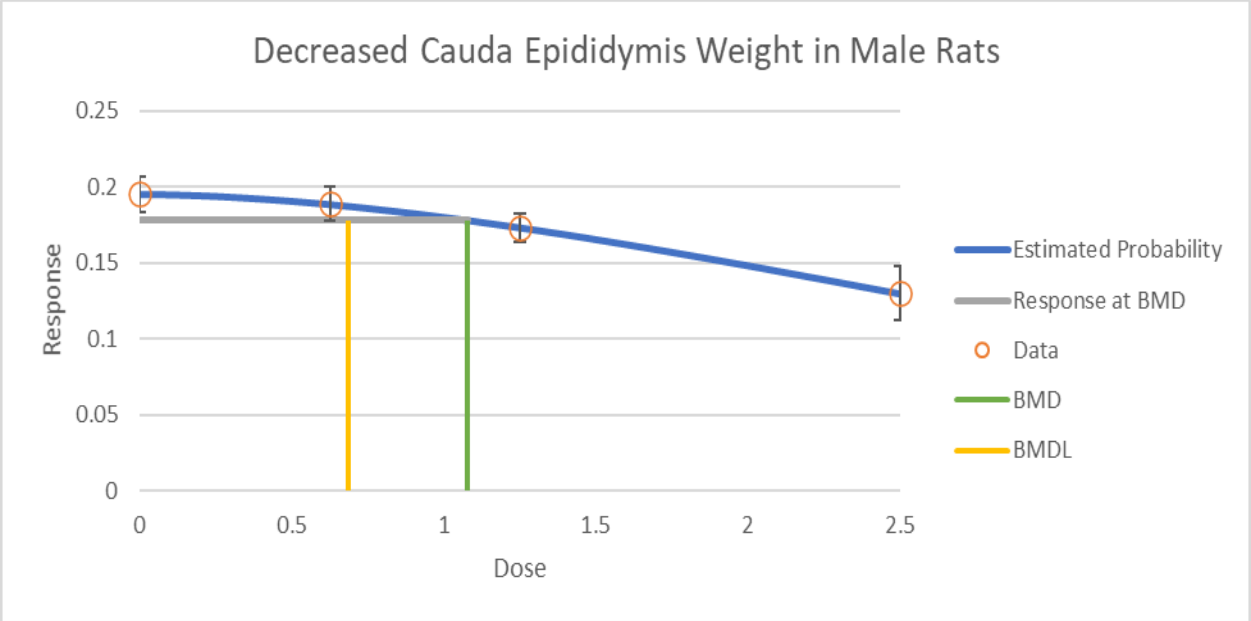

Figure D-5. Dose-response data and curve of the exponential degree 3 model for absolute decreased cauda epididymis weight in male rats (NTP, 2018)[a].

[a]X-axis is dose (mg/kg-d), and y-axis is absolute cauda epididymis weight (g).

Decreased Epididymis Weight (Absolute) in Rats (NTP, 2018)

Table D-23. Dose-response data for decreased absolute epididymis weight in rats (NTP, 2018)

Dose (mg/kg-d)	n	Mean (g)	SD
0	10	0.555	0.04110961
0.625	10	0.515	0.031622777
1.25	10	0.482	0.015811388
2.5	10	0.363	0.069570109

Table D-24. Benchmark dose results for decreased absolute epididymis weight in male rats (highest dose removed) — non-constant variance, BMR = 1 standard deviation (NTP, 2018)

Models	Test 3 (*p*-value)	1 standard deviation		Goodness of fit (*p*-value)	AIC	BMDS classification[a]	BMDS notes
		BMD	BMDL				
Exponential 2 (NCV—normal)	0.4234	0.7304	0.4671	0.8231	−125.1820	Viable – Alternate	
Exponential 3 (NCV—normal)	0.4234	0.7453	0.4673	NA	−123.2258	Questionable	d.f. = 0, saturated model (Goodness-of-fit test cannot be calculated)
Exponential 4 (NCV—normal)	0.4234	0.7200	0.4653	0.8299	−125.1858	Viable – Alternate	
Exponential 5 (NCV—normal)	0.4234	0.7572	0.4670	<0.0001	−121.2312	Questionable	Goodness-of-fit *p*-value < 0.1
Hill (NCV—normal)	0.4234	0.6404	0.3603	<0.0001	−121.2311	Questionable	Goodness-of-fit *p*-value < 0.1
Polynomial (2 degree) (NCV—normal)	0.4234	0.7566	0.4935	NA	−123.2303	Questionable	d.f. = 0, saturated model (Goodness-of-fit test cannot be calculated)
Power (NCV—normal)	0.4234	0.7559	0.4936	NA	−123.2305	Questionable	d.f. = 0, saturated model (Goodness-of-fit test cannot be calculated)
Linear (NCV—normal)	**0.4234**	**0.7451**	**0.4933**	**0.9265**	**−125.2235**	**Viable – Recommended**	**Lowest AIC**

[a]"Classification" column denotes whether a model can be considered for model selection purposes. See BMDS User Guide: https://www.epa.gov/bmds.

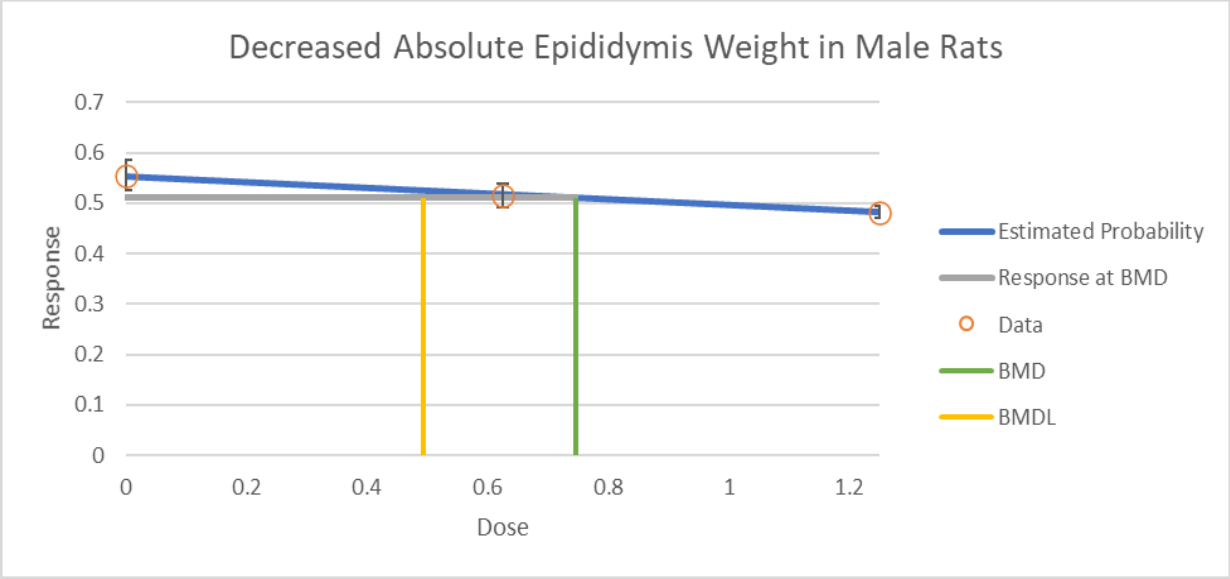

Figure D-6. Dose-response data and curve of the linear model for absolute decreased epididymis weight in male rats (NTP, 2018)[a].

[a]X-axis is dose (mg/kg-d), and y-axis is epididymis weight (g).

Decreased Right Testis Weight (Absolute) in Rats (NTP, 2018)

Table D-25. Dose-response data for decreased absolute right testis weight in rats (NTP, 2018)

Dose (mg/kg-d)	n	Mean (g)	SD
0	10	1.87	0.14230249
0.625	10	1.793	0.11067972
1.25	10	1.757	0.10119289
2.5	10	1.493	0.17392527
5	2	0.636	0.03252691

Table D-26. Benchmark dose results for decreased absolute right testis weight in rats — constant variance, BMR = 1 standard deviation (NTP, 2018)

Models	Test 2 (*p*-value)	1 standard deviation		Goodness of fit (*p*-value)	AIC	BMDS classification[a]	BMDS notes
		BMD	BMDL				
Exponential 2 (CV—normal)	0.0732	0.7202	0.5576	<0.0001	−24.8848	Questionable	Goodness-of-fit *p*-value < 0.1
Exponential 3 (CV—normal)	0.0732	1.5510	1.2235	0.5448	−46.1578	Viable – Alternate	
Exponential 4 (CV—normal)	0.0732	0.7202	0.5576	<0.0001	−24.8848	Questionable	Goodness-of-fit *p*-value < 0.1
Exponential 5 (CV—normal)	0.0732	1.5510	1.2235	0.5448	−46.1578	Viable – Alternate	
Hill (CV—normal)	0.0732	1.3749	1.0346	0.3800	−44.6017	Viable – Alternate	
Polynomial (4 degree) (CV—normal)	0.0732	1.2586	0.7457	0.4531	−44.8095	Viable – Alternate	
Polynomial (3 degree) (CV—normal)	0.0732	1.2586	0.7831	0.4531	−44.8095	Viable – Alternate	
Polynomial (2 degree) (CV—normal)	0.0732	1.2836	0.9005	0.7512	−46.8004	Viable – Recommended	Lowest AIC
Power (CV—normal)	0.0732	1.3718	1.0295	0.6823	−46.6078	Viable – Alternate	
Linear (CV—normal)	0.0732	0.7225	0.5842	0.0012	−33.4421	Questionable	Goodness-of-fit *p*-value < 0.1

[a]"Classification" column denotes whether a model can be considered for model selection purposes. See BMDS User Guide: https://www.epa.gov/bmds.

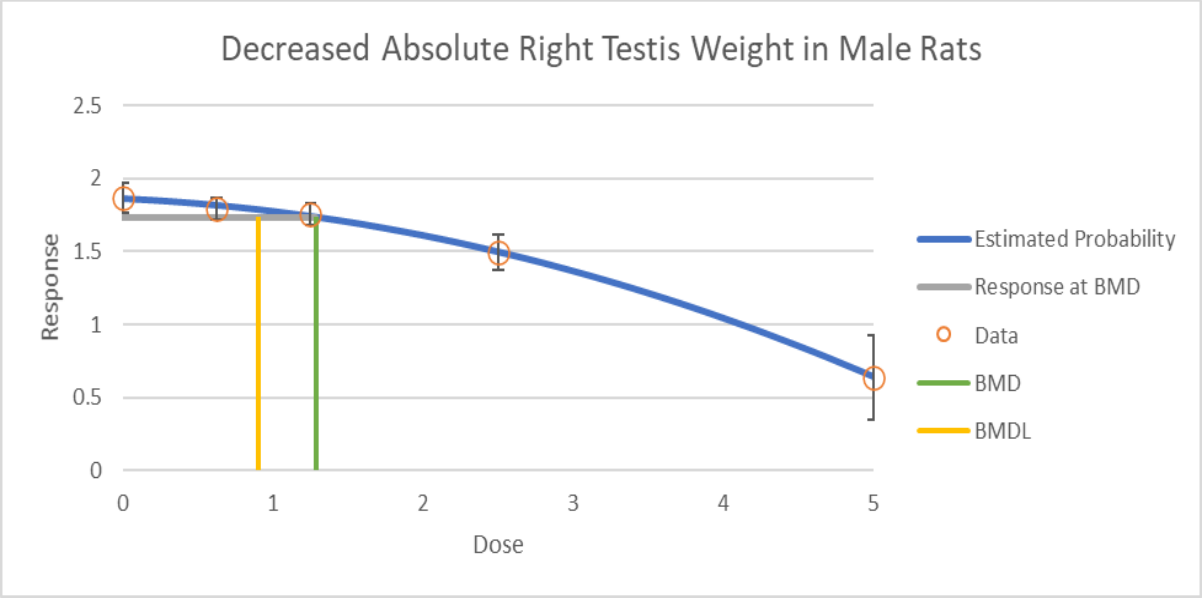

Figure D-7. Dose-response data and curve of the polynomial degree 2 model for decreased absolute right testis weight in male rats (NTP, 2018)[a].

[a]X-axis is dose (mg/kg-d), and y-axis is absolute right testis weight (g).

Decreased Left Testis Weight (Absolute) in Rats (NTP, 2018)

Table D-27. Dose-response data for decreased absolute left testis weight in rats (NTP, 2018)

Dose (mg/kg-d)	n	Mean (g)	SD
0	10	1.885	0.129653384
0.625	10	1.82	0.110679718
1.25	10	1.762	0.098030607
2.5	10	1.507	0.164438438

Table D-28. Benchmark dose results for decreased absolute left testis weight in rats — constant variance, BMR = 1 standard deviation (NTP, 2018)

Models	Test 2 (*p*-value)	1 standard deviation		Goodness of fit (*p*-value)	AIC	BMDS classification[a]	BMDS notes
		BMD	BMDL				
Exponential 2 (CV—normal)	0.3792	0.7747	0.5830	0.2704	−46.4356	Viable – Alternate	
Exponential 3 (CV—normal)	0.3792	1.2221	0.6891	0.5852	−46.7534	Viable – Alternate	
Exponential 4 (CV—normal)	0.3792	0.7747	0.5830	0.2704	−46.4356	Viable – Alternate	
Exponential 5 (CV—normal)	0.3792	1.2228	0.6891	0.5852	−46.7534	Viable – Alternate	
Hill (CV—normal)	0.3792	1.2159	0.6886	NA	−44.7949	Questionable	d.f. = 0, saturated model (Goodness-of-fit test cannot be calculated)
Polynomial (3 degree) (CV—normal)	0.3792	1.2295	0.7036	0.8083	−46.9924	Viable – Alternate	
Polynomial (2 degree) (CV—normal)	0.3792	1.2125	0.6928	0.6918	−46.8942	Viable – Alternate	
Power (CV—normal)	0.3792	1.2184	0.6927	0.6142	−46.7972	Viable – Alternate	
Linear (CV—normal)	**0.3792**	**0.8184**	**0.6312**	**0.3786**	**−47.1089**	**Viable – Recommended**	**Lowest AIC**

[a]"Classification" column denotes whether a model can be considered for model selection purposes. See BMDS User Guide: https://www.epa.gov/bmds.

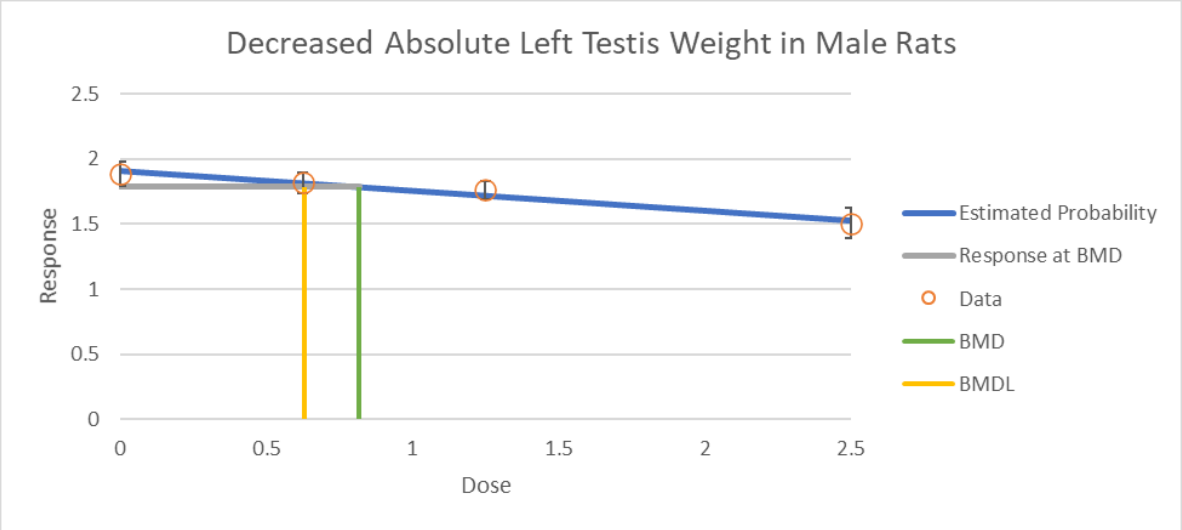

Figure D-8. Dose-response data and curve of the linear model for decreased absolute left testis weight in rats (NTP, 2018)[a].

[a]X-axis is dose (mg/kg-d), and y-axis is absolute left testis weight (g).

Increased Interstitial (Leydig) Cell Atrophy (Testis) in Rats (NTP, 2018)

Table D-29. Dose-response data for increased interstitial (Leydig) cell atrophy (testis) in rats (NTP, 2018)

Dose (mg/kg-d)	N	Incidence
0	10	0
0.625	10	0
1.25	10	1
2.5	10	10
5	9	9
10	10	10

Table D-30. Benchmark dose results for increased interstitial (Leydig) cell atrophy (testis) in rats, BMR = 10% extra risk (NTP, 2018)

Models	10% extra risk		Goodness of fit (*p*-value)	AIC	BMDS classification[a]	BMDS notes
	BMD	BMDL				
Dichotomous Hill	1.2409	1.0124	0.9908	12.7130	Viable – Alternate	
Gamma	1.1865	0.9390	0.9924	9.3600	Viable – Alternate	
Log-Logistic	1.2409	1.0124	0.9986	10.7130	Viable – Alternate	
Multistage (Degree 5)	1.1703	0.7867	0.9985	8.8997	Viable – Alternate	
Multistage (Degree 4)	1.0476	0.7428	0.9608	10.0757	Viable – Alternate	
Multistage (Degree 3)	0.8747	0.6258	0.7431	12.7481	Viable – Alternate	
Multistage (Degree 2)	0.6295	0.4336	0.3048	17.9460	Viable – Alternate	
Multistage (Degree 1)	0.2188	0.1487	0.0080	31.4363	Questionable	Goodness-of-fit *p*-value < 0.1 BMDL 3× lower than lowest non-zero dose
Weibull	0.8899	0.8152	0.5398	15.5983	Viable – Alternate	
Logistic	**1.2502**	**0.9609**	**1.0000**	**8.5066**	**Viable – Recommended**	**Lowest AIC**
Log-Probit	1.2500	1.0202	1.0000	10.5017	Viable – Alternate	
Probit	1.0592	0.7568	0.8966	11.3399	Viable – Alternate	

[a]"Classification" column denotes whether a model can be considered for model selection purposes. See BMDS User Guide: https://www.epa.gov/bmds.

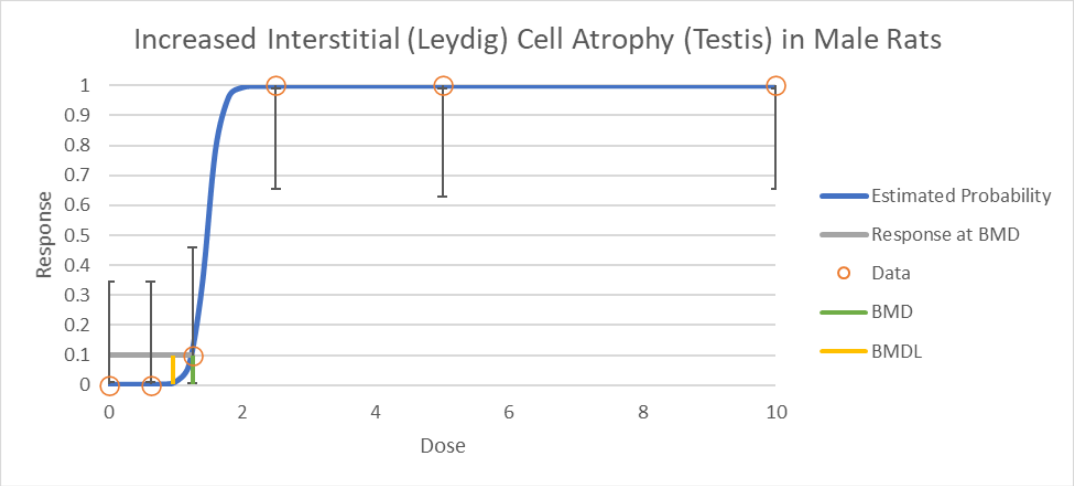

Figure D-9. Dose-response data and curve of the logistic model for increased interstitial (Leydig) cell atrophy (testis) in rats (NTP, 2018)[a].

[a]X-axis is dose (mg/kg-d), and y-axis is percent incidence of interstitial cell atrophy (testis).

Increased Germinal Epithelium Degeneration (Testis) in Rats (NTP, 2018)

Table D-31. Dose-response data for increased germinal epithelium degeneration (testis) in male rats (NTP, 2018)

Dose (mg/kg-d)	N	Incidence
0	10	0
0.625	10	0
1.25	10	0
2.5	10	6
5	9	9
10	10	10

Table D-32. Benchmark dose results for increased germinal epithelium degeneration (testis) in rats, BMR = 10% extra risk (NTP, 2018)

Models	10% extra risk		Goodness of fit (*p*-value)	AIC	BMDS classification[a]	BMDS notes
	BMD	BMDL				
Dichotomous Hill	2.0367	1.2758	1.0000	19.4666	Viable – Alternate	
Gamma	1.7196	1.1964	0.9992	17.6171	Viable – Alternate	
Log-Logistic	2.0367	1.2758	1.0000	15.4666	Viable – Alternate	
Multistage (Degree 5)	1.6388	1.1225	0.9977	16.0358	Viable – Alternate	
Multistage (Degree 4)	1.4936	1.0453	0.9871	16.6158	Viable – Alternate	
Multistage (Degree 3)	1.2924	0.8959	0.9331	17.8245	Viable – Alternate	
Multistage (Degree 2)	0.9324	0.6431	0.6666	21.2781	Viable – Alternate	
Multistage (Degree 1)	0.3345	0.2286	0.0418	34.4466	Questionable	Goodness-of-fit *p*-value < 0.1
Weibull	1.4382	0.0000	0.9667	17.0865	Unusable	BMD computation failed BMDL not estimated
Logistic[b]	2.1465	1.3040	1.0000	15.4633	Viable – Recommended	Lowest AIC
Log-Probit	2.2146	1.2403	1.0000	17.4602	Viable – Alternate	
Probit	1.6914	1.1861	0.9986	15.8960	Viable – Alternate	

[a]"Classification" column denotes whether a model can be considered for model selection purposes. See BMDS User Guide: https://www.epa.gov/bmds.

[b]Note that while BMDS 3.2 recommends a viable model, the NOAEL/LOAEL approach was applied to this endpoint given that the response was much greater than the BMR in the lowest responding dose group.

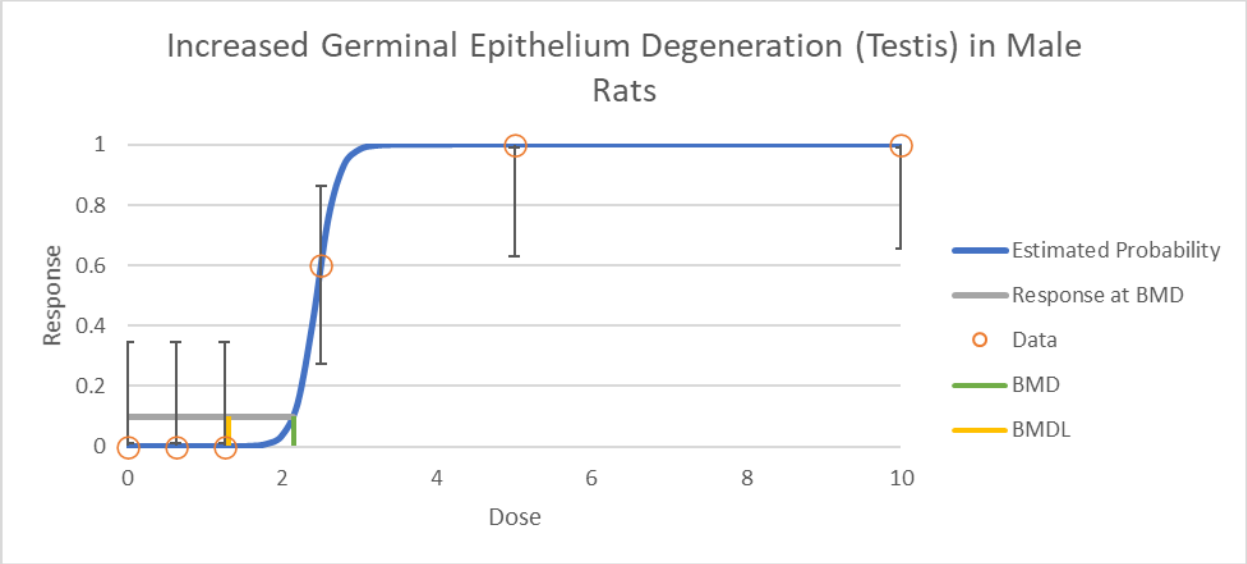

Figure D-10. Dose-response data and curve of the logistic model for increased germinal epithelium degeneration (testis) in male rats (NTP, 2018)[a].

[a]X-axis is dose (mg/kg-d), and y-axis is percent incidence of germinal epithelium degeneration (testis).

Increased Spermatid Retention (Seminiferous Tubule) in Rats (NTP, 2018)

Table D-33. Dose-response data for increased spermatid retention (seminiferous tubule) in male rats (NTP, 2018)

Dose (mg/kg-d)	N	Incidence
0	10	0
0.625	10	0
1.25	10	0
2.5	10	6
5	9	9
10	10	10

Table D-34. Benchmark dose results for increased spermatid retention (seminiferous tubule) in rats, BMR = 10% extra risk (NTP, 2018)

Models	10% extra risk		Goodness of fit (*p*-value)	AIC	BMDS classification[a]	BMDS notes
	BMD	BMDL				
Dichotomous Hill	2.0367	1.2758	1.0000	19.4666	Viable – Alternate	
Gamma	1.7196	1.1964	0.9992	17.6171	Viable – Alternate	
Log-Logistic	2.0367	1.2758	1.0000	15.4666	Viable – Alternate	
Multistage (Degree 5)	1.6388	1.1225	0.9977	16.0358	Viable – Alternate	
Multistage (Degree 4)	1.4936	1.0453	0.9871	16.6158	Viable – Alternate	
Multistage (Degree 3)	1.2924	0.8959	0.9331	17.8245	Viable – Alternate	
Multistage (Degree 2)	0.9324	0.6431	0.6666	21.2781	Viable – Alternate	
Multistage (Degree 1)	0.3345	0.2286	0.0418	34.4466	Questionable	Goodness-of-fit *p*-value < 0.1
Weibull	1.4382	0.0000	0.9667	17.0865	Unusable	BMD computation failed BMDL not estimated
Logistic[b]	**2.1465**	**1.3040**	**1.0000**	**15.4633**	**Viable – Recommended**	**Lowest AIC**
Log-Probit	2.2146	1.2403	1.0000	17.4602	Viable – Alternate	
Probit	1.6914	1.1861	0.9986	15.8960	Viable – Alternate	

[a]"Classification" column denotes whether a model can be considered for model selection purposes. See BMDS User Guide: https://www.epa.gov/bmds.

[b]Note that while BMDS 3.2 recommends a viable model, the NOAEL/LOAEL approach was applied to this endpoint given that the response was much greater than the BMR in the lowest responding dose group.

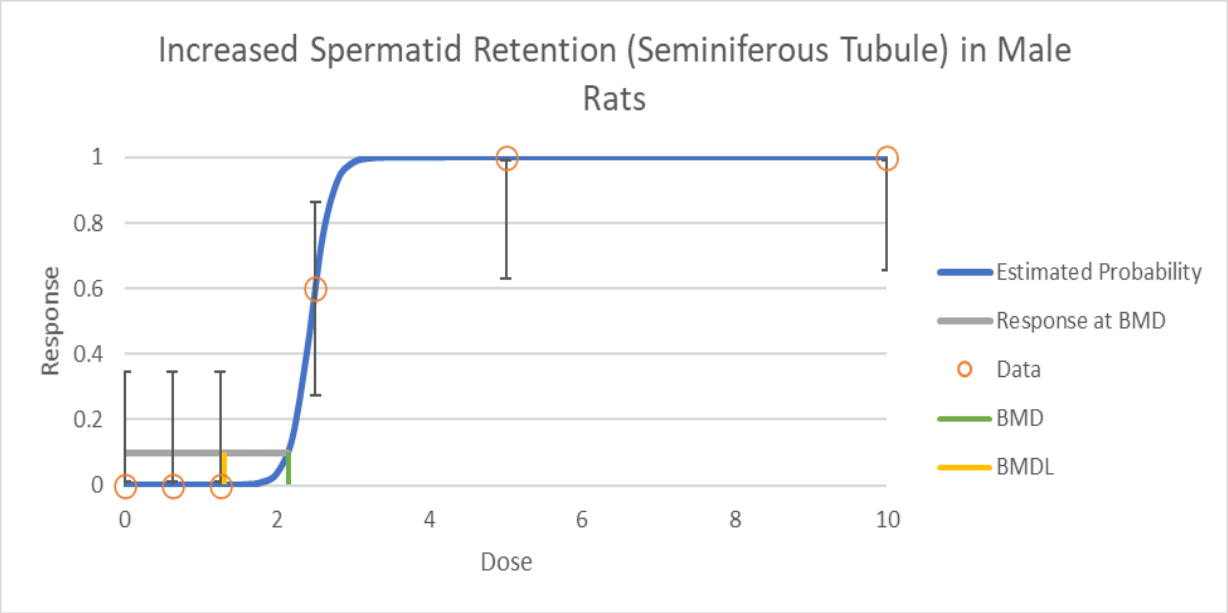

Figure D-11. Dose-response data for the logistic model for increased spermatid retention (seminiferous tubule) in rats (NTP, 2018)[a].

[a]X-axis is dose (mg/kg-d), and y-axis is percent incidence of spermatid retention (seminiferous tubule).

Increased Duct Exfoliated Germ Cell (Epididymis) in Rats (NTP, 2018)

Table D-35. Dose-response data for increased duct exfoliated germ cell (epididymis) in rats (NTP, 2018)

Dose (mg/kg-d)	N	Incidence
0	10	0
0.625	10	0
1.25	10	0
2.5	10	6
5	9	9
10	10	10

Table D-36. Benchmark dose results for increased duct exfoliated germ cell (epididymis) in rats, BMR = 10% extra risk (NTP, 2018)

Models	10% extra risk		Goodness of fit (*p*-value)	AIC	BMDS classification[a]	BMDS notes
	BMD	BMDL				
Dichotomous Hill	2.0367	1.2758	1.0000	19.4666	Viable – Alternate	
Gamma	1.7196	1.1964	0.9992	17.6171	Viable – Alternate	
Log-Logistic	2.0367	1.2758	1.0000	15.4666	Viable – Alternate	
Multistage (Degree 5)	1.6388	1.1225	0.9977	16.0358	Viable – Alternate	
Multistage (Degree 4)	1.4936	1.0453	0.9871	16.6158	Viable – Alternate	
Multistage (Degree 3)	1.2924	0.8959	0.9331	17.8245	Viable – Alternate	
Multistage (Degree 2)	0.9324	0.6431	0.6666	21.2781	Viable – Alternate	
Multistage (Degree 1)	0.3345	0.2286	0.0418	34.4466	Questionable	Goodness-of-fit *p*-value < 0.1
Weibull	1.4382	0.0000	0.9667	17.0865	Unusable	BMD computation failed BMDL not estimated
Logistic[b]	**2.1465**	**1.3040**	**1.0000**	**15.4633**	**Viable – Recommended**	**Lowest AIC**
Log-Probit	2.2146	1.2403	1.0000	17.4602	Viable – Alternate	
Probit	1.6914	1.1861	0.9986	15.8960	Viable – Alternate	

[a]"Classification" column denotes whether a model can be considered for model selection purposes. See BMDS User Guide: https://www.epa.gov/bmds.

[b]Note that while BMDS 3.2 recommends a viable model, the NOAEL/LOAEL approach was applied to this endpoint given that the response was much greater than the BMR in the lowest responding dose group.

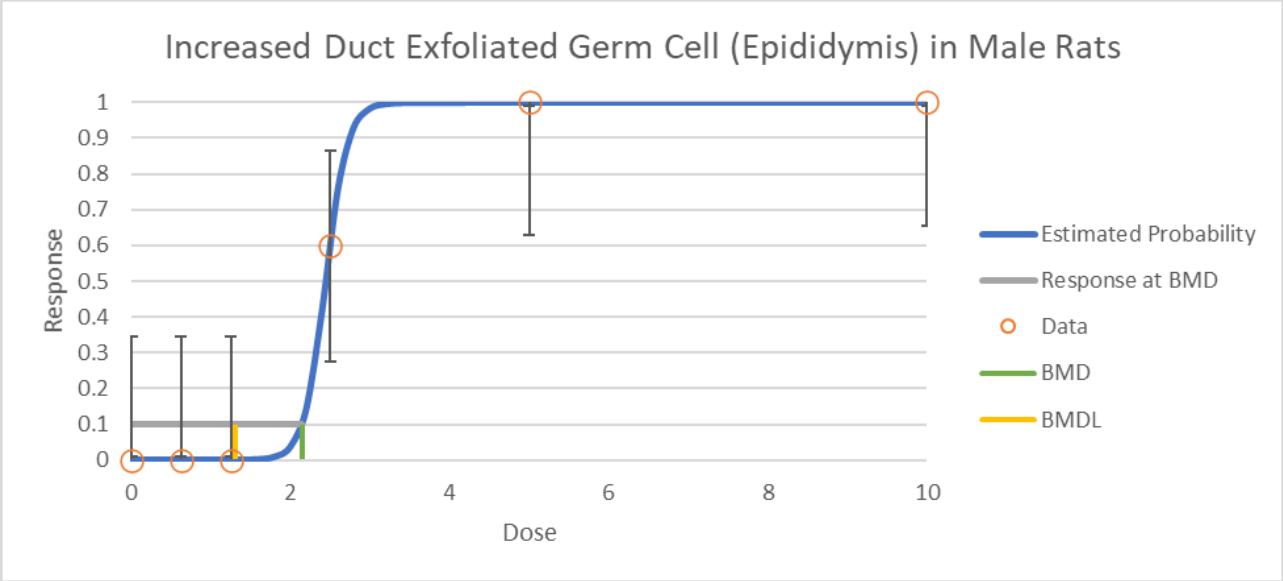

Figure D-12. Dose-response data and curve of the logistic model for increased duct exfoliated germ cell (epididymis) in male rats (NTP, 2018)[a].

[a]X-axis is dose (mg/kg-d), and y-axis is percent incidence of duct exfoliated germ cell (epididymis).

Increased Epithelium Apoptosis (Epididymis) in Rats (NTP, 2018)

Table D-37. Dose-response data for increased epithelium apoptosis (epididymis) in rats (NTP, 2018)

Dose (mg/kg-d)	N	Incidence
0	10	0
0.625	10	0
1.25	10	0
2.5	10	0
5	9	8
10	10	10

Table D-38. Benchmark dose results for increased epithelium apoptosis (epididymis) in rats, BMR = 10% extra risk (NTP, 2018)

Models	10% extra risk		Goodness of fit (*p*-value)	AIC	BMDS classification[a]	BMDS notes
	BMD	BMDL				
Dichotomous Hill	3.9427	2.4042	1.0000	10.2796	Viable – Alternate	
Gamma	2.8683	2.2482	0.9923	9.1482	Viable – Alternate	
Log-Logistic	3.9427	2.4042	1.0000	10.2796	Viable – Alternate	
Multistage (Degree 5)	2.7885	2.1252	0.9819	9.6135	Viable – Alternate	
Multistage (Degree 4)	2.4739	1.9155	0.9163	10.8868	Viable – Alternate	
Multistage (Degree 3)	2.0825	1.5959	0.6995	13.3118	Viable – Alternate	
Multistage (Degree 2)	1.5289	1.1189	0.2932	18.1367	Viable – Alternate	
Multistage (Degree 1)	0.5960	0.3985	0.0055	33.5080	Questionable	Goodness-of-fit *p*-value < 0.1
Weibull	3.0110	2.9287	0.9757	11.1280	Viable – Alternate	
Logistic	**3.9354**	**2.4580**	**1.0000**	**8.2860**	**Viable – Recommended**	**Lowest AIC**
Log-Probit	4.1792	2.4010	1.0000	10.2790	Viable – Alternate	
Probit	3.6130	2.3998	1.0000	8.2893	Viable – Alternate	

[a]"Classification" column denotes whether a model can be considered for model selection purposes. See BMDS User Guide: https://www.epa.gov/bmds.

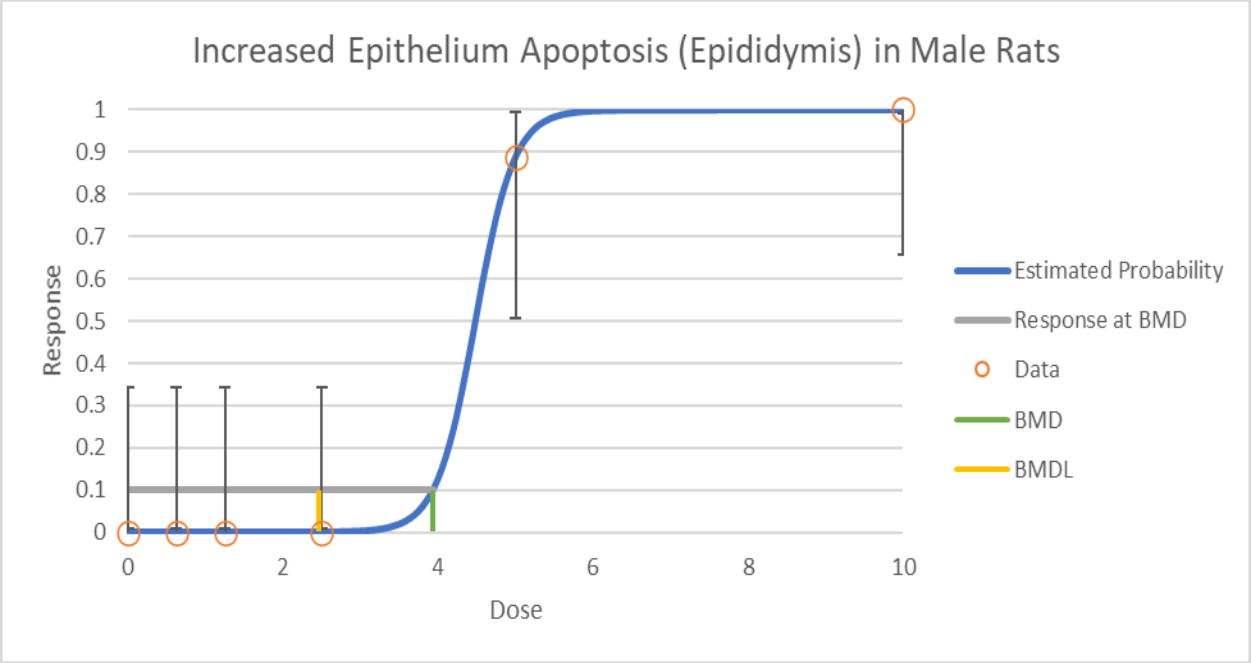

Figure D-13. Dose-response data and curve of the logistic model for increased epithelium apoptosis (epididymis) in rats (NTP, 2018)[a].

[a]X-axis is dose (mg/kg-d), and y-axis is percent incidence of epithelium apoptosis (epididymis).

Increased Hypospermia (Epididymis) in Rats (NTP, 2018)

Table D-39. Dose-response data for increased hypospermia (epididymis) in rats (NTP, 2018)

Dose (mg/kg-d)	N	Incidence
0	10	0
0.625	10	0
1.25	10	0
2.5	10	2
5	9	9
10	10	10

Table D-40. Benchmark dose results for increased hypospermia (epididymis) in rats, BMR = 10% extra risk (NTP, 2018)

Models	10% extra risk		Goodness of fit (*p*-value)	AIC	BMDS classification[a]	BMDS notes
	BMD	BMDL				
Dichotomous Hill	2.3591	1.7910	1.0000	14.0128	Viable – Alternate	
Gamma	2.1964	1.6658	0.9983	14.2298	Viable – Alternate	
Log-Logistic	2.3591	1.7910	1.0000	14.0128	Viable – Alternate	
Multistage (Degree 5)	2.1554	1.4545	0.9999	12.1660	Viable – Alternate	
Multistage (Degree 4)	1.9842	1.4285	0.9961	12.6836	Viable – Alternate	
Multistage (Degree 3)	1.6747	1.2334	0.9105	14.5925	Viable – Alternate	
Multistage (Degree 2)	1.2201	0.8773	0.4952	19.3373	Viable – Alternate	
Multistage (Degree 1)	0.4601	0.3117	0.0292	32.0993	Questionable	Goodness-of-fit *p*-value < 0.1
Weibull	2.1037	0.0000	0.9992	12.3892	Unusable	BMD computation failed BMDL not estimated
Logistic	**2.3780**	**1.6976**	**1.0000**	**12.0093**	**Viable – Recommended**	**Lowest AIC**
Log-Probit	2.3841	1.7632	1.0000	14.0080	Viable – Alternate	
Probit	2.2589	1.6127	1.0000	12.0303	Viable – Alternate	

[a]"Classification" column denotes whether a model can be considered for model selection purposes. See BMDS User Guide: https://www.epa.gov/bmds.

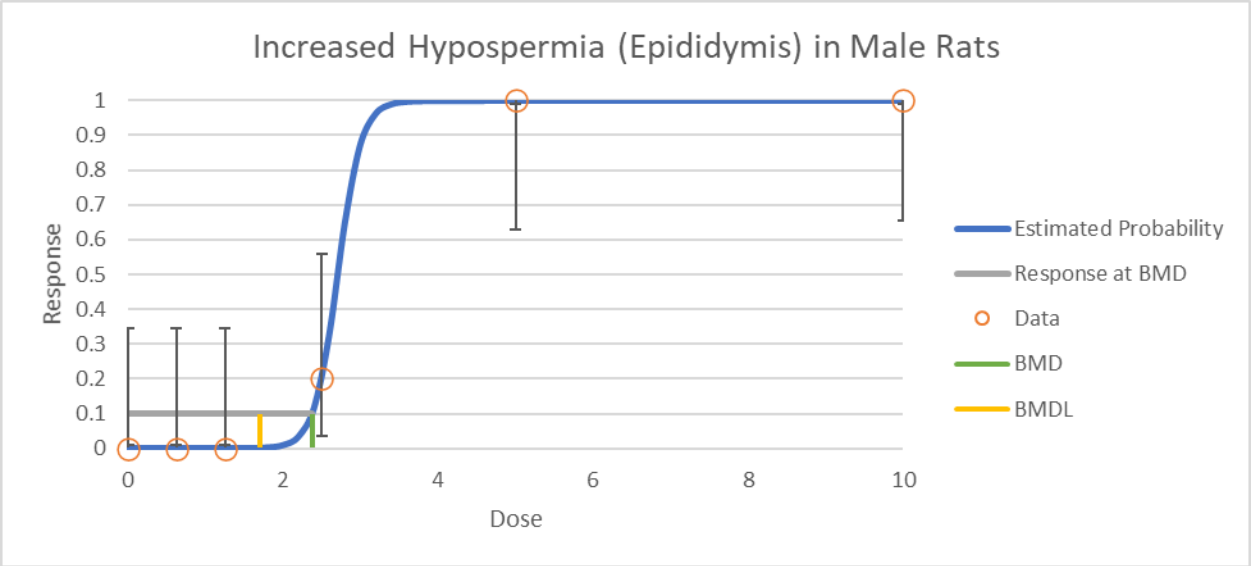

Figure D-14. Dose-response data and curve of the logistic model for increased hypospermia (epididymis) in rats (NTP, 2018)[a].

[a]X-axis is dose (mg/kg-d), and y-axis is percent incidence of hypospermia (epididymis).

Decreased Serum Testosterone in Male Rats (NTP, 2018)

Table D-41. Dose-response data for decreased serum testosterone in male rats (NTP, 2018)

Dose (mg/kg-d)	n	Mean (ng/mL)	SD
0	10	4.483	4.13625918
0.625	10	4.859	4.20266701
1.25	10	3.233	4.35129406
2.5	9	0.847	1.536

Table D-42. Benchmark dose results for decreased serum in male rats — non-constant variance, BMR = 1 standard deviation (NTP, 2018)

Models	Test 3 (*p*-value)	1 standard deviation		Goodness of fit (*p*-value)	AIC	BMDS classification[a]	BMDS notes
		BMD	BMDL				
Exponential 2 (NCV—normal)	0.7563	4.1901	1.1972	0.0638	214.7644	Questionable	Goodness-of-fit *p*-value < 0.1 BMD/BMDL ratio > 3 BMD higher than maximum dose
Exponential 3 (NCV—normal)	0.7563	2.9118	1.3718	0.8054	211.3206	Viable – Alternate	BMD higher than maximum dose
Exponential 4 (NCV—normal)	0.7563	4.1902	1.1972	0.0638	214.7644	Questionable	Goodness-of-fit *p*-value < 0.1 BMD/BMDL ratio > 3 BMD higher than maximum dose
Exponential 5 (NCV—normal)	0.7563	−9,999	0.0000	NA	213.2975	Unusable	BMD computation failed BMD not estimated BMDL not estimated d.f. = 0, saturated model (Goodness-of-fit test cannot be calculated)
Hill (NCV—normal)	0.7563	−9,999	0.0000	NA	213.2997	Unusable	BMD computation failed BMD not estimated BMDL not estimated d.f. = 0, saturated model (Goodness-of-fit test cannot be calculated)
Polynomial (3 degree) (NCV—normal)	0.7563	2.6412	1.8662	0.7657	211.3487	Viable – Alternate	BMD higher than maximum dose
Polynomial (2 degree) (NCV—normal)	**0.7563**	**2.6511**	**1.8552**	**0.9322**	**209.4003**	**Viable – Recommended**	**Lowest AIC BMD higher than maximum dose**
Power (NCV—normal)	0.7563	2.6471	1.8716	0.7741	211.3423	Viable – Alternate	BMD higher than maximum dose
Linear (NCV—normal)	0.7563	2.5438	1.5642	0.4556	210.8322	Viable – Alternate	BMD higher than maximum dose

[a]"Classification" column denotes whether a model can be considered for model selection purposes. See BMDS User Guide: https://www.epa.gov/bmds.

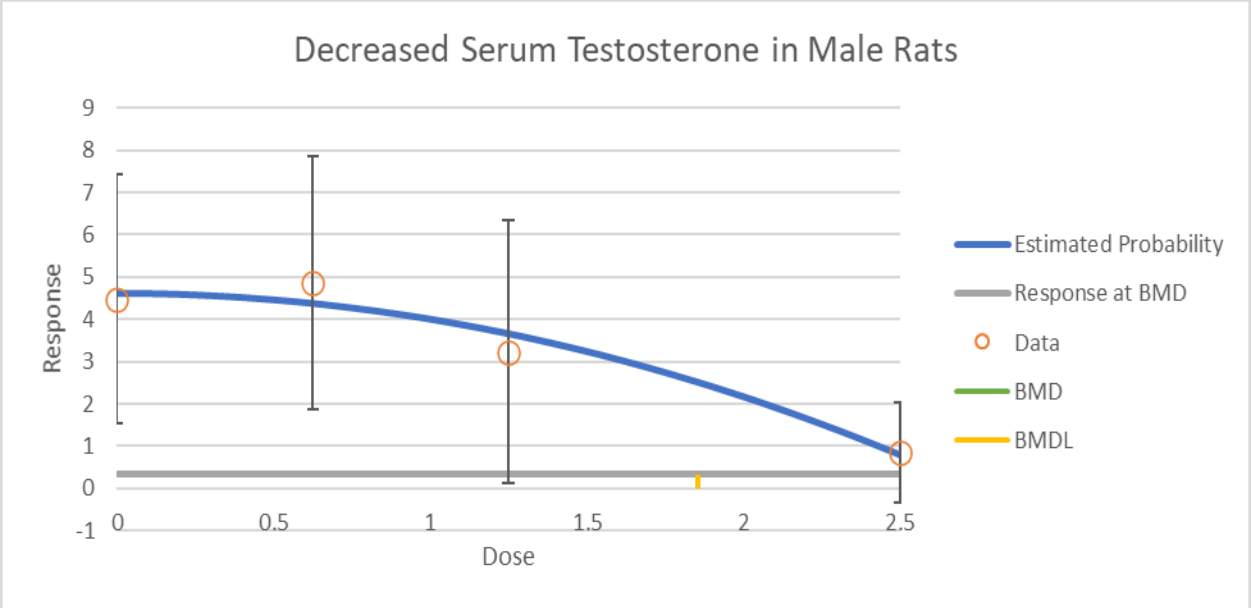

Figure D-15. Dose-response data for the polynomial degree 2 model of decreased serum testosterone in male rats (NTP, 2018)[a].

[a]X-axis is dose (mg/kg-d), and y-axis is serum testosterone concentration (ng/mL).

Decreased Cauda Epididymis Sperm Count (Absolute) in Rats (NTP, 2018)

Table D-43. Dose-response data for decreased absolute sperm count (cauda epididymis) in rats (NTP, 2018)

Dose (mg/kg-d)	n	Mean ($\times 10^6$)	SD
0	10	142.3	29.72541001
0.625	10	136.2	24.98199352
1.25	10	116	19.92234926
2.5	10	98.1	28.46049894

Table D-44. Benchmark dose results for decreased absolute sperm count (cauda epididymis) in rats — constant variance, BMR = 1 standard deviation (NTP, 2018)

Models	Test 2 (*p*-value)	1 standard deviation		Goodness of fit (*p*-value)	AIC	BMDS classification[a]	BMDS notes
		BMD	BMDL				
Exponential 2 (CV—normal)	0.6163	1.2171	0.7965	0.7254	376.7470	Viable – Alternate	
Exponential 3 (CV—normal)	0.6163	1.3271	0.8011	0.4554	378.6621	Viable – Alternate	
Exponential 4 (CV—normal)	0.6163	1.2171	0.7965	0.7254	376.7470	Viable – Alternate	
Exponential 5 (CV—normal)	0.6163	1.2037	0.6530	NA	380.1049	Questionable	d.f. = 0, saturated model (Goodness-of-fit test cannot be calculated)
Hill (CV—normal)	0.6163	1.1974	0.6484	NA	380.1049	Questionable	d.f. = 0, saturated model (Goodness-of-fit test cannot be calculated)
Polynomial (3 degree) (CV—normal)	0.6163	1.3429	0.9449	0.7261	376.7450	Viable – Alternate	
Polynomial (2 degree) (CV—normal)	0.6163	1.3429	0.9449	0.7261	376.7450	Viable – Alternate	
Power (CV—normal)	0.6163	1.3481	0.9449	0.4237	378.7448	Viable – Alternate	
Linear (CV—normal)	**0.6163**	**1.3429**	**0.9449**	**0.7261**	**376.7450**	**Viable – Recommended**	**Lowest AIC**

[a]"Classification" column denotes whether a model can be considered for model selection purposes. See BMDS User Guide: https://www.epa.gov/bmds.

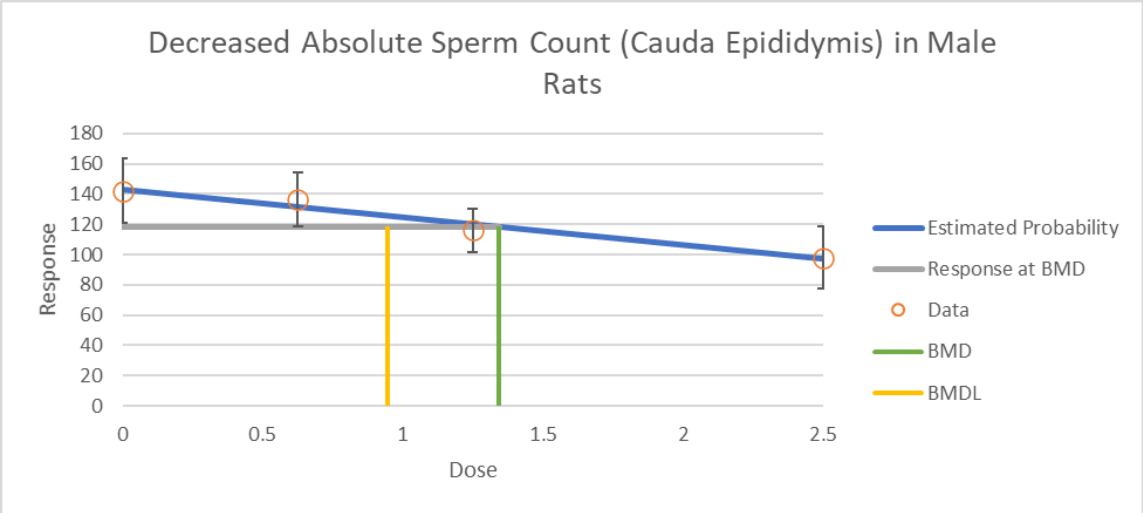

Figure D-16. Dose-response data and curve of the linear model for decreased absolute sperm count (cauda epididymis) in rats (NTP, 2018)[a].

[a]X-axis is dose (mg/kg-d), and y-axis is sperm count ($\times 10^6$).

Increased Liver Weight (Relative) in Male Rats (NTP, 2018)

Table D-45. Dose-response data for increased relative liver weight in male rats (NTP, 2018)

Dose (mg/kg-d)	n	Mean (ng/mL)	SD
0	10	34.14	1.011928851
0.625	10	42.12	1.834121043
1.25	10	54.47	1.865743819
2.5	10	63.37	5.881836448
5	2	81.01	3.210264787

Table D-46. Benchmark dose results for increased relative liver weight in male rats (two highest dose groups removed) – constant variance, BMR = 10% relative deviation (NTP, 2018)

Models	Test 2 (*p*-value)	10% relative deviation		Goodness of fit (*p*-value)	AIC	BMDS classification[a]	BMDS notes
		BMD	BMDL				
Exponential 2 (CV—normal)	**0.1295**	**0.2511**	**0.2366**	**0.1055**	**119.5259**	**Viable – Recommended**	**Lowest AIC Modeled control response std. dev. > |1.5| actual response std. dev.**
Exponential 3 (CV—normal)	0.1295	0.3150	0.2481	NA	118.9051	Questionable	Modeled control response std. dev. > |1.5| actual response std. dev. d.f. = 0, saturated model (Goodness-of-fit test cannot be calculated)
Exponential 4 (CV—normal)	0.1295	0.2052	0.1878	NA	130.0932	Questionable	BMD 3× lower than lowest non-zero dose BMDL 3× lower than lowest non-zero dose Modeled control response std. dev. > |1.5| actual response std. dev. d.f. = 0, saturated model (Goodness-of-fit test cannot be calculated)
Exponential 5 (CV—normal)	0.1295	0.3769	0.2692	<0.0001	120.9051	Questionable	Goodness-of-fit *p*-value < 0.1 Modeled control response std. dev. > |1.5| actual response std. dev.
Hill (CV—normal)	0.1295	0.5859	0.5781	NA	118.9051	Questionable	Modeled control response std. dev. > |1.5| actual response std. dev. d.f. = 0, saturated model (Goodness-of-fit test cannot be calculated)
Polynomial (2 degree) (CV—normal)	0.1295	0.3102	0.2508	NA	118.9051	Questionable	Modeled control response std. dev. > |1.5| actual response std. dev. d.f. = 0, saturated model (Goodness-of-fit test cannot be calculated)

Models	Test 2 (*p*-value)	10% relative deviation		Goodness of fit (*p*-value)	AIC	BMDS classification[a]	BMDS notes
		BMD	BMDL				
Power (CV—normal)	0.1295	0.3331	0.2692	NA	118.9051	Questionable	Modeled control response std. dev. > |1.5| actual response std. dev. d.f. = 0, saturated model (Goodness-of-fit test cannot be calculated)
Linear (CV—normal)	0.1295	0.2054	0.1879	0.0008	128.0399	Questionable	Goodness-of-fit *p*-value < 0.1 BMD 3× lower than lowest non-zero dose BMDL 3× lower than lowest non-zero dose Modeled control response std. dev. > |1.5| actual response std. dev.

[a]"Classification" column denotes whether a model can be considered for model selection purposes. See BMDS User Guide: https://www.epa.gov/bmds.

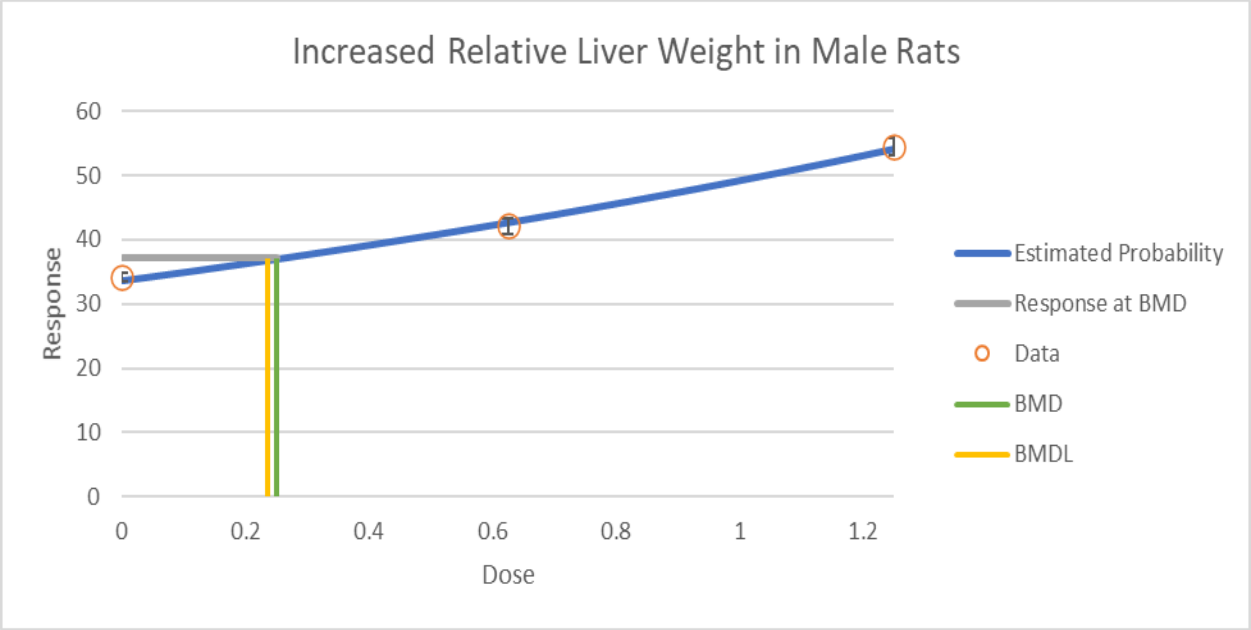

Figure D-17. Dose-response data for the exponential 2 model of increased relative liver weight in male rats (NTP, 2018)[a].

[a]X-axis is dose (mg/kg-d), and y-axis is relative liver weight (mg/g).

Increased Liver Weight (Relative) in Female Rats (NTP, 2018)

Table D-47. Dose-response data for increased relative liver weight in female rats (NTP, 2018)

Dose (mg/kg-d)	n	Mean (ng/mL)	SD
0	10	33.29	2.213594362
1.56	10	40.3	2.877672671
3.12	10	44.95	2.340085469
6.25	10	48.92	2.150348809

Table D-48. Benchmark dose results for increased relative liver weight in female rats — constant variance, BMR = 10% relative deviation (NTP, 2018)

Models	Test 2 (*p*-value)	10% relative deviation		Goodness of fit (*p*-value)	AIC	BMDS classification[a]	BMDS notes
		BMD	BMDL				
Exponential 2 (CV—normal)	0.7758	1.7654	1.5406	<0.0001	208.8211	Questionable	Goodness-of-fit *p*-value < 0.1 |Residual at control| > 2
Exponential 3 (CV—normal)	0.7758	1.7653	1.5406	<0.0001	208.8211	Questionable	Goodness-of-fit *p*-value < 0.1 |Residual at control| > 2
Exponential 4 (CV—normal)	**0.7758**	**0.6243**	**0.4705**	**0.7477**	**187.8578**	**Viable – Recommended**	**Lowest AIC BMDL 3× lower than lowest non-zero dose**
Exponential 5 (CV—normal)	0.7758	0.7056	0.4731	NA	189.7544	Questionable	BMDL 3× lower than lowest non-zero dose d.f. = 0, saturated model (Goodness-of-fit test cannot be calculated)
Hill (CV—normal)	0.7758	0.7598	0.4254	NA	189.7544	Questionable	BMDL 3× lower than lowest non-zero dose d.f. = 0, saturated model (Goodness-of-fit test cannot be calculated)
Polynomial (3 degree) (CV—normal)	0.7758	1.4710	1.2584	0.0001	204.1038	Questionable	Goodness-of-fit *p*-value < 0.1 |Residual at control| > 2
Polynomial (2 degree) (CV—normal)	0.7758	1.4710	1.2584	0.0001	204.1038	Questionable	Goodness-of-fit *p*-value < 0.1 |Residual at control| > 2
Power (CV—normal)	0.7758	1.4710	1.2584	0.0001	204.1038	Questionable	Goodness-of-fit *p*-value < 0.1 |Residual at control| > 2
Linear (CV—normal)	0.7758	1.4710	1.2584	0.0001	204.1038	Questionable	Goodness-of-fit *p*-value < 0.1 |Residual at control| > 2

[a]"Classification" column denotes whether a model can be considered for model selection purposes. See BMDS User Guide: https://www.epa.gov/bmds.

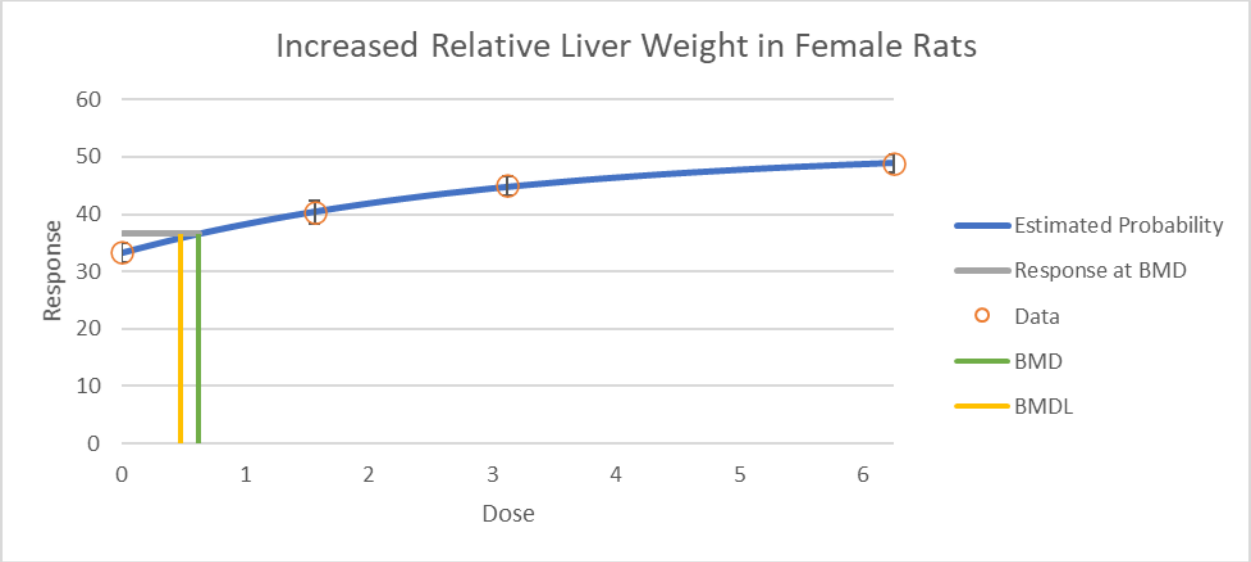

Figure D-18. Dose-response data and curve of the exponential 4 model of increased relative liver weight in female rats (NTP, 2018)[a].

[a]X-axis is dose (mg/kg-d), and y-axis is relative liver weight (mg/g).

Increased Liver Weight (Relative) in Male Mice (Wang et al., 2015)

Table D-49. Dose-response data for increased relative liver weight in male mice (Wang et al., 2015)

Dose (mg/kg-d)	n	Mean (ng/mL)	SD
0	6	0.053288288	0.002317217
0.2	6	0.062117117	0.002317217
1	6	0.086711712	0.001545628
5	6	0.130225225	0.003088807

Table D-50. Benchmark dose results for increased relative liver weight in male mice — constant variance, BMR = 10% relative deviation (Wang et al., 2015)

Models	Test 2 (*p*-value)	10% relative deviation		Goodness of fit (*p*-value)	AIC	BMDS classification[a]	BMDS notes
		BMD	BMDL				
Exponential 2 (CV—normal)	0.4393	0.6476	0.5872	<0.0001	−153.0001	Questionable	Goodness-of-fit *p*-value < 0.1 |Residual for Dose Group Near BMD| > 2 |Residual at control| > 2 Modeled control response std. dev. > |1.5| actual response std. dev.
Exponential 3 (CV—normal)	0.4393	0.6476	0.5872	<0.0001	−153.0001	Questionable	Goodness-of-fit *p*-value < 0.1 |Residual for Dose Group Near BMD| > 2 |Residual at control| > 2 Modeled control response std. dev. > |1.5| actual response std. dev.
Exponential 4 (CV—normal)	0.4393	0.1304	0.1179	0.5306	−217.8131	Viable – Alternate	
Exponential 5 (CV—normal)	0.4393	0.1304	0.1179	0.5306	−217.8131	Viable – Alternate	
Hill (CV—normal)	**0.4393**	**0.1184**	**0.1050**	**0.9310**	**−218.1989**	**Viable – Recommended**	**Lowest AIC**
Polynomial (3 degree) (CV—normal)	0.4393	0.4256	0.3758	<0.0001	−161.6418	Questionable	Goodness-of-fit *p*-value < 0.1 |Residual at control| > 2 Modeled control response std. dev. > |1.5| actual response std. dev.
Polynomial (2 degree) (CV—normal)	0.4393	0.4256	0.3758	<0.0001	−161.6418	Questionable	Goodness-of-fit *p*-value < 0.1 |Residual at control| > 2 Modeled control response std. dev. > |1.5| actual response std. dev.
Power (CV—normal)	0.4393	0.4256	0.3758	<0.0001	−161.6418	Questionable	Goodness-of-fit *p*-value < 0.1 |Residual at control| > 2 Modeled control response std. dev. > |1.5| actual response std. dev.
Linear (CV—normal)	0.4393	0.4256	0.3758	<0.0001	−161.6418	Questionable	Goodness-of-fit *p*-value < 0.1 |Residual at control| > 2 Modeled control response std. dev. > |1.5| actual response std. dev.

[a]"Classification" column denotes whether a model can be considered for model selection purposes. See BMDS User Guide: https://www.epa.gov/bmds.

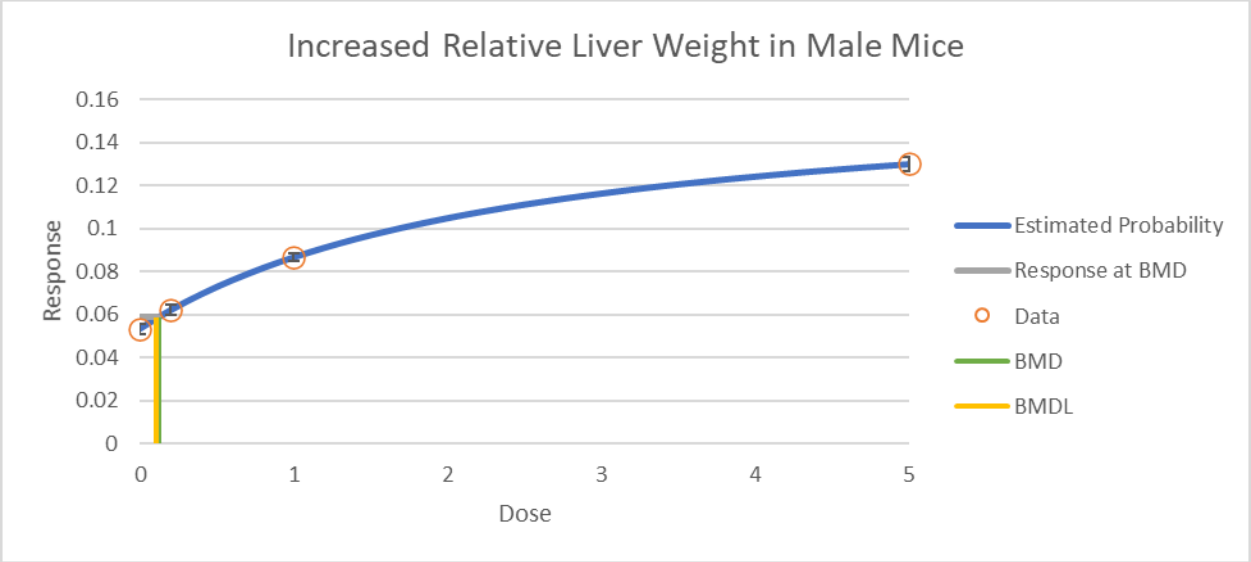

Figure D-19. Dose-response data and curve for the Hill model of increased relative liver weight in male mice (Wang et al., 2015)[a].

[a]X-axis is dose (mg/kg-d), and y-axis is relative liver weight (mg/g).

Increased Liver Weight (Relative) in Nonpregnant Mice (Das et al., 2015)

Table D-51. Dose-response data for increased relative liver weight in nonpregnant mice (Das et al., 2015)

Dose (mg/kg-d)	n	Mean (mg/g)	SD
0	4	4.4	0.503428247
1	7	7.64	0.608092098
3	5	11.15	1.970105327
5	2	10.96	0.46348247

Table D-52. Benchmark dose results for increased relative liver weight in nonpregnant mice — non-constant variance, BMR = 10% relative deviation (Das et al., 2015)

Models	Test 3 (*p*-value)	10% relative deviation		Goodness of fit (*p*-value)	AIC	BMDS classification[a]	BMDS notes
		BMD	BMDL				
Exponential 2 (NCV—normal)	0.0502	0.4211	0.2813	<0.0001	74.8726	Questionable	Goodness-of-fit *p*-value < 0.1 |Residual for Dose Group Near BMD| > 2 BMDL 3× lower than lowest non-zero dose |Residual at control| > 2 Modeled control response std. dev. > |1.5| actual response std. dev.
Exponential 3 (NCV—normal)	0.0502	0.4211	0.2813	<0.0001	74.8726	Questionable	Goodness-of-fit *p*-value < 0.1 |Residual for Dose Group Near BMD| > 2 BMDL 3× lower than lowest non-zero dose |Residual at control| > 2 Modeled control response std. dev. > |1.5| actual response std. dev.
Exponential 4 (NCV—normal)	0.0502	0.1070	0.0772	0.1455	55.7026	Questionable	BMD 3× lower than lowest non-zero dose BMDL 3× lower than lowest non-zero dose BMDL 10× lower than lowest non-zero dose
Exponential 5 (NCV—normal)	0.0502	0.4465	0.0898	NA	55.8305	Questionable	BMD/BMDL ratio > 3 BMDL 3× lower than lowest non-zero dose BMDL 10× lower than lowest non-zero dose d.f. = 0, saturated model (Goodness-of-fit test cannot be calculated)
Hill (NCV—normal)	0.0502	0.7715	0.7412	NA	55.8306	Questionable	d.f. = 0, saturated model (Goodness-of-fit test cannot be calculated)
Polynomial (3 degree) (NCV—normal)	0.0502	0.1871	0.1450	0.0012	65.1120	Questionable	Goodness-of-fit *p*-value < 0.1 BMD 3× lower than lowest non-zero dose BMDL 3× lower than lowest non-zero dose

Models	Test 3 (*p*-value)	10% relative deviation		Goodness of fit (*p*-value)	AIC	BMDS classification[a]	BMDS notes
		BMD	BMDL				
Polynomial (2 degree) (NCV—normal)	0.0502	0.1871	0.1450	0.0012	65.1120	Questionable	Goodness-of-fit *p*-value < 0.1 BMD 3× lower than lowest non-zero dose BMDL 3× lower than lowest non-zero dose
Power (NCV—normal)	0.0502	0.1871	0.1450	0.0012	65.1120	Questionable	Goodness-of-fit *p*-value < 0.1 BMD 3× lower than lowest non-zero dose BMDL 3× lower than lowest non-zero dose
Linear (NCV—normal)	0.0502	0.1871	0.1450	0.0012	65.1120	Questionable	Goodness-of-fit *p*-value < 0.1 BMD 3× lower than lowest non-zero dose BMDL 3× lower than lowest non-zero dose

No viable BMD or BMDL identified by BMDS.

[a]"Classification" column denotes whether a model can be considered for model selection purposes. See BMDS User Guide: https://www.epa.gov/bmds.

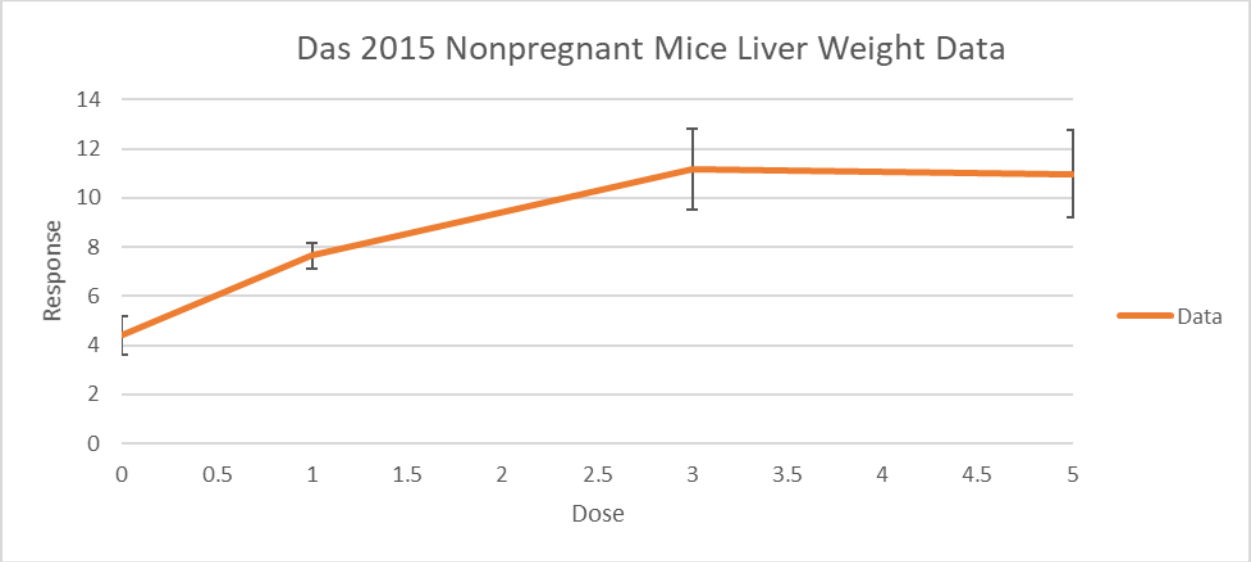

Figure D-20. Dose-response data for increased relative liver weight in nonpregnant mice (Das et al., 2015)[a].

[a]X-axis is dose (mg/kg-d), and y-axis is relative liver weight (mg/g).

Increased Liver Weight (Relative) in Nonpregnant Wild Type Mice (Wolf et al., 2010)

Table D-53. Dose-response data for increased relative liver weight in nonpregnant mice (WT) (Wolf et al., 2010)

Dose (mg/kg-d)	n	Mean (g)	SD
0	13	3.762	0.28195411
0.83	13	6.504	0.511267171
1.1	25	7.495	0.47315
1.5	22	8.115	0.549716727
2	23	9.008	0.725609309

Table D-54. Benchmark dose results for increased relative liver weight in nonpregnant wild type mice — non-constant variance, BMR = 10% relative deviation (Wolf et al., 2010)

Models	Test 3 (*p*-value)	10% relative deviation		Goodness of fit *p*-value	AIC	BMDS classification[a]	BMDS notes
		BMD	BMDL				
Exponential 2 (NCV—normal)	0.6396	0.3137	0.2741	<0.0001	220.9390	Questionable	Goodness-of-fit *p*-value < 0.1 |Residual for Dose Group Near BMD| > 2 BMDL 3× lower than lowest non-zero dose |Residual at control| > 2 Modeled control response std. dev. > |1.5| actual response std. dev.
Exponential 3 (NCV—normal)	0.6396	0.3135	0.2741	<0.0001	220.9390	Questionable	Goodness-of-fit *p*-value < 0.1 |Residual for Dose Group Near BMD| > 2 BMDL 3× lower than lowest non-zero dose |Residual at control| > 2 Modeled control response std. dev. > |1.5| actual response std. dev.
Exponential 4 (NCV—normal)	0.6396	0.0882	0.0770	0.1676	153.6919	Questionable	BMD 3× lower than lowest non-zero dose BMDL 3× lower than lowest non-zero dose BMDL 10× lower than lowest non-zero dose
Exponential 5 (NCV—normal)	0.6396	0.1354	0.0780	0.0787	155.2118	Questionable	Goodness-of-fit *p*-value < 0.1 BMD 3× lower than lowest non-zero dose BMDL 3× lower than lowest non-zero dose BMDL 10× lower than lowest non-zero dose
Hill (NCV—normal)	0.6396	0.1822	0.0756	0.0951	154.9051	Questionable	Goodness-of-fit *p*-value < 0.1 BMD 3× lower than lowest non-zero dose BMDL 3× lower than lowest non-zero dose BMDL 10× lower than lowest non-zero dose

Models	Test 3 (*p*-value)	10% relative deviation		Goodness of fit *p*-value	AIC	BMDS classification[a]	BMDS notes
		BMD	BMDL				
Polynomial (4 degree) (NCV—normal)	0.6396	0.1366	0.1268	<0.0001	185.2253	Questionable	Goodness-of-fit *p*-value < 0.1 BMD 3× lower than lowest non-zero dose BMDL 3× lower than lowest non-zero dose
Polynomial (3 degree) (NCV—normal)	0.6396	0.1366	0.1254	<0.0001	185.2253	Questionable	Goodness-of-fit *p*-value < 0.1 BMD 3× lower than lowest non-zero dose BMDL 3× lower than lowest non-zero dose
Polynomial (2 degree) (NCV—normal)	0.6396	0.1366	0.1254	<0.0001	185.2253	Questionable	Goodness-of-fit *p*-value < 0.1 BMD 3× lower than lowest non-zero dose BMDL 3× lower than lowest non-zero dose
Power (NCV—normal)	0.6396	0.1366	0.1254	<0.0001	185.2253	Questionable	Goodness-of-fit *p*-value < 0.1 BMD 3× lower than lowest non-zero dose BMDL 3× lower than lowest non-zero dose
Linear (NCV—normal)	0.6396	0.1366	0.1254	<0.0001	185.2253	Questionable	Goodness-of-fit *p*-value < 0.1 BMD 3× lower than lowest non-zero dose BMDL 3× lower than lowest non-zero dose

No viable BMD or BMDL identified by BMDS.

[a]"Classification" column denotes whether a model can be considered for model selection purposes. See BMDS User Guide: https://www.epa.gov/bmds.

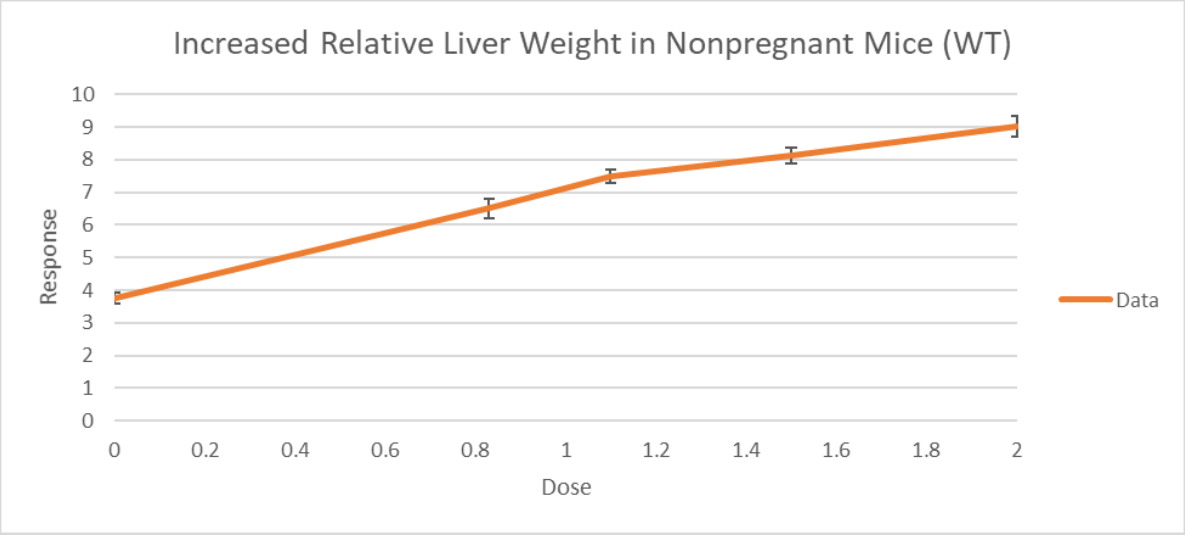

Figure D-21. Dose-response data for increased relative liver weight in nonpregnant mice (WT) (Wolf et al., 2010)[a].

[a]X-axis is dose (mg/kg-d), and y-axis is relative liver weight (mg/g).

Increased Liver Weight (Relative, Developmental) in Mouse Pups on PND 1 (Das et al., 2015)

Table D-55. Dose-response data for increased relative liver weight in mouse pups on PND 1 (Das et al., 2015)

Dose (mg/kg-d)	n	Mean (ng/mL)	SD
0	13	4.687	0.403821743
1	11	6.183	0.39467835
3	13	7.155	0.414638397
5	16	7.179	0.608

Table D-56. Benchmark dose results for increased relative liver weight in mouse pups on PND 1 — constant variance, BMR = 5% relative deviation (Das et al., 2015)

Models	Test 2 (*p*-value)	5% relative deviation		Goodness of fit (*p*-value)	AIC	BMDS classification[a]	BMDS notes
		BMD	BMDL				
Exponential 2 (CV—normal)	0.2353	0.7180	0.6073	<0.0001	117.6727	Questionable	Goodness-of-fit *p*-value < 0.1 |Residual for Dose Group Near BMD| > 2 |Residual at control| > 2 Modeled control response std. dev. > |1.5| actual response std. dev.
Exponential 3 (CV—normal)	0.2353	0.7180	0.6073	<0.0001	117.6727	Questionable	Goodness-of-fit *p*-value < 0.1 |Residual for Dose Group Near BMD| > 2 |Residual at control| > 2 Modeled control response std. dev. > |1.5| actual response std. dev.
Exponential 4 (CV—normal)	0.2353	0.1047	0.0761	0.4672	76.1867	Questionable	BMD 3× lower than lowest non-zero dose BMDL 3× lower than lowest non-zero dose BMDL 10× lower than lowest non-zero dose
Exponential 5 (CV—normal)	0.2353	0.2163	0.0787	NA	77.6583	Questionable	BMD 3× lower than lowest non-zero dose BMDL 3× lower than lowest non-zero dose BMDL 10× lower than lowest non-zero dose d.f. = 0, saturated model (Goodness-of-fit test cannot be calculated)
Hill (CV—normal)	0.2353	0.4557	0.0631	NA	77.6607	Questionable	BMD/BMDL ratio > 3 BMDL 3× lower than lowest non-zero dose BMDL 10× lower than lowest non-zero dose d.f. = 0, saturated model (Goodness-of-fit test cannot be calculated)

Models	Test 2 (*p*-value)	5% relative deviation		Goodness of fit (*p*-value)	AIC	BMDS classification[a]	BMDS notes
		BMD	BMDL				
Polynomial (3 degree) (CV—normal)	0.2353	0.5753	0.4736	<0.0001	113.2049	Questionable	Goodness-of-fit *p*-value < 0.1 |Residual for Dose Group Near BMD| > 2 |Residual at control| > 2 Modeled control response std. dev. > |1.5| actual response std. dev.
Polynomial (2 degree) (CV—normal)	0.2353	0.5753	0.4736	<0.0001	113.2049	Questionable	Goodness-of-fit *p*-value < 0.1 |Residual for Dose Group Near BMD| > 2 |Residual at control| > 2 Modeled control response std. dev. > |1.5| actual response std. dev.
Power (CV—normal)	0.2353	0.5754	0.4736	<0.0001	113.2049	Questionable	Goodness-of-fit *p*-value < 0.1 |Residual for Dose Group Near BMD| > 2 |Residual at control| > 2 Modeled control response std. dev. > |1.5| actual response std. dev.
Linear (CV—normal)	0.2353	0.5753	0.4736	<0.0001	113.2049	Questionable	Goodness-of-fit *p*-value < 0.1 |Residual for Dose Group Near BMD| > 2 |Residual at control| > 2 Modeled control response std. dev. > |1.5| actual response std. dev.

No viable BMD or BMDL identified by BMDS.

[a]"Classification" column denotes whether a model can be considered for model selection purposes. See BMDS User Guide: https://www.epa.gov/bmds.

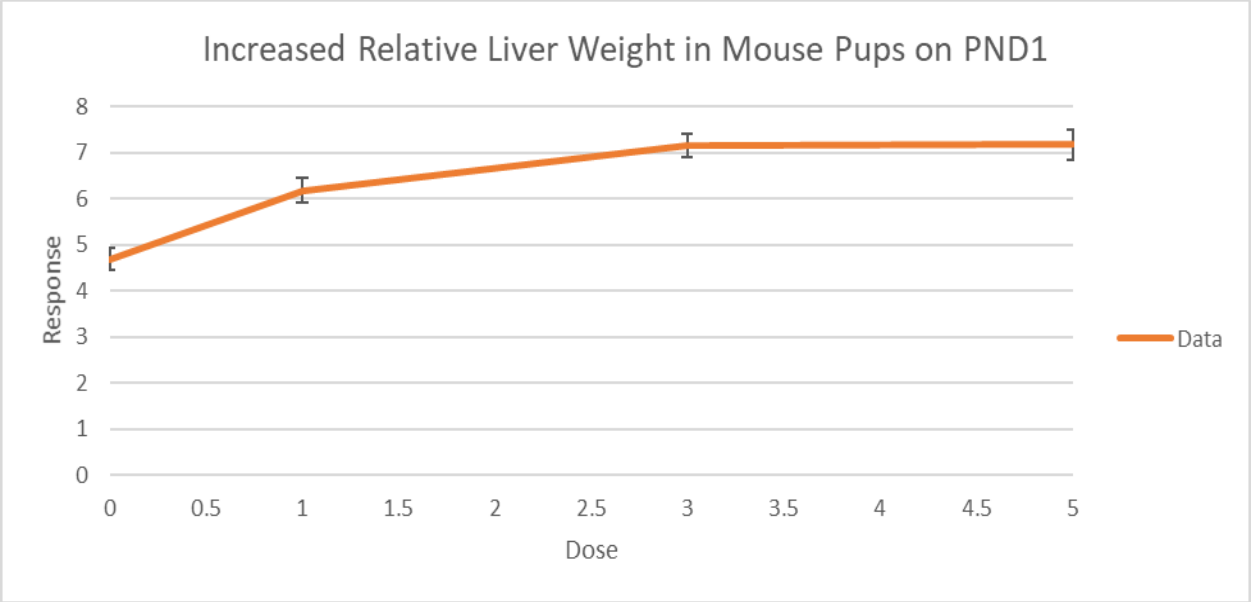

Figure D-22. Dose-response data for increased relative liver weight in mouse pups on PND 1(Das et al., 2015)[a].

[a]X-axis is dose (mg/kg-d), and y-axis is relative liver weight (mg/g).

Increased Liver Weight (Relative, Developmental) in Mouse Pups on PND 24 (Das et al., 2015)

Table D-57. Dose-response data for increased relative liver weight in mouse pups on PND 24 (Das et al., 2015)

Dose (mg/kg-d)	n	Mean (ng/mL)	SD
0	13	5.519	0.454299461
1	11	6.926	0.461010846
3	13	8.171	0.411032845
5	8	9.425	1.527350647

Table D-58. Benchmark dose results for increased relative liver weight in mouse pups on PND 24 — non-constant variance, BMR = 5% relative deviation (Das et al., 2015)

Models	Test 3 (*p*-value)	5% relative deviation		Goodness of fit (*p*-value)	AIC	BMDS classification[a]	BMDS notes
		BMD	BMDL				
Exponential 2 (NCV—normal)	0.0029	0.4465	0.3900	0.0013	102.5940	Questionable	Non-constant variance test failed (Test 3 *p*-value < 0.05) Goodness-of-fit *p*-value < 0.1 |Residual for Dose Group Near BMD| > 2 |Residual at control| > 2
Exponential 3 (NCV—normal)	0.0029	0.4465	0.3900	0.0013	102.5940	Questionable	Non-constant variance test failed (Test 3 *p*-value < 0.05) Goodness-of-fit *p*-value < 0.1 |Residual for Dose Group Near BMD| > 2 |Residual at control| > 2
Exponential 4 (NCV—normal)	0.0029	0.2151	0.1548	0.0646	94.7346	Questionable	Non-constant variance test failed (Test 3 *p*-value < 0.05) Goodness-of-fit *p*-value < 0.1 BMD 3× lower than lowest non-zero dose BMDL 3× lower than lowest non-zero dose
Exponential 5 (NCV—normal)	0.0029	0.2150	0.1548	0.0646	94.7346	Questionable	Non-constant variance test failed (Test 3 *p*-value < 0.05) Goodness-of-fit *p*-value < 0.1 BMD 3× lower than lowest non-zero dose BMDL 3× lower than lowest non-zero dose
Hill (NCV—normal)	0.0029	0.2009	0.1365	0.0859	94.2683	Questionable	Non-constant variance test failed (Test 3 *p*-value < 0.05) Goodness-of-fit *p*-value < 0.1 BMD 3× lower than lowest non-zero dose BMDL 3× lower than lowest non-zero dose
Polynomial (3 degree) (NCV—normal)	0.0029	0.3425	0.2940	0.0154	97.6648	Questionable	Non-constant variance test failed (Test 3 *p*-value < 0.05) Goodness-of-fit *p*-value < 0.1 BMDL 3× lower than lowest non-zero dose
Polynomial (2 degree) (NCV—normal)	0.0029	0.3425	0.2940	0.0154	97.6648	Questionable	Non-constant variance test failed (Test 3 *p*-value < 0.05) Goodness-of-fit *p*-value < 0.1 BMDL 3× lower than lowest non-zero dose

Models	Test 3 (*p*-value)	5% relative deviation		Goodness of fit (*p*-value)	AIC	BMDS classification[a]	BMDS notes
		BMD	BMDL				
Power (NCV—normal)	0.0029	0.3425	0.2940	0.0154	97.6648	Questionable	Non-constant variance test failed (Test 3 *p*-value < 0.05) Goodness-of-fit *p*-value < 0.1 BMDL 3× lower than lowest non-zero dose
Linear (NCV—normal)	0.0029	0.3425	0.2940	0.0154	97.6648	Questionable	Non-constant variance test failed (Test 3 *p*-value < 0.05) Goodness-of-fit *p*-value < 0.1 BMDL 3× lower than lowest non-zero dose

The variance of the data cannot be modeled.

[a]"Classification" column denotes whether a model can be considered for model selection purposes. See BMDS User Guide: https://www.epa.gov/bmds.

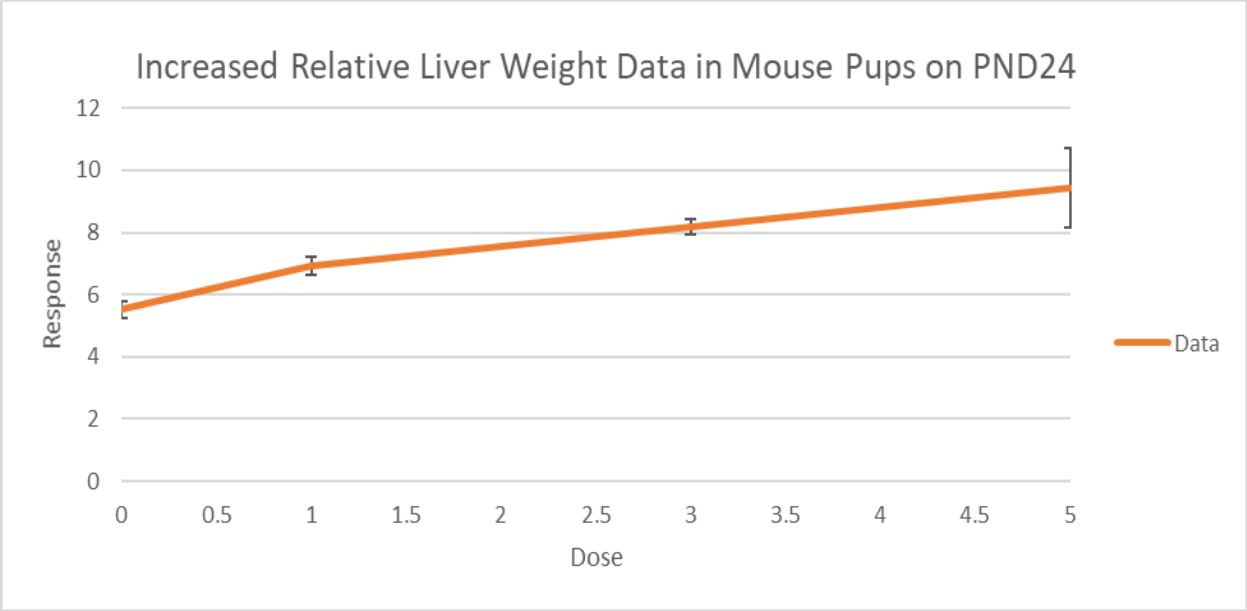

Figure D-23. Dose-response data for increased relative liver weight in mouse pups on PND 24 (Das et al., 2015)[a].

[a]X-axis is dose (mg/kg-d), and y-axis is relative liver weight (mg/g).

Increased Liver Weight (Relative, Developmental) in Mouse Pups on PND 70 (Das et al., 2015)

Table D-59. Dose-response data for increased relative liver weight in mouse pups on PND 70 (Das et al., 2015)

Dose (mg/kg-d)	n	Mean (ng/mL)	SD
0	3	4.806	0.661643408
1	5	5.554	0.366715148
3	4	6.119	0.744
5	2	6.216	0.028284271

Table D-60. Benchmark dose results for increased relative liver weight in mouse pups on PND 70 — non-constant variance, BMR = 5% relative deviation

Models	Test 3 (*p*-value)	5% relative deviation		Goodness of fit (*p*-value)	AIC	BMDS classification[a]	BMDS notes
		BMD	BMDL				
Exponential 2 (NCV—normal)	0.0017	1.1243	0.6482	0.2089	29.6394	Questionable	Non-constant variance test failed (Test 3 *p*-value < 0.05)
Exponential 3 (NCV—normal)	0.0017	1.1233	0.6583	0.2089	29.6394	Questionable	Non-constant variance test failed (Test 3 *p*-value < 0.05)
Exponential 4 (NCV—normal)	0.0017	0.2454	0.0819	0.9495	28.5112	Questionable	Non-constant variance test failed (Test 3 *p*-value < 0.05) BMD 3× lower than lowest non-zero dose BMDL 3× lower than lowest non-zero dose BMDL 10× lower than lowest non-zero dose
Exponential 5 (NCV—normal)	0.0017	0.2738	0.0820	NA	30.5074	Questionable	Non-constant variance test failed (Test 3 *p*-value < 0.05) BMD/BMDL ratio > 3 BMD 3× lower than lowest non-zero dose BMDL 3× lower than lowest non-zero dose BMDL 10× lower than lowest non-zero dose d.f. = 0, saturated model (Goodness-of-fit test cannot be calculated)
Hill (NCV—normal)	0.0017	0.3950	0.0391	NA	30.5072	Questionable	Non-constant variance test failed (Test 3 *p*-value < 0.05) BMD/BMDL ratio > 3 BMDL 3× lower than lowest non-zero dose BMDL 10× lower than lowest non-zero dose d.f. = 0, saturated model (Goodness-of-fit test cannot be calculated)
Polynomial (3 degree) (NCV—normal)	0.0017	0.9703	0.5368	0.2447	29.3230	Questionable	Non-constant variance test failed (Test 3 *p*-value < 0.05)

Models	Test 3 (*p*-value)	5% relative deviation		Goodness of fit (*p*-value)	AIC	BMDS classification[a]	BMDS notes
		BMD	BMDL				
Polynomial (2 degree) (NCV—normal)	0.0017	0.9703	0.5367	0.2447	29.3230	Questionable	Non-constant variance test failed (Test 3 *p*-value < 0.05)
Power (NCV—normal)	0.0017	0.9703	0.5368	0.2447	29.3230	Questionable	Non-constant variance test failed (Test 3 *p*-value < 0.05)
Linear (NCV—normal)	0.0017	0.9703	0.5368	0.2447	29.3230	Questionable	Non-constant variance test failed (Test 3 *p*-value < 0.05)

The variance of the data cannot be modeled.

[a]"Classification" column denotes whether a model can be considered for model selection purposes. See BMDS User Guide: https://www.epa.gov/bmds.

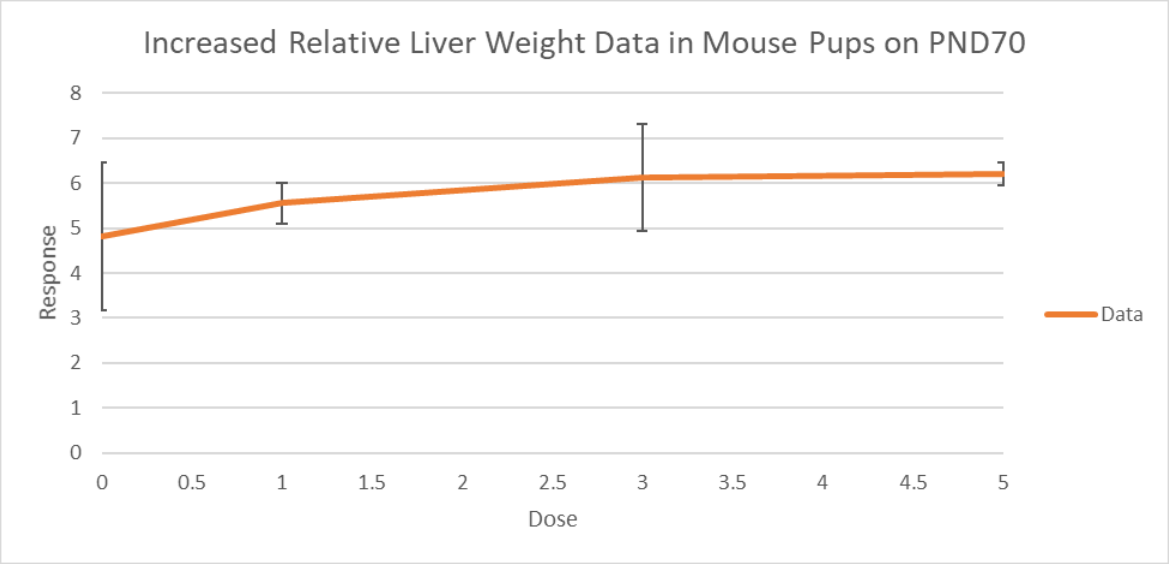

Figure D-24. Dose-response data for increased relative liver weight in mouse pups on PND 70 (Das et al., 2015)[a].

[a]X-axis is dose (mg/kg-d), and y-axis is relative liver weight (mg/g).

Increased Liver Weight (Relative) in Mouse Pups (WT) on PND 21(Wolf et al., 2010)

Table D-61. Dose-response data for increased relative liver weight in mouse pups (WT) on PND 21 (Wolf et al., 2010)

Dose (mg/kg-d)	n	Mean (g)	SD
0	10	3.951	0.241155294
0.83	8	5.62	0.418324372
1.1	5	6.268	0.519438591
1.5	10	6.419	0.266832989
2	7	6.83	0.528091962

Table D-62. Benchmark dose results for increased relative liver weight in mouse pups (WT) on PND 21 — constant variance, BMR = 5% relative deviation (Wolf et al., 2010)

Models	Test 2 (*p*-value)	5% relative deviation		Goodness of fit (*p*-value)	AIC	BMDS classification[a]	BMDS notes
		BMD	BMDL				
Exponential 2 (CV—normal)	0.1069	0.1912	0.1687	<0.0001	62.6276	Questionable	Goodness-of-fit *p*-value < 0.1 |Residual for Dose Group Near BMD| > 2 BMD 3× lower than lowest non-zero dose BMDL 3× lower than lowest non-zero dose |Residual at control| > 2 Modeled control response std. dev. > |1.5| actual response std. dev.
Exponential 3 (CV—normal)	0.1069	0.1912	0.1687	<0.0001	62.6276	Questionable	Goodness-of-fit *p*-value < 0.1 |Residual for Dose Group Near BMD| > 2 BMD 3× lower than lowest non-zero dose BMDL 3× lower than lowest non-zero dose |Residual at control| > 2 Modeled control response std. dev. > |1.5| actual response std. dev.
Exponential 4 (CV—normal)	0.1069	0.0699	0.0523	0.331	41.6646	Questionable	BMD 3× lower than lowest non-zero dose BMDL 3× lower than lowest non-zero dose BMD 10× lower than lowest non-zero dose BMDL 10× lower than lowest non-zero dose Modeled control response std. dev. > |1.5| actual response std. dev.
Exponential 5 (CV—normal)	0.1069	0.1155	0.0528	0.152	43.5090	Questionable	BMD 3× lower than lowest non-zero dose BMDL 3× lower than lowest non-zero dose BMDL 10× lower than lowest non-zero dose Modeled control response std. dev. > |1.5| actual response std. dev.

Models	Test 2 (*p*-value)	5% relative deviation		Goodness of fit (*p*-value)	AIC	BMDS classification[a]	BMDS notes
		BMD	BMDL				
Hill (CV—normal)	0.1069	0.2006	0.0453	0.171	43.3278	Questionable	BMD/BMDL ratio > 3 BMD 3× lower than lowest non-zero dose BMDL 3× lower than lowest non-zero dose BMDL 10× lower than lowest non-zero dose Modeled control response std. dev. > |1.5| actual response std. dev.
Polynomial (4 degree) (CV—normal)	0.1069	0.1399	0.1228	0.001	53.8951	Questionable	Goodness-of-fit *p*-value < 0.1 BMD 3× lower than lowest non-zero dose BMDL 3× lower than lowest non-zero dose Modeled control response std. dev. > |1.5| actual response std. dev.
Polynomial (3 degree) (CV—normal)	0.1069	0.1399	0.1204	0.001	53.8951	Questionable	Goodness-of-fit *p*-value < 0.1 BMD 3× lower than lowest non-zero dose BMDL 3× lower than lowest non-zero dose Modeled control response std. dev. > |1.5| actual response std. dev.
Polynomial (2 degree) (CV—normal)	0.1069	0.1399	0.1204	0.001	53.8951	Questionable	Goodness-of-fit *p*-value < 0.1 BMD 3× lower than lowest non-zero dose BMDL 3× lower than lowest non-zero dose Modeled control response std. dev. > |1.5| actual response std. dev.
Power (CV—normal)	0.1069	0.1399	0.1204	0.001	53.8951	Questionable	Goodness-of-fit *p*-value < 0.1 BMD 3× lower than lowest non-zero dose BMDL 3× lower than lowest non-zero dose Modeled control response std. dev. > |1.5| actual response std. dev.

Models	Test 2 (*p*-value)	5% relative deviation		Goodness of fit (*p*-value)	AIC	BMDS classification[a]	BMDS notes
		BMD	BMDL				
Linear (CV—normal)	0.1069	0.1399	0.1204	0.001	53.8951	Questionable	Goodness-of-fit *p*-value < 0.1 BMD 3× lower than lowest non-zero dose BMDL 3× lower than lowest non-zero dose Modeled control response std. dev. > |1.5| actual response std. dev.

No viable BMD or BMDL identified by BMDS.

[a]"Classification" column denotes whether a model can be considered for model selection purposes. See BMDS User Guide: https://www.epa.gov/bmds.

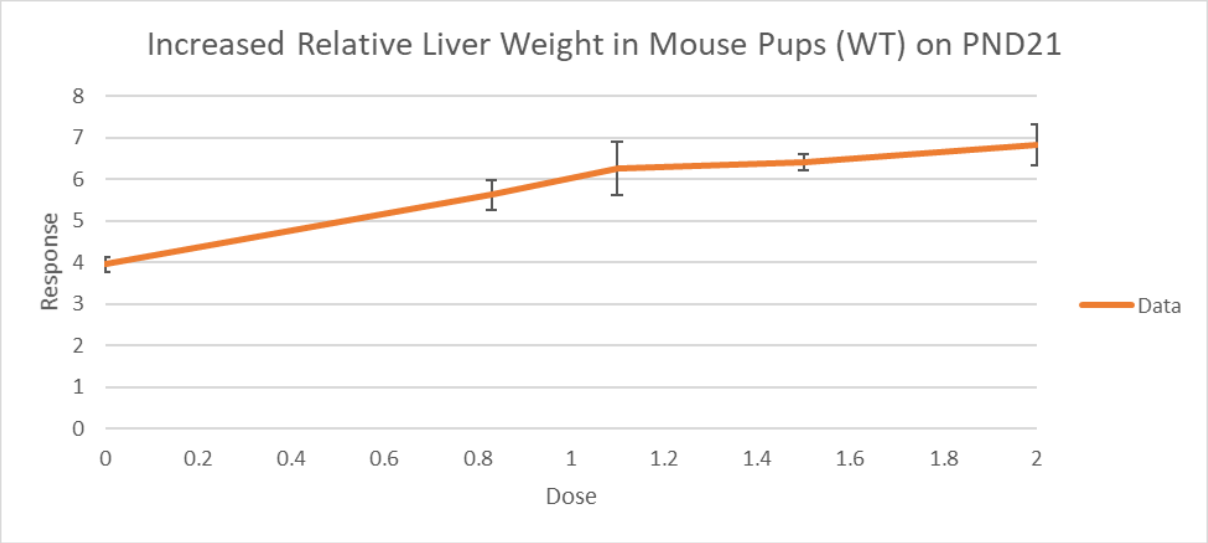

Figure D-25. Dose-response data for increased relative liver weight in mouse pups on PND 21 (Wolf et al., 2010)[a].

[a]X-axis is dose (mg/kg-d), and y-axis is relative liver weight (mg/g).

Increased Hepatic Hypertrophy in Male Rats (NTP, 2018)

Table D-63. Dose-response data for increased hepatic hypertrophy in male rats (NTP, 2018)

Dose (mg/kg-d)	N	Incidence
0	10	0
0.625	10	7
1.25	10	10
2.5	10	10
5	9	9
10	10	10

Table D-64. Benchmark dose results for increased hepatic hypertrophy in male rats, BMR = 10% extra risk (NTP, 2018)

Models	10% extra risk		Goodness of fit (*p*-value)	AIC	BMDS classification[a]	BMDS notes
	BMD	BMDL				
Dichotomous Hill	0.3806	0.0649	0.9996	16.3353	Viable – Alternate	BMD/BMDL ratio > 3 BMDL 3× lower than lowest non-zero dose
Gamma	0.2611	0.0300	0.9993	16.3638	Questionable	BMD/BMDL ratio > 3 BMDL 3× lower than lowest non-zero dose BMDL 10× lower than lowest non-zero dose
Log-Logistic	0.3806	0.0649	1.0000	14.3353	Viable – Alternate	BMD/BMDL ratio > 3 BMDL 3× lower than lowest non-zero dose
Multistage (Degree 5)	0.2848	0.0304	1.0000	14.2176	Questionable	BMD/BMDL ratio > 3 BMDL 3× lower than lowest non-zero dose BMDL 10× lower than lowest non-zero dose
Multistage (Degree 4)	0.2842	0.0306	1.0000	14.2177	Questionable	BMD/BMDL ratio > 3 BMDL 3× lower than lowest non-zero dose BMDL 10× lower than lowest non-zero dose
Multistage (Degree 3)	0.2774	0.0306	1.0000	14.2186	Questionable	BMD/BMDL ratio > 3 BMDL 3× lower than lowest non-zero dose BMDL 10× lower than lowest non-zero dose
Multistage (Degree 2)	0.1803	0.0300	0.9999	14.3600	Questionable	BMD/BMDL ratio > 3 BMD 3× lower than lowest non-zero dose BMDL 3× lower than lowest non-zero dose BMDL 10× lower than lowest non-zero dose
Multistage (Degree 1)	0.0430	0.0264	0.9207	17.6010	Questionable	BMD 3× lower than lowest non-zero dose BMDL 3× lower than lowest non-zero dose BMD 10× lower than lowest non-zero dose BMDL 10× lower than lowest non-zero dose

Models	10% extra risk		Goodness of fit (*p*-value)	AIC	BMDS classification[a]	BMDS notes
	BMD	BMDL				
Weibull	0.1235	0.1182	0.9920	16.6827	Viable – Alternate	BMD 3× lower than lowest non-zero dose BMDL 3× lower than lowest non-zero dose
Logistic[b]	**0.3266**	**0.1303**	**1.0000**	**14.3231**	**Viable – Recommended**	**Lowest AIC** **BMDL 3× lower than lowest non-zero dose**
Log-Probit	0.4693	0.0443	1.0000	16.2173	Questionable	BMD/BMDL ratio > 3 BMDL 3× lower than lowest non-zero dose BMDL 10× lower than lowest non-zero dose
Probit	0.1489	0.0972	0.5916	20.6639	Viable – Alternate	BMD 3× lower than lowest non-zero dose BMDL 3× lower than lowest non-zero dose

[a]"Classification" column denotes whether a model can be considered for model selection purposes. See BMDS User Guide: https://www.epa.gov/bmds.

[b]Note that while BMDS 3.2 recommends a viable model, the NOAEL/LOAEL approach was applied to this endpoint given that the response was much greater than the BMR in the lowest responding dose group.

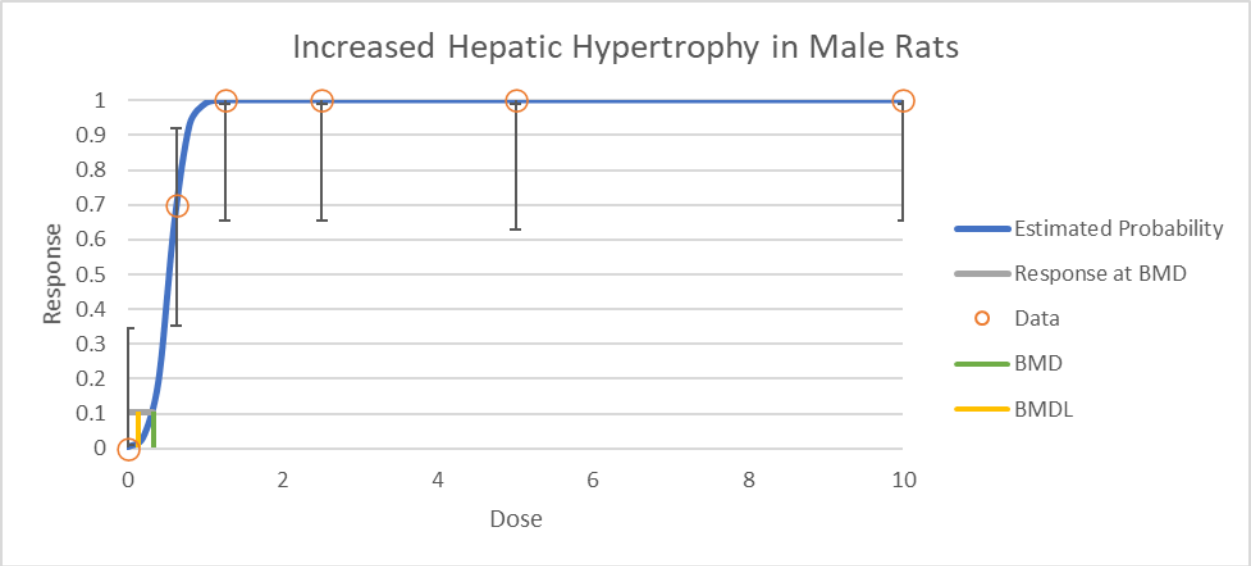

Figure D-26. Dose-response data and curve of the logistic model for increased hepatic hypertrophy in male rats (NTP, 2018)[a].

[a]X-axis is dose (mg/kg-d), and y-axis is percent incidence of hepatic hypertrophy.

Increased Hepatic Hypertrophy in Female Rats (NTP, 2018)

Table D-65. Dose-response data for increased hepatic hypertrophy in female rats (NTP, 2018)

Dose (mg/kg-d)	N	Incidence
0	10	0
1.56	10	0
3.12	10	2
6.25	10	10
12.5	10	10
25	10	10

Table D-66. Benchmark dose results for increased hepatic hypertrophy in female rats, BMR = 10% extra risk (NTP, 2018)

Models	10% extra risk		Goodness of fit (*p*-value)	AIC	BMDS classification[a]	BMDS notes
	BMD	BMDL				
Dichotomous Hill	2.8529	2.2284	0.9995	14.1386	Viable – Alternate	
Gamma	2.7046	2.0587	0.9944	14.4191	Viable – Alternate	
Log-Logistic	2.8529	2.2284	0.9999	12.1386	Viable – Alternate	
Multistage (Degree 5)	2.6887	1.4859	0.9999	12.1624	Viable – Alternate	
Multistage (Degree 4)	2.4682	1.5559	0.9960	12.6830	Viable – Alternate	
Multistage (Degree 3)	2.0688	1.3925	0.9077	14.5840	Viable – Alternate	
Multistage (Degree 2)	1.4739	0.9835	0.4998	19.0935	Viable – Alternate	
Multistage (Degree 1)	0.5001	0.3410	0.0210	31.8454	Questionable	Goodness-of-fit *p*-value < 0.1 BMD 3× lower than lowest non-zero dose BMDL 3× lower than lowest non-zero dose
Weibull	2.0283	0.0000	0.8404	15.6262	Unusable	BMD computation failed; lower limit includes zero BMDL not estimated
Logistic[b]	**2.9180**	**2.0646**	**1.0000**	**12.0181**	**Viable – Recommended**	**Lowest AIC**
Log-Probit	2.9720	2.2131	1.0000	14.0080	Viable – Alternate	
Probit	2.3662	1.6506	0.9554	14.0668	Viable – Alternate	

[a]"Classification" column denotes whether a model can be considered for model selection purposes. See BMDS User Guide: https://www.epa.gov/bmds.

[b]Note that while BMDS 3.2 recommends a viable model, the NOAEL/LOAEL approach was applied to this endpoint given that the response was much greater than the BMR in the lowest responding dose group.

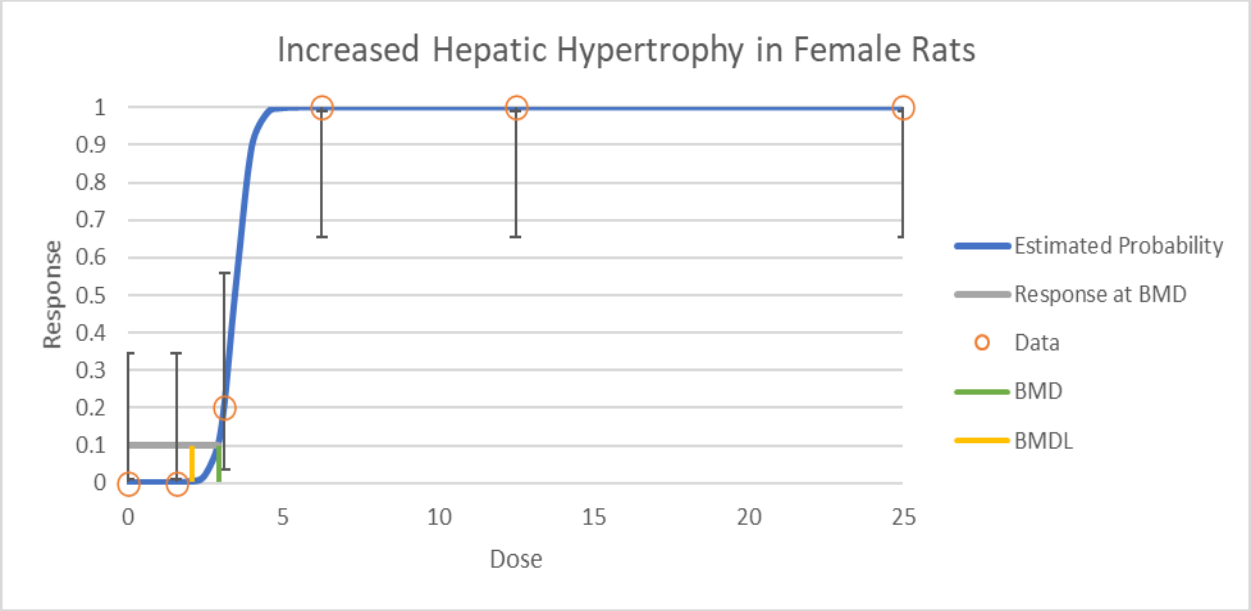

Figure D-27. Dose-response data and curve of the logistic model for increased hepatic hypertrophy in female rats (NTP, 2018)[a].

[a]X-axis is dose (mg/kg-d), and y-axis is percent incidence of hepatic hypertrophy.

Decreased Thyroxine Total T4 in Female Rats (NTP, 2018)

Table D-67. Dose-response data for decreased thyroxine total T4 in female rats (NTP, 2018)

Dose (mg/kg-d)	n	Mean (µg/dL)	SD
0	10	4.37	1.2934
1.56	10	3.57	0.8949
3.12	10	2.81	0.5313
6.25	10	2.61	0.7495

Table D-68. Benchmark dose results for decreased thyroxine total T4 in female rats— non-constant variance, BMR = 1 standard deviation (NTP, 2018)

Models	Test 3 (*p*-value)	1 standard deviation		Goodness-of-fit (*p*-value)	AIC	BMDS classification[a]	BMDS notes
		BMD	BMDL				
Exponential 2 (NCV—normal)	0.4279	3.7284	2.1056	0.0511	109.4539	Questionable	Goodness-of-fit *p*-value < 0.1
Exponential 3 (NCV—normal)	0.4279	3.7266	2.1056	0.0511	109.4539	Questionable	Goodness-of-fit *p*-value < 0.1
Exponential 4 (NCV—normal)	**0.4279**	**1.7933**	**0.8367**	**0.2493**	**106.8322**	**Viable – Recommended**	**Lowest AIC**
Exponential 5 (NCV—normal)	0.4279	1.9785	1.0198	NA	107.5049	Questionable	d.f. = 0, saturated model (Goodness-of-fit test cannot be calculated)
Hill (NCV—normal)	0.4279	1.8580	1.0393	NA	107.5049	Questionable	d.f. = 0, saturated model (Goodness-of-fit test cannot be calculated)
Polynomial (3 degree) (NCV—normal)	0.4279	4.5182	2.8230	0.0244	110.9336	Questionable	Goodness-of-fit *p*-value < 0.1
Polynomial (2 degree) (NCV—normal)	0.4279	4.5182	2.8230	0.0244	110.9336	Questionable	Goodness-of-fit *p*-value < 0.1
Power (NCV—normal)	0.4279	4.5182	2.8228	0.0244	110.9336	Questionable	Goodness-of-fit *p*-value < 0.1
Linear (NCV—normal)	0.4279	4.5182	2.8230	0.0244	110.9336	Questionable	Goodness-of-fit *p*-value < 0.1

[a]"Classification" column denotes whether a model can be considered for model selection purposes. See BMDS User Guide: https://www.epa.gov/bmds.

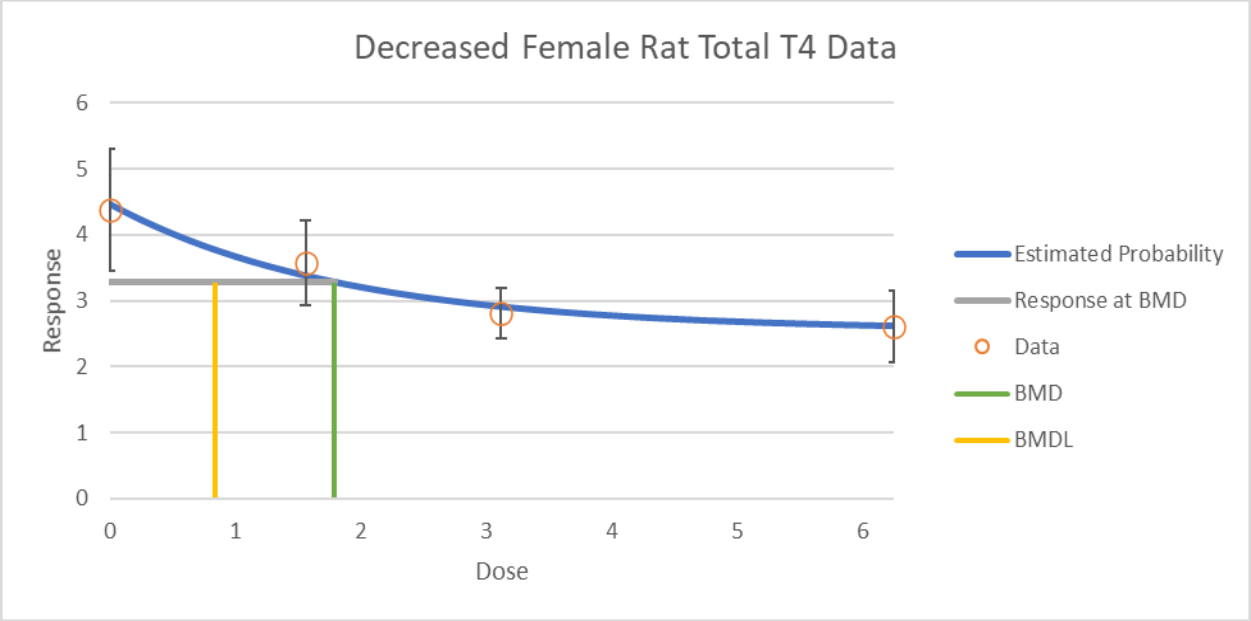

Figure D-28. Dose-response data and curve of the exponential 4 model for decreased female rat Total T4 (NTP, 2018)[a].

[a]X-axis is dose (mg/kg-d), and y-axis is level of Total T4 (µg/dL).

Decreased Free T4 in Female Rats (NTP, 2018)

Table D-69. Dose-response data for decreased Free T4 in female rats (NTP, 2018)

Dose (mg/kg-d)	n	Mean (ng/dL)	SD
0	10	1.702	0.6293
1.56	10	1.473	0.4870
3.12	10	1.096	0.3067
6.25	10	0.797	0.3036

Table D-70. Benchmark dose results for decreased Free T4 in female rats—constant variance, BMR = 1 standard deviation (NTP, 2018)

Models	Test 2 (*p*-value)	1 standard deviation		Goodness of fit (*p*-value)	AIC	BMDS classification[a]	BMDS notes
		BMD	BMDL				
Exponential 2 (CV—normal)	0.0523	2.2834	1.4681	0.7992	52.3308	Viable – Recommended	Lowest AIC
Exponential 3 (CV—normal)	0.0523	2.3517	1.4689	0.5067	54.3234	Viable – Alternate	
Exponential 4 (CV—normal)	0.0523	2.2294	1.0902	0.5055	54.3259	Viable – Alternate	
Exponential 5 (CV—normal)	0.0523	2.3560	1.1549	NA	55.8825	Questionable	d.f. = 0, saturated model (Goodness-of-fit test cannot be calculated)
Hill (CV—normal)	0.0523	2.3155	1.1066	NA	55.8825	Questionable	d.f. = 0, saturated model (Goodness-of-fit test cannot be calculated)
Polynomial (3 degree) (CV—normal)	0.0523	2.9468	2.1345	0.6263	52.8185	Viable – Alternate	
Polynomial (2 degree) (CV—normal)	0.0523	2.9468	2.1345	0.6263	52.8185	Viable – Alternate	
Power (CV—normal)	0.0523	2.9468	2.1346	0.6263	52.8185	Viable – Alternate	
Linear (CV—normal)	0.0523	2.9468	2.1345	0.6263	52.8185	Viable – Alternate	

[a]"Classification" column denotes whether a model can be considered for model selection purposes. See BMDS User Guide: https://www.epa.gov/bmds.

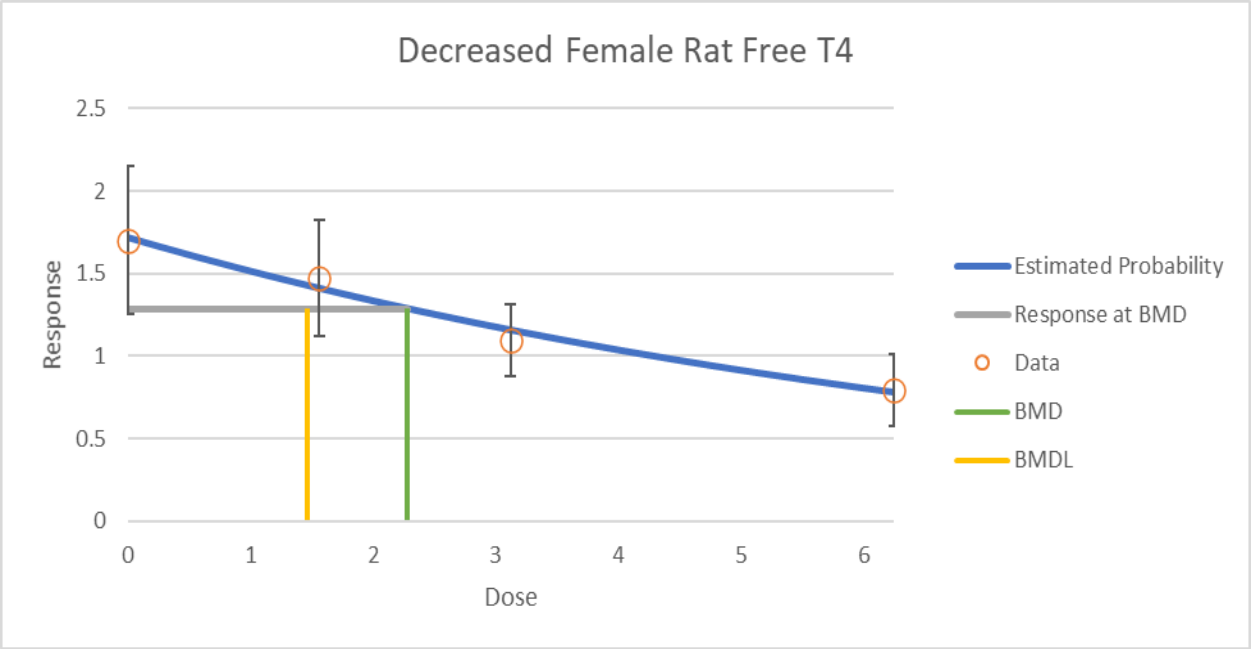

Figure D-29. Dose-response data and curve of the exponential 2 model for decreased female rat Free T4 (NTP, 2018)[a].

[a]X-axis is dose (mg/kg-d), and y-axis is level of Free T4 (ng/dL).

Decreased Survival Rate in Mice (Das et al., 2015)

Table D-71. Decreased survival rate in mice (NTP, 2018; Das et al., 2015)

Dose (mg/kg-d)	n	Mean (%)	SD
0	13	83.7	11.18
1	11	85.9	10.61
3	13	84.5	10.10
5	17	17.3	23.91

Table D-72. Benchmark dose results for decreased survival rate in mice — non-constant variance, BMR = 0.01 relative deviation (Das et al., 2015)

Models	Test 3 (*p*-value)	0.01 relative deviation		Goodness of fit (*p*-value)	AIC	BMDS classification[a]	BMDS notes
		BMD	BMDL				
Exponential 2 (NCV—normal)	0.9414	0.1232	0.0774	<0.0001	487.6169	Questionable	Goodness-of-fit *p*-value < 0.1 BMD 3× lower than lowest non-zero dose BMDL 3× lower than lowest non-zero dose BMDL 10× lower than lowest non-zero dose
Exponential 3 (NCV—normal)	0.9414	3.5203	2.1619	0.5874	442.2736	Viable – Alternate	
Exponential 4 (NCV—normal)	0.9414	0.1231	0.0774	<0.0001	487.6169	Questionable	Goodness-of-fit *p*-value < 0.1 BMD 3× lower than lowest non-zero dose BMDL 3× lower than lowest non-zero dose BMDL 10× lower than lowest non-zero dose
Exponential 5 (NCV—normal)	0.9414	3.3922	2.1614	NA	444.2736	Questionable	d.f. = 0, saturated model (Goodness-of-fit test cannot be calculated)
Hill (NCV—normal)[b]	**0.9414**	**3.3648**	**2.6883**	**0.5875**	**442.2736**	**Viable – Recommended**	**Lowest AIC**
Polynomial (3 degree) (NCV—normal)	0.9414	1.1928	0.7252	0.0010	453.8360	Questionable	Goodness-of-fit *p*-value < 0.1
Polynomial (2 degree) (NCV—normal)	0.9414	0.6317	0.3998	<0.0001	467.7543	Questionable	Goodness-of-fit *p*-value < 0.1
Power (NCV—normal)	0.9414	4.4957	4.4307	0.5869	442.2745	Viable – Alternate	
Linear (NCV—normal)	0.9414	0.1241	0.0887	<0.0001	484.5091	Questionable	Goodness-of-fit *p*-value < 0.1 BMD 3× lower than lowest non-zero dose BMDL 3× lower than

Models	Test 3 (*p*-value)	0.01 relative deviation		Goodness of fit (*p*-value)	AIC	BMDS classification[a]	BMDS notes
		BMD	BMDL				
							lowest non-zero dose BMDL 10× lower than lowest non-zero dose

[a]"Classification" column denotes whether a model can be considered for model selection purposes. See BMDS User Guide: https://www.epa.gov/bmds.

[b]Although an effect is observed only in the highest dose group, technical guideline supports BMD modeling in favor of the NOAEL/LOAEL approach for the derivation of reference values since this dataset can successfully be BMD modeled and the BMR is near an observed response.

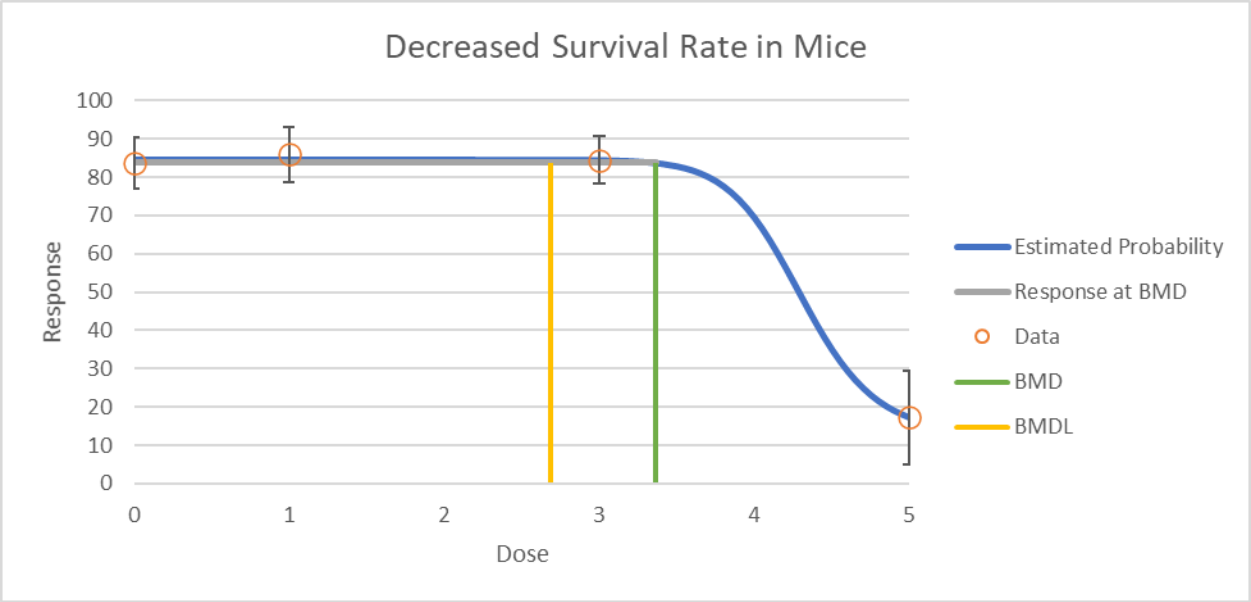

Figure D-30. Dose-response data and curve of the Hill model for decreased survival rate in mice (Das et al., 2015)[a].

[a]X-axis is dose (mg/kg-d), and y-axis is survival (%).

Decreased Survival Rate in Mice (WT) (Wolf et al., 2010)

Table D-73. Dose-response data for decreased survival rate in mice (WT) (Wolf et al., 2010)

Dose (mg/kg-d)	n	Mean (%)	SD
0	12	72.08	37.00
0.83	10	61.31	37.16
1.1	10	26.50	29.63
1.5	13	55.48	35.53
2	13	22.84	24.28

Table D-74. Benchmark dose results for decreased survival rate in mice — constant variance, BMR = 0.01 relative deviation (Wolf et al., 2010)

Models	Test 2 (*p*-value)	0.01 relative deviation		Goodness of fit (*p*-value)	AIC	BMDS classification[a]	BMDS notes
		BMD	BMDL				
Exponential 2 (CV—normal)	0.5595	0.0237	0.0156	0.0335	579.5559	Questionable	Goodness-of-fit *p*-value < 0.1 BMD 3× lower than lowest non-zero dose BMDL 3× lower than lowest non-zero dose BMD 10× lower than lowest non-zero dose BMDL 10× lower than lowest non-zero dose
Exponential 3 (CV—normal)	0.5595	0.0644	0.0158	0.0139	581.4034	Questionable	Goodness-of-fit *p*-value < 0.1 BMD/BMDL ratio > 3 BMD 3× lower than lowest non-zero dose BMDL 3× lower than lowest non-zero dose BMD 10× lower than lowest non-zero dose BMDL 10× lower than lowest non-zero dose
Exponential 4 (CV—normal)	0.5595	0.0237	0.0156	0.0335	579.5559	Questionable	Goodness-of-fit *p*-value < 0.1 BMD 3× lower than lowest non-zero dose BMDL 3× lower than lowest non-zero dose BMD 10× lower than lowest non-zero dose BMDL 10× lower than lowest non-zero dose
Exponential 5 (CV—normal)	0.5595	0.0644	0.0158	0.0139	581.4034	Questionable	Goodness-of-fit *p*-value < 0.1 BMD/BMDL ratio > 3 BMD 3× lower than lowest non-zero dose BMDL 3× lower than lowest non-zero dose BMD 10× lower than lowest non-zero dose BMDL 10× lower than lowest non-zero dose
Hill (CV—normal)	0.5595	0.0476	0.0038	0.0037	583.2650	Questionable	Goodness-of-fit *p*-value < 0.1 BMD/BMDL ratio > 3 BMD 3× lower than lowest non-zero dose BMDL 3× lower than lowest non-zero dose BMD 10× lower than lowest non-zero dose BMDL 10× lower than lowest non-zero dose

Models	Test 2 (*p*-value)	0.01 relative deviation		Goodness of fit (*p*-value)	AIC	BMDS classification[a]	BMDS notes
		BMD	BMDL				
Polynomial (3 degree) (CV—normal)	0.5595	0.0383	0.0254	0.0162	581.1804	Questionable	Goodness-of-fit *p*-value < 0.1 BMD 3× lower than lowest non-zero dose BMDL 3× lower than lowest non-zero dose BMD 10× lower than lowest non-zero dose BMDL 10× lower than lowest non-zero dose
Polynomial (2 degree) (CV—normal)	0.5595	0.0377	0.0253	0.0155	581.2332	Questionable	Goodness-of-fit *p*-value < 0.1 BMD 3× lower than lowest non-zero dose BMDL 3× lower than lowest non-zero dose BMD 10× lower than lowest non-zero dose BMDL 10× lower than lowest non-zero dose
Power (CV—normal)	0.5595	0.0381	0.0253	0.0151	581.2539	Questionable	Goodness-of-fit *p*-value < 0.1 BMD 3× lower than lowest non-zero dose BMDL 3× lower than lowest non-zero dose BMD 10× lower than lowest non-zero dose BMDL 10× lower than lowest non-zero dose
Linear (CV—normal)	0.5595	0.0329	0.0253	0.0150	579.2568	Questionable	Goodness-of-fit *p*-value < 0.1 BMD 3× lower than lowest non-zero dose BMDL 3× lower than lowest non-zero dose BMD 10× lower than lowest non-zero dose BMDL 10× lower than lowest non-zero dose

The means of the data could not be modeled.

[a]"Classification" column denotes whether a model can be considered for model selection purposes. See BMDS User Guide: https://www.epa.gov/bmds.

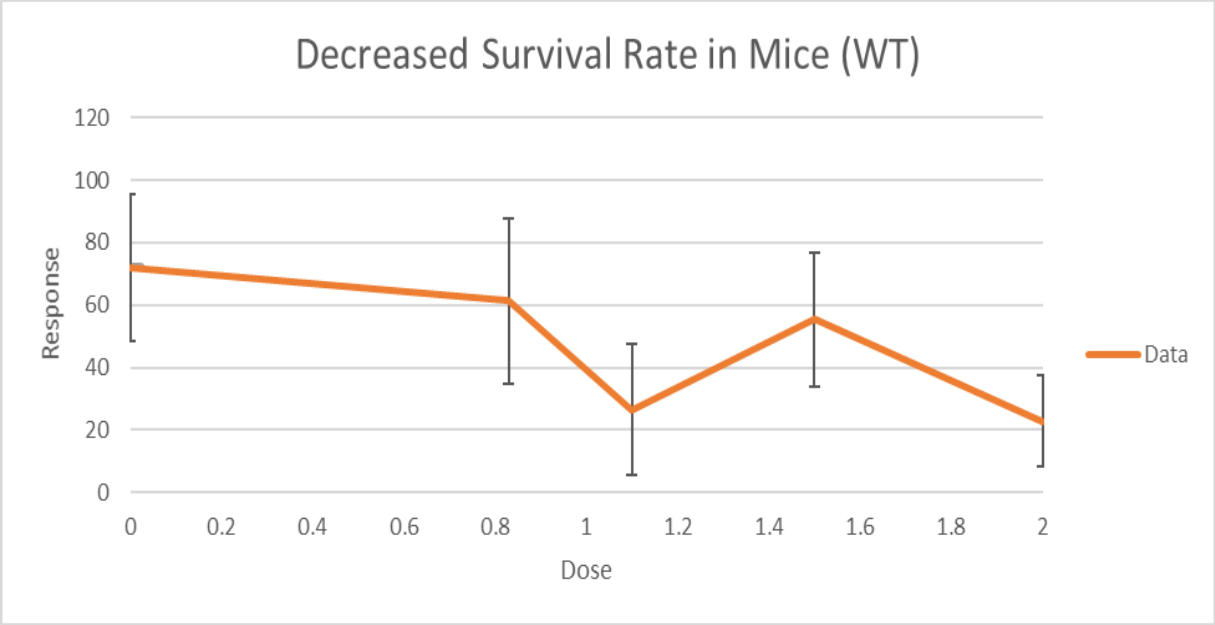

Figure D-31. Dose-response data for decreased survival rate in mice (Wolf et al., 2010)[a].

[a]X-axis is dose (mg/kg-d), and y-axis is survival rate in mice (%).

Offspring Body Weight on PND 7 in Mice (Das et al., 2015)

Table D-75. Dose-response data for offspring body weight on PND 7 in mice (Das et al., 2015)

Dose (mg/kg-d)	n	Mean (g)	SD
0	13	4.465	0.707
1	11	4.045	0.328
3	13	3.408	0.516
5	16	1.748	0.400

Table D-76. Benchmark dose results for offspring body weight on PND 7 in mice— non-constant variance, BMR = 0.05 relative deviation (Das et al., 2015)

Models	Test 3 (*p*-value)	0.05 relative deviation		Goodness of fit (*p*-value)	AIC	BMDS classification[a]	BMDS notes
		BMD	BMDL				
Exponential 2 (NCV—normal)	0.0575	0.3202	0.2754	<0.0001	103.0437	Questionable	Goodness-of-fit *p*-value < 0.1 BMD 3× lower than lowest non-zero dose BMDL 3× lower than lowest non-zero dose
Exponential 3 (NCV—normal)	0.0575	1.5981	1.0966	0.0825	84.9016	Questionable	Goodness-of-fit *p*-value < 0.1
Exponential 4 (NCV—normal)	0.0575	0.3202	0.2754	<0.0001	103.0437	Questionable	Goodness-of-fit *p*-value < 0.1 BMD 3× lower than lowest non-zero dose BMDL 3× lower than lowest non-zero dose
Exponential 5 (NCV—normal)	0.0575	1.6000	1.0966	0.0825	84.9016	Questionable	Goodness-of-fit *p*-value < 0.1
Hill (NCV—normal)	0.0575	2.5393	0.6798	NA	87.8486	Questionable	BMD/BMDL ratio > 3 d.f. = 0, saturated model (Goodness-of-fit test cannot be calculated)
Polynomial (3 degree) (NCV—normal)	**0.0575**	**0.8627**	**0.5624**	**0.3401**	**82.7960**	**Viable – Recommended**	**Lowest AIC**
Polynomial (2 degree) (NCV—normal)	0.0575	1.1174	0.6282	0.1673	83.7928	Viable – Alternate	
Power (NCV—normal)	0.0575	1.3146	0.7927	0.1311	84.1650	Viable – Alternate	
Linear (NCV—Normal)	0.0575	0.4197	0.3901	0.0023	92.0319	Viable – Alternate	Goodness-of-fit *p*-value < 0.1

[a]"Classification" column denotes whether a model can be considered for model selection purposes. See BMDS User Guide: https://www.epa.gov/bmds.

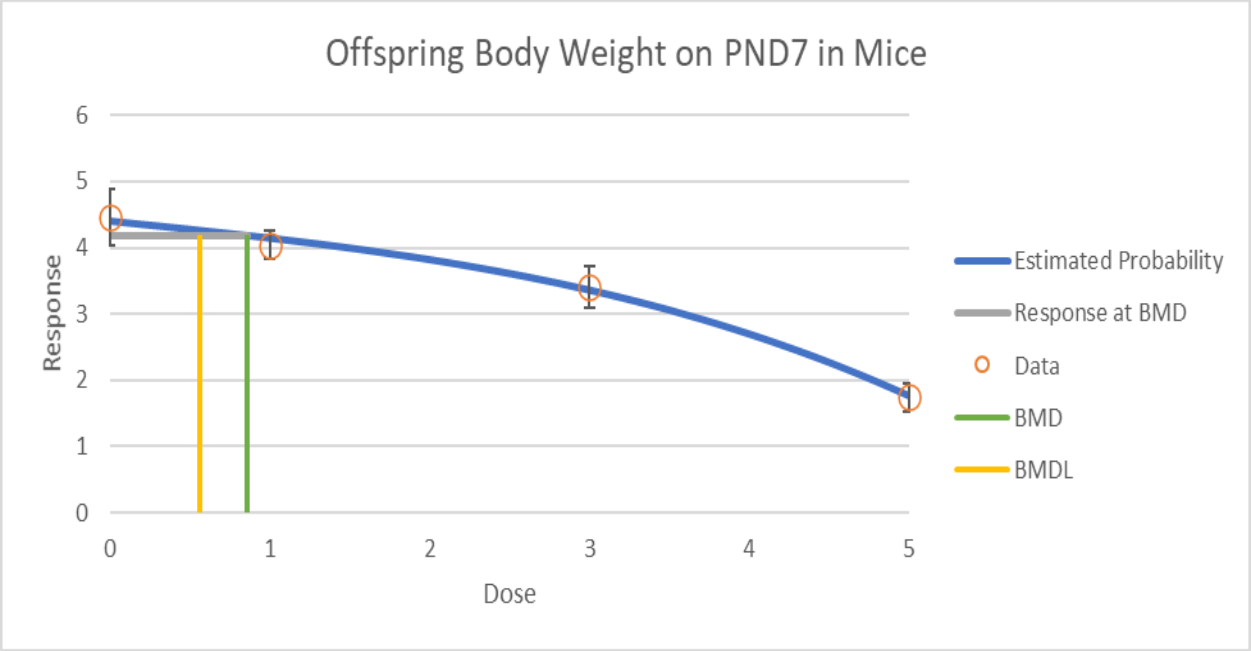

Figure D-32. Dose-response data and curve of the polynomial degree 3 model for offspring body weight on PND 7 in mice (Das et al., 2015)[a].

[a]X-axis is dose (mg/kg-d), and y-axis is offspring body weight (g).

Offspring Body Weight on PND 7 in Male Mice (WT) (Wolf et al., 2010)

Table D-77. Dose-response data for offspring body weight on PND 7 in male mice (WT) (Wolf et al., 2010)

Dose (mg/kg-d)	n	Mean (g)	SD
0	10	4.016666	0.399229965
0.83	5	3.60934	0.337791609
1.1	5	4.02	0.637965399
1.5	9	3.632963	0.5450037
2	4	2.5375	0.4190764

Table D-78. Benchmark dose results for offspring body weight on PND 7 in male mice (WT) — constant variance, BMR = 0.05 relative deviation (Wolf et al., 2010)

Models	Test 2 (*p*-value)	0.05 relative deviation		Goodness of fit (*p*-value)	AIC	BMDS classification[a]	BMDS notes
		BMD	BMDL				
Exponential 2 (CV—normal)	0.5450	0.4105	0.2780	0.7821	0.0033	Questionable	Goodness-of-fit *p*-value < 0.1
Exponential 3 (CV—normal)	0.5450	1.4130	1.0366	1.8036	0.2015	Viable – Alternate	
Exponential 4 (CV—normal)	0.5450	0.4105	0.2780	0.7821	0.0033	Questionable	Goodness-of-fit *p*-value < 0.1
Exponential 5 (CV—normal)	0.5450	1.4129	1.0366	1.8035	0.2015	Viable – Alternate	
Hill (CV – normal)	0.5450	1.4637	1.3838	1.7205	0.2150	Viable – Alternate	
Polynomial Degree 4 (CV – normal)	**0.5450**	**1.2332**	**0.6540**	**1.3478**	**0.2844**	**Viable – Recommended**	**Lowest AIC**
Polynomial Degree 3 (CV – normal)	0.5450	1.0665	0.6479	1.2076	0.1558	Viable – Alternate	
Polynomial Degree 2 (CV – normal)	0.5450	0.8193	0.5216	1.0110	0.0444	Questionable	Goodness-of-fit *p*-value < 0.1
Power (CV – normal)	0.5450	1.4035	0.9906	1.7421	0.2009	Viable – Alternate	
Linear (CV – normal)	0.5450	0.4253	0.3054	0.7482	0.0045	Questionable	Goodness-of-fit *p*-value < 0.1

[a]"Classification" column denotes whether a model can be considered for model selection purposes. See BMDS User Guide: https://www.epa.gov/bmds.

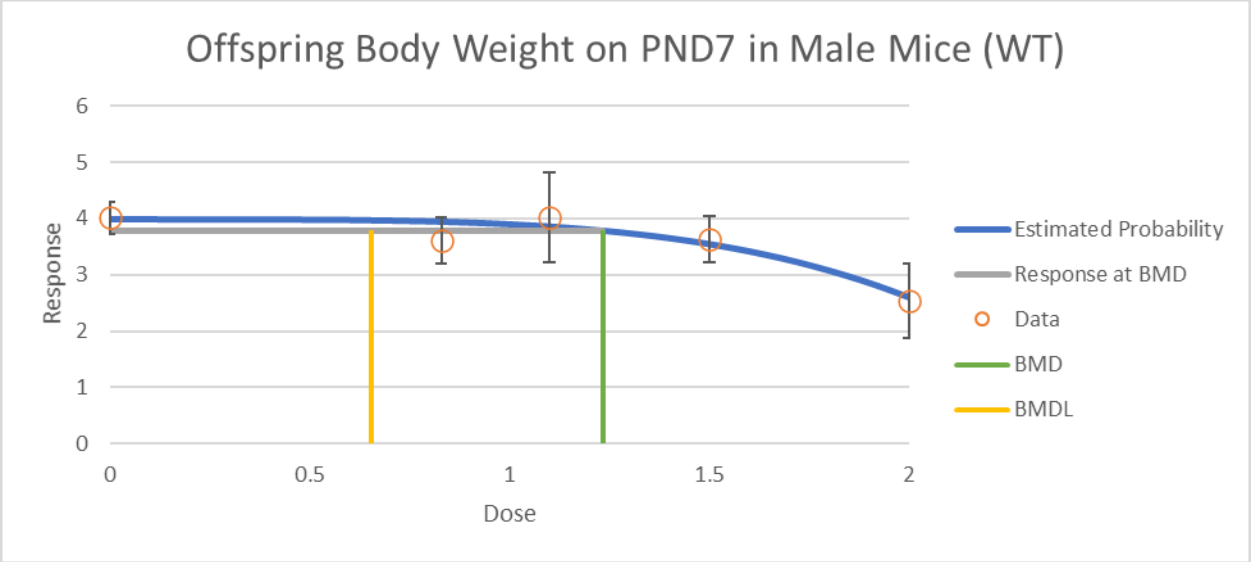

Figure D-33. Dose-response data and curve of the polynomial degree 4 model for offspring body weight on PND 7 in male mice (WT) (Wolf et al., 2010)[a].

[a]X-axis is dose (mg/kg-d), and y-axis is offspring body weight (g).

Offspring Body Weight on PND 7 in Female Mice (WT) (Wolf et al., 2010)

Table D-79. Dose-response data for offspring body weight on PND 7 in female mice (WT) — constant variance, BMR = 5% relative deviation (Wolf et al., 2010)

Dose (mg/kg-d)	n	Mean (g)	SD
0	9	4.097778	0.4861785
0.83	7	3.711429	0.478101549
1.1	6	3.561112	1.094718607
1.5	10	3.423809	0.736661435
2	6	2.63	0.270924343

Table D-80. Benchmark dose results for offspring body weight on PND 7 in female mice (WT) (highest dose group removed) — constant variance, BMR = 0.05 relative deviation (Wolf et al., 2010)

Models	Test 2 (*p*-value)	0.05 relative deviation		Goodness of fit (*p*-value)	AIC	BMDS classification[a]	BMDS notes
		BMD	BMDL				
Exponential 2 (CV—normal)	0.0902	0.4234	0.2454	0.9949	70.6836	Viable – Alternate	BMDL 3× lower than lowest non-zero dose
Exponential 3 (CV—normal)	**0.0902**	**0.4234**	**0.2464**	**0.9949**	**70.6836**	**Viable – Recommended**	**Lowest AIC BMDL 3× lower than lowest non-zero dose**
Exponential 4 (CV—normal)	0.0902	0.4088	0.0000	0.9251	72.6822	Unusable	BMD computation failed; lower limit includes zero BMDL not estimated
Exponential 5 (CV—normal)	0.0902	0.4234	0.0000	0.9195	72.6836	Unusable	BMD computation failed; lower limit includes zero BMDL not estimated
Hill (CV—normal)	0.0902	0.5678	0.0000	NA	74.6734	Unusable	BMD computation failed; lower limit includes zero BMDL not estimated d.f. = 0, saturated model (Goodness-of-fit test cannot be calculated)
Polynomial (3 degree) (CV—normal)	0.0902	0.4499	0.2763	0.9911	70.6914	Viable – Alternate	BMDL 3× lower than lowest non-zero dose
Polynomial (2 degree) (CV—normal)	0.0902	0.4499	0.2764	0.9911	70.6914	Viable – Alternate	BMDL 3× lower than lowest non-zero dose
Power (CV—normal)	0.0902	0.4499	0.2764	0.9911	70.6914	Viable – Alternate	BMDL 3× lower than lowest non-zero dose
Linear (CV—normal)	0.0902	0.4499	0.2763	0.9911	70.6914	Viable – Alternate	BMDL 3× lower than lowest non-zero dose

[a]"Classification" column denotes whether a model can be considered for model selection purposes. See BMDS User Guide: https://www.epa.gov/bmds.

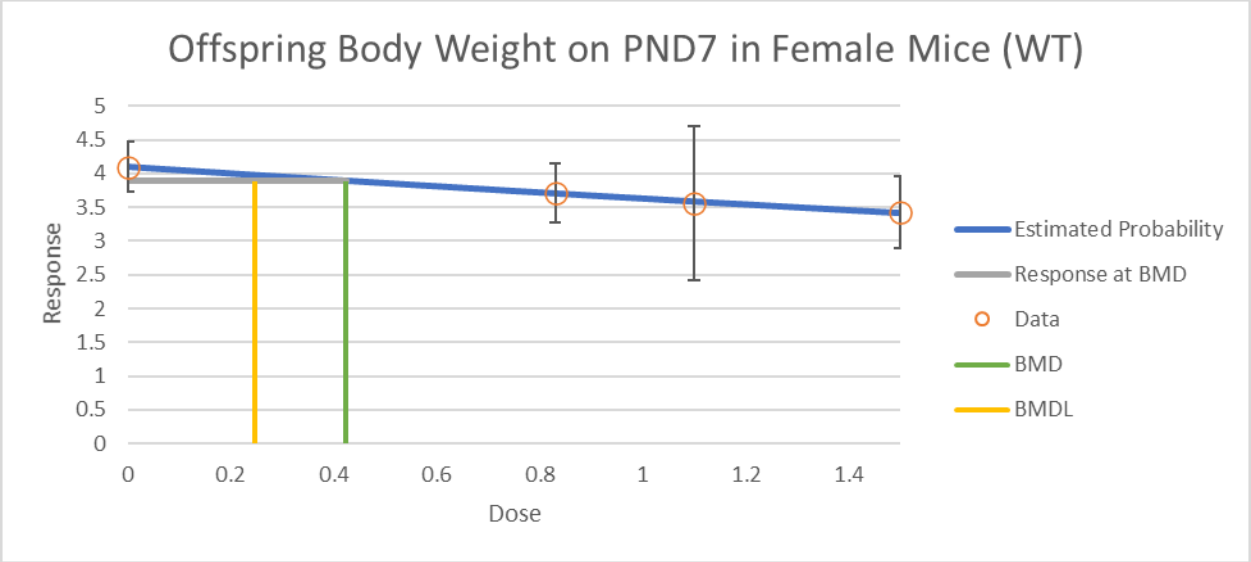

Figure D-34. Dose-response data and curve of the exponential 3 model for offspring body weight on PND 7 in female mice (WT) (Wolf et al., 2010)[a].

[a]X-axis is dose (mg/kg-d), and y-axis is offspring body weight (g).

Offspring Body Weight on PND 21 in Mice (Das et al., 2015)

Table D-81. Dose-response data for offspring body weight on PND 21 in mice (Das et al., 2015)

Dose (mg/kg-d)	n	Mean (g)	SD
0	13	13.45	2.383
1	11	11.62	1.585
3	13	10.07	1.709
5	13	6.59	2.427

Table D-82. Benchmark dose results for offspring body weight on PND 21 in mice — constant variance, BMR = 0.05 relative deviation (Das et al., 2015)

Models	Test 2 (*p*-value)	0.05 relative deviation		Goodness of fit (*p*-value)	AIC	BMDS classification[a]	BMDS notes
		BMD	BMDL				
Exponential 2 (CV—normal)	0.3164	0.4037	0.3325	0.1753	220.4399	Viable – Alternate	BMDL 3× lower than lowest non-zero dose
Exponential 3 (CV—normal)	0.3164	0.8413	0.3464	0.1129	221.4705	Viable – Alternate	
Exponential 4 (CV—normal)	0.3164	0.4036	0.3325	0.1753	220.4399	Viable – Alternate	BMDL 3× lower than lowest non-zero dose
Exponential 5 (CV—normal)	0.3164	0.8431	0.3459	0.1129	221.4705	Viable – Alternate	
Hill (CV—normal)	0.3164	2.7099	2.6010	NA	225.7456	Questionable	d.f. = 0, saturated model (Goodness-of-fit test cannot be calculated)
Polynomial (3 degree) (CV—normal)	0.3164	0.6548	0.4566	0.2677	220.1863	Viable – Alternate	
Polynomial (2 degree) (CV—normal)	0.3164	0.6791	0.4534	0.2218	220.4505	Viable – Alternate	
Power (CV—normal)	0.3164	0.6841	0.4496	0.1771	220.7798	Viable – Alternate	
Linear (CV—normal)	**0.3164**	**0.5137**	**0.4479**	**0.3711**	**218.9406**	**Viable – Recommended**	**Lowest AIC**

[a]"Classification" column denotes whether a model can be considered for model selection purposes. See BMDS User Guide: https://www.epa.gov/bmds.

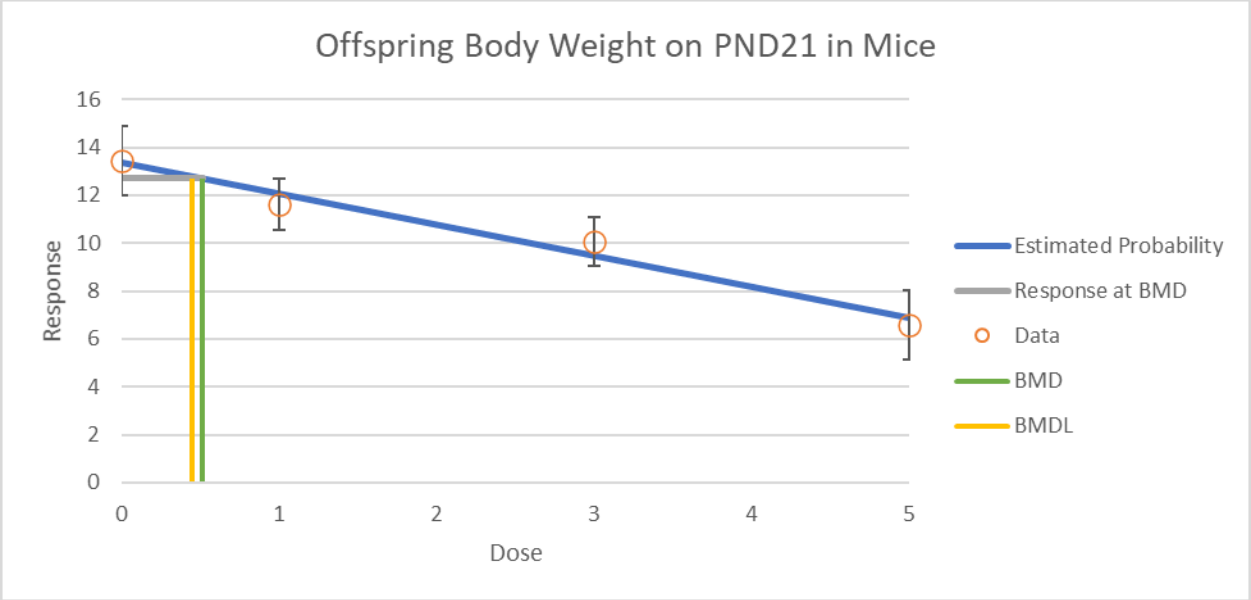

Figure D-35. Dose-response data and curve of the linear model for offspring body weight on PND 21 in mice (Das et al., 2015)[a].

[a]X-axis is dose (mg/kg-d), and y-axis is offspring body weight (g).

Offspring Body Weight on PND 21 in Male Mice (WT) (Wolf et al., 2010)

Table D-83. Dose-response data for offspring body weight on PND 21 in male mice (WT) (Wolf et al., 2010)

Dose (mg/kg-d)	n	Mean (g)	SD
0	10	9.641	1.142
0.83	6	9.527	0.649
1.1	5	10.344	1.960
1.5	9	9.686	0.950
2	3	8.400	0.100

Table D-84. Benchmark dose results for offspring body weight on PND 7 in male mice (WT) — constant variance, BMR = 0.05 relative deviation (Wolf et al., 2010)

Models	Test 2 (*p*-value)	0.05 relative deviation		Goodness of fit (*p*-value)	AIC	BMDS classification[a]	BMDS notes
		BMD	BMDL				
Exponential 2 (CV—normal)	0.5600	0.0237	0.0156	0.0335	579.5559	Questionable	Goodness-of-fit *p*-value < 0.1 BMD 3× lower than lowest non-zero dose BMDL 3× lower than lowest non-zero dose BMD 10× lower than lowest non-zero dose BMDL 10× lower than lowest non-zero dose
Exponential 3 (CV—normal)	0.5600	0.0644	0.0158	0.0139	581.4034	Questionable	Goodness-of-fit *p*-value < 0.1 BMD/BMDL ratio > 3 BMD 3× lower than lowest non-zero dose BMDL 3× lower than lowest non-zero dose BMD 10× lower than lowest non-zero dose BMDL 10× lower than lowest non-zero dose
Exponential 4 (CV—normal)	0.5600	0.0237	0.0156	0.0335	579.5559	Questionable	Goodness-of-fit *p*-value < 0.1 BMD 3× lower than lowest non-zero dose BMDL 3× lower than lowest non-zero dose BMD 10× lower than lowest non-zero dose BMDL 10× lower than lowest non-zero dose
Exponential 5 (CV—normal)	0.5600	0.0644	0.0158	0.0139	581.4034	Questionable	Goodness-of-fit *p*-value < 0.1 BMD/BMDL ratio > 3 BMD 3× lower than lowest non-zero dose BMDL 3× lower than lowest non-zero dose BMD 10× lower than lowest non-zero dose BMDL 10× lower than lowest non-zero dose

Models	Test 2 (*p*-value)	0.05 relative deviation		Goodness of fit (*p*-value)	AIC	BMDS classification[a]	BMDS notes
		BMD	BMDL				
Hill (CV—normal)	0.5600	0.0476	0.0038	0.0037	583.2650	Questionable	Goodness-of-fit *p*-value < 0.1 BMD/BMDL ratio > 3 BMD 3× lower than lowest non-zero dose BMDL 3× lower than lowest non-zero dose BMD 10× lower than lowest non-zero dose BMDL 10× lower than lowest non-zero dose
Polynomial (3 degree) (CV—normal)	0.5600	0.0391	0.0254	0.0162	581.0983	Questionable	Goodness-of-fit *p*-value < 0.1 BMD 3× lower than lowest non-zero dose BMDL 3× lower than lowest non-zero dose BMD 10× lower than lowest non-zero dose BMDL 10× lower than lowest non-zero dose
Polynomial (2 degree) (CV—normal)	0.5600	0.0383	0.0254	0.0155	581.1804	Questionable	Goodness-of-fit *p*-value < 0.1 BMD 3× lower than lowest non-zero dose BMDL 3× lower than lowest non-zero dose BMD 10× lower than lowest non-zero dose BMDL 10× lower than lowest non-zero dose
Power (CV—normal)	0.5600	0.0377	0.0253	0.0151	581.2332	Questionable	Goodness-of-fit *p*-value < 0.1 BMD 3× lower than lowest non-zero dose BMDL 3× lower than lowest non-zero dose BMD 10× lower than lowest non-zero dose BMDL 10× lower than lowest non-zero dose
Linear (CV—normal)	0.5600	0.0381	0.0253	0.0150	581.2539	Questionable	Goodness-of-fit *p*-value < 0.1 BMD 3× lower than lowest non-zero dose BMDL 3× lower than lowest non-zero dose BMD 10× lower than lowest non-zero dose BMDL 10× lower than lowest non-zero dose

The means of the data could not be modeled.

[a]"Classification" column denotes whether a model can be considered for model selection purposes. See BMDS User Guide: https://www.epa.gov/bmds.

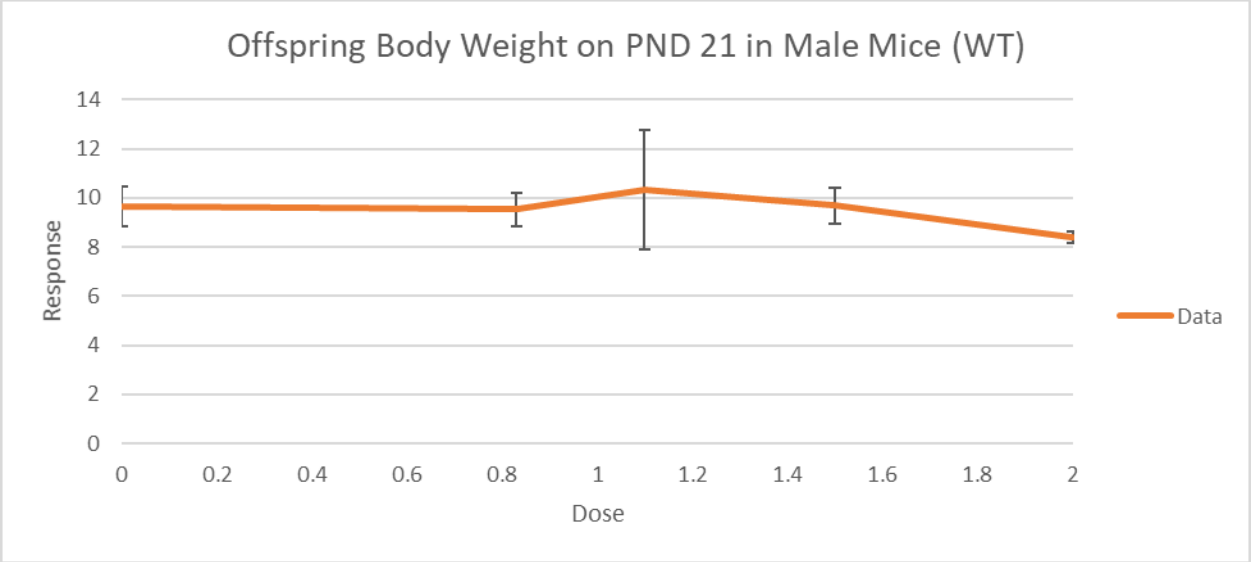

Figure D-36. Dose-response data for offspring body weight on PND 21 in male mice (WT) (Wolf et al., 2010).

Offspring Body Weight on PND 21 in Female Mice (WT) (Wolf et al., 2010)

Table D-85. Dose-response data for offspring body weight on PND 21 in female mice (WT) (Wolf et al., 2010)

Dose (mg/kg-d)	n	Mean (g)	SD
0	9	9.753	1.066
0.83	8	9.513	0.785
1.1	4	10.400	1.635
1.5	9	9.460	0.966
2	7	7.679	1.145

Table D-86. Benchmark dose results for offspring body weight on PND 21 in female mice (WT) — constant variance, BMR = 0.05 relative deviation (Wolf et al., 2010)

Models	Test 2 (*p*-value)	0.05 relative deviation		Goodness of fit (*p*-value)	AIC	BMDS classification[a]	BMDS notes
		BMD	BMDL				
Exponential 2 (CV—normal)	0.6109	0.6382	0.4005	0.0060	123.2125	Questionable	Goodness-of-fit *p*-value < 0.1
Exponential 3 (CV—normal)	0.6109	1.6304	1.2298	0.3318	114.9644	Viable – Alternate	
Exponential 4 (CV—normal)	0.6109	0.6382	0.4005	0.0060	123.2125	Questionable	Goodness-of-fit *p*-value < 0.1
Exponential 5 (CV—normal)	0.6109	1.6322	1.2324	0.3318	114.9644	Viable – Alternate	
Hill (CV – normal)	0.6109	1.5431	1.4168	0.3538	114.8357	Viable – Alternate	
Polynomial Degree 4 (CV – normal)[b]	**0.6109**	**1.3924**	**0.9775**	**0.3370**	**114.1357**	**Viable – Recommended**	**Lowest AIC**
Polynomial Degree 3 (CV – normal)	0.6109	1.2464	0.8855	0.1853	115.5796	Viable – Alternate	
Polynomial Degree 2 (CV – normal)	0.6109	1.0191	0.7021	0.0593	118.1896	Questionable	Goodness-of-fit *p*-value < 0.1
Power (CV – normal)	0.6109	1.6389	1.2178	0.3301	114.9748	Viable – Alternate	
Linear (CV – normal)	0.6109	0.6417	0.4247	0.0071	122.8321	Questionable	Goodness-of-fit *p*-value < 0.1

[a]"Classification" column denotes whether a model can be considered for model selection purposes. See BMDS User Guide: https://www.epa.gov/bmds.

[b]Although an effect is observed only in the highest dose group, technical guideline supports BMD modeling in favor of the NOAEL/LOAEL approach for the derivation of reference values since this dataset can successfully be BMD modeled and the BMR is near an observed response.

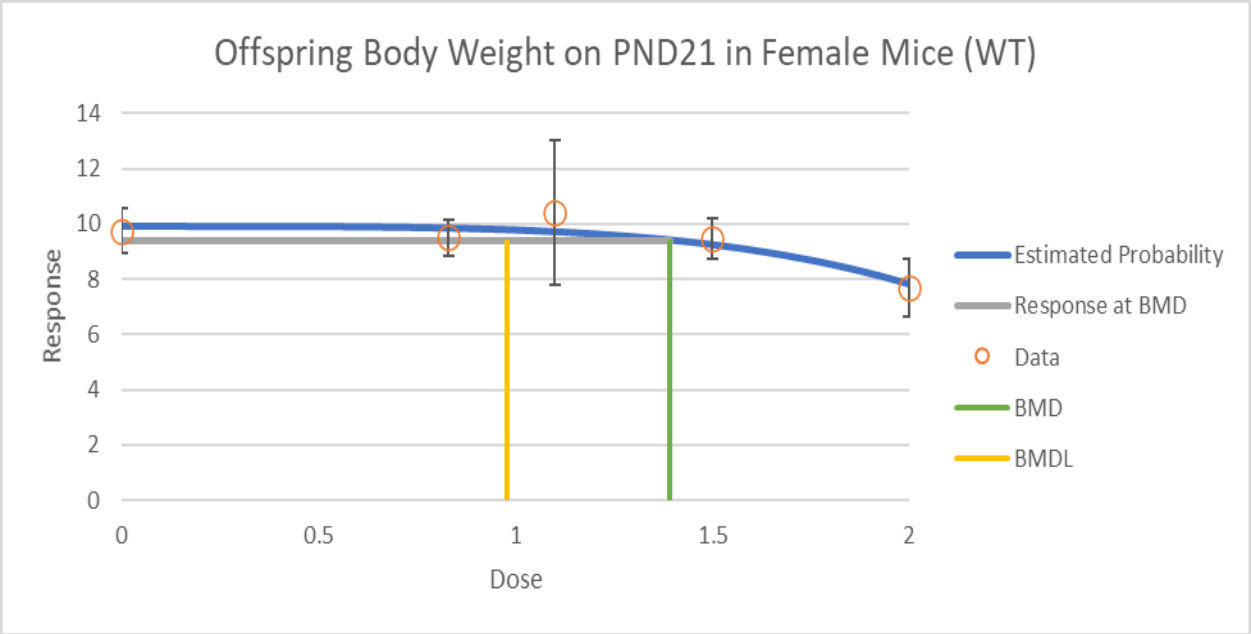

Figure D-37. Dose-response data and curve of the polynomial degree 4 model for offspring body weight on PND 21 in female mice (WT) (Wolf et al., 2010).

Offspring Body Weight on PND 24 in Male Mice (Das et al., 2015)

Table D-87. Dose-response data for offspring body weight on PND 24 in male mice (Das et al., 2015)

Dose (mg/kg-d)	n	Mean (g)	SD
0	13	17.7	3.606
1	11	15.8	1.990
3	13	13.6	2.163
5	7	8.4	2.910

Table D-88. Benchmark dose results for offspring body weight on PND 24 in male mice — constant variance, BMR = 0.05 relative deviation (Das et al., 2015)

Models	Test 2 (*p*-value)	0.05 relative deviation		Goodness of fit (*p*-value)	AIC	BMDS classification[a]	BMDS notes
		BMD	BMDL				
Exponential 2 (CV—normal)	0.1359	0.4290	0.3411	0.1187	219.9678	Viable – Alternate	
Exponential 3 (CV—normal)	0.1359	1.2613	0.3951	0.1700	219.5881	Viable – Alternate	BMD/BMDL ratio > 3
Exponential 4 (CV—normal)	0.1359	0.4289	0.3411	0.1187	219.9678	Viable – Alternate	
Exponential 5 (CV—normal)	0.1359	1.2613	0.3951	0.1700	219.5881	Viable – Alternate	BMD/BMDL ratio > 3
Hill (CV—normal)	0.1359	2.7262	2.6253	NA	222.7271	Questionable	d.f. = 0, saturated model (Goodness-of-fit test cannot be calculated)
Polynomial (3 degree) (CV—normal)	0.1359	0.7776	0.4727	0.4271	218.3362	Viable – Alternate	
Polynomial (2 degree) (CV—normal)	0.1359	0.8798	0.4647	0.3191	218.6980	Viable – Alternate	
Power (CV—normal)	0.1359	1.0283	0.4576	0.2416	219.0765	Viable – Alternate	
Linear (CV—normal)	**0.1359**	**0.5218**	**0.4420**	**0.2944**	**218.1511**	**Viable – Recommended**	**Lowest AIC**

[a]"Classification" column denotes whether a model can be considered for model selection purposes. See BMDS User Guide: https://www.epa.gov/bmds.

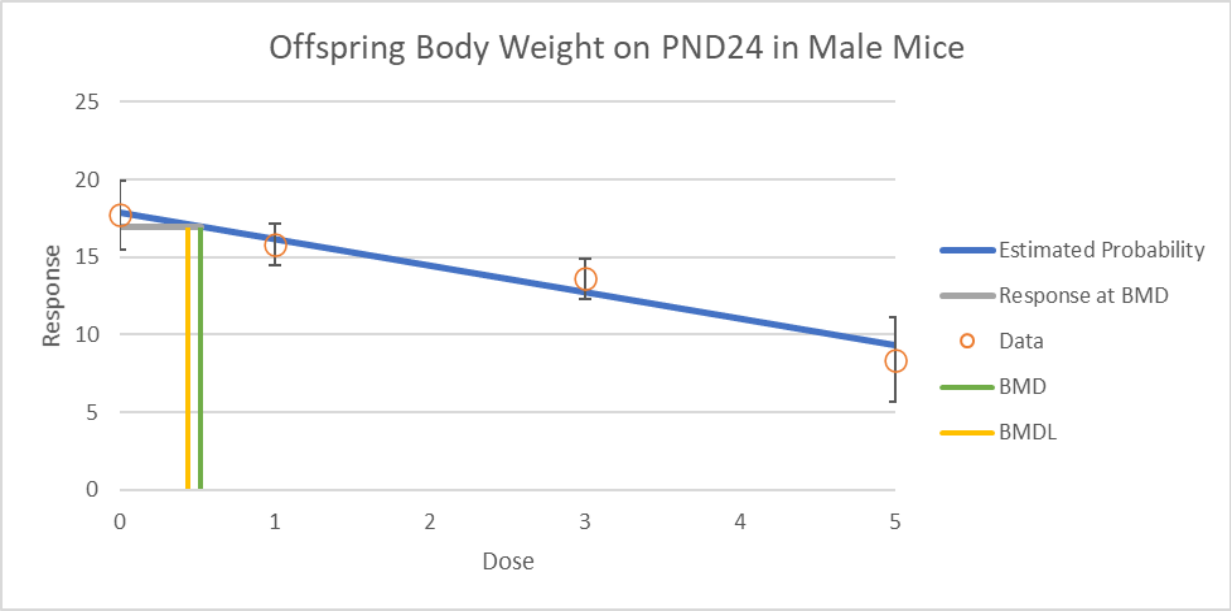

Figure D-38. Dose-response data and curve of linear model for offspring body weight on PND 24 in male mice (Das et al., 2015)[a].

[a]X-axis is dose (mg/kg-d), and y-axis is offspring body weight (g).

Offspring Body Weight on PND 24 in Female Mice (Das et al., 2015)

Table D-89. Dose-response data for offspring body weight on PND 24 in female mice (Das et al., 2015)

Dose (mg/kg-d)	n	Mean (g)	SD
0	13	16	2.524
1	11	14.6	1.658
3	13	13.1	1.803
5	7	9.5	2.910

Table D-90. Benchmark dose results for offspring body weight on PND 24 in female mice — constant variance, BMR = 0.05 relative deviation (Das et al., 2015)

Models	Test 2 (*p*-value)	0.05 relative deviation		Goodness of fit (*p*-value)	AIC	BMDS classification[a]	BMDS notes
		BMD	BMDL				
Exponential 2 (CV—normal)	0.2659	0.5830	0.4556	0.2484	198.8793	Viable – Alternate	
Exponential 3 (CV—normal)	0.2659	1.3267	0.4877	0.2250	199.5659	Viable – Alternate	
Exponential 4 (CV—normal)	**0.2659**	**0.5830**	**0.4556**	**0.2484**	**198.8793**	**Viable – Recommended**	**Lowest BMDL**
Exponential 5 (CV—normal)	0.2659	1.3267	0.4873	0.2250	199.5659	Viable – Alternate	
Hill (CV—normal)	0.2659	2.7716	2.6495	0.1086	200.6687	Viable – Alternate	
Polynomial (3 degree) (CV—normal)	0.2659	0.9770	0.5822	0.4451	198.6767	Viable – Alternate	
Polynomial (2 degree) (CV—normal)	0.2659	1.0601	0.5749	0.3522	198.9591	Viable – Alternate	
Power (CV—normal)	0.2659	1.1782	0.5679	0.2785	199.2679	Viable – Alternate	
Linear (CV—normal)	0.2659	0.6735	0.5546	0.3979	197.9368	Viable – Alternate	

[a]"Classification" column denotes whether a model can be considered for model selection purposes. See BMDS User Guide: https://www.epa.gov/bmds.

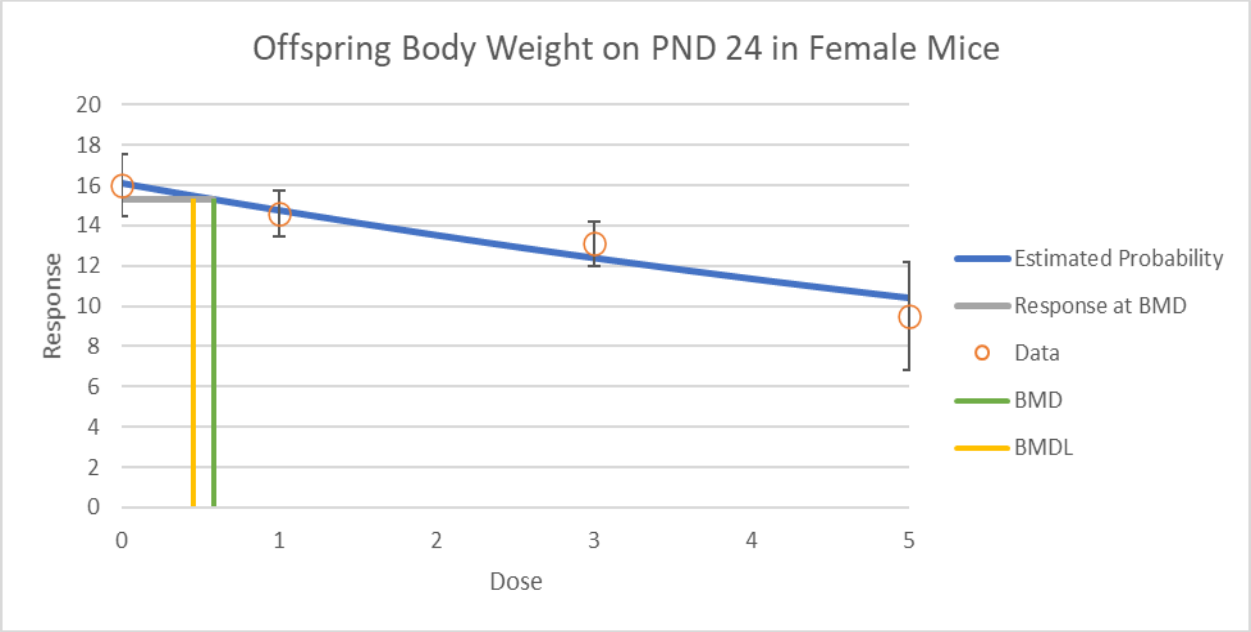

Figure D-39. Dose-response data and curve of exponential 4 model for offspring body weight on PND 24 in female mice (Das et al., 2015)[a].

[a]X-axis is dose (mg/kg-d), and y-axis is offspring body weight (g).

Offspring Body Weight on PND 42 in Female Mice (Das et al., 2015)

Table D-91. Dose-response data for offspring body weight on PND 42 in female mice (Das et al., 2015)

Dose (mg/kg-d)	n	Mean (ng/dL)	SD
0	13	36.42	3.208940635
1	11	34.49	2.653299832
3	13	32.44	4.18243948
5	6	31.06	4.066152973

Table D-92. Benchmark dose results for offspring body weight on PND 42 in female mice — constant variance, BMR = 0.05 relative deviation (Das et al., 2015)

Models	Test 2 (*p*-value)	0.05 relative deviation		Goodness of fit (*p*-value)	AIC	BMDS classification[a]	BMDS notes
		BMD	BMDL				
Exponential 2 (CV—normal)	0.4352	1.5517	1.0604	0.7859	232.8346	Viable – Alternate	
Exponential 3 (CV—normal)	0.4352	1.5517	1.0639	0.7859	232.8346	Viable – Alternate	
Exponential 4 (CV—normal)	0.4352	1.0233	0.3035	0.8692	234.3798	Viable – Alternate	BMD/BMDL ratio > 3 BMDL 3× lower than lowest non-zero dose
Exponential 5 (CV—normal)	0.4352	1.0233	0.3041	0.8692	234.3798	Viable – Alternate	BMD/BMDL ratio > 3 BMDL 3× lower than lowest non-zero dose
Hill (CV—normal)	**0.4352**	**0.9809**	**0.1938**	**0.9129**	**234.3646**	**Viable – Recommended**	**Lowest BMDL BMD/BMDL ratio > 3 BMDL 3× lower than lowest non-zero dose**
Polynomial (3 degree) (CV—normal)	0.4352	1.6419	1.1571	0.7394	232.9565	Viable – Alternate	
Polynomial (2 degree) (CV—normal)	0.4352	1.6419	1.1571	0.7394	232.9565	Viable – Alternate	
Power (CV—normal)	0.4352	1.6419	1.1571	0.7394	232.9565	Viable – Alternate	
Linear (CV—normal)	0.4352	1.6419	1.1571	0.7394	232.9565	Viable – Alternate	

[a]"Classification" column denotes whether a model can be considered for model selection purposes. See BMDS User Guide: https://www.epa.gov/bmds.

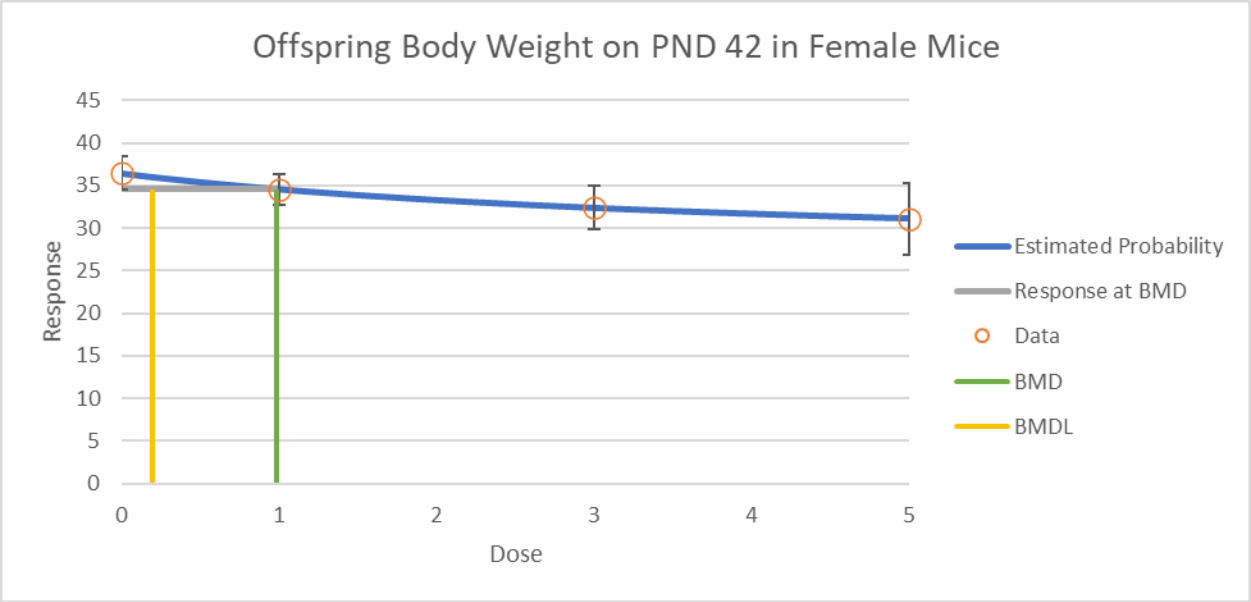

Figure D-40. Dose-response data and curve of Hill model for offspring body weight on PND 42 in female mice (Das et al., 2015)[a].

[a]X-axis is dose (mg/kg-d), and y-axis is offspring body weight (g).

Offspring Body Weight on PND 287 in Male Mice (Das et al., 2015)

Table D-93. Dose-response data for offspring body weight on PND 287 in male mice (Das et al., 2015)

Dose (mg/kg-d)	n	Mean (g)	SD
0	13	60.29	7.319
1	11	54.95	8.093
3	13	53.32	8.978
5	5	51.49	7.357

Table D-94. Benchmark dose results for offspring body weight on PND 287 in male mice — constant variance, BMR = 0.05 relative deviation (Das et al., 2015)

Models	Test 2 (*p*-value)	0.05 relative deviation		Goodness of fit (*p*-value)	AIC	BMDS classification[a]	BMDS notes
		BMD	BMDL				
Exponential 2 (CV—normal)	0.8527	1.6045	0.9385	0.5041	297.8758	Viable – Alternate	
Exponential 3 (CV—normal)	**0.8527**	**1.6045**	**0.9437**	**0.5041**	**297.8758**	**Viable – Recommended**	**Lowest AIC**
Exponential 4 (CV—normal)	0.8527	0.4550	0.0000	0.6916	298.6632	Unusable	BMD computation failed; lower limit includes zero BMDL not estimated
Exponential 5 (CV—normal)	0.8527	0.4693	0.0000	0.6908	298.6641	Unusable	BMD computation failed; lower limit includes zero BMDL not estimated
Hill (CV—normal)	0.8527	0.3860	0.0000	0.7676	298.5932	Unusable	BMD computation failed; lower limit includes zero BMDL not estimated
Polynomial (3 degree) (CV—normal)	0.8527	1.7041	1.0403	0.4797	297.9752	Viable – Alternate	
Polynomial (2 degree) (CV—normal)	0.8527	1.7041	1.0403	0.4797	297.9752	Viable – Alternate	
Power (CV—normal)	0.8527	1.7041	1.0405	0.4797	297.9752	Viable – Alternate	
Linear (CV—normal)	0.8527	1.7041	1.0404	0.4797	297.9752	Viable – Alternate	

[a]"Classification" column denotes whether a model can be considered for model selection purposes. See BMDS User Guide: https://www.epa.gov/bmds.

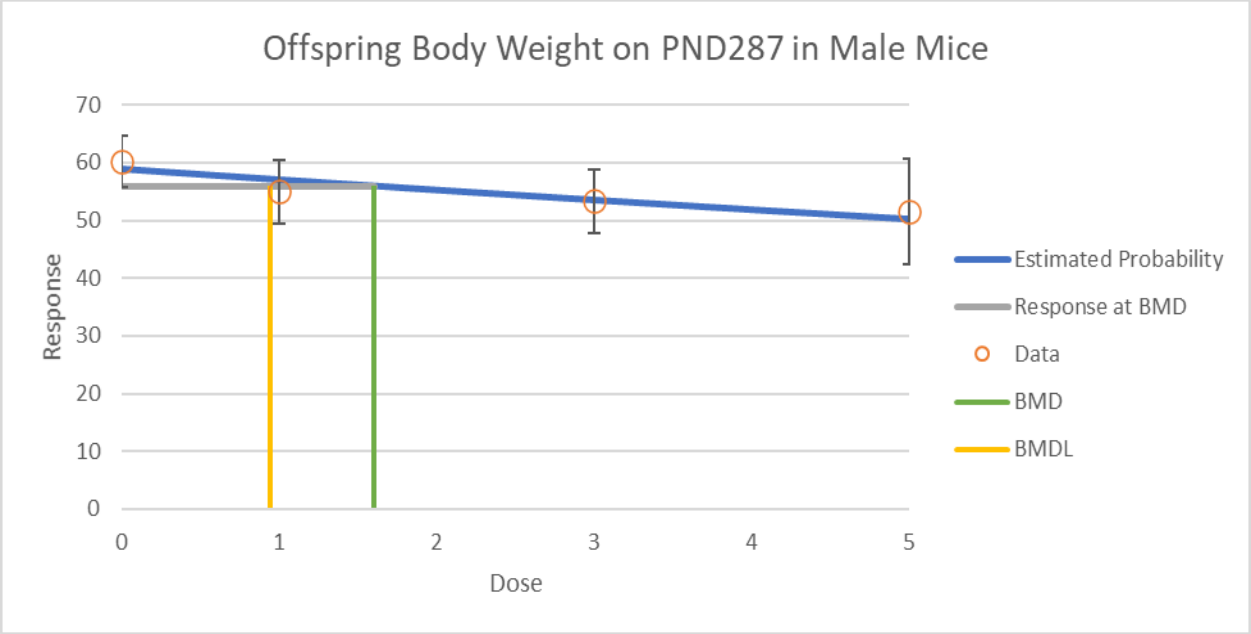

Figure D-41. Dose-response data and curve of exponential 3 model for offspring body weight on PND 287 in male mice (Das et al., 2015)[a].

[a]X-axis is dose (mg/kg-d), and y-axis is offspring body weight (g).

Delayed Eye Opening in Mice (Das et al., 2015)

Table D-95. Dose-response data for delayed eye opening in mice (Das et al., 2015)

Dose (mg/kg-d)	n	Mean (d)	SD
0	13	15.4	0.553
1	11	15.8	0.696
3	13	17.3	1.102
5	6	20.3	1.580

Table D-96. Benchmark dose results for delayed eye opening in mice — non-constant variance, BMR = 0.05 relative deviation (Das et al., 2015)

Models	Test 3 (*p*-value)	0.05 relative deviation		Goodness of fit (*p*-value)	AIC	BMDS classification[a]	BMDS notes
		BMD	BMDL				
Exponential 2 (NCV—normal)	0.6047	1.0664	0.9030	0.1438	115.3434	Viable – Alternate	
Exponential 3 (NCV—normal)	0.6047	1.6453	1.1100	0.7381	113.5759	Viable – Alternate	
Exponential 4 (NCV—normal)	0.6047	1.0280	0.8270	0.0244	118.5271	Questionable	Goodness-of-fit *p*-value < 0.1
Exponential 5 (NCV—normal)	0.6047	−9,999.000	0.0000	<0.0001	185.3896	Unusable	BMD computation failed; lower limit includes zero BMD not estimated BMDL not estimated Goodness-of-fit *p*-value < 0.1 |Residual at control| > 2 Modeled control response std. dev. > |1.5| actual response std. dev.
Hill (NCV—normal)	0.6047	2.8196	2.7888	0.0989	116.1872	Questionable	Goodness-of-fit *p*-value < 0.1
Polynomial (3 degree) (NCV—normal)	0.6047	1.5911	1.0477	NA	115.4663	Questionable	d.f. = 0, saturated model (Goodness-of-fit test cannot be calculated)
Polynomial (2 degree) (NCV—normal)	**0.6047**	**1.6271**	**1.0951**	**0.8410**	**113.5044**	**Viable – Recommended**	**Lowest AIC**
Power (NCV—normal)	0.6047	1.6763	1.1307	0.6376	113.6860	Viable – Alternate	
Linear (NCV—normal)	0.6047	1.0275	0.8301	0.0795	116.5270	Questionable	Goodness-of-fit *p*-value < 0.1

[a]"Classification" column denotes whether a model can be considered for model selection purposes. See BMDS User Guide: https://www.epa.gov/bmds.

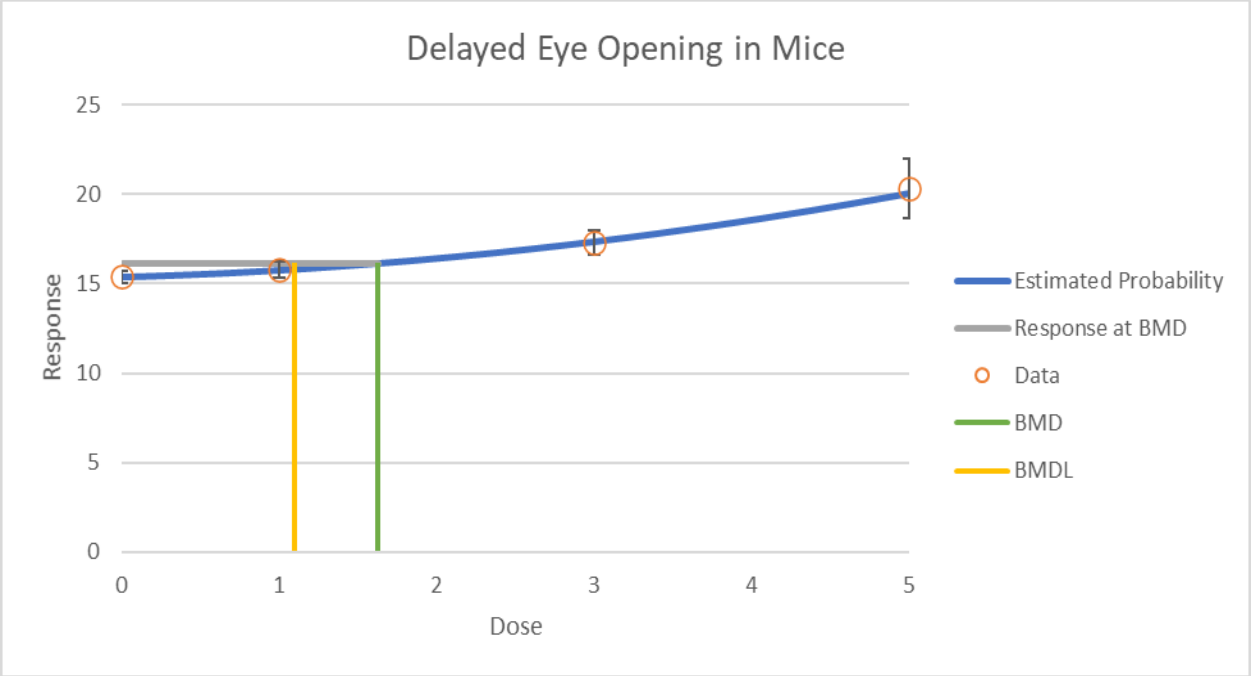

Figure D-42. Dose-response data and curve of polynomial degree 2 model for delayed eye opening in mice (Das et al., 2015)[a].

[a]X-axis is dose (mg/kg-d), and y-axis is eye opening time (d).

Delayed Preputial Separation in Mice (Das et al., 2015)

Table D-97. Dose-response data for delayed preputial separation in mice (Das et al., 2015)

Dose (mg/kg-d)	n	Mean (d)	SD
0	13	28.52	1.061
1	11	28.91	1.015
3	13	30.67	0.758
5	6	33.84	1.204

Table D-98. Benchmark dose results for delayed preputial separation in mice — constant variance, BMR = 0.05 relative deviation (Das et al., 2015)

Models	Test 2 (*p*-value)	0.05 relative deviation		Goodness of fit (*p*-value)	AIC	BMDS classification[a]	BMDS notes
		BMD	BMDL				
Exponential 2 (CV—normal)	0.5798	1.4777	1.2872	0.0290	129.7563	Questionable	Goodness-of-fit *p*-value < 0.1
Exponential 3 (CV—normal)	0.5798	2.3702	1.8167	0.8763	124.6994	Viable – Alternate	
Exponential 4 (CV—normal)	0.5798	1.4166	1.2150	0.0035	133.1978	Questionable	Goodness-of-fit *p*-value < 0.1
Exponential 5 (CV—normal)	0.5798	2.3885	1.8212	NA	126.7317	Questionable	d.f. = 0, saturated model (Goodness-of-fit test cannot be calculated)
Hill (CV—normal)	0.5798	2.9221	2.8557	0.3198	125.6650	Viable – Alternate	
Polynomial (3 degree) (CV—normal)	0.5798	2.3511	1.6857	NA	126.6752	Questionable	d.f. = 0, saturated model (Goodness-of-fit test cannot be calculated)
Polynomial (2 degree) (CV—normal)	**0.5798**	**2.3575**	**1.7585**	**0.9624**	**124.6774**	**Viable – Recommended**	**Lowest AIC**
Power (CV—normal)	0.5798	2.3870	1.8219	0.8228	124.7253	Viable – Alternate	
Linear (CV—normal)	0.5798	1.4171	1.2158	0.0142	131.1834	Questionable	Goodness-of-fit *p*-value < 0.1

[a]"Classification" column denotes whether a model can be considered for model selection purposes. See BMDS User Guide: https://www.epa.gov/bmds.

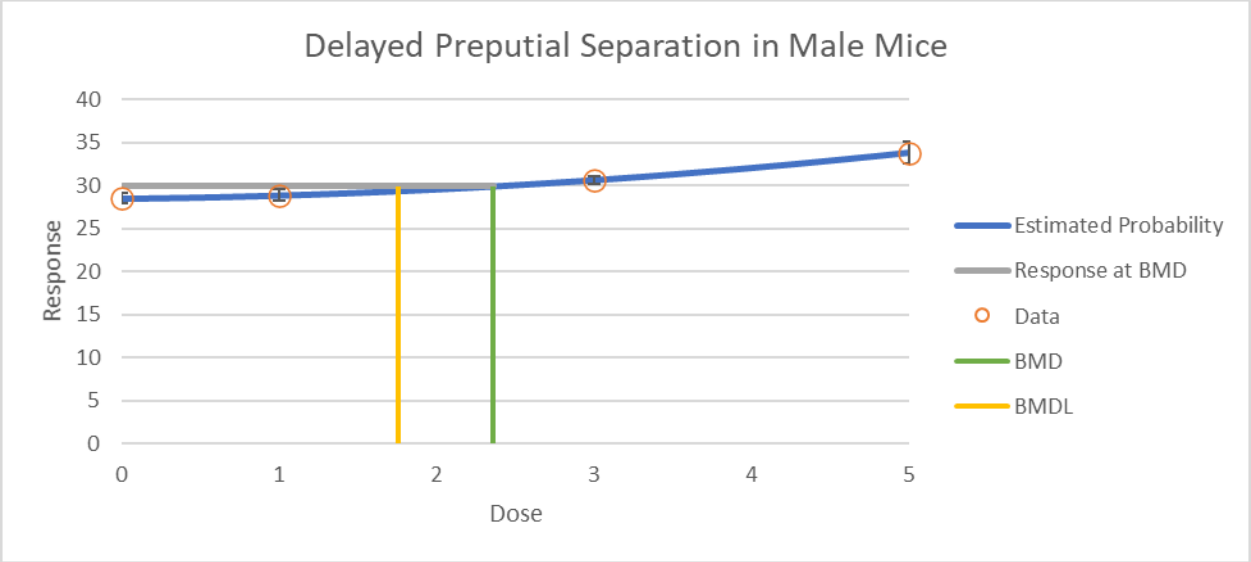

Figure D-43. Dose-response data and curve of polynomial degree 2 model for delayed preputial separation in mice (Das et al., 2015)[a].

[a]X-axis is dose (mg/kg-d), and y-axis is preputial separation (d).

Delayed Vaginal Opening in Mice (Das et al., 2015)

Table D-99. Dose-response data for delayed vaginal opening in mice (Das et al., 2015)

Dose (mg/kg-d)	n	Mean (d)	SD
0	13	29.856	2.084
1	11	31.177	1.645
3	13	32.871	1.457
5	6	36.500	1.516

Table D-100. Benchmark dose results for delayed vaginal opening in mice — constant variance, BMR = 0.05 relative deviation (Das et al., 2015)

Models	Test 2 (*p*-value)	0.05 relative deviation		Goodness of fit (*p*-value)	AIC	BMDS classification[a]	BMDS notes
		BMD	BMDL				
Exponential 2 (CV—normal)	**0.5468**	**1.2948**	**1.0798**	**0.3719**	**172.7406**	**Viable – Recommended**	**Lowest AIC**
Exponential 3 (CV—normal)	0.5468	1.7643	1.1070	0.2615	174.0232	Viable – Alternate	
Exponential 4 (CV—normal)	0.5468	1.2213	0.9043	0.1140	175.2603	Viable – Alternate	
Exponential 5 (CV—normal)	0.5468	1.7233	0.9938	NA	176.1922	Questionable	d.f. = 0, saturated model (Goodness-of-fit test cannot be calculated)
Hill (CV—normal)	0.5468	2.8893	2.7917	0.0548	176.4502	Questionable	Goodness-of-fit *p*-value < 0.1
Polynomial (3 degree) (CV—normal)	0.5468	1.6955	1.0904	0.4374	173.3655	Viable – Alternate	
Polynomial (2 degree) (CV—normal)	0.5468	1.7397	1.0657	0.3229	173.7393	Viable – Alternate	
Power (CV—normal)	0.5468	1.7977	1.0434	0.2347	174.1745	Viable – Alternate	
Linear (CV—normal)	0.5468	1.2220	0.9983	0.2877	173.2540	Viable – Alternate	

[a]"Classification" column denotes whether a model can be considered for model selection purposes. See BMDS User Guide: https://www.epa.gov/bmds.

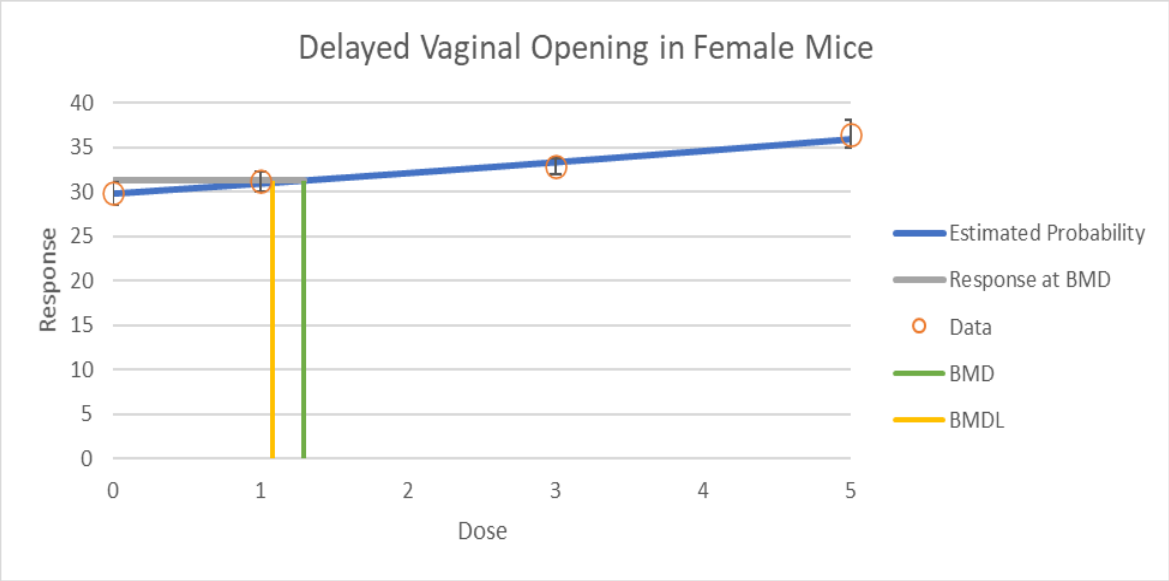

Figure D-44. Dose-response data and curve of exponential 2 model for delayed vaginal opening in mice (Das et al., 2015)[a].

[a]X-axis is dose (mg/kg-d), and y-axis is vaginal opening (d).

APPENDIX E. DETAILED PHARMACOKINETIC ANALYSES

E.1. PARTIAL POOLING OF PFNA PHARMACOKINETIC DATA FOR HIERARCHICAL BAYESIAN ANALYSIS

We estimated the sex-specific pharmacokinetic parameters (half-life, volume of distribution, and clearance) of PFNA in rats and mice by fitting one- and two-compartment models to the available concentration versus time data. A Bayesian hierarchical methodology was developed to fit these models because of the need to pool time-course concentration data across numerous studies with varying exposure scenarios within each study. This allowed for each concentration versus time dataset to be fit to each model, wherein fitted parameters for each dataset are sampled from a population-level distribution that models the similarities between each dataset. In addition, the Bayesian analysis allowed for the generation of central estimates and credible intervals for the pharmacokinetic parameter of interest, e.g., half-life, volume of distribution and clearance, using posterior distributions from the estimated variables. Finally, the Bayesian methodology allowed for hypothesis testing of the one- and two-compartment formulations to decide which model more appropriately fit the data.

E.1.1. Pharmacokinetic Model

To determine pharmacokinetic parameters for PFNA, constants were estimated for both one- and two-compartment model assumptions. The implementation of this model and other pharmacokinetic calculations is available in HERO (Schlosser, 2024). For a one-compartment model assumption, the following exponential decay functions were fit to the available data:

$$C_{1-cmpt}^{IV}(t) = \frac{f_a \cdot D}{V} e^{-k_e t} \quad \text{(E-1)}$$

$$C_{1-cmpt}^{oral}(t) = \frac{f_a \cdot D}{V} \left(\frac{k_a}{k_a - k_e}\right) \left(e^{-k_e t} - e^{-k_a t}\right) \quad \text{(E-2)}$$

where D represents the administered dose and V, k_e, f_a, and k_a represent the central compartment volume, elimination constant, fraction absorbed (when IV and oral data available) and absorption constant (for oral only), respectively, to be fit. From these fitted constants, pharmacokinetic parameters are derived:

$$V_d = \frac{V}{BW} \quad \text{(E-3)}$$

$$t_{\frac{1}{2}} = \frac{\ln 2}{k_e} \quad \text{(E-4)}$$

$$CLC = V_d * k_e \quad \text{(E-5)}$$

where V_d, $t_{1/2}$, and CLC represent the volume of distribution, terminal half-life, and clearance, respectively, and BW represents the animal body weight.

For the two-compartment model assumption, the following exponential decay functions were fit to available data:

$$A^{IV} = \frac{\alpha - k_{dc}}{\alpha - \beta};\ A^{oral} = k_a\left(\frac{k_{dc} - \alpha}{(k_a - \alpha)(\beta - \alpha)}\right) \quad \text{(E-6)}$$

$$B^{IV} = \frac{\beta - k_{dc}}{\beta - \alpha};\ B^{oral} = k_a\left(\frac{k_{dc} - \beta}{(k_a - \beta)(\alpha - \beta)}\right) \quad \text{(E-7)}$$

$$C_{2-cmpt}^{IV}(t) = \frac{f_a \cdot D}{V}\left(A^{IV}e^{-\alpha t} + B^{IV}e^{-\beta t}\right) \quad \text{(E-8)}$$

$$C_{2-cmpt}^{oral}(t) = \frac{f_a \cdot D}{V}\left(A^{oral}e^{-\alpha t} + B^{oral}e^{-\beta t} - \left(A^{oral} + B^{oral}\right)e^{-k_a t}\right) \quad \text{(E-9)}$$

where D represents the administered dose and V, α, β, k_{dc}, f_a, and k_a represent central compartment volume, alpha-phase elimination constant, beta-phase elimination constant, deep-to-central compartment rate constant, fraction absorbed (when IV and oral data available) and absorption constant (for oral only), respectively, to be fit. From these fitted constants, the remaining two-compartment constants (k_{cd}: central-to-deep compartment rate constant and k_e: elimination constant) and the deep compartment volume (V_{deep}) are derived by solving:

$$\alpha + \beta = k_{cd} + k_{dc} + k_e \quad \text{(E-10)}$$

$$\alpha * \beta = k_{dc} * k_e \quad \text{(E-11)}$$

$$V_d = V\frac{k_{cd}}{k_{dc}} \quad \text{(E-12)}$$

which allows for the desired pharmacokinetic parameters to be derived using the following equations:

$$V_{d-ss} = \frac{V + V_{deep}}{BW} = \frac{V}{BW}\left(\frac{k_{cd} + k_{dc}}{k_{dc}}\right) \quad \text{(E-13)}$$

$$t_{\frac{1}{2}} = \frac{\ln 2}{\beta} \quad \text{(E-14)}$$

$$CLC = \frac{V}{BW} * k_e \quad \text{(E-15)}$$

where $V_{d\text{-}ss}$, $t_{1/2}$, and CLC represent the steady-state volume of distribution, terminal half-life, and clearance, respectively, and BW represents the animal body weight.

Finally, fraction absorbed was determined for PFNA in rats where IV and oral gavage datasets were available using a hierarchical beta-distribution to ensure the population fraction absorbed (ω_{f_a}) was bounded on the interval (0,1). Therefore, the fraction absorbed for the i^{th} dataset gives $f_{a,i} \sim Beta(\alpha, \beta)$, where

$$\alpha = \omega_{f_a}(\kappa - 2) + 1$$
$$\beta = (1 - \omega_{f_a})(\kappa - 2) + 1 \quad \text{(E-16)}$$

Here, ω_{f_a} is the population fraction absorbed mode and κ is the population "concentration".

E.1.2. Bayesian Inference

The fitted constants for each model structure (described above) were determined using available time-course concentration data reported in mice and rats with the parameters for each model estimated using a Bayesian calibration approach. For the mice fits, time-course data from only one study Tatum-Gibbs et al. (2011) were available, and all sex-specific data were pooled into a single dataset and fit to the one- and two-compartment models described above. However, a hierarchical Bayesian calibration approach was used to fit the observed time-course concentration data for male and female rats using data reported from multiple studies (Kim et al., 2019; Iwabuchi et al., 2017; Tatum-Gibbs et al., 2011; Ohmori et al., 2003); Iwabuchi et al. (2017) had only male rat data, the other three had data for both male and female rats. To aid in parameter identifiability, the one- and two-compartment model structures were reparametrized in terms of clearance and steady-state volume of distribution (equations above). Therefore, fitted parameters for the one-compartment model were k_a (gavage only), f_a (when IV and gavage datasets were available), V_d, and CLC while the fitted parameters for the two-compartment model were k_a (gavage only), f_a (when IV and gavage datasets were available), V_{d-ss}, CLC, k_{cd}, and R (the ratio V: V_{deep}). Finally, priors for each pharmacokinetic parameter were chosen to be "weakly informative" based on prior knowledge of PFAS pharmacokinetics (ATSDR, 2021) with 95% equal-tailed intervals spanning multiple orders of magnitude.

Prior parameter distributions for model-specific variables are presented in Table E-1. Two-compartment priors for k_{cd} (d^{-1}) and R (unitless) are defined such that $k_{cd} \ll 1$ and $R \gg 1$ which ensures two-compartment behavior for predicted concentrations is only exhibited when driven by the observed data.

Table E-1. Prior distributions for population mean parameters used for one- and two-compartment model fitting. All instances of log represent a natural log

Parameter (units)	Summary	Prior distribution	2.5th – 97.5th percentile	Two-compartment model only
$M_{\tilde{C}_L}$ (L/kg/d)	Clearance	$\log M_{CLC} \sim N(\log(0.07), 2.68)$	0.00037 – 13.3	
$M_{\tilde{V}_d}$ (L/kg)	Volume of distribution[1]	$\log M_{V_d} \sim N(\log(0.36), 1)$	0.05 – 2.5	
$M_{k_{12}}$ (d^{-1})	Rate of transfer from central to deep compartment	$\log M_{k_{12}} \sim N(\log(0.01), 1)$	$1.4x10^{-3}$ – $7.1x10^{-2}$	✓
M_R (unitless)	Ratio of volumes for central and deep compartments	$\log M_R \sim N(\log(100), 1)$	14 – 710	✓
M_{k_a} (d^{-1})	Absorption rate constant	$\log M_{k_a} \sim N(\log(81), 0.25)$	50 – 132	
ω_{fa} (unitless)	Fraction absorbed	$\omega_{fa} \sim \text{Beta}(6,1.5)$	0.47 – 0.98	

Corresponding prior distributions for pharmacokinetic parameters of interest are presented in Table E-2. Finally, a sensitivity analysis on the model priors is shown in the *Prior sensitivity analysis* section.

Table E-2. Weakly informed prior distributions for pharmacokinetic parameters used in the Bayesian analysis

	Median	MAD	ETI_3%	ETI_97%
Half-life (d)	3.5	3.5	0.01	710
Clearance (mL/kg-d)	70	66	0.47	10,000
Vd-ss (mL/kg)	360	217	53.5	2,500

For the mouse data where data is only available from one study (Tatum-Gibbs et al. (2011)), priors are used from Table E-1to fit a single set of pharmacokinetic parameters for either male or female mice. The likelihood for the individual mouse data is described using

$$C_i = \begin{cases} C_{1-cmpt}^{route} & \text{for 1-compartment model,} \\ C_{2-cmpt}^{route} & \text{for 2-compartment model} \end{cases}$$

$$\breve{\sigma} \sim Exp(1)$$
$$C_i \sim LN(\bar{x}_i, \tilde{\sigma}),$$

where $\bar{x}_i$ is the sample mean of the observed concentrations at time t_i for all times reported in Tatum-Gibbs et al. (2011). For model parameters, V (L), CLC $(L/kg/d)$, and k_a (d^{-1}), priors are defined based on the available PFAS pharmacokinetic information available in (ATSDR, 2021).

For the hierarchical approach, the concentration versus time data comprised a population and dataset level for which model parameters were estimated. Here, each dataset represented each study/sex/dose concentration versus time dataset extracted from the literature and was fit using the model:

$$C_{ij} = \begin{cases} C_{1-cmpt}^{route} & \text{for 1-compartment model,} \\ C_{2-cmpt}^{route} & \text{for 2-compartment model} \end{cases}$$
$$C_{ik} \sim LN(\bar{x}_{ij}, \tilde{\sigma}_k)$$

where $\bar{x}_{ij}$ is the sample mean of the observed concentrations at time t_{ij} for dataset j, and $\tilde{\sigma}_k$ is study-level log-transformed standard deviation for the relative errors based on study k. Study-level priors for $\tilde{\sigma}_k$ were determined using the average log-transformed standard deviations:

$$\bar{\sigma}_{i,j}^2 = \ln\left(1 + \frac{s_{i,j}^2}{\bar{x}_{i,j}^2}\right)$$
$$\gamma_k = \frac{\sum_i \bar{\sigma}_{i,j \in k}}{n_k}$$

where $s_{i,j}$ is the sample standard deviation on the observed concentrations at time $t_{i,j}$ for study k. If s_{ij} was available, $\bar{\sigma}_{i,j}$ is the log-transformed standard deviation using the sample mean and standard deviation. For studies in which sample standard deviations could not be extracted, an average of all log-transformed standard deviations was used. This allowed for study-level prior distributions on the error model log-transformed standard deviation:

$$\tilde{\sigma}_k \sim \begin{cases} \text{Exp}\left(1/\gamma_k\right) & \text{if } \gamma_k \text{ available,} \\ \text{Exp}\left(1/\gamma\right) & \text{otherwise.} \end{cases}$$

Using this model, dataset-level fitted constants were assigned priors based on a non-centered parameterization of a population-level distribution. This reparameterization of a typical hierarchical Bayesian model allows for increased sampling efficiency and can be more efficient for sampling when there is limited data (Betancourt and Girolami, 2013). In addition, population standard deviation priors for the pharmacokinetic parameters were assigned HalfNormal(0.5). This weakly informative, half-normal prior helps to regularize (i.e., constrain, the population mean and allows for stringer pooling so a common population pharmacokinetic parameter while allowing for

discrepancies between datasets. Therefore, dataset level parameters were determined through the non-centered sampling approach as $\ln(k_a, V, CLC, R, k_{cd})_j \sim N(\mu_{k_a,V,\mathrm{CLC},R,k_{cd}}, \sigma_{k_a,V,CLC,R,k_{cd}})$ for the j^{th} dataset. For both the single-level and hierarchical approaches, one- and two-compartment model goodness of fits were compared using the leave-one-out cross validation (LOO-CV) method. Pharmacokinetic parameters from the most appropriate model, as judged by the LOO-CV comparison, were reported. To estimate the resulting pharmacokinetic parameters, posterior probability densities of the parameters from the LOO-CV-determined model were examined, and distributional estimates of the half-life, volume of distribution, and clearance were calculated using the equations described above. The parameter space was sampled using PyMC (Salvatier et al., 2016), using four independent Markov chains run for 10,000 iterations per chain. Posterior parameter distributions were determined using the final 5,000 iterations of each chain, ensuring an effective sample size (ESS) greater than 10,000 (Kruschke, 2021). Convergence was assessed using a potential scale $\hat{R} = 1.05$ (Kruschke, 2021) with visualizations of chains and accompanying analysis code located in HERO (Zurlinden, 2024).

E.1.3. Prior Sensitivity Analysis

To investigate the impact of prior selection on posterior pharmacokinetic parameter estimation, a sensitivity analysis was conducted on the priors used in the Bayesian analysis. Priors were classified into three categories: weakly informed, broad, and uninformed. Weakly informed priors are defined using the half-life, clearance, and volume of distribution described above based on reported ranges of PFNA pharmacokinetics with a prior predictive check demonstrating available data for fitting fall within the prior 90% credible interval.

Broad priors are defined as uniform distributions spanning the 3% and 97% ETI defined from the weakly informed priors, and uninformed priors represent uniform priors spanning multiple orders of magnitude and are essentially flat priors (Figure E-1). Figure E-2 compares these three classes of priors and their impact on the posterior pharmacokinetic parameter distributions.

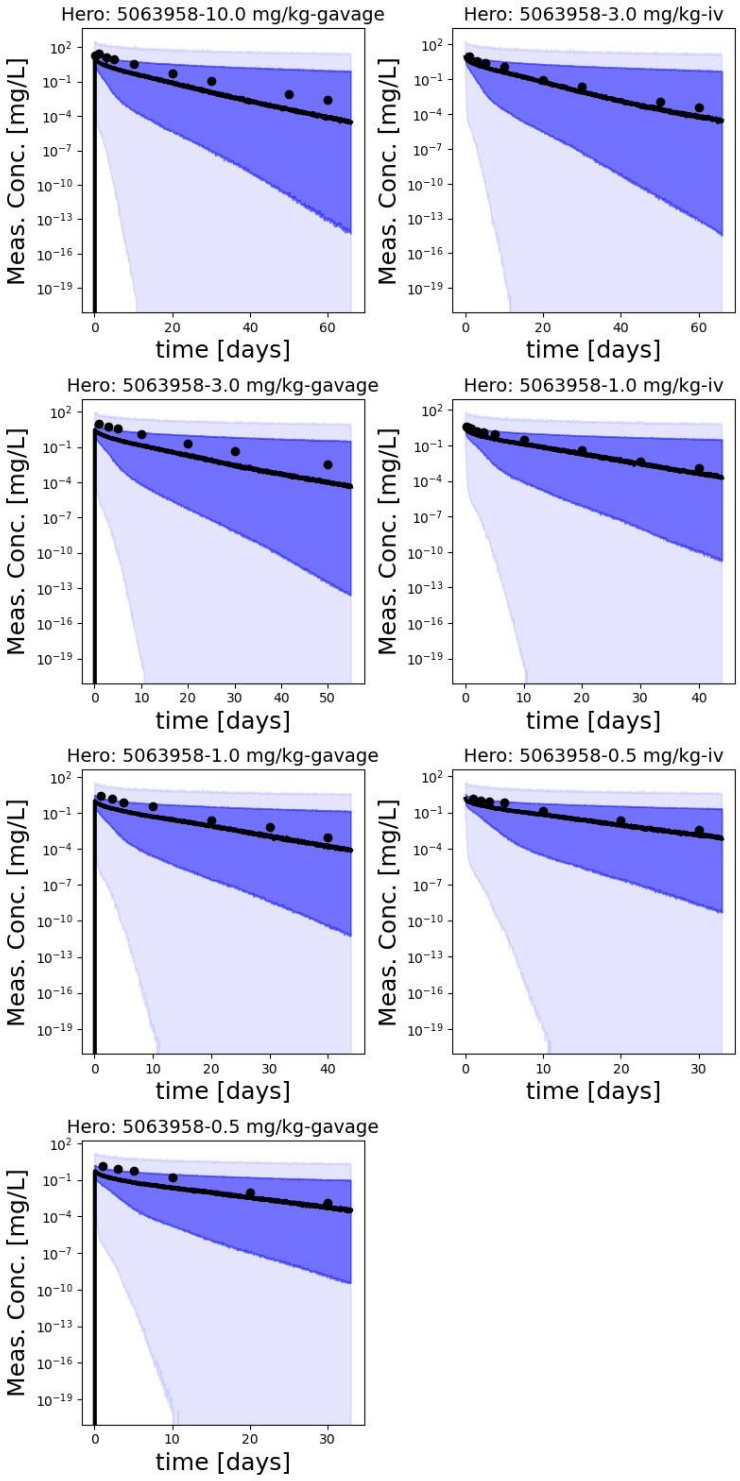

Figure E-1. Prior predictive check to ensure equal-tailed interval from prior distributions encompass the available time-course concentration data for fitting. The dark blue represents the interquartile range (25th to 75th percentile) while the light blue represents the 3% to 97% equal tailed intervals.

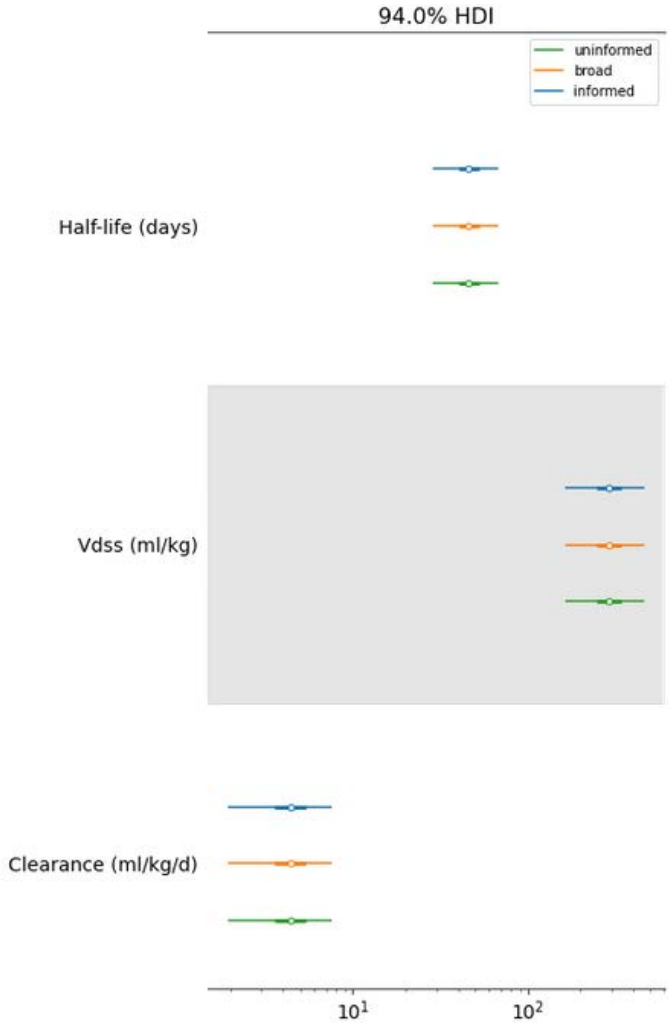

Figure E-2. Prior sensitivity on half-life, steady-state volume of distribution, and clearance to ensure weakly informed priors do not bias posterior distributions of the pharmacokinetic parameters.

Given these findings, the weakly informed pharmacokinetic priors were used for fitting available time-course concentration data.

E.1.4. Study-specific Clearance Values and Model Fits

As described above, three datasets were used for the female rat-specific parameter estimation, which had a mixture of gavage and i.v. exposure routes and follow-up times extending up to 150 days (Kim et al., 2019; Tatum-Gibbs et al., 2011; Ohmori et al., 2003). In addition to these three, a fourth dataset (Iwabuchi et al., 2017) was used for male rats. The sex-specific clearance value distribution obtained from fitting the three datasets together had means and 90% credible intervals of 71.1 (63.8–79.6) mL/kg-day in female rats and 3.68 (2.29–5.01) mL/kg-day in male rats. For these data, a two-compartment PK model was deemed superior. Visual inspection shows some of the data have a distinguishable distribution and excretion phase (e.g., female rat data in Fig.

1 of Tatum-Gibbs et al. (2011)), which is appropriate for a two-compartment model. A two-compartment model is also able to fit data that appear linear as is evidenced in fits to other datasets. Because data were available for different individual rats, sampled at different time points, a single concentration versus time simulation cannot be compared to data plotted in that format. Therefore, model results are presented as predicted versus measured concentration in Figure E-3. Credible intervals for the fits to individual datasets are qualitatively small showing good model fits to the data from individual studies. The relatively large credible interval for the pooled male rat data is due to the large variation between studies. For example, in male rats, the mean clearance values for individual studies ranged from 2.29 to 6.91 mL/kg-day. The range in female rats (60.1–100.7) was more modest by comparison.

Kim et al. (2019) was the only study to directly compare PK after both i.v. and gavage doses, but no particular trend was apparent when comparing the terminal clearance following these doses. For example, at 0.5 mg/kg in female rats, the mean CL was 65.8 mL/kg-day after the i.v. dose and 70.9 mL/kg-day after the gavage dose, but at 3 mg/kg, mean CL was 69.5 mL/kg-day after the i.v. dose and 60.1 mL/kg-day after the oral gavage (Kim et al., 2019). Hence, the decision to model the data assuming 100% or bioavailability appears consistent in that regard (no apparent bias in resulting parameters), and the PK model fit the data for both routes adequately.

For mice only, the data from Tatum-Gibbs et al. (2011) were available for analysis, and since Fujii et al. (2015) only observed the serum time-course for 24 hours, those data would not have informed the long-term clearance. Therefore, the data for 1 and 10 mg/kg (IV) from Tatum-Gibbs et al. (2011) were pooled to obtain a single mean and credible interval for each mouse sex: 7.65 (5.98–9.41) mL/kg-day for male mice and 6.65 (4.76–8.68) mL/kg-day for female mice. The predicted versus estimated concentrations are shown in Figure E-4. While these clearance values do not seem to indicate a significant sex difference, the volume of distribution in male mice was estimated to be 639 (574–707) mL/kg, whereas that in female mice was estimated to be 341 (290–386) mL/kg. Hence, it would not be appropriate to pool the data from the two sexes.

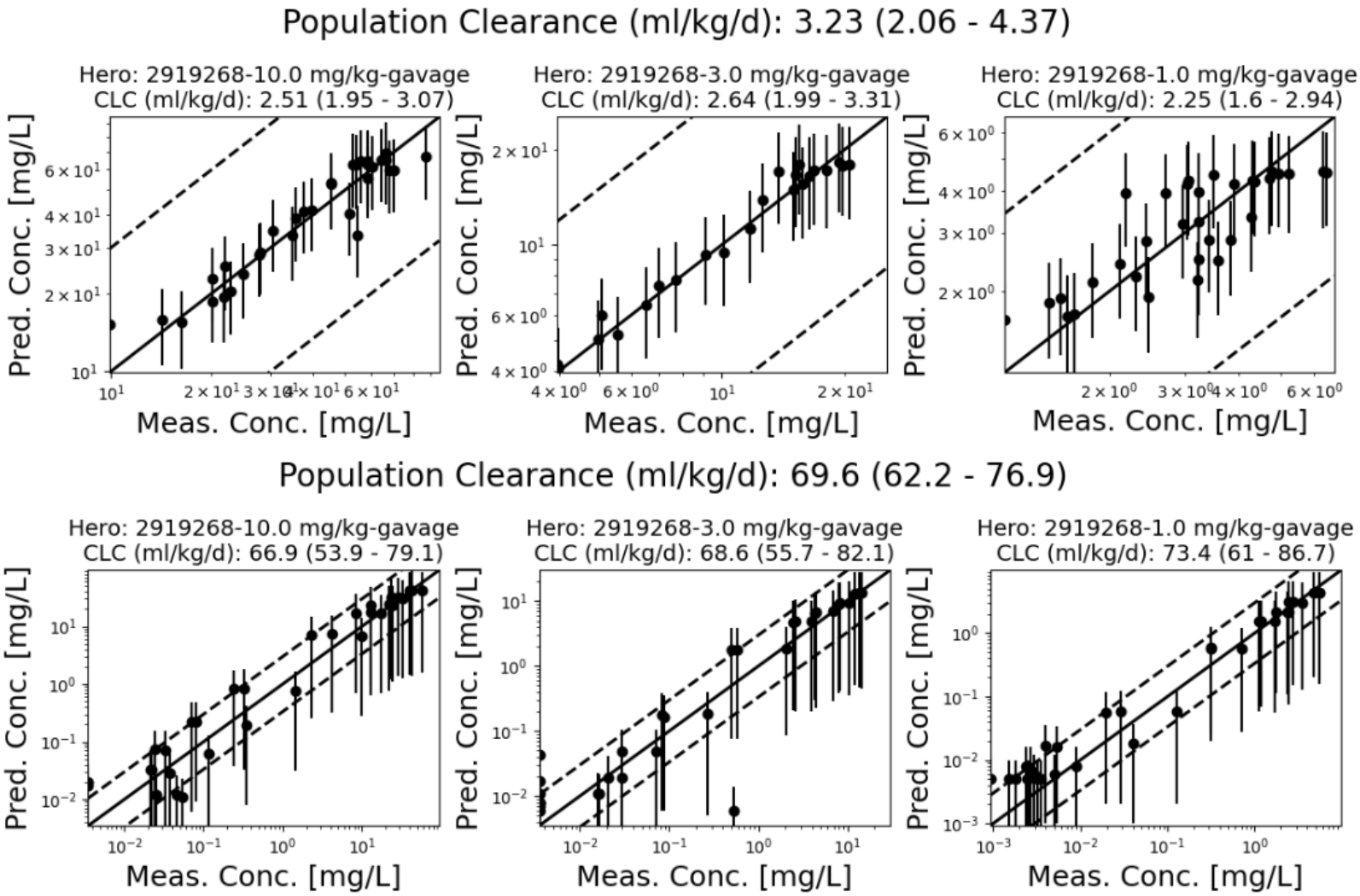

Figure E-3. PK model fits versus observational data for female and male rats. Results for male rats shown in upper panels and female rats in lower panels. See text for sources of measured concentrations. Points and error bars show mean and 90% credible interval of model simulations. Solid line is y = x, dashed lines are ± a factor of 3.

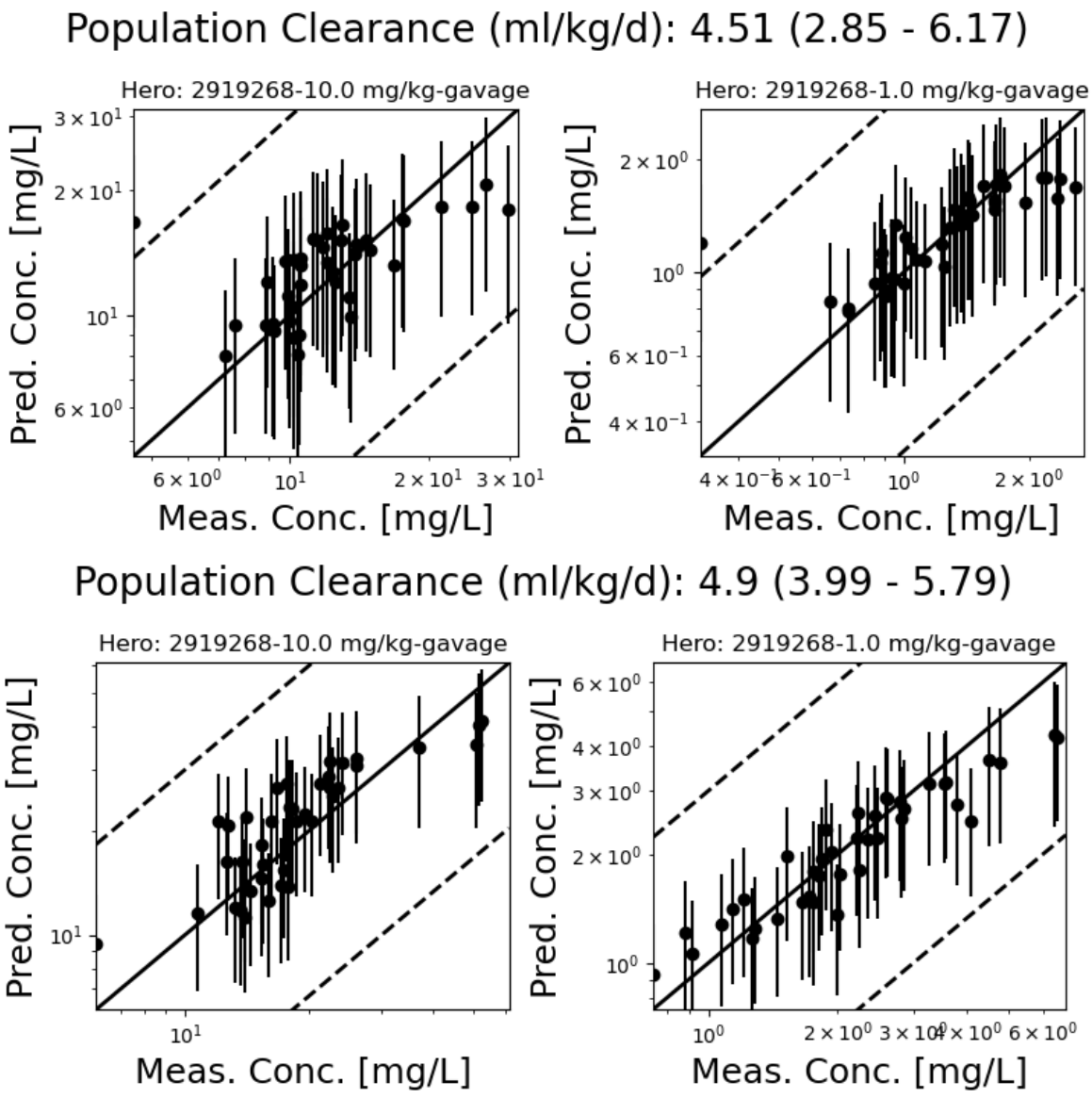

Figure E-4. PK model fits versus observational data for male and female mice. Results for male mice shown in upper panels and female mice in lower panels. Data are from **Tatum-Gibbs et al. (2011)**. Points and error bars show mean and 90% credible interval of model simulations. Solid line is y = x, dashed lines are ± a factor of 3.

E.2. ADDITIONAL DETAILS ON PFNA DISTRIBUTION

Some of the calculations presented in Kim et al. (2019) appear to have been reported inconsistently with each other and the PK parameter units given or perhaps are in error. The Vd and CL reported by Kim et al. (2019) were given in units of mL and mL/day, respectively rather than the standard normalized units of mL/kg and mL/kg-day. Therefore, EPA used known relationships among PK parameters to check these values before converting them to standard units.

Since clearance can be calculated as dose/area-under-the-concentration-curve (AUC), and AUC is normalized to plasma volume, it appears that this study determined the CL for female rats using a BW of 0.25 kg. In particular, for the dose of 3 mg/kg = 3,000 µg/kg (mg converted to µg), the total mass of PFNA administered to a 0.25 kg rat would be 750 µg. If this absolute dose of 750 µg is divided by the reported AUC for female rats, the result is identical to the reported female rat CL. Thus, the PK parameters reported for female rats are consistent with one another and with the units listed in the table, assuming a BW of 0.25 kg. Normalizing the reported Vd for female rats by 0.25 kg yields a mean value of 183.4 mL/kg, which matches the value calculated as dose/C0 (assuming the reported C_{max} = C0) and is in the range of values reported for female rats by Ohmori et al. (2003) and Tatum-Gibbs et al. (2011). On the other hand, using the same calculation for clearance indicates that either the male rat calculations used ~1 kg for body weight, which is unlikely, or that the Vd reported for male rats, 363.09, is the normalized value (mL/kg). Thus, the numerical value of Vd listed for male rats appears to be inconsistent with the units listed for that parameter and was apparently calculated in a manner not consistent with the calculation for female rats. Further, 363.09 mL/kg is much higher than the Vd values reported for male rats by Tatum-Gibbs et al. (2011) and Ohmori et al. (2003). If instead one calculates Vd = dose/C_{max} for male rats, one obtains 282 mL/kg, which is very close to the value reported by Ohmori et al. (2003). Hence, it appears there was an error in Vd calculation for male rats in addition to its being inconsistent with the calculation for female rats.

In mice, Tatum-Gibbs et al. (2011) reported mean Vd of 328 mL/kg BW for males and 192 mL/kg BW for females, whereas Fujii et al. (2015) reported 220 mL/kg in males and 150 mL/kg in females. However, the uncertainty range for Vd in male mice reported by Tatum-Gibbs et al. (2011) was very large (0–1,060 L/kg). Only a single value was reported for Vd, although two doses were used in the study, and the reported value is lower than the Vd obtained by calculating it from dose/C_{max} at each dose level, which results in 503 mL/kg for the 1 mg/kg dose and 348 mL/kg for the 10 mg/kg dose. The Vd values calculated from dose/C_{max} are listed in Table 3-1, because they have much tighter confidence bounds than the reported Vd value for male mice. For consistency, Vd calculated as dose/C_{max} is also used for the female mice in Tatum-Gibbs et al. (2011), yielding somewhat higher values than the reported mean (262 and 207 mL/kg at 1 and 10 mg/kg, respectively, versus a reported overall mean of 191 mL/kg). For Fujii et al. (2015), the reported mean Vd values are almost identical to dose/C_{max} for the fitted curve, e.g., 140 versus 150 mL/kg for female mice, so the reported values are used. While the Vd values for mice calculated from Tatum-Gibbs et al. (2011) are much larger than those reported by Fujii et al. (2015), the 95% confidence interval in the C_{max} reported by Tatum-Gibbs et al. (2011) was approximately a factor of two (upper/lower bound), so the C_{max} values are considered a robust measure of distribution in that study. The difference between the two studies may result from the difference in mouse strain used, CD-1 versus FVB/NJc1.

Gao et al. (2015) and Iwabuchi et al. (2017) examined the distribution of PFNA to various tissues in rats after drinking water exposure (vs. gavage dosing), while Benskin et al. (2009) evaluated distribution after gavage dosing and Kim et al. (2019) evaluated distribution after i.v. dosing. Gao et al. (2015) found that the hair concentration, which could be a useful marker for exposure in humans, was significantly correlated with concentration in serum and other tissues (Table E-3). Benskin et al. (2009) showed the highest distribution in rats to liver, followed by blood > kidney > lung > heart > spleen > testes > muscle > fat > intestines > brain after gavage dosing (Table E-4). Also, Benskin et al. (2009) distinguished between n- and iso-PFNA, showing that distribution of the isomers was generally similar (Table E-4). Kim et al. (2019) reported sex-specific distribution, with higher relative liver levels in male rats and higher relative kidney levels in female rats after i.v. administration (Table E-5). Iwabuchi et al. (2017) showed that tissue-to-serum concentration ratios were relatively consistent between a single exposure and 3 months of drinking water exposure to a mixture of 4 PFAS (Table E-6). The one exception was liver, which showed a higher tissue-to-serum ratio after 1 and 3 months of drinking water exposure compared to the single gavage exposure. The high concentration of PFNA found in liver is likely related to its high affinity for liver fatty acid binding protein (Yang et al., 2020).

Table E-3. Ratio between mean tissue concentrations and mean serum concentrations in rats exposed to PFNA-containing drinking water (Gao et al., 2015)

	Tissue (ng/g) to serum (ng/mL) concentration ratio							
Dose	**0.05 mg/L**		**0.5 mg/L**		**5 mg/L**		**Mean**	
Sex	Female	Male	Female	Male	Female	Male	Female	Male
Hair	0.127	0.035	0.055	0.034	0.024	0.020	0.069	0.029
Liver	0.225	0.776	0.314	0.601	0.176	0.283	0.238	0.553
Kidney	0.750	0.358	0.759	0.289	0.327	0.489	0.612	0.379
Spleen	0.061	0.070	0.086	0.088	0.048	0.067	0.065	0.075
Lung	0.186	0.177	0.180	0.159	0.129	0.283	0.165	0.206
Brain	0.010	0.011	0.006	0.004	0.003	0.011	0.007	0.009
Heart	0.169	0.126	0.142	0.127	0.060	0.066	0.123	0.106

Table E-4. Ratio between mean tissue concentrations and mean whole blood concentrations for n-PFNA and iso-PFNA after a single gavage dose to rats (Benskin et al., 2009)

Dose (mg/kg)	0.189	0.199
Isomer	iso-	n-
Brain	0.015	0.024
Muscle	0.101	0.098
Fat	0.082	0.084
Intestines	0.071	0.076
Testes	0.136	0.158
Lungs	0.224	0.536
Heart	0.229	0.241
Spleen	0.146	0.170
Kidneys	0.607	0.819
Liver	3.398	5.325

Table E-5. Ratio between mean tissue concentrations and mean whole blood concentrations for male and female rats after an i.v. dose of 3 mg/kg (Kim et al., 2019)

Sex	Male	Female
Brain	0.000	0.004
Heart	0.018	0.035
Lung	0.032	0.058
Kidney	0.127	0.247
Liver	1.188	0.464
Spleen	0.012	0.023
GI tract	0.008	0.006
Adipose tissue	0.006	0.018
Muscle	0.006	0.006

Table E-6. Ratio between tissue concentration and serum concentration for male and female rats after either a gavage dose or chronic drinking water exposure of a mixture of PFAS, including PFNA (Iwabuchi et al., 2017)

Exposure	Single dose	Contaminated drinking water	
	C_0	1 mo	3 mo
Brain	0.027	0.014	0.022
heart	0.017	0.015	0.016
liver	6.7	12	11
spleen	0.11	0.11	0.11
kidney	0.73	0.9	0.76
whole blood	0.41	0.55	0.51

C_0 = Ratio of initial concentrations.

E.2.1. PFNA Distribution in Human Blood

Examination of blood components in humans revealed that serum and plasma had similar PFNA concentrations, with a median serum:plasma ratio of 1.26 (Poothong et al., 2017). The median ratio between plasma and whole blood was higher (1.86), and the median ratio between serum and whole blood was higher still (2.34) (Poothong et al., 2017), indicating very little distribution into red blood cells. Another examination of humans revealed a mass fraction in plasma of 0.79 (Jin et al., 2016). The preferential distribution to plasma in the blood may be driven by interactions between PFNA and albumin, which has a measured association constant on the order of 105 M-1, which is consistent with a specific high affinity interaction (Bischel et al., 2010). Binding between PFNA and liver fatty acid binding protein (L-FABP) has also been observed (Sheng et al., 2016; Woodcroft et al., 2010). PFNA has also been shown, via in vitro methods, to bind to transthyretin and liver fatty acid binding protein (Yang et al., 2020; Weiss et al., 2009).

E.2.2. PFNA Distribution during Human Gestation

Besides studies described in detail in Section 3.1.2 of the main document, other studies listed that compared maternal and cord PFNA concentrations are summarized in Table E-7. For example, Li et al. (2020a) measured PFNA in maternal and cord serum for 86 preterm and 187 full-term pregnancies (maternal blood collected 1 week prior to birth, cord blood collected at birth) and calculated matched cord:maternal serum ratios when both cord and maternal concentrations were greater than the limit of quantitation (LOQ). While not all of the mean values in Table E-7 are based on the same statistical analysis (e.g., Kato et al. (2014) reported the geometric mean of maternal

serum (at delivery)/cord serum[10], a simple overall mean, weighted by study sample sizes, was calculated from these results, indicating an average cord/maternal serum ratio of 0.575.

Li et al. (2020a) demonstrated a significant increase in the cord/maternal serum ratio between preterm and full-term pregnancies, from a median ratio of 0.34 to 0.59. The authors evaluated the correlation of the cord/maternal serum ratio with multiple placental transporters and identified a significant, positive correlation with multiple transporters: p-glycoprotein (MDR1), multidrug resistance-associated protein 2 (MRP2), breast cancer resistance protein (BCRP), and organic cation/carnitine transporter 2 (OCTN2). These positive correlations, significant for full-term but not preterm pregnancies, may indicate that the placenta acts as a passive barrier to PFNA in early pregnancy and this function is partly defeated by the expression of these transporters late in pregnancy.

Table E-7. Reported ratios between cord and maternal serum concentrations of PFNA

Reference	Sample size	Detection frequency (%) (maternal/cord serum)	Cord/maternal concentration ratio (range)	Notes[a]
Cariou et al. (2015)	22	98 / 74	0.51 ± 0.05	Mean ± SD. Subjects undergoing planned caesarean delivery.
Glynn et al. (2012)	19	NS	0.13/0.55 = 0.24	Ratio calculated from mean cord serum concentration given in text to mean third trimester maternal serum concentration digitized from Figure 3
Gutzkow et al. (2012)	123	NS	0.40 [0.12, 0.74]	Mean [10th, 90th percentile]. Values digitized from Figure 2.
Han et al. (2018)	369	100 / 100	0.44/0.81 = 0.54	Ratio calculated from 50th percentiles in Table 2. Same value obtained using geometric mean (GM) values in Table 2.
Hanssen et al. (2013)	7	52 / 17	0.54 ± 0.14	Ratios calculated from matched individual data in Table S2.
Kato et al. (2014)	71	100 / 98.6	0.64 [0.61, 0.68]	1/GM [1/95% confidence interval] for maternal/cord serum in Table S3.
Kim et al. (2011)	20	100 / 100	0.47 ± 0.1	Mean ± SD from Table S4.
Li et al. (2020a)	77 185	94.8 99.5	0.34 [0.23, 0.45] 0.59 [0.39, 0.93]	Median [Q1, Q3] in Table S4 for preterm / full term deliveries. Rate of quantification is % of paired samples.
Liu et al. (2011)	50	100 / 100	0.61	Mean. Maternal sample during first wk after delivery

[10] The value for Kato et al. (2014) in Table E-7 is 1 divided by the reported maternal/cord serum ratio.

Reference	Sample size	Detection frequency (%) (maternal/cord serum)	Cord/maternal concentration ratio (range)	Notes[a]
Manzano-Salgado et al. (2017)	66	100 / 100	0.42 [0.38, 0.44]	1/GM [1/95% confidence interval] for maternal/cord serum in Table 2.
Monroy et al. (2008)	28	100 / 26	0.72/0.69 = 1.04	Median cord blood (UBC) / median maternal serum at delivery in Table 3. N = 101 maternal serum and 28 UBC.
Needham et al. (2011)	12	100 / 100	0.50	Mean ratio in Table 3.
Ode et al. (2013)	237	NS	0.93 [0.46, 1.40]	Mean [5th, 95th percentile] in Table 1.
Yang et al. (2016b)	50	100 / 100	0.35/0.55 0.64	Median cord/maternal serum in Table 5.
Yang et al. (2016a)	157	100 / 100	0.49 ± 0.29	Mean ± SD in Table 2.
Zhang et al. (2013)	31	100 / 100	0.39 ± 0.15	Mean ± SD of ratios calculated from data in Table S2.
Overall mean	**1,524**	**–**	**0.575**	Sample-size-weighted mean of study-specific mean values above

[a]Tables and figures listed are those in the corresponding publications / supplemental materials.

Monroy et al. (2008) collected maternal serum both at the second trimester and at delivery and paired cord serum. In this study, PFNA was above the level of quantitation (0.51 ng/mL) in only 26% of the cord blood samples. The publication is ambiguous regarding the level of detection in maternal serum, with a value of 100% given in Table 3 for both time points and 85% suggested by the text. Levels below the level of quantitation (LOQ) were replaced with LOQ/2. The mean ± SD PFNA concentrations were 0.86 ± 0.81 ng/mL in maternal serum at 24–28 weeks gestation, 0.80 ± 0.93 ng/mL maternal serum at delivery, and 0.94 ± 1.04 ng/mL in cord serum. The lack of a substantial decrease over gestation and between maternal serum at delivery and in cord serum may be due to the greater censorship (more non-detects) of the data.

Mamsen et al. (2017) measured PFNA in paired samples of maternal plasma, placenta, and fetal organs from terminated pregnancies in the first trimester, when the mother chose to terminate pregnancy for reasons other than fetal abnormality, and Mamsen et al. (2019) extended the analysis to second- and third-trimester data, wherein intrauterine fetal death occurred and an autopsy was conducted to determine the cause of death. In Mamsen et al. (2017), the average placental concentration was only 11% of maternal plasma levels, and the average of fetal organ concentration was only 9% of maternal plasma levels. Specifically, the average maternal plasma concentration was 0.98 ng/g with a range of 0.41–1.64 ng/g. The fetal organs were also analyzed separately, with the highest median level in liver (0.791 ng/g) followed by intestine (0.744 ng/g), placenta (0.130 ng/g), lung (0.129 ng/g), connective tissue (0.064 ng/g), extremities (0.060 ng/g),

spinal cord (0.055 ng/g), ribs (0.050 ng/g), and heart (0.040 ng/g). The fetal samples were 52 days post-conception on average with a range of 37–68 days. A positive, linear correlation between gestational age and fetal-to-maternal ratio was noted, implying that the PFNA concentration in the fetus increases with gestational age. If one assumes a Vd in adult women obtained by Chiu et al. (2022), 0.19 L/kg, then given the average maternal plasma concentration, one would predict an average maternal tissue concentration of 0.19 ng/g. The observed range of fetal tissue concentrations indicates that if weighted by tissue volume, a similar level of overall distribution occurs in the early-gestation fetus as in the mother.

The results of Mamsen et al. (2019) are complicated by the fact that the maternal serum samples to which the fetal and placental tissue data were compared were collected in the first trimester, so it is possible that the maternal serum concentration at the time of fetal death was significantly different than at the time the banked sample was collected. In addition, the factors leading to fetal death may have altered the fetal tissue distribution relative to a healthy fetus. With those caveats noted, the tissue concentrations in the third trimester group were significantly higher relative to the (first trimester) maternal serum than in the first trimester described above. Specifically, the average maternal serum concentration was 0.53 ng/g with a range of 0.14–1.8 ng/g. The fetal organs were also analyzed separately, with the highest median levels in placenta and adipose (0.17 ng/g), followed by lung (0.16 ng/g), liver (0.15 ng/g), spinal cord (0.12 ng/g [n = 1]), and heart (0.11 ng/g). (Other tissues for which Mamsen et al. (2017) reported concentrations were not analyzed and reported by Mamsen et al. (2019).) While this fetal liver concentration was much lower than observed in the first trimester, other tissue levels were comparable or higher, and when compared to a maternal serum concentration that is 46% lower, the distribution to the placenta and fetal tissues appears to be much higher in these second- and third-trimester samples. If the Vd estimated for adult men and women, 0.19 L/kg, is applied to the average maternal serum concentration, the resulting expected average tissue concentration would be 0.1 ng/g; while the observed median fetal tissue concentrations in the third trimester are all greater than 0.1 ng/g, they are less than 0.2 ng/g, i.e., within a factor of 2 of the expected value. Further, risk estimates for developmental effects are based either on observed maternal serum concentrations for human data or on estimates of maternal serum concentrations for data from mice—in which case, the distribution from mother to fetus is implicit and need not be quantified, though it must be acknowledged that mouse-to-human extrapolation assumes that distribution to fetal (and newborn) mice is similar to distribution to fetal (and newborn) humans.

While the data discussed above suggest that distribution to mid- and late-gestation human fetuses is greater than distribution in the first trimester and to maternal tissues, the difference appears to be within a factor of 2, which is unlikely to significantly change the volume of distribution in the mother and fetus as a whole because the mass of the fetus is a small fraction of the mass of the maternal tissues and because the distribution to cord serum from maternal serum was estimated to be 0.575. (The lower distribution to cord blood (or fetal serum) could occur

because of lower levels of albumin or a lower overall extent of serum binding of PFNA in the fetus.) Therefore, it will be assumed that the overall volume of distribution of the mother and fetus is the same as estimated in the general adult population, 0.19 L/kg (Chiu et al., 2022).

Zhang et al. (2013) evaluated placenta, as well as maternal and cord blood, and found that the three concentrations were highly correlated with correlation values of 0.776 for maternal blood and placenta, 0.643 for maternal blood and cord blood, and 0.793 for placenta and cord blood. Levels were highest in maternal blood, with a median level of 2.00 ng/mL, then placenta (0.96 ng/g) and cord blood (0.63 ng/mL). The ratio of placenta concentration to maternal serum was 0.56 ± 0.23 (mean ± SD calculated from data in Table S3 of Zhang et al. (2013)), almost the same as the overall average cord blood/maternal serum estimated in Table E-7. Zhang et al. (2013) also looked at PFNA concentrations in amniotic fluid and found only 38% of samples were higher than the level of quantitation, which was 0.01 ng/mL.

E.2.3. Longitudinal PFNA Changes during Pregnancy in Taibl et al. (2023)

In contrast to results of other longitudinal observations of PFNA (and other PFAS) over the course of pregnancy (see Section 3.1.2, "Human distribution during gestation and childhood"), Taibl et al. (2023) report higher serum levels of PFNA in second- (GM = 0.37 ng/mL) and third-trimester (GM = 0.41 ng/mL) women than first-trimester women (GM = 0.26 ng/mL), with the difference between the third and first trimester indicated as statistically significant ($p < 0.05$). In part, this difference may be due to the fact that the population of women sampled in each trimester was somewhat different. While 85 of the 110 women who participated in the third trimester had participated in the first trimester, the number of women sampled for serum in the first trimester was 190, so (at least) 105 of the 190 first-trimester samples did not have matched samples in the third trimester. However, 113 subjects participated in both the first and second trimester, and 127 serum samples were taken in the second trimester; it is between the first and second trimester that the largest increase appears to have occurred. Analyzing those data more specifically, if one assumes that the serum levels observed in the first trimester (median gestation week [GW] = 11) represent pre-pregnancy values that are near steady state for women of childbearing age, for whom the estimated clearance rate is 0.124 mL/kg-day (see Section 3.1.4, "Total clearance in humans"), this first trimester concentration corresponds to an exposure rate of 0.26 ng/mL × 0.124 mL/kg-day = 0.032 ng/kg-day. The median gestational age for the second trimester observations was GW 24, or 13 weeks = 91 days after the first trimester cadre. Assuming a constant volume of distribution (Vd) of 190 mL/kg (Chiu et al., 2022) and ignoring gestational weight gain, the increase in serum levels between the first and second trimesters corresponds to an increased body burden of (0.37-0.26 ng/mL) × 190 mL/kg = 20.9 ng/kg. If total body volume into which the PFNA distributes increases over this period as would generally be predicted, the increase in body burden would be higher. Given that this difference occurred over a median period of 91 days, the increase then indicates an exposure of at least 0.23 ng/kg-day or about 7 times higher than the steady-state exposure estimated for the reported concentration during the first trimester, even assuming zero

excretion during that time period. If excretion had decreased to zero and there was no increase in exposure, the predicted increase in serum levels would be only 0.015 ng/mL in 91 days, one-seventh of that observed. Similar results are obtained if one analyzes the third versus first trimester concentrations.

Other possible explanations exist for the subjects of the Taibl et al. (2023) study compared to the results of other studies discussed in Section 3.1.2. EPA noted that samples in the Taibl et al. (2023) study were analyzed in two laboratories; however, based on communication with the study authors, it seems unlikely that this aspect introduced significant bias between the trimesters. It is also noted that Taibl and colleagues selected a specifically African American population, whereas Oh et al. (2022a), for example, had a population that was 57% non-Hispanic White, 19% Hispanic, 21% Asian, and only 2% listed as "multiracial." Thus, an alternative to a significant increase in exposure during pregnancy for the subjects of Taibl et al. (2023) is that the African American population experienced a significant decrease in tissue distribution, wherein PFNA previously stored in the subjects' body tissues was transferred back to their serum over the course of pregnancy, although such a large change has not been observed in populations from other ethnic groups. However, EPA is not aware of specific biological differences between these ethnic groups that would result in such disparate outcomes for PFNA (and other PFAS). A second hypothesis is that there was significantly greater clearance in the Taibl subjects during the first trimester, such that the observed first-trimester serum concentrations were far lower than would occur given a relatively constant exposure and clearance (resulting in serum concentrations that were not at equilibrium with the rest of the body due to the short time scale), and that clearance then decreased significantly in subsequent trimesters. However, the steady increase in glomerular filtration shown by Taibl et al. (2023) over the entire study period contraindicates such an explanation. Therefore, EPA's conclusion is that the most likely explanation for the results of Taibl et al. (2023) is a significant increase in or difference between exposure levels of the subjects, resulting in the observed increase in serum PFNA levels of close to 60% between the first and third trimester. Such an increase might have occurred as much as several months before the period of observation, such that even the women in the first trimester were not at steady state, or after the first trimester observations. Given a constant exposure and other known changes in physiology and expected variation in distribution over the course of pregnancy, the most likely longitudinal change in PFNA concentration in maternal blood is a modest decline in serum levels such as that reported by Glynn et al. (2012) and Oh et al. (2022a), although the results of Chen et al. (2021) suggest that more substantial decreases can occur. EPA is not aware of a mechanism that could result in a 60% increase in maternal serum concentration between the first and third trimester of pregnancy under conditions of constant exposure and fairly constant Vd.

E.3. URINARY CLEARANCE VERSUS GLOMERULA FILTRATION OF PFNA

Some mechanistic insight can be gained by comparing the clearance values (shown in Table 3-3 for rats, mice and humans) with species-specific glomerular filtration rate (GFR), with and without adjustment for serum protein binding. Davies and Morris (1993) summarized GFR for multiple species. Considering the time period when those data were collected, it seems appropriate to use the species average body weight values listed in Table III of Davies and Morris (1993): 0.02 kg for the mouse, 0.25 kg for the rat, and 70 kg for the human. Using these values, the GFR/BW for these species are 20.2 L/kg-day in mice, 7.55 L/kg-day in rats, and 2.57 L/kg-day in humans, which are, respectively, 4,500 and 4,100 times higher than PFNA clearance in male and female mice, 2,000 and 106 times higher than male and female rats, 29,000 times higher than estimated in men and non-reproductive-age women, and 21,000 times higher than in reproductive age women.

Binding to serum proteins plays a likely role in the differences between animal and human urinary clearance. As discussed above in the context of distribution, PFNA binds to albumin with high affinity, and it is the major carrier of PFNA in blood (Forsthuber et al., 2020; Bischel et al., 2010). PFNA does not appear to interact with lipoproteins (Forsthuber et al., 2020); its binding may play a role in limiting the rate of renal excretion of PFNA. Kim et al. (2019) reported PFNA free fractions (f_{free}) of 0.00272 and 0.00332 in male and female rat plasma and 0.00148 and 0.00122 in male and female human plasma. Using these values, GFR × f_{free} = 20.5 and 25.1 mL/kg-day in male and female rats and 3.8 and 3.1 mL/kg-day in male and female humans, respectively. If one assumes an average f_{free} also applies to mice, GFR f_{free} = 60.5 mL/kg-day for that species. With the exception of female rats, these estimates are still 5.5- to 40-fold greater than the respective empirical clearance values, suggesting that a biological mechanism besides plasma protein binding is at play, renal resorption in particular.

While we expect that serum protein binding limits renal excretion (and tissue distribution), the extent of the limitation on urinary clearance appears to be less than predicted by assuming it is strictly limited to the free fraction in female rats. In particular, the empirically estimated clearance of 71.0 mL/kg-day for female rats is almost three-fold greater than the GFR × f_{free} = 25.1 mL/kg-day calculated from the rat GFR of Davies and Morris (1993) and the female rat f_{free} from Kim et al. (2019). Section 3.1.6 and Appendix E.4 provide further discussion of the fact that the PBPK model of Kim et al. (2019), which assumes that tissue distribution is similarly limited by the free fraction, underpredicts the short-term distribution of PFNA in rats. Hence, it appears that serum protein binding is less limiting of both urinary clearance and tissue distribution than predicted by assuming these processes are strictly limited to the free fraction at equilibrium.

Renal resorption was previously put forward as a general explanation for the slow clearance of per- and polyfluoroalkyl substances (PFAS) through the urine (Andersen et al., 2008). In vitro experiments have since identified PFNA as a potential substrate for transporters in the OATP family, such as human OATP1B1, OATP1B3, and OATP2B1 (Zhao et al., 2017). Another in vitro study identified rat organic anion transporter (OAT) 3 and oatp1a1, as well (Weaver et al.,

2010). Thus, active transport is a plausible and likely explanation for part of the difference between GFR, or GFR × f_{free} and urinary clearance of PFNA.

E.4. EVALUATION OF PBPK AND PK MODELING

A PBPK model is available for PFNA in rats and humans by Kim et al. (2019). The computational code for this model was obtained from the model authors and evaluated for consistency with the written description in the published paper, the PK data for PFNA, known physiology, and the accepted practices of PBPK modeling. Several flaws were found in the model. One flaw, an error in the balance of blood flow through the liver, had only a moderate impact on model predictions. A much larger issue is that the model had only been calibrated to fit the oral PK data for rats, and the set of model parameters selected by the model authors to match those data included an oral bioavailability lower than is otherwise supported by the empirical PK data. For example, the fraction absorbed by the male rat was effectively set to 40% in the model when the empirical PK analysis presented in Kim et al. (2019) showed 77% bioavailability. Further, when the model was used to simulate the intravenous PK data, which are data to which a PK model should be calibrated, the parameters were found to be completely inconsistent with those data. Figure E-5 compares results obtained with a replication of the PBPK model, which exactly matches the published PBPK model results for oral dosimetry, to the data and empirical PK fit for the 3 mg/kg i.v. dose to male rats.

The overprediction (approximately three to four times higher than the data for male rats during the first 14 days) of the i.v. data by the Kim et al. (2019) model indicates that distribution into the body is significantly underpredicted by the model, which was offset in the simulations of oral dosimetry data by using an unrealistically low oral bioavailability. Initial efforts to re-fit the model to the data did not produce acceptable fits to both the i.v. and oral dose PK data and involved changing model assumptions in a way that would require separate experimental validation before use. Specifically, the limitation to tissue distribution had to be significantly reduced in order to fit the blood concentration data at short times. Further, once these changes were made to accurately predict the distribution phase, the cumulative amount of PFNA reported in urine and feces was not enough to account for the subsequent decline in blood concentration, indicating that some other route of excretion was active. But no data to demonstrate a third route of excretion were available, and the data might also be explained by a time-dependent distribution to body tissues for which the limited tissue-concentration data were not sufficient to identify. It was therefore determined that the published model structure and underlying assumptions did not allow a sufficiently sound calibration of the model to the currently available PK data.

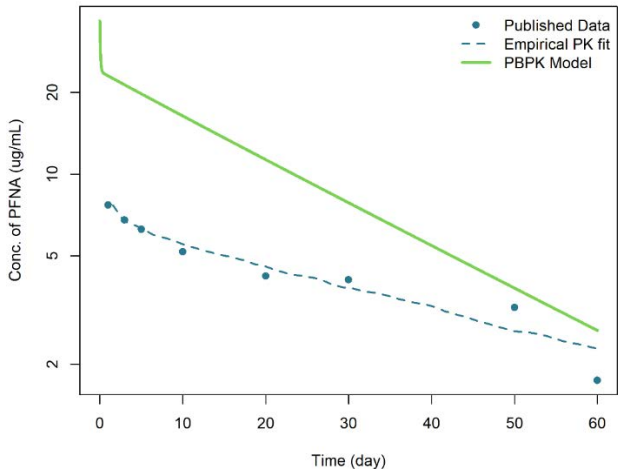

Figure E-5. Comparison of PFNA PBPK model predictions to i.v. dosimetry data (circles) of Kim et al. (2019) for a 3 mg/kg dose. The blue, dashed line is the result of an empirical PK analysis shown by **Kim et al. (2019)** (digitized). EPA's replication of the PBPK model (solid green line) exactly reproduces the PBPK model results of **Kim et al. (2019)** for oral dosimetry (results not shown – simulation here is for i.v. dose) and hence is considered an accurate reproduction of the model. The blue dashed line shows the fit of an empirical (non-physiologically based) model to the i.v. data. The discrepancy between the PBPK model prediction and the data demonstrates that the published model structure and parameters are inconsistent with the empirical data to an extent that indicates a significant flaw in the model.

E.4.1. One- and Two-Compartment PK Modeling for Rats and Mice

Empirical PK data from all published studies, including Kim et al. (2019), were evaluated and are summarized in Section 3.1.5 (ADME Summary). PK data that could be obtained for rats and mice were analyzed as described Appendix E.1 to obtain PK parameter values for a one- or two-compartment (1-C or 2-C) classic PK model for male and female rats and mice. The choice of model type, 1-C or 2-C, for each individual sex and species was based on model performance, as measured by the widely applicable information criteria (WAIC). Parameter values obtained included the fraction absorbed for oral exposure (F_{abs}, rats only), volume of distribution (Vd, mL/kg) and clearance (CL, mL/kg/d) for the 1-C model, with the addition of rate constants for transfer between the central and deep compartment (k_{cd}, k_{dc}, 1/d) for the 2-C model. Since oral dosimetry data were not available for mice, F_{abs} could not be estimated for that species and is assumed to be 1 (100%) when simulating oral exposures in mice.

The clearance in rats is sufficiently slow, so that PFNA is expected to accumulate throughout the course of the NTP 28-day exposure (NTP, 2018), although female rats are predicted to approach steady state by the end of the study, as will be illustrated below. Further, given the slow clearance of PFNA in male rats, the growth of rats during these toxicity studies can be a significant factor as increases in BW dilute the body burden from earlier exposures. Therefore, a PK model was developed to evaluate the accumulation and elimination of PFNA during these experiments, using parameters from the posterior probabilistic samples from the Bayesian analysis (E.1.4) and dose-

dependent changes in BW over time based on the empirical measurements from the NTP 28-day exposure (see Figure E-6) (NTP, 2018). (While the period of accumulation is much longer for male rats, female rats were modeled in the same way for consistency.)

Internal doses of PFNA predicted by the PK model as a function of exposure day are shown in Figure E-7. The dose is assumed to be adjusted for changes in BW each day. Since the animals were necropsied on day 29, 1 day after the final dose, the model simulations include a final day with zero exposure. Notice that the accumulation in male rats is fairly constant for the entire 28 days, whereas for female rats, it slows considerably later in the study as they begin to approach steady state. The inflection in the simulated concentration curves for the highest dose of male rats is the result of the observed decrease in the rate of weight loss between day 8 and day 22 followed by a constant BW between day 22 and day 29 (see Figure E-6).

Mean plasma PFNA concentrations from the NTP study, collected at time of necropsy, are shown for comparison in Figure E-7. The terminal plasma concentration data in the male rat were not proportional to dose, indicating a nonlinear pharmacokinetic process. For example, the measured concentration more than doubled between the 1.25 and 2.5 mg/kg-day dose groups, then was slightly lower at 5 mg/kg-day than 2.5 mg/kg-day. This nonlinearity may result both from the effects on BW and nonlinear clearance. (The model includes the time- and dose-specific body weight changes but assumes clearance is linear and dose independent.) For male rats, the model predictions show qualitative agreement with the observed greater-than-proportional increase in concentration with dose between doses of 0.625 and 2.5 mg/kg-day. At 5 mg/kg-day dose levels, all but two of the male rats died prior to the end of the study due to overt toxicity, with many of them having an annotation of "thin," so the relatively low serum levels in the remaining two animals may have occurred because of wasting. While simulations were conducted and results shown for comparison at 5 mg/kg-day, model predictions are not considered reliable at or above this dose level.

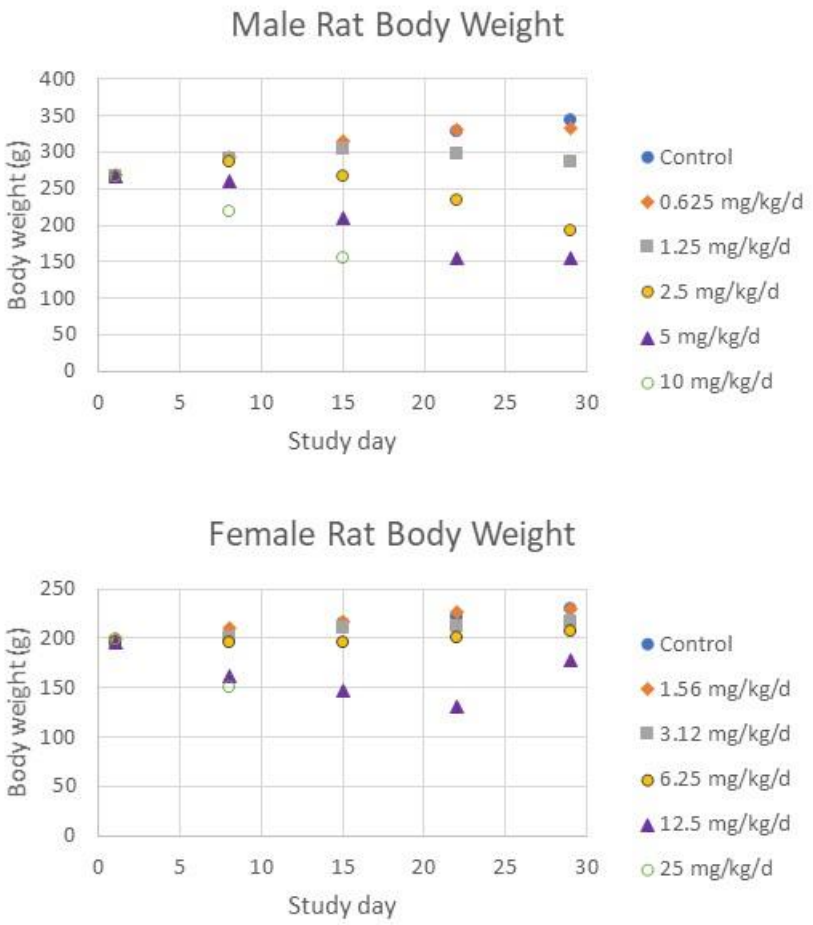

Figure E-6. Male and female rat body weight changes during 28-day PFNA bioassay (NTP, 2018). Datasets are identified by the dose (mg/kg/d). At the highest dose levels, 10 mg/kg-day in males and 25 mg/kg-day in females, the study was terminated prior to 28-days due to overt toxicity. (Note that in the 5 mg/kg-day dose group only two males remained at the final time-point and in the 12.5 mg/kg-day group only one female remained.)

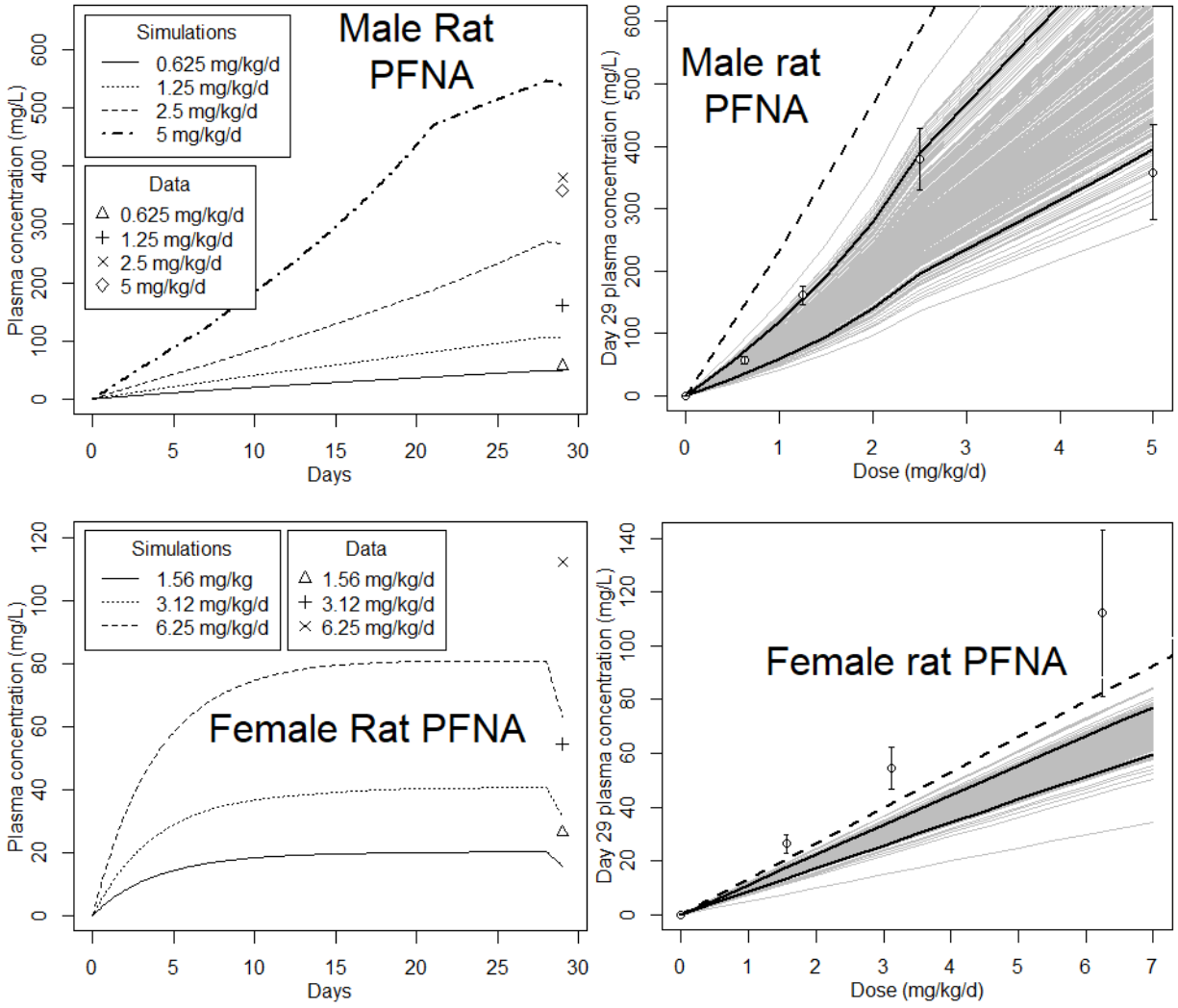

Figure E-7. Predicted accumulation and observed end-of-study plasma concentrations of PFNA in male and female rats in the NTP bioassay (NTP, 2018) as a function of dose. The end-of-study plasma concentrations were measured 1 day after the final dose, study day 29. Exposure is treated as continuous for 28 days. See text for other details. Left panels: Model simulations versus time using mean model parameters. Right panels: Model-predicted concentration using 1,000 samples from the Bayesian posterior parameter distribution (grey lines are individual exposure-dose curves, solid black lines are 5th and 95th percentiles). Dashed lines show predicted steady-state concentrations. Observed end-of-study concentration are plotted with error bars for ±1 standard deviation.

To facilitate the comparison of the PK model predictions (using mean PK parameters), estimated steady concentrations, and measured end-of-study concentrations, their values are compared in Table E-8.

Table E-8. Measured and predicted plasma PFNA concentrations (mg/L) in male and female rats in the NTP bioassay

Dose (mg/kg-d)	Measured concentration (mean ± SD)	PK model predictions	Estimated steady-state concentration[a]
Male rats			
0.625	56.7 ± 5.9	48	146
1.25	161 ± 16	105	292
2.5	380 ± 50	266	584
5	358 ± 76	838	1,170
Female rats			
1.56	26.4 ± 3.4	15.8	20.6
3.12	54.4 ± 7.9	31.6	41.2
6.25	112 ± 31	63	83

[a] Dose times fraction absorbed divided by sex-specific clearance (dose × F_{abs}/CL).

The PK model simulations with mean parameter values underpredict the concentration for the 0.625–2.5 mg/kg-day doses by 15%–35%, while the upper 95th percentile results come close to the data. Model results for 5 mg/kg-day overpredict the measured concentration in males, which may be due to toxicity at this dose level significantly altering the PK in the animals. This suggests the model should only be applied for extrapolation at doses of 2.5 mg/kg-day and below. By comparison, the estimated steady-state concentrations in male rats for doses 0.625–2.5 mg/kg-day, using only the mean estimated F_{abs} and CL, are 54% to 160% higher than the observed data. The male rat simulation results for 2.5 mg/kg-day and lower are within a factor of 2 of the observed means (see Table E-8), which is generally an acceptable level of agreement. However, the systematic underprediction of the observed levels and the mild nonlinearity in the data for 0–2.5 mg/kg-day encourage consideration of an alternate approach based on direct interpolation of the data. Specifically, the final concentration expected for POD concentrations ≤2.5 mg/kg-day could reasonably be estimated using a linear interpolation between the two closest observed concentrations. Then, the qualitative prediction of the PK model, which reflects the relatively long half-life of PFNA, indicates an essentially linear increase in blood concentration from the start of the study to the day of observation, i.e., the simulated time courses in the top-left panel of Figure E-7 are close to a straight line from zero at the beginning to the final concentration. Modest variation in the PK parameters will not impact this general feature. Given such a time course, the average blood concentration over the study duration is just one-half the final concentration. Hence, the average concentration for a given POD dose used for extrapolation of 28-day male rat endpoints to humans

was estimated as one-half of the final concentration in a 28-day study, calculated by linear interpolation between the observed concentrations.

The female rat concentration data versus dose in Figure E-7 (lower right panel, 1.56–6.25 mg/kg-day) are very close to linear, with an upward curvature versus dose much less than observed in the males, indicating that PK is linear with dose over that range. Female rat simulations over that dose range are likewise linear versus dose. However, the mean model predictions are 42%–55% of the serum concentration data at those dose levels (see Table E-8), and even the highest simulation from the posterior sample was 30% lower than observed in female rats. As demonstrated in the female time course (lower-left panel, Figure E-7), female rats are predicted to be close to steady state after 28 days; however, due to the assumption of a full day of elimination prior to sacrifice, the predicted concentration then decreases about 20%. In this case, the use of the predicted steady state or measured plasma concentrations appears to be a better option than the PK model. That the PK model predicts female serum concentrations near to steady state over 75% of the exposure period suggests that assuming steady-state plasma concentrations is reasonable for female rats. Since the observed plasma concentrations are systematically underpredicted by both the PK model and the estimated steady-state concentration, the simple approach of linear interpolation to estimate final concentrations for various POD values will be more accurate than using either the model or steady-state calculation. Given the robust analysis of rat PK data described in Appendix E.1, EPA considers it quite likely that the half-life in female rats is in the range of three days and therefore that steady state is reached fairly quickly in female rats, with a time-course similar to that predicted by the PK model (Figure E-7), though the plasma concentration at which steady state occurs must be higher than predicted by the PK analysis. Therefore, the average plasma concentration for a given POD dose used for extrapolation of 28-day female rat endpoints to humans was simply estimated as equal to the measured end-of-study plasma concentration or calculated by linear interpolation of those measured values.

The performance of the classic PK model was also validated against data in mice. Das et al. (2015) evaluated the effects of PFNA in pregnant mice and their offspring, as well as nonpregnant females, in which the dams and nonpregnant females were dosed from gestation day (GD) 1 to 16 or 17. Some dams and nonpregnant mice were exposed from GD 1 to GD 16 and then sacrificed on GD 17, when serum concentrations and liver weights were measured. For simplicity, model simulations treated PFAS intake as a 24-hour infusion; the internal dose is simulated as occurring from GD 0.5 to GD 16.5 for these animals. An Excel workbook obtained from the study authors contained body weights of pregnant dams from GD 1 to GD 17 and at PND 28 and BWs of nonpregnant females on day 17. The mean BWs for the pregnant dams for all dose groups were used as inputs for linear interpolation as was done previously for the NTP rat bioassay, to obtain a growth curve for any applied or estimated dose. Pregnant dams were assumed to grow at the same rate between GD 17 and GD 19 (parturition) as between GD 16 and GD 17 for each dose group, but this extrapolation does not impact model evaluation at GD 17. PK model results and maternal

serum concentration data from Das et al. (2015) are shown in Figure E-8. The model predictions are 2.3- to 4.5-fold higher than reported at GD 17 in dams.

Mouse fetuses were assumed to have the same serum concentration as the dams until birth, and simulations after birth were performed using the average milk ingestion rate (per pup weight) for mice built into the model and the measured milk/maternal serum ratio (0.3) as described in Section 3.1.4. The mean estimated concentrations in PND 1 pups were then only 19%–66% higher than the observed concentrations, but at later time points, the discrepancy increased due to the high rate of lactational transfer predicted in combination with the high predictions of maternal concentrations. While the resulting model predictions are mostly much farther from the observed data than is generally considered acceptable, the corresponding steady-state concentrations (shown as the solid dashed line for the 1 mg/kg-day dose in Figure E-8) are much farther from the observed data.

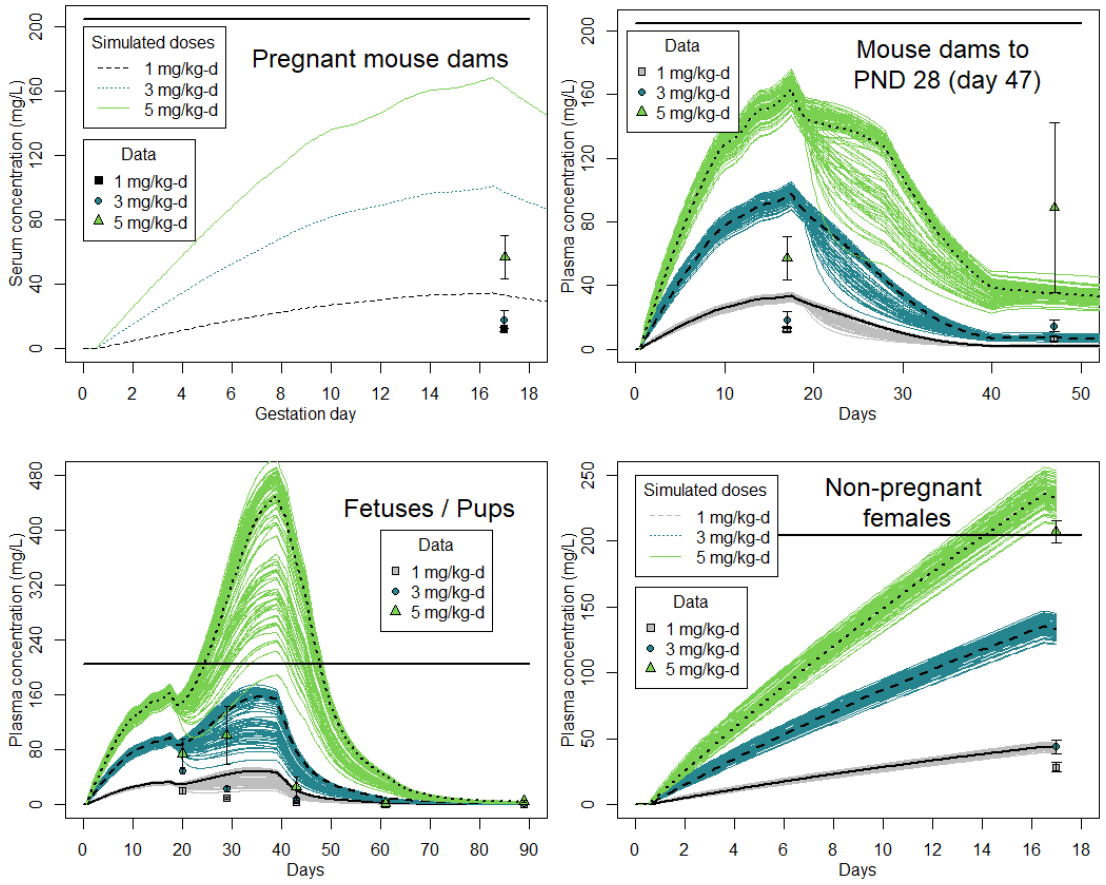

Figure E-8. Predicted and observed PFNA serum concentrations in pregnant female mice from Das et al. (2015). Simulations in upper left panel performed with the 2-compartment PK model using mean parameter values for female mice from Bayesian analysis and F_{abs} = 1. Curves in other panels were generated using 100 random samples from the posterior distribution of the Bayesian analysis. Black, heavy curves show median simulated value versus time. Black solid horizontal lines show steady-state concentrations given 1 mg/kg-day doses.

It is not clear why the PK model overpredicts the serum concentration of female mice as much as is shown in Figure E-8. One possibility that could explain the results at 1 and 3 mg/kg-day is that with the increasing body burden after multiple days of dosing, resorption in the kidney becomes saturated leading to higher clearance, and this is a factor that did not impact the single-dose PK studies used to estimate the mouse PK parameters. (The highest dose of the mouse PK study used for model calibration was 10 mg/kg at which the maximum serum concentration in female mice was 48 mg/L (Tatum-Gibbs et al., 2011).) Unfortunately, a method of efficiently performing Bayesian calibration with a nonlinear PK model that includes saturable resorption is not yet available in the Python environment described above. (While Bayesian fitting of a PK model with saturable renal resorption has been reported by Wambaugh et al. (2013), with analysis conducted in R, for which the model code is available, the method for computational analysis used was not considered fast enough for the current application.)

While saturable resorption can explain the discrepancies between model predictions and the 1 and 3 mg/kg-day data (i.e., resulting in much more rapid clearance at 3 mg/kg-day than 1 mg/kg-day, hence a disproportionately lower plasma concentration), some other mechanism must then come into play at 5 mg/kg-day, for which the serum levels are disproportionately higher than the 1 and 3 mg/kg-day serum levels. EPA is not aware of a mechanism associated with PFAS exposures that could explain that nonlinearity. That the model simulations for nonpregnant mice exposed to 5 mg/kg-day matched almost exactly the observed serum levels on day 17 may be the result of saturable resorption and a second mechanism leading to reduced clearance just happening to cancel one another at that dose.

While the underprediction for female rats shown in Figure E-7 is not as large as the underprediction for male rats, both show a systematic error in the model relative to the observations, which suggests a mechanism leading to reduced clearance after multiple doses, like that suggested by the mouse plasma data. It is also possible that distribution in the body is different under multiple-dose conditions than after single doses, but tissue-concentration data other than mouse liver data discussed below are not available to evaluate that hypothesis.

Recall that the PK model accounts for the change in total BW of the pregnant dams versus nonpregnant females, which is why the simulated serum concentrations at GD 17 for the pregnant females were 125–150 mg/L, whereas those for nonpregnant females were 180–220 mg/L. The fact that observed serum concentrations in the pregnant females were still overpredicted (while those in PND 1 pups were only modestly overpredicted), while observed serum levels in the pregnant females were less than half of those in the nonpregnant females on day 17, suggests yet another factor affecting the clearance or distribution to non-fetal tissues during pregnancy.

Further insight can be gained from liver concentration data obtained from Das et al. (2015), shown in Figure E-9. First, it is notable that maternal liver concentrations on GD 17 increase almost linearly with dose, although the increase from 3 to 5 mg/kg-day is slightly less than proportional to the dose. In contrast, the fetal liver concentration increases at a rate greater than proportional to

dose from 3 to 5 mg/kg-day. Then, in PND 1 and 10 pups, the liver concentration appears to saturate slightly between 1 and 3 mg/kg-day and more strongly between 3 and 5 mg/kg-day.

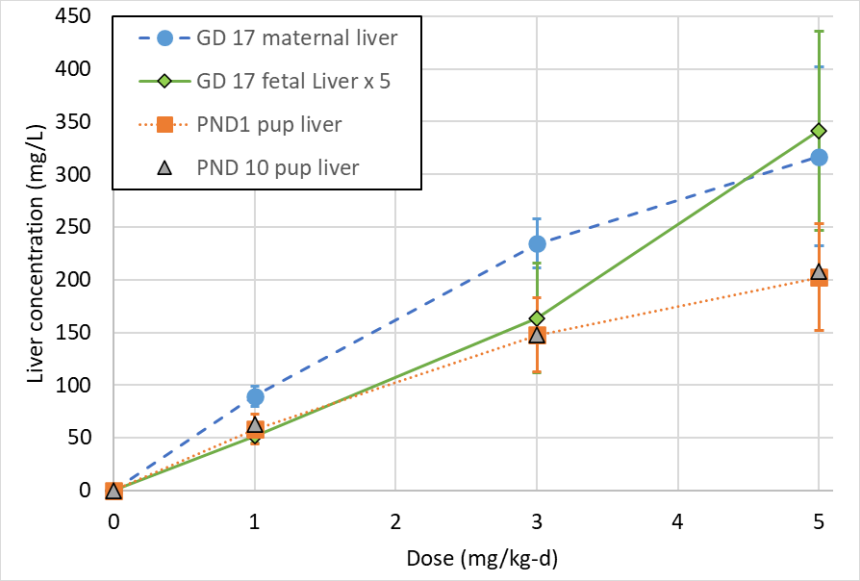

Figure E-9. Observed PFNA liver concentrations in pregnant female mice, mouse fetuses and pups from Das et al. (2015). Concentrations in fetal liver were multiplied by five for easier comparison of the relationship between concentration and dose.

Wolf et al. (2010) also conducted a developmental study in mice but with more limited data. In particular, serum levels were measured only at PND 21 (study day 40) in dams, pups, and nonpregnant females. Simulations were conducted similarly to those of Das et al. (2015), accounting for BW changes in the pregnant dams and pups. BW was assumed constant for nonpregnant females. Model simulations versus observed serum data are shown in Figure E-10. While the final concentrations in the dams are underpredicted and the simulations for the pups overpredict the observed means, the latter are mostly within one standard deviation of the means and are considered by EPA to be a good match to the data. Simulations for the nonpregnant females also appear to be quite good.

A complete understanding of the Das et al. (2015) data and their nonlinearities will likely require additional PK data to evaluate the effects of repeated dosing and higher serum concentrations versus pregnancy on PK and almost certainly a PBPK or PK model that can adequately describe the observed nonlinearities and pregnancy-related differences, i.e., science that is not currently available. In the meantime, simulations using the two-compartment classic PK model tested here, shown in Figures E-8 and E-10, although clearly imperfect, are closer to the observed serum concentrations than if one assumes steady state is reached (with the same clearance value), which is effectively what occurs when a data-derived extrapolation factor (DDEF) is used.

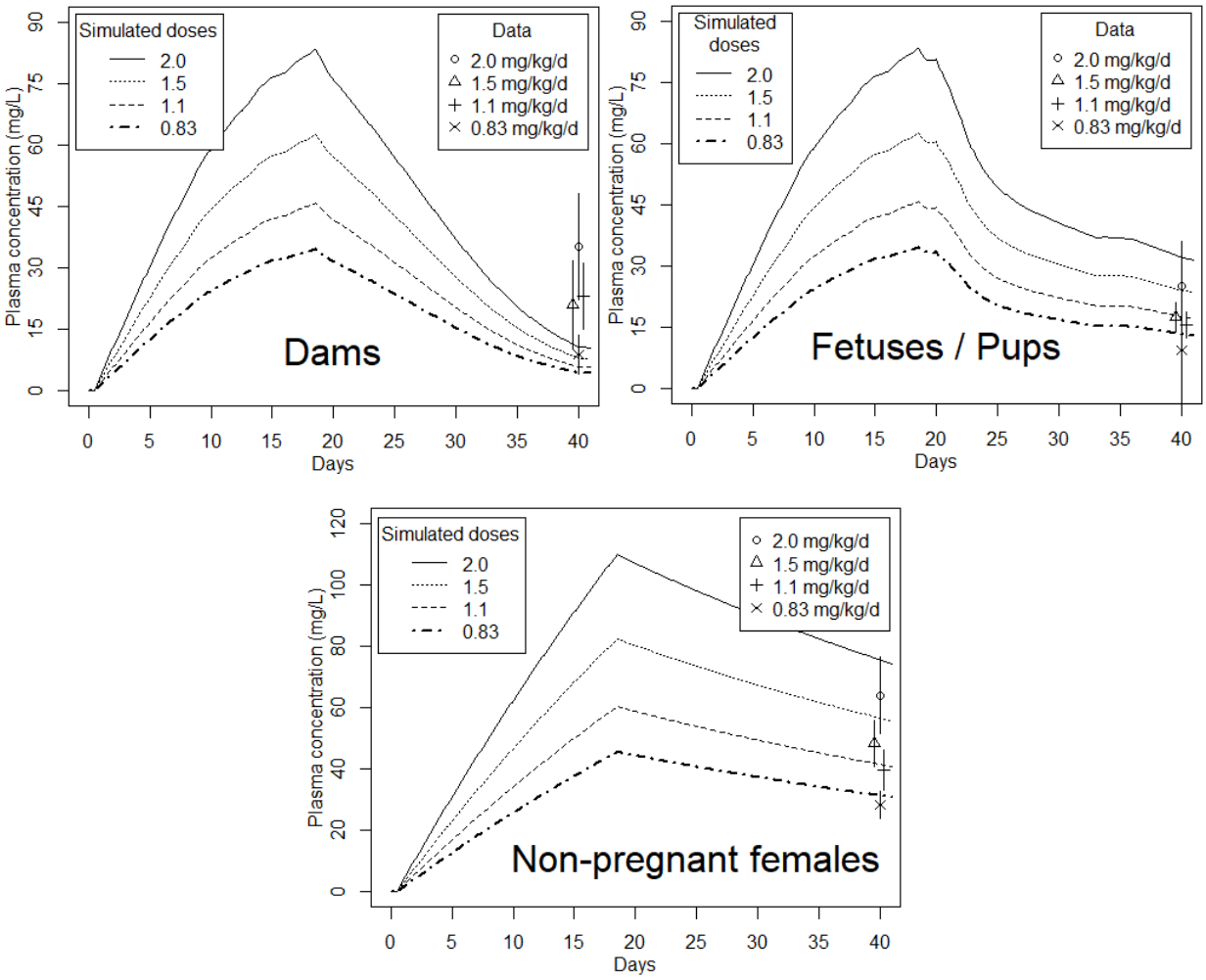

Figure E-10. Model simulations and observed PFNA plasma concentrations in female dams, pups and nonpregnant females from Das et al. (2015). Animals were sacrificed on PND 21, study day 40. Data are shown as mean ± SD with middle two doses plotted on day 39.5 or 40.5 to avoid over-lap.

E.4.2. Human PK Simulations with a One-Compartment Model

Separate values of CL were estimated for women of child-bearing age (12.4–50 years of age) and for men and all other women (see Table 3-3), with F_{abs} assumed to be 1 in humans. The model of Kapraun et al. (2022) was adapted for the current analysis, which includes body weight as a function of age in a woman from birth through pregnancy, between ages 24.25 (average age of first pregnancy, (Portier et al., 2007)) and 25 years. However, the rate of breast-milk ingestion for breast-fed children was revised to use the mean milk intake rate from Table 15-1 of EPA's Exposure Factors Handbook (U.S. EPA, 2011), rather than the upper percentile (mean + 2 × SD). Human PK parameters were set as described in Section 3 (see Table 3-3), and distribution of PFNA to breast milk was defined using a milk/maternal serum ratio of 0.05 (see Section 3.1.4, "Lactation in humans"). The time course of PFNA in three generations of human women, continuously exposed to

1 mg/kg-day, was simulated.[11] The first-generation (F0) woman is assumed to become pregnant at age 24.25 years and to give birth to a female child at age 25. The child (F1) is assumed to have the same growth over time, also become pregnant at age 24.25, and give birth to a female child (F2). It is assumed that both daughters are breast fed for a year, and this is the sole source of PFNA exposure during that time, after which they are exposed to 1 mg/kg-day. As discussed in Section 3.1.2 ("Human distribution in pregnancy and childhood"), fetal serum concentrations are assumed equal to 0.575 times maternal serum concentrations at birth, whereas the Vd for the fetus and infant at childbirth is assumed to be double that of the mother and to decline to adult Vd at age 10. The results of simulating continuous exposure to 1 mg/kg-day to all three generations (except for the 1 year of breastfeeding, when exposure to the infant is determined by that rate) are shown in Figure E-11.

[11]Since the model is linear with dose, results would be proportionately lower at 1 μg/kg-day or 1 ng/kg-day. A dose of 1 mg/kg-day was used for illustrative purposes since mg is the native mass unit for the model.

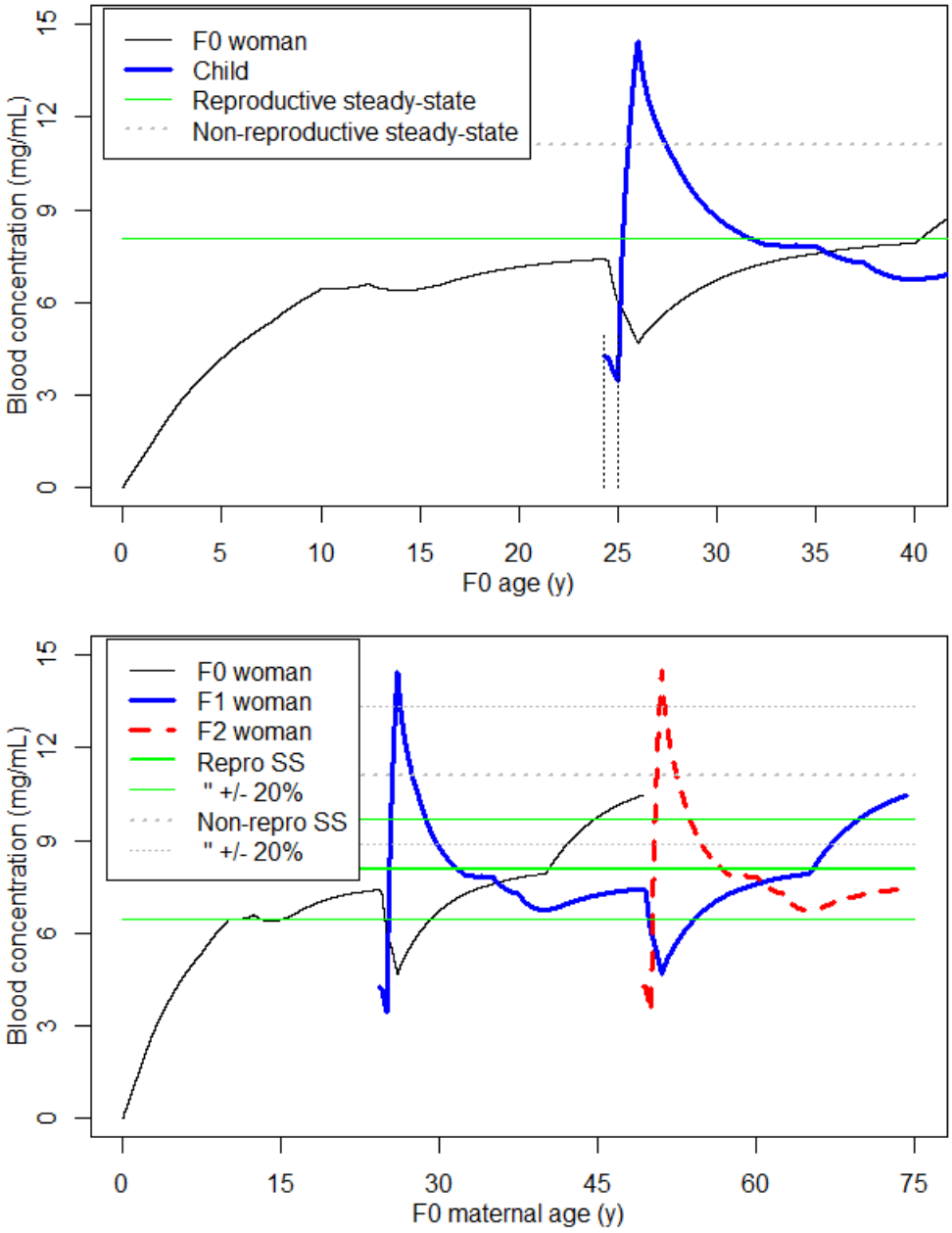

Figure E-11. Predicted blood concentration time-course in three generations of women from continuous exposure to 1 mg/kg-day PFNA. PK model simulations were conducted as described in the text. In the upper panel the vertical dashed lines show the beginning and end of pregnancy, where fetal blood concentration is assumed to be 0.575 times the maternal concentration. The heavy horizontal lines show the steady-state (SS) concentrations for women of childbearing age (solid green) and older and younger women (dotted grey). The lighter horizontal lines above and below the heavy lines are ±20% of the SS levels.

The model simulation results in Figure E-11 indicate that if a child is born with zero PFNA body burden and is not exposed through breast feeding but ingests 1 mg/kg-day (F0 woman), they will reach 80% of steady-state levels by around age 10. The time it takes to reach this level of

accumulation is the result of both the half-life of PFNA (predicted to be 4 years for all males and non-reproductive age women) and the ongoing growth of the child, which dilutes the PFNA ingested prior to a given age. The young woman is then predicted to be between 80% and 100% of the steady state for reproductive age women through the first trimester of pregnancy. Because the total growth during pregnancy and subsequent breastfeeding is predicted to significantly reduce her blood concentration, the model predicts that it is then not until age 29 that her blood concentration returns to 80% of steady state. Her blood concentration is predicted to begin another period of rapid increase at age 40, when her clearance is assumed to decrease to that estimated for men and older women (see Section 3.1.4, "Total clearance in humans").

While fetal serum levels are predicted to decrease in parallel with maternal serum levels during pregnancy (due to growth dilution), the infant is then predicted to have a very large spike in blood concentration due to the high exposure of breast-feeding. Even though the concentration in breast milk is assumed to be only 5% of that in maternal serum, the maternal serum concentration has been accumulated by the mother's lifetime exposure, and infants ingest a larger volume of milk per kg BW than adult food ingestion so are predicted to receive much more than 1 mg/kg-day until weaning at age 1. The decline in concentration in the child after age 1 is due to a combination of the reduced ingestion and the growth of the child. The child is predicted to be within 20% of the steady state for men and non-reproductive age women between ages 5 and 10 but then to fall below that level due to continued growth and (at age 12.4) the onset of higher clearance assumed for women of reproductive age.

To evaluate one aspect of model predictions against observational human data, simulations were conducted in which the F1 child is assumed to be breast-fed for varying lengths of time, from 0 to 12 months, after which they were exposed to the same daily dose as the mother.

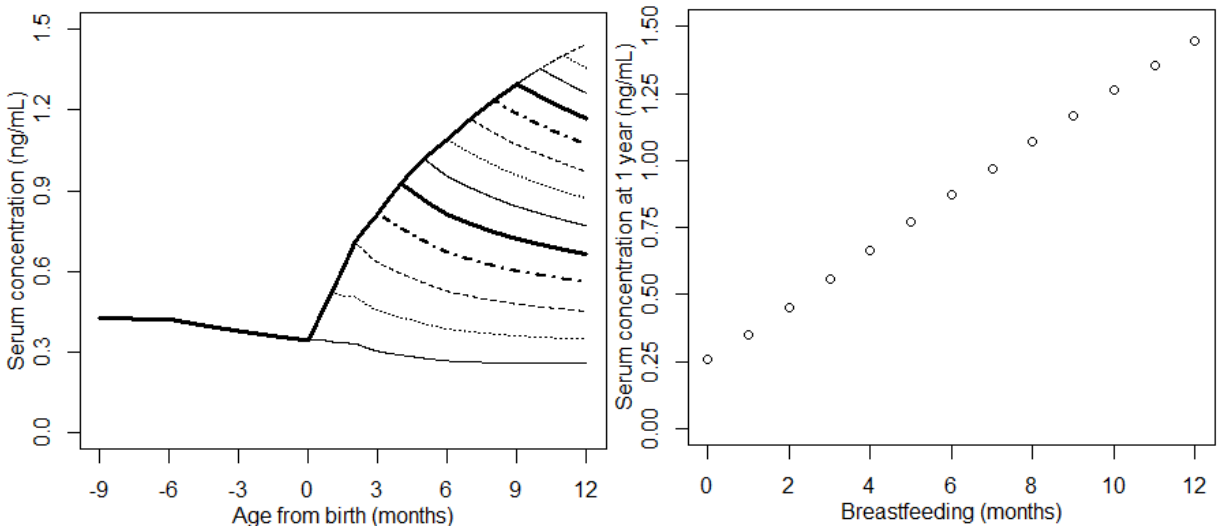

Figure E-12. Simulated PFNA time-courses in fetuses (age < 0) and infants of mothers ingesting 0.1 ng/kg-day PFNA, with breastfeeding for 0–12 months. PK model simulations were conducted as described for Figure E-11 for the F0 woman and F1 fetuses, except that the dose was set to 0.1 ng/kg-day. After birth (age 0 months in left panel), the child was assumed to be either not breast-fed (lowest curve) or breast-fed for durations of 1–12 months. *Left panel:* serum concentration time-courses. The upper-most curve is for the child breast-fed for 12 months. After weaning and for the non-breast-fed child exposure is assumed to be 0.1 ng/kg-day. Results are identical until the end of breast-feeding. *Right panel:* Serum concentration predicted at age 1 year versus months of breast-feeding.

A dose of 0.1 ng/kg-day was selected for the simulations in Figure E-12 since the resulting predicted serum concentration in the 1-year-old child, approximately 0.25 ng/mL, is similar to that observed by Koponen et al. (2018) in a longitudinal study of Finnish children for whom the duration of breastfeeding was recorded and a correlation between the serum levels at age 1 year and the months of breastfeeding obtained. Koponen et al. (2018) observed a statistically significant increase in the serum PFNA levels of their population with the length of breastfeeding, with a slope of 0.07 ng/mL-month. The model simulations shown in Figure E-12 yield a slope of 0.1 ng/mL-month, and the predicted concentration for a child breast-fed for an entire 12 months, 1.44 ng/mL, is well within the range observed by Koponen et al. (2018). When simulations were repeated based on the upper percentile milk ingestion, the slope was 0.14 ng/mL-month, and the predicted concentration at 12 months was 1.9 ng/mL, just below the highest individual in the Koponen et al. (2018) population. This indicates that the milk ingestion rates evaluated, along with other parameters for PK in the infants and mother during the first year postpartum, are fairly accurate, although the predicted lactational transfer is 40% higher than estimated when using the mean estimated breast milk ingestion rate.

As discussed in Section 3.1.6, the PK model simulations shown in Figure E-11 are considered highly uncertain due to the many assumptions involved. In particular, there are almost no data that can be used to directly evaluate how clearance and volume of distribution for PFNA

may or may not differ between children and adults. However, the results in Figure E-11 show an overall pattern of serum concentration that indicates that chronic exposure to PFNA will result in blood concentrations near or above steady-state levels for most of a person's lifetime. Therefore, estimation of human equivalent doses based on the dose-corresponding steady-state levels, i.e., the blood concentration multiplied by the clearance, should provide an estimate of that exposure level that is within a factor of 2 of the value one might obtain with a detailed PK (or PBPK analysis), given lifestage-specific values for the various parameters.

E.5. DERIVATION OF DATA-DERIVED EXTRAPOLATION FACTORS

The data-derived extrapolation factor (DDEF) approach applies the ratio of human clearance to clearance in the animal species and sex used to identify a specific point of departure (POD), adjusted for differences in oral bioavailability, to estimate HEDs. For example, if a male rat is continuously exposed to a chemical dose (the POD) and reaches steady state, or a period of time over which the daily average serum concentration (C_{avg}) is the same from day to day, then at that steady state, the total amount of the chemical cleared each day, given by $C_{avg,rat,m} \times CL_{rat,m}$, must equal the absorbed portion of the daily POD dose, which is $F_{abs,rat,m} \times POD$, where $CL_{rat,m}$ is the clearance and $F_{abs,rat,m}$ is the fraction absorbed in male rats. In short, at steady state, the daily amount absorbed must equal the daily amount cleared, or

$$F_{abs,rat,m} \times POD = C_{avg,rat,m} \times CL_{rat,m}, \quad \text{(E-16)}$$

from which we can derive:

$$C_{avg,rat,m} = POD \times (F_{abs,rat,m}/CL_{rat,m}) \quad \text{(E-17)}$$

The same analysis applies to a human male (for example) exposed on a daily basis, but the corresponding fraction absorbed is $F_{abs,H}$, the corresponding clearance is $CL_{H,m}$, and the dose being estimated is the HED_{DDEF}:

$$C_{avg,H,m} = HED_{DDEF} \times (F_{abs,H}/C_{H,m}) \quad \text{(E-18)}$$

We assume that the health effect in a human male will be the same as in the male rat if C_{avg} is the same in both receptors, i.e., when

$$C_{avg,H,m} = HED_{DDEF} \times (F_{abs,H}/C_{H,m}) = C_{avg,rat,m} = POD \times (F_{abs,rat,m}/CL_{rat,m}) \quad \text{(E-19)}$$

Solving for the HED_{DDEF} to extrapolate from a POD from the NTP bioassay for an endpoint in male rats to male humans:

$$HED_{DDEF} = POD \times (F_{abs,rat,m}/F_{abs,H}) \times CL_{H,m}/CL_{rat,m}. \quad \text{(E-20)}$$

The factor that multiplies the POD, $(F_{abs,rat,m}/F_{abs,H}) \times CL_{H,m}/CL_{rat,m}$, is the DDEF.

As described in Excretion in Humans (see Section 3.1.4), the estimated sex- and lifestage-specific average clearance values in Section 3.1.5, Table 3-3 are considered sound for animal-human extrapolation of (population average) PFNA dosimetry. The key assumptions in calculating a DDEF for a given endpoint evaluated are then as follows:

1) For effects observed in adult male and female rats and mice (liver and endocrine), the corresponding CL for the animal species and sex are from Section 3.1.5, Table 3-3.

2) Developmental effects observed in mice are assumed to depend on CL in both the dam and the offspring, with the extent of dependence on the dam depending on the age of the pup. It is recognized that the amount transferred through lactation also depends on maternal CL, but the CL in the offspring is assumed to be a significant factor in postnatal dosimetry. At birth, the concentration in the pup is assumed to depend only on maternal CL since urinary excretion by the fetus becomes amniotic fluid in which the pup is immersed. As the pup grows after birth, its serum concentration depends to an increasing extent on CL of the pup, which determines how much of the dose from the dam is eliminated. Evaluation of the quantitative dependence on maternal versus pup CL during this time would require either an accurate PK model or additional PK studies, such as from cross-fostered pups, neither of which is currently available.

    a. Effects observed in all pups on or before PND 7 and in all older female mouse pups use CL for the female mouse, 4.89 mL/kg-day, since the dose to younger pups is assumed to be largely determined by maternal CL, and CL in older female pups is assumed to be the same as maternal female CL.

    b. Effects observed in male mouse pups on or after PND 21 use CL for the male mouse, 4.51 mL/kg-day, since CL in the pups is assumed to be the same as adult males.

    c. Effects for combined male and female pups on or after PND 21 use the average CL, 4.70 mL/kg-day.

    d. Since there is only a modest difference between CL in adult male and female mice, we presume that dosimetry in pups is approximately equally dependent on maternal and pup CL between PND 7 and 21.

3) CL_H is set to the value of 0.090 mL/kg-day for effects in adults other than reproductive effects in females, observations in human children at age 7, and observations in animal pups after PND 7. CL_H is set to the value of 0.124 mL/kg-day for reproductive effects in adult women, effects on birth weight, or observations in animal pups on or before PND 7. Because these values are used in conjunction with the uncertainty factor for inter-individual variability among humans, UF_H, which is understood to account for variability in both pharmacokinetics and pharmacodynamics across the entire human population relative to an average adult, their use is assumed to result in an adequate degree of health protection for all human lifestages.

Table E-9 shows the resulting DDEFs. Since $F_{abs,H}$ is assumed to be 1, it is not listed for the sake of brevity.

Table E-9. DDEF calculations

Sex and species of observation (lifestage)	CL_A (mL/kg-d)	$F_{abs,A.s}$	CL_H (mL/kg-d)	DDEF
Male rats (adult)	3.68	0.86	0.090	2.10×10^{-2}
Female rats (adult), non-reproductive	71.1	0.94	0.090	1.19×10^{-3}
Female rats (adult), reproductive	71.1	0.94	0.124	1.64×10^{-3}
Male mice (≥PND 15)	4.51	1	0.090	2.00×10^{-2}
Female mice repro; Mouse pups (≤PND 7)	4.89	1	0.124	2.54×10^{-2}
Female mice, non-repro (≥PND 21)	4.89	1	0.090	1.84×10^{-2}
Male + female mouse pups (≥PND 15)	4.70	1	0.090	1.91×10^{-2}

[a]DDEF = $(CL_H/CL_A) \times (F_{abs,A}/F_{abs,H})$, with $F_{abs,H}$ assumed to be 1. CL values from Table 3-3.

APPENDIX F. QUALITY ASSURANCE FOR THE IRIS TOXICOLOGICAL REVIEW OF PERFLUORONONANOIC ACID AND RELATED SALTS

This assessment is prepared under the auspices of the U.S. Environmental Protection Agency's (EPA's) Integrated Risk Information System (IRIS) Program. The IRIS Program is housed within the Office of Research and Development (ORD) in the Center for Public Health and Environmental Assessment (CPHEA). EPA has an Agency-wide quality assurance (QA) policy that is outlined in the *EPA Quality Manual for Environmental Programs* (see CIO 2105-P-01.3) and follows the specifications outlined in EPA Order CIO 2105.3.

As required by CIO 2105.3, ORD maintains a Quality Management Program, which is documented in an internal Quality Management Plan (QMP). The latest version was developed in 2013 using Guidance for Developing Quality Systems for Environmental Programs (QA/G-1). An NCEA/CPHEA-specific QMP was also developed in 2013 as an appendix to the ORD QMP. Quality assurance for products developed within CPHEA is managed under the ORD QMP and applicable appendices.

The IRIS Toxicological Review of Perfluorononanoic Acid (PFNA) is designated as Highly Influential Scientific Information (HISA)/Influential Scientific Information (ISI) and is classified as QA Category A. Category A designations require reporting of all critical QA activities, including audits. The development of IRIS assessments is done through a seven-step process. Documentation of this process is available on the IRIS website: https://www.epa.gov/iris/basic-information-about-integrated-risk-information-system#process.

Specific management of quality assurance within the IRIS Program is documented in a Programmatic Quality Assurance Project Plan (PQAPP). A PQAPP is developed using the EPA Guidance for Quality Assurance Project Plans (QA/G-5), and the latest approved version is dated April 2021. All IRIS assessments follow the IRIS PQAPP, and all assessment leads and team members are required to receive QA training on the IRIS PQAPP. During assessment development, additional QAPPs may be applied for quality assurance management. They include:

Title	Document number	Date
Program Quality Assurance Project Plan (PQAPP) for PFAS Assessments	L-CPAD-0031652-QP-1-5	February 2023
Program Quality Assurance Project Plan (PQAPP) for the Integrated Risk Information System (IRIS) Program	L-CPAD-0030729-QP-1-6	June 2023
An Umbrella Quality Assurance Project Plan (QAPP) for Dosimetry and Mechanism-Based Models (PBPK)	L-CPAD-0032188-QP-1-3	May 2023
Quality Assurance Project Plan (QAPP) for Enhancements to Benchmark Dose Software (BMDS)	L-HEEAD-0032189-QP-1-3	June 2023
ICF-General Support of CPHEA Human Health Assessment Activities QAPP	L-CPAD-0031961-QP-1-5	September 2022

During assessment development, this project undergoes four quality audits, including:

Date	Type of audit	Major findings	Actions taken
August 2020	Technical system audit	None	None
July 2021	Technical system audit	None	None
August 2022	Technical system audit	None	None
June 2023	Technical system audit	None	Note

During Step 3 and Step 6 of the IRIS process, the IRIS toxicological review is subjected to external reviews by other federal agency partners, including the Executive Office of the President. Comments during these IRIS process steps are available in the docket EPA-HQ-ORD-2021-0560 on http://www.regulations.gov.

REFERENCES

ACOG (American College of Obstetricians and Gynecologists). (2020). How your fetus grows during pregnancy. Available online at https://www.acog.org/womens-health/faqs/how-your-fetus-grows-during-pregnancy (accessed

Ames, JL; Burjak, M; Avalos, LA; Braun, JM; Bulka, CM; Croen, LA; Dunlop, AL; Ferrara, A; Fry, RC; Hedderson, MM; Karagas, MR; Liang, D; Lin, PID; Lyall, K; Moore, B; Morello-Frosch, R; O'Connor, TG; Oh, J; Padula, AM; Woodruff, TJ; Zhu, Y; Hamra, GB. (2023). Prenatal exposure to per- and polyfluoroalkyl substances and childhood autism-related outcomes. Epidemiology. http://dx.doi.org/10.1097/EDE.0000000000001587.

Ammitzbøll, C; Börnsen, L; Petersen, ER; Oturai, AB; Søndergaard, HB; Grandjean, P; Sellebjerg, F. (2019). Perfluorinated substances, risk factors for multiple sclerosis and cellular immune activation. J Neuroimmunol 330: 90-95. http://dx.doi.org/10.1016/j.jneuroim.2019.03.002.

Andersen, ME; Butenhoff, JL; Chang, SC; Farrar, DG; Kennedy, GL; Lau, C; Olsen, GW; Seed, J; Wallace, KB. (2008). Perfluoroalkyl acids and related chemistries--toxicokinetics and modes of action. Toxicol Sci 102: 3-14. http://dx.doi.org/10.1093/toxsci/kfm270.

Arrebola, JP; Ramos, JJ; Bartolomé, M; Esteban, M; Huetos, O; Cañas, AI; López-Herranz, A; Calvo, E; Pérez-Gómez, B; Castaño, A; BIOAMBIENT.ES. (2019). Associations of multiple exposures to persistent toxic substances with the risk of hyperuricemia and subclinical uric acid levels in BIOAMBIENT.ES study. Environ Int 123: 512-521. http://dx.doi.org/10.1016/j.envint.2018.12.030.

ATSDR (Agency for Toxic Substances and Disease Registry). (2021). Toxicological profile for perfluoroalkyls [ATSDR Tox Profile]. Atlanta, GA: U.S. Department of Health and Human Services, Public Health Service. http://dx.doi.org/10.15620/cdc:59198.

Averina, M; Brox, J; Huber, S; Furberg, AS; Sørensen, M. (2019). Serum perfluoroalkyl substances (PFAS) and risk of asthma and various allergies in adolescents. The Tromsø study Fit Futures in Northern Norway. Environ Res 169: 114-121. http://dx.doi.org/10.1016/j.envres.2018.11.005.

Bach, CC; Bech, BH; Nohr, EA; Olsen, J; Matthiesen, NB; Bonefeld-Jørgensen, EC; Bossi, R; Henriksen, TB. (2016). Perfluoroalkyl acids in maternal serum and indices of fetal growth: The Aarhus Birth Cohort. Environ Health Perspect 124: 848-854. http://dx.doi.org/10.1289/ehp.1510046.

Bassler, J; Ducatman, A; Elliott, M; Wen, S; Wahlang, B; Barnett, J; Cave, MC. (2019). Environmental perfluoroalkyl acid exposures are associated with liver disease characterized by apoptosis and altered serum adipocytokines. Environ Pollut 247: 1055-1063. http://dx.doi.org/10.1016/j.envpol.2019.01.064.

Batzella, E; Zare Jeddi, M; Pitter, G; Russo, F; Fletcher, T; Canova, C. (2022). Associations between Mixture of Perfluoroalkyl Substances and Lipid Profile in a Highly Exposed Adult Community in the Veneto Region. Int J Environ Res Public Health 19. http://dx.doi.org/10.3390/ijerph191912421.

Benskin, JP; De Silva, AO; Martin, LJ; Arsenault, G; Mccrindle, R; Riddell, N; Mabury, SA; Martin, JW. (2009). Disposition of perfluorinated acid isomers in Sprague-Dawley rats; part 1: single dose. Environ Toxicol Chem 28: 542-554. http://dx.doi.org/10.1897/08-239.1.

Beste, LA; Icardi, M; Hunt, CM; Gylys-Colwell, I; Lowry, E; Taylor, L; Morgan, TR; Chang, MF; Maier, MM; Cheung, R. (2020). Alanine aminotransferase results differ by analyzer manufacturer in

a national integrated health setting, 2012-2017. Arch Pathol Lab Med 144: 748-754. http://dx.doi.org/10.5858/arpa.2018-0622-OA.

Betancourt, MJ; Girolami, M. (2013). Hamiltonian monte carlo for hierarchical models. Betancourt, MJ; Girolami, M. http://dx.doi.org/10.48550/arXiv.1312.0906.

Bischel, HN; Macmanus-Spencer, LA; Luthy, RG. (2010). Noncovalent Interactions of Long-Chain Perfluoroalkyl Acids with Serum Albumin. Environ Sci Technol 44: 5263-5269. http://dx.doi.org/10.1021/es101334s.

Bjerregaard-Olesen, C; Bach, CC; Long, M; Ghisari, M; Bech, BH; Nohr, EA; Henriksen, TB; Olsen, J; Bonefeld-Jørgensen, EC. (2016). Determinants of serum levels of perfluorinated alkyl acids in Danish pregnant women. Int J Hyg Environ Health 219: 867-875. http://dx.doi.org/10.1016/j.ijheh.2016.07.008.

Bjerregaard-Olesen, C; Bach, CC; Long, M; Wielsøe, M; Bech, BH; Henriksen, TB; Olsen, J; Bonefeld-Jørgensen, EC. (2019). Associations of Fetal Growth Outcomes with Measures of the Combined Xenoestrogenic Activity of Maternal Serum Perfluorinated Alkyl Acids in Danish Pregnant Women. Environ Health Perspect 127: 17006. http://dx.doi.org/10.1289/EHP1884.

Blomberg, A; Mortensen, J; Weihe, P; Grandjean, P. (2022). Bone mass density following developmental exposures to perfluoroalkyl substances (PFAS): a longitudinal cohort study. Environ Health 21: 113. http://dx.doi.org/10.1186/s12940-022-00929-w.

Bonefeld-Jørgensen, EC. (2022). RE: Hjermitslev et al. Persistent organic pollutants in Greenlandic pregnant women and indices of foetal growth: The ACCEPT study. Available online at (accessed

Borenstein, M; Hedges, LV; Higgins, JPT; Rothstein, HR. (2009). Introduction to meta-analysis. Chichester, UK: John Wiley & Sons.

Borghese, MM; Liang, CL; Owen, J; Fisher, M. (2022). Individual and mixture associations of perfluoroalkyl substances on liver function biomarkers in the Canadian Health Measures Survey. Environ Health 21: 85. http://dx.doi.org/10.1186/s12940-022-00892-6.

Brantsæter, AL; Whitworth, KW; Ydersbond, TA; Haug, LS; Haugen, M; Knutsen, HK; Thomsen, C; Meltzer, HM; Becher, G; Sabaredzovic, A; Hoppin, JA; Eggesbø, M; Longnecker, MP. (2013). Determinants of plasma concentrations of perfluoroalkyl substances in pregnant Norwegian women. Environ Int 54: 74-84. http://dx.doi.org/10.1016/j.envint.2012.12.014.

Brosset, E; Ngueta, G. (2022). Exposure to per- and polyfluoroalkyl substances and glycemic control in older US adults with type 2 diabetes mellitus. Environ Res 216: 114697. http://dx.doi.org/10.1016/j.envres.2022.114697.

Buck Louis, GM; Sundaram, R; Schisterman, EF; Sweeney, AM; Lynch, CD; Gore-Langton, RE; Maisog, J; Kim, S; Chen, Z; Barr, DB. (2013). Persistent environmental pollutants and couple fecundity: The LIFE study. Environ Health Perspect 121: 231-236. http://dx.doi.org/10.1289/ehp.1205301.

Buck Louis, GM; Zhai, S; Smarr, MM; Grewal, J; Zhang, C; Grantz, KL; Hinkle, SN; Sundaram, R; Lee, S; Honda, M; Oh, J; Kannan, K. (2018). Endocrine disruptors and neonatal anthropometry, NICHD Fetal Growth Studies - Singletons. Environ Int 119: 515-526. http://dx.doi.org/10.1016/j.envint.2018.07.024.

Budtz-Jørgensen, E; Grandjean, P. (2018a). Application of benchmark analysis for mixed contaminant exposures: Mutual adjustment of perfluoroalkylate substances associated with immunotoxicity. PLoS ONE 13: e0205388. http://dx.doi.org/10.1371/journal.pone.0205388.

Budtz-Jørgensen, E; Grandjean, P. (2018b). Computational details for the paper "Application of benchmark analysis for mixed contaminant exposures: Mutual adjustment of perfluoroalkylate substances associated with immunotoxicity".

Callan, AC; Rotander, A; Thompson, K; Heyworth, J; Mueller, JF; Odland, JØ; Hinwood, AL. (2016). Maternal exposure to perfluoroalkyl acids measured in whole blood and birth outcomes in offspring. Sci Total Environ 569-570: 1107-1113. http://dx.doi.org/10.1016/j.scitotenv.2016.06.177.

Cao, W; Liu, X; Liu, X; Zhou, Y; Zhang, X; Tian, H; Wang, J; Feng, S; Wu, Y; Bhatti, P; Wen, S; Sun, X. (2018). Perfluoroalkyl substances in umbilical cord serum and gestational and postnatal growth in a Chinese birth cohort. Environ Int 116: 197-205. http://dx.doi.org/10.1016/j.envint.2018.04.015.

Cardenas, A; Hauser, R; Gold, DR; Kleinman, KP; Hivert, MF; Fleisch, AF; Lin, PD; Calafat, AM; Webster, TF; Horton, ES; Oken, E. (2018). Association of perfluoroalkyl and polyfluoroalkyl substances with adiposity. JAMA Netw Open 1: e181493. http://dx.doi.org/10.1001/jamanetworkopen.2018.1493.

Cardenas, A; Hivert, MF; Gold, DR; Hauser, R; Kleinman, KP; Lin, PD; Fleisch, AF; Calafat, AM; Ye, X; Webster, TF; Horton, ES; Oken, E. (2019). Associations of perfluoroalkyl and polyfluoroalkyl substances with incident diabetes and microvascular disease. Diabetes Care 42: 1824-1832. http://dx.doi.org/10.2337/dc18-2254.

Cariou, R; Veyrand, B; Yamada, A; Berrebi, A; Zalko, D; Durand, S; Pollono, C; Marchand, P; Leblanc, JC; Antignac, JP; Le Bizec, B. (2015). Perfluoroalkyl acid (PFAA) levels and profiles in breast milk, maternal and cord serum of French women and their newborns. Environ Int 84: 71-81. http://dx.doi.org/10.1016/j.envint.2015.07.014.

Cellesi, C; Michelangeli, C; Rossolini, GM; Giovannoni, F; Rossolini, A. (1989). Immunity to diphtheria, six to 15 years after a basic three-dose immunization schedule. Journal of Biological Standardization 17: 29-34. http://dx.doi.org/10.1016/0092-1157(89)90025-5.

Chang, CJ; Barr, DB; Ryan, PB; Panuwet, P; Smarr, MM; Liu, K; Kannan, K; Yakimavets, V; Tan, Y; Ly, V; Marsit, CJ; Jones, DP; Corwin, EJ; Dunlop, AL; Liang, D. (2022). Per- and polyfluoroalkyl substance (PFAS) exposure, maternal metabolomic perturbation, and fetal growth in African American women: A meet-in-the-middle approach. Environ Int 158: 106964. http://dx.doi.org/10.1016/j.envint.2021.106964.

Chang, CJ; Ryan, PB; Smarr, MM; Kannan, K; Panuwet, P; Dunlop, AL; Corwin, EJ; Barr, DB. (2020). Serum per- and polyfluoroalkyl substance (PFAS) concentrations and predictors of exposure among pregnant African American women in the Atlanta area, Georgia. Environ Res 198: 110445. http://dx.doi.org/10.1016/j.envres.2020.110445.

Chapman, AB; Abraham, WT; Zamudio, S; Coffin, C; Merouani, A; Young, D; Johnson, A; Osorio, F; Goldberg, C; Moore, LG; Dahms, T; Schrier, RW. (1998). Temporal relationships between hormonal and hemodynamic changes in early human pregnancy. Kidney Int 54: 2056-2063. http://dx.doi.org/10.1046/j.1523-1755.1998.00217.x.

Chen, L; Tong, C; Huo, X; Zhang, J; Tian, Y. (2021). Prenatal exposure to perfluoroalkyl and polyfluoroalkyl substances and birth outcomes: A longitudinal cohort with repeated measurements. Chemosphere 267: 128899. http://dx.doi.org/10.1016/j.chemosphere.2020.128899.

Chen, MH; Ha, EH; Wen, TW; Su, YN; Lien, GW; Chen, CY; Chen, PC; Hsieh, WS. (2012). Perfluorinated compounds in umbilical cord blood and adverse birth outcomes. PLoS ONE 7: e42474. http://dx.doi.org/10.1371/journal.pone.0042474.

Chiu, WA; Lynch, MT; Lay, CR; Antezana, A; Malek, P; Sokolinski, S; Rogers, RD. (2022). Bayesian estimation of human population toxicokinetics of PFOA, PFOS, PFHxS, and PFNA from studies of contaminated drinking water. Environ Health Perspect 130: 127001. http://dx.doi.org/10.1289/EHP10103.

Christensen, KY; Raymond, MR; Thompson, BA; Anderson, HA. (2016). Fish consumption, levels of nutrients and contaminants, and endocrine-related health outcomes among older male

anglers in Wisconsin. J Occup Environ Med 58: 668-675. http://dx.doi.org/10.1097/JOM.0000000000000758.

Christenson, B; Böttiger, M. (1986). Serological immunity to diphtheria in Sweden in 1978 and 1984. Scand J Infect Dis 18: 227-233. http://dx.doi.org/10.3109/00365548609032331.

Cohen, NJ; Yao, M; Midya, V; India-Aldana, S; Mouzica, T; Andra, SS; Narasimhan, S; Meher, AK; Arora, M; Chan, JKY; Chan, SY; Loy, SL; Minguez-Alarcon, L; Oulhote, Y; Huang, J; Valvi, D. (2023). Exposure to perfluoroalkyl substances and women's fertility outcomes in a Singaporean population-based preconception cohort. Sci Total Environ 873: 162267. http://dx.doi.org/10.1016/j.scitotenv.2023.162267.

Colicino, E; Pedretti, NF; Busgang, SA; Gennings, C. (2020). Per- and poly-fluoroalkyl substances and bone mineral density: Results from the Bayesian weighted quantile sum regression. Environmental Epidemiology 4: 1. http://dx.doi.org/10.1097/EE9.0000000000000092.

Colles, A; Bruckers, L; Den Hond, E; Govarts, E; Morrens, B; Schettgen, T; Buekers, J; Coertjens, D; Nawrot, T; Loots, I; Nelen, V; De Henauw, S; Schoeters, G; Baeyens, W; van Larebeke, N. (2020). Perfluorinated substances in the Flemish population (Belgium): Levels and determinants of variability in exposure. Chemosphere 242: 125250. http://dx.doi.org/10.1016/j.chemosphere.2019.125250.

Collier, RJ. (1975). Diphtheria toxin: Mode of action and structure [Review]. Bacteriol Rev 39: 54-85. http://dx.doi.org/10.1128/br.39.1.54-85.1975.

Cui, F; Liu, H; Li, Y; Zheng, TZ; Xu, S; Xia, W; Sheng, X. (2022). Association of exposure to per- and polyfluoroalkyl substances with hemoglobin and hematocrit during pregnancy. Ecotoxicol Environ Saf 248: 114319. http://dx.doi.org/10.1016/j.ecoenv.2022.114319.

Das, KP; Grey, BE; Rosen, MB; Wood, CR; Tatum-Gibbs, KR; Zehr, RD; Strynar, MJ; Lindstrom, AB; Lau, C. (2015). Developmental toxicity of perfluorononanoic acid in mice. Reprod Toxicol 51: 133-144. http://dx.doi.org/10.1016/j.reprotox.2014.12.012.

Davies, B; Morris, T. (1993). Physiological parameters in laboratory animals and humans [Review]. Pharm Res 10: 1093-1095. http://dx.doi.org/10.1023/A:1018943613122.

Derakhshan, A; Kortenkamp, A; Shu, H; Broeren, MAC; Lindh, CH; Peeters, RP; Bornehag, CG; Demeneix, B; Korevaar, TIM. (2022). Association of per- and polyfluoroalkyl substances with thyroid homeostasis during pregnancy in the SELMA study. Environ Int 167: 107420. http://dx.doi.org/10.1016/j.envint.2022.107420.

Ding, N; Harlow, SD; Randolph, JF; Calafat, AM; Mukherjee, B; Batterman, S; Gold, EB; Park, SK. (2020). Associations of perfluoroalkyl substances with incident natural menopause: The study of women's health across the nation. J Clin Endocrinol Metab 105: E3169-E3182. http://dx.doi.org/10.1210/clinem/dgaa303.

Ding, N; Karvonen-Gutierrez, CA; Mukherjee, B; Calafat, AM; Harlow, SD; Park, SK. (2022). Per- and Polyfluoroalkyl Substances and Incident Hypertension in Multi-Racial/Ethnic Women: The Study of Women's Health Across the Nation. Hypertension 79: 101161HYPERTENSIONAHA12118809. http://dx.doi.org/10.1161/HYPERTENSIONAHA.121.18809.

Donat-Vargas, C; Bergdahl, IA; Tornevi, A; Wennberg, M; Sommar, J; Kiviranta, H; Koponen, J; Rolandsson, O; Åkesson, A. (2019a). Perfluoroalkyl substances and risk of type II diabetes: A prospective nested case-control study. Environ Int 123: 390-398. http://dx.doi.org/10.1016/j.envint.2018.12.026.

Donat-Vargas, C; Bergdahl, IA; Tornevi, A; Wennberg, M; Sommar, J; Koponen, J; Kiviranta, H; Åkesson, A. (2019b). Associations between repeated measure of plasma perfluoroalkyl substances and cardiometabolic risk factors. Environ Int 124: 58-65. http://dx.doi.org/10.1016/j.envint.2019.01.007.

Dufour, DR; Lott, JA; Nolte, FS; Gretch, DR; Koff, RS; Seeff, LB. (2000). Diagnosis and monitoring of hepatic injury. I. Performance characteristics of laboratory tests [Review]. Clin Chem 46: 2027-2049.

Dufour, P; Pirard, C; Petrossians, P; Beckers, A; Charlier, C. (2020). Association between mixture of persistent organic pollutants and thyroid pathologies in a Belgian population. Environ Res 181: 108922. http://dx.doi.org/10.1016/j.envres.2019.108922.

Dunder, L; Salihovic, S; Elmståhl, S; Lind, PM; Lind, L. (2023). Associations between per- and polyfluoroalkyl substances (PFAS) and diabetes in two population-based cohort studies from Sweden. J Expo Sci Environ Epidemiol. http://dx.doi.org/10.1038/s41370-023-00529-x.

Dzierlenga, M, .W.; Crawford, L, .; Longnecker, M, .P. (2020). Birth weight and perfluorooctane sulfonic acid: a random-effects meta-regression analysis. Environmental Epidemiology 4: e095. http://dx.doi.org/10.1097/EE9.0000000000000095.

E, L; Zhang, S; Jiang, X. (2023). Association between perfluoroalkyl substances exposure and the prevalence of nonalcoholic fatty liver disease in the different sexes: a study from the National Health and Nutrition Examination Survey 2005-2018. Environ Sci Pollut Res Int 30: 44292-44303. http://dx.doi.org/10.1007/s11356-023-25258-4.

Eick, SM; Demicco, E; Valeri, L; Woodruff, TJ; Morello-Frosch, R; Hom Thepaksorn, EK; Izano, MA; Cushing, LJ; Wang, Y; Smith, SC; Gao, S; Park, JS; Padula, AM. (2020). Associations between prenatal maternal exposure to per- and polyfluoroalkyl substances (PFAS) and polybrominated diphenyl ethers (PBDEs) and birth outcomes among pregnant women in San Francisco. Environ Health 19: 100-100. http://dx.doi.org/10.1186/s12940-020-00654-2.

Eick, SM; Enright, EA; Geiger, SD; Dzwilewski, KLC; DeMicco, E; Smith, S; Park, JS; Aguiar, S; Woodruff, TJ; Morello-Frosch, R; Schantz, SL. (2021). Associations of maternal stress, prenatal exposure to per- and polyfluoroalkyl substances (PFAS), and demographic risk factors with birth outcomes and offspring neurodevelopment: An overview of the ECO.CA.IL prospective birth cohorts [Review]. Int J Environ Res Public Health 18: 742. http://dx.doi.org/10.3390/ijerph18020742.

Fan, S; Wu, Y; Bloom, MS; Lv, J; Chen, L; Wang, W; Li, Z; Jiang, Q; Bu, L; Shi, J; Shi, T; Zeng, X; Zhang, L; Zhang, Z; Yang, B; Dong, G; Feng, W. (2023). Associations of per- and polyfluoroalkyl substances and their alternatives with bone mineral density levels and osteoporosis prevalence: A community-based population study in Guangzhou, Southern China. Sci Total Environ 862: 160617-160617. http://dx.doi.org/10.1016/j.scitotenv.2022.160617.

Fan, Y; Lu, C; Li, X; Xu, Q; Zhang, Y; Yang, X; Han, X; Du, G; Xia, Y; Wang, X. (2020). Serum albumin mediates the effect of multiple per- and polyfluoroalkyl substances on serum lipid levels. Environ Pollut 266 Pt 2: 115138. http://dx.doi.org/10.1016/j.envpol.2020.115138.

Fassler, CS; Pinney, SE; Xie, C; Biro, FM; Pinney, SM. (2019). Complex relationships between perfluorooctanoate, body mass index, insulin resistance and serum lipids in young girls. Environ Res 176: 108558. http://dx.doi.org/10.1016/j.envres.2019.108558.

Feng, X; Long, G; Zeng, G; Zhang, Q; Song, B; Wu, KH. (2022a). Association of increased risk of cardiovascular diseases with higher levels of perfluoroalkylated substances in the serum of adults. Environ Sci Pollut Res Int 29: 89081-89092. http://dx.doi.org/10.1007/s11356-022-22021-z.

Feng, Y; Bai, Y; Lu, Y; Chen, M; Fu, M; Guan, X; Cao, Q; Yuan, F; Jie, J; Li, M; Meng, H; Wang, C; Hong, S; Zhou, Y; Zhang, X; He, M; Guo, H. (2022b). Plasma perfluoroalkyl substance exposure and incidence risk of breast cancer: A case-cohort study in the Dongfeng-Tongji cohort. Environ Pollut 306: 119345. http://dx.doi.org/10.1016/j.envpol.2022.119345.

Feng, Y; Fu, M; Guan, X; Wang, C; Meng, H; Zhou, Y; He, M; Guo, H. (2022c). Associations of exposure to perfluoroalkyl substances with serum uric acid change and hyperuricemia among

Chinese women: Results from a longitudinal study. Chemosphere 308: 136438. http://dx.doi.org/10.1016/j.chemosphere.2022.136438.

Forsthuber, M; Kaiser, AM; Granitzer, S; Hassl, I; Hengstschläger, M; Stangl, H; Gundacker, C. (2020). Albumin is the major carrier protein for PFOS, PFOA, PFHxS, PFNA and PFDA in human plasma. Environ Int 137: 105324. http://dx.doi.org/10.1016/j.envint.2019.105324.

Fujii, Y; Niisoe, T; Harada, KH; Uemoto, S; Ogura, Y; Takenaka, K; Koizumi, A. (2015). Toxicokinetics of perfluoroalkyl carboxylic acids with different carbon chain lengths in mice and humans. J Occup Health 57: 1-12. http://dx.doi.org/10.1539/joh.14-0136-OA.

Galazka, A; Kardymowicz, B. (1989). Immunity against diphtheria in adults in Poland. Epidemiol Infect 103: 587-593. http://dx.doi.org/10.1017/s0950268800030983.

Galazka, AM; Milstien, JB; Robertson, SE; Cutts, FT. (1993). The immunological basis for immunization module 2 : Diphtheria. (WHO/EPI/Gen/93.11-18). Galazka, AM; Milstien, JB; Robertson, SE; Cutts, FT. http://apps.who.int/iris/bitstream/handle/10665/58891/WHO-EPI-GEN-93.12-mod2-eng.pdf?sequence=38&isAllowed=y.

Gao, B; He, X; Liu, W; Zhang, H; Saito, N; Tsuda, S. (2015). Distribution of perfluoroalkyl compounds in rats: Indication for using hair as bioindicator of exposure. J Expo Sci Environ Epidemiol 25: 632-638. http://dx.doi.org/10.1038/jes.2014.54.

Gao, Y; Luo, J; Zhang, Y; Pan, C; Ren, Y; Zhang, J; Tian, Y; Cohort, SB. (2022). Prenatal Exposure to Per- and Polyfluoroalkyl Substances and Child Growth Trajectories in the First Two Years. Environ Health Perspect 130: 37006. http://dx.doi.org/10.1289/EHP9875.

Gaylord, A; Berger, KI; Naidu, M; Attina, TM; Gilbert, J; Koshy, TT; Han, X; Marmor, M; Shao, Y; Giusti, R; Goldring, RM; Kannan, K; Trasande, L. (2019). Serum perfluoroalkyl substances and lung function in adolescents exposed to the World Trade Center disaster. Environ Res 172: 266-272. http://dx.doi.org/10.1016/j.envres.2019.02.024.

Gaylord, A; Trasande, L; Kannan, K; Thomas, KM; Lee, S; Liu, M; Levine, J. (2020). Persistent organic pollutant exposure and celiac disease: A pilot study. Environ Res 186: 109439. http://dx.doi.org/10.1016/j.envres.2020.109439.

Gibson, H, .M. (1973). Plasma volume and glomerular filtration rate in pregnancy and their relation to differences in fetal growth. Br J Obstet Gynaecol 80: 1067-1074. http://dx.doi.org/10.1111/j.1471-0528.1973.tb02981.x.

Glynn, A; Berger, U; Bignert, A; Ullah, S; Aune, M; Lignell, S; Darnerud, PO. (2012). Perfluorinated alkyl acids in blood serum from primiparous women in Sweden: serial sampling during pregnancy and nursing, and temporal trends 1996-2010. Environ Sci Technol 46: 9071-9079. http://dx.doi.org/10.1021/es301168c.

Goodrich, JA; Walker, D; Lin, X; Wang, H; Lim, T; McConnell, R; Conti, DV; Chatzi, L; Setiawan, VW. (2022). Exposure to perfluoroalkyl substances and risk of hepatocellular carcinoma in a multiethnic cohort. JHEP Rep 4: 100550. http://dx.doi.org/10.1016/j.jhepr.2022.100550.

Gowda, S; Desai, PB; Hull, VV; Math, AAK; Vernekar, SN; Kulkarni, SS. (2009). A review on laboratory liver function tests. Pan African Medical Journal 3: 17.

Grandjean, P; Andersen, EW; Budtz-Jørgensen, E; Nielsen, F; Mølbak, K; Weihe, P; Heilmann, C. (2012). Serum vaccine antibody concentrations in children exposed to perfluorinated compounds. JAMA 307: 391-397. http://dx.doi.org/10.1001/jama.2011.2034.

Grandjean, P; Heilmann, C; Weihe, P; Nielsen, F; Mogensen, UB; Timmermann, A; Budtz-Jørgensen, E. (2017). Estimated exposures to perfluorinated compounds in infancy predict attenuated vaccine antibody concentrations at age 5-years. J Immunotoxicol 14: 188-195. http://dx.doi.org/10.1080/1547691X.2017.1360968.

Guo, J; Huang, S; Yang, L; Zhou, J; Xu, X; Lin, S; Li, H; Xie, X; Wu, S. (2023). Association between polyfluoroalkyl substances exposure and sex steroids in adolescents: The mediating role of serum albumin. Ecotoxicol Environ Saf 253: 114687. http://dx.doi.org/10.1016/j.ecoenv.2023.114687.

Gutzkow, KB; Haug, LS; Thomsen, C; Sabaredzovic, A; Becher, G; Brunborg, G. (2012). Placental transfer of perfluorinated compounds is selective - A Norwegian Mother and Child sub-cohort study. Int J Hyg Environ Health 215: 216-219. http://dx.doi.org/10.1016/j.ijheh.2011.08.011.

Gyllenhammar, I; Diderholm, B; Gustafsson, J; Berger, U; Ridefelt, P; Benskin, JP; Lignell, S; Lampa, E; Glynn, A. (2018). Perfluoroalkyl acid levels in first-time mothers in relation to offspring weight gain and growth. Environ Int 111: 191-199. http://dx.doi.org/10.1016/j.envint.2017.12.002.

Hack, M; Klein, NK; Taylor, HG. (1995). Long-term developmental outcomes of low birth weight infants [Review]. Future Child 5: 176-196. http://dx.doi.org/10.2307/1602514.

Hall, AP; Elcombe, CR; Foster, JR; Harada, T; Kaufmann, W; Knippel, A; Küttler, K; Malarkey, DE; Maronpot, RR; Nishikawa, A; Nolte, T; Schulte, A; Strauss, V; York, MJ. (2012). Liver hypertrophy: A review of adaptive (adverse and non-adverse) changes—Conclusions from the 3rd International ESTP Expert Workshop [Review]. Toxicol Pathol 40: 971-994. http://dx.doi.org/10.1177/0192623312448935.

Hall, SM; Zhang, S; Hoffman, K; Miranda, ML; Stapleton, HM. (2022). Concentrations of per- and polyfluoroalkyl substances (PFAS) in human placental tissues and associations with birth outcomes. Chemosphere 295: 133873. http://dx.doi.org/10.1016/j.chemosphere.2022.133873.

Han, W; Gao, Y; Yao, Q; Yuan, T; Wang, Y; Zhao, S; Shi, R; Bonefeld-Jorgensen, EC; Shen, X; Tian, Y. (2018). Perfluoroalkyl and polyfluoroalkyl substances in matched parental and cord serum in Shandong, China. Environ Int 116: 206-213. http://dx.doi.org/10.1016/j.envint.2018.04.025.

Hanssen, L; Dudarev, AA; Huber, S; Odland, JØ; Nieboer, E; Sandanger, TM. (2013). Partition of perfluoroalkyl substances (PFASs) in whole blood and plasma, assessed in maternal and umbilical cord samples from inhabitants of arctic Russia and Uzbekistan. Sci Total Environ 447: 430-437. http://dx.doi.org/10.1016/j.scitotenv.2013.01.029.

Harris, MH; Rifas-Shiman, SL; Calafat, AM; Ye, X; Mora, AM; Webster, TF; Oken, E; Sagiv, SK. (2017). Predictors of per- and polyfluoroalkyl substance (PFAS) plasma concentrations in 6-10 year old American children. Environ Sci Technol 51: 5193-5204. http://dx.doi.org/10.1021/acs.est.6b05811.

Higgins, JPT; Thomas, J; Chandler, J; Cumpston, M; Li, T; Page, MJ; Welch, VA. (2022). Cochrane handbook for systematic reviews of interventions version 6.3. Higgins, JPT; Thomas, J; Chandler, J; Cumpston, M; Li, T; Page, MJ; Welch, VA. http://www.training.cochrane.org/handbook.

Hjermitslev, MH; Long, M; Wielsøe, M; Bonefeld-Jørgensen, EC. (2020). Persistent organic pollutants in Greenlandic pregnant women and indices of foetal growth: The ACCEPT study. Sci Total Environ 698: 134118. http://dx.doi.org/10.1016/j.scitotenv.2019.134118.

Højsager, FD; Andersen, M; Juul, A; Nielsen, F; Möller, S; Christensen, HT; Grøntved, A; Grandjean, P; Jensen, TK. (2022). Prenatal and early postnatal exposure to perfluoroalkyl substances and bone mineral content and density in the Odense child cohort. Environ Int 167: 107417. http://dx.doi.org/10.1016/j.envint.2022.107417.

Hong, A; Zhuang, L; Cui, W; Lu, Q; Yang, P; Su, S; Wang, B; Zhang, G; Chen, D. (2022). Per- and polyfluoroalkyl substances (PFAS) exposure in women seeking in vitro fertilization-embryo transfer treatment (IVF-ET) in China: Blood-follicular transfer and associations with IVF-ET outcomes. Sci Total Environ 838: 156323. http://dx.doi.org/10.1016/j.scitotenv.2022.156323.

Huang, H; Wang, Q; He, X; Wu, Y; Xu, C. (2019). Association between polyfluoroalkyl chemical concentrations and leucocyte telomere length in US adults. Sci Total Environ 653: 547-553. http://dx.doi.org/10.1016/j.scitotenv.2018.10.400.

Huang, H; Yu, K; Zeng, X; Chen, Q; Liu, Q; Zhao, Y; Zhang, J; Zhang, X; Huang, L. (2020). Association between prenatal exposure to perfluoroalkyl substances and respiratory tract infections in preschool children. Environ Res 191: 110156. http://dx.doi.org/10.1016/j.envres.2020.110156.

Huedo-Medina, TB; Sánchez-Meca, J; Marín-Martínez, F; Botella, J. (2006). Assessing heterogeneity in meta-analysis: Q statistic or I2 index? Psychol Methods 11: 193-206. http://dx.doi.org/10.1037/1082-989X.11.2.193.

Huo, X; Huang, R; Gan, Y; Luo, K; Aimuzi, R; Nian, M; Ao, J; Feng, L; Tian, Y; Wang, W; Ye, W; Zhang, J. (2020). Perfluoroalkyl substances in early pregnancy and risk of hypertensive disorders of pregnancy: A prospective cohort study. Environ Int 138: 105656. http://dx.doi.org/10.1016/j.envint.2020.105656.

Hutcheson, R; Innes, K; Conway, B. (2020). Perfluoroalkyl substances and likelihood of stroke in persons with and without diabetes. Diab Vasc Dis Res 17: 1-8. http://dx.doi.org/10.1177/1479164119892223.

Infusino I, M, auro P. (2009). Standardization in clinical enzymology. EJIFCC 20: 141-147.

Ipsen, J. (1946). Circulating antitoxin at the onset of diphtheria in 425 patients. J Immunol 54: 325-347.

Iwabuchi, K; Senzaki, N; Mazawa, D; Sato, I; Hara, M; Ueda, F; Liu, W; Tsuda, S. (2017). Tissue toxicokinetics of perfluoro compounds with single and chronic low doses in male rats. J Toxicol Sci 42: 301-317. http://dx.doi.org/10.2131/jts.42.301.

Jain, RB. (2014). Contribution of diet and other factors to the levels of selected polyfluorinated compounds: data from NHANES 2003-2008. Int J Hyg Environ Health 217: 52-61. http://dx.doi.org/10.1016/j.ijheh.2013.03.008.

Jain, RB; Ducatman, A. (2019). Perfluoroalkyl acids and thyroid hormones across stages of kidney function. Sci Total Environ 696: 133994. http://dx.doi.org/10.1016/j.scitotenv.2019.133994.

Jain, RB; Ducatman, A. (2022). Serum concentrations of selected perfluoroalkyl substances for US females compared to males as they age. Sci Total Environ 842: 156891. http://dx.doi.org/10.1016/j.scitotenv.2022.156891.

Jensen, RC; Glintborg, D; Timmermann, CAG; Nielsen, F; Boye, H; Madsen, JB; Bilenberg, N; Grandjean, P; Jensen, TK; Andersen, MS. (2022). Higher free thyroxine associated with PFAS exposure in first trimester. The Odense Child Cohort. Environ Res 212: 113492. http://dx.doi.org/10.1016/j.envres.2022.113492.

Ji, K; Kim, S; Kho, Y; Sakong, J; Paek, D; Choi, K. (2012). Major perfluoroalkyl acid (PFAA) concentrations and influence of food consumption among the general population of Daegu, Korea. Sci Total Environ 438: 42-48. http://dx.doi.org/10.1016/j.scitotenv.2012.08.007.

Jin, H; Zhang, Y; Jiang, W; Zhu, L; Martin, JW. (2016). Isomer-Specific Distribution of Perfluoroalkyl Substances in Blood. Environ Sci Technol 50: 7808-7815. http://dx.doi.org/10.1021/acs.est.6b01698.

Kapraun, D, ustin F.; Zurlinden, T, odd J.; Verner, M, arc-André; Chiang, C, atheryne; Dzierlenga, M, ichael W.; Carlson, L, aura M.; Schlosser, P, aul M.; Lehmann, G, eniece M. (2022). A generic pharmacokinetic model for quantifying mother-to-offspring transfer of lipophilic persistent environmental chemicals. Toxicol Sci 2022: kfac084. http://dx.doi.org/10.1093/toxsci/kfac084.

Kashino, I; Sasaki, S; Okada, E; Matsuura, H; Goudarzi, H; Miyashita, C; Okada, E; Ito, YM; Araki, A; Kishi, R. (2020). Prenatal exposure to 11 perfluoroalkyl substances and fetal growth: A large-scale, prospective birth cohort study. Environ Int 136: 105355. http://dx.doi.org/10.1016/j.envint.2019.105355.

Kato, K; Wong, LY; Chen, A; Dunbar, C; Webster, GM; Lanphear, BP; Calafat, AM. (2014). Changes in serum concentrations of maternal poly- and perfluoroalkyl substances over the course of

pregnancy and predictors of exposure in a multiethnic cohort of Cincinnati, Ohio pregnant women during 2003-2006. Environ Sci Technol 48: 9600-9608. http://dx.doi.org/10.1021/es501811k.

Kaur, K; Lesseur, C; Chen, L; Andra, SS; Narasimhan, S; Pulivarthi, D; Midya, V; Ma, Y; Ibroci, E; Gigase, F; Lieber, M; Lieb, W; Janevic, T; De Witte, LD; Bergink, V; Rommel, AS; Chen, J. (2023). Cross-sectional associations of maternal PFAS exposure on SARS-CoV-2 IgG antibody levels during pregnancy. Environ Res 219: 115067. http://dx.doi.org/10.1016/j.envres.2022.115067.

Kavlock, RJ; Allen, BC; Faustman, EM; Kimmel, CA. (1995). Dose-response assessments for developmental toxicity. IV. Benchmark doses for fetal weight changes. Toxicol Sci 26: 211-222. http://dx.doi.org/10.1006/faat.1995.1092.

Kim, JH; Park, HY; Jeon, JD; Kho, Y; Kim, SK; Park, MS; Hong, YC. (2015). The modifying effect of vitamin C on the association between perfluorinated compounds and insulin resistance in the Korean elderly: a double-blind, randomized, placebo-controlled crossover trial. Eur J Nutr 55: 1011-1020. http://dx.doi.org/10.1007/s00394-015-0915-0.

Kim, JI; Kim, BN; Lee, YA; Shin, CH; Hong, YC; Døssing, LD; Hildebrandt, G; Lim, YH. (2023a). Association between early-childhood exposure to perfluoroalkyl substances and ADHD symptoms: A prospective cohort study. Sci Total Environ 879: 163081. http://dx.doi.org/10.1016/j.scitotenv.2023.163081.

Kim, K; Bennett, DH; Calafat, AM; Hertz-Picciotto, I; Shin, HM. (2020). Temporal trends and determinants of serum concentrations of per- and polyfluoroalkyl substances among Northern California mothers with a young child, 2009-2016. Environ Res 186: 109491. http://dx.doi.org/10.1016/j.envres.2020.109491.

Kim, OJ; Kim, S; Park, EY; Oh, JK; Jung, SK; Park, S; Hong, S; Jeon, HL; Kim, HJ; Park, B; Park, B; Kim, S; Kim, B. (2023b). Exposure to serum perfluoroalkyl substances and biomarkers of liver function: The Korean national environmental health survey 2015-2017. Chemosphere 322: 138208. http://dx.doi.org/10.1016/j.chemosphere.2023.138208.

Kim, SJ; Choi, EJ; Choi, GW; Lee, YB; Cho, HY. (2019). Exploring sex differences in human health risk assessment for PFNA and PFDA using a PBPK model. Arch Toxicol 93: 311-330. http://dx.doi.org/10.1007/s00204-018-2365-y.

Kim, SK; Lee, KT; Kang, CS; Tao, L; Kannan, K; Kim, KR; Kim, CK; Lee, JS; Park, PS; Yoo, YW; Ha, JY; Shin, YS; Lee, JH. (2011). Distribution of perfluorochemicals between sera and milk from the same mothers and implications for prenatal and postnatal exposures. Environ Pollut 159: 169-174. http://dx.doi.org/10.1016/j.envpol.2010.09.008.

Kishi, R; Nakajima, T; Goudarzi, H; Kobayashi, S; Sasaki, S; Okada, E; Miyashita, C; Itoh, S; Araki, A; Ikeno, T; Iwasaki, Y; Nakazawa, H. (2015). The association of prenatal exposure to perfluorinated chemicals with maternal essential and long-chain polyunsaturated fatty acids during pregnancy and the birth weight of their offspring: the hokkaido study. Environ Health Perspect 123: 1038-1045. http://dx.doi.org/10.1289/ehp.1408834.

Kobayashi, S; Azumi, K; Goudarzi, H; Araki, A; Miyashita, C; Kobayashi, S; Itoh, S; Sasaki, S; Ishizuka, M; Nakazawa, H; Ikeno, T; Kishi, R. (2017). Effects of prenatal perfluoroalkyl acid exposure on cord blood IGF2/H19 methylation and ponderal index: The Hokkaido Study. J Expo Sci Environ Epidemiol 27: 251-259. http://dx.doi.org/10.1038/jes.2016.50.

Koponen, J; Winkens, K; Airaksinen, R; Berger, U; Vestergren, R; Cousins, IT; Karvonen, AM; Pekkanen, J; Kiviranta, H. (2018). Longitudinal trends of per- and polyfluoroalkyl substances in children's serum. Environ Int 121: 591-599. http://dx.doi.org/10.1016/j.envint.2018.09.006.

Kruschke, JK. (2021). Bayesian analysis reporting guidelines. Nat Hum Behav 5: 1282-1291. http://dx.doi.org/10.1038/s41562-021-01177-7.

Kwon, EJ; Shin, JS; Kim, BM; Shah-Kulkarni, S; Park, H; Kho, YL; Park, EA; Kim, YJ; Ha, EH. (2016). Prenatal exposure to perfluorinated compounds affects birth weight through GSTM1 polymorphism. J Occup Environ Med 58: e198-e205. http://dx.doi.org/10.1097/JOM.0000000000000739.

Larsen, A. (2022). Meta-analysis of maternal serum PFNA effects on birth weight [Computer Program].

Leary, DB; Takazawa, M; Kannan, K; Khalil, N. (2020). Perfluoroalkyl substances and metabolic syndrome in firefighters a pilot study. J Occup Environ Med 62: 52-57. http://dx.doi.org/10.1097/JOM.0000000000001756.

Lee, E; Kinninger, A; Ursin, G; Tseng, C; Hurley, S; Wang, M; Wang, Y; Park, JS; Petreas, M; Deapen, D; Reynolds, P. (2020). Serum levels of commonly detected persistent organic pollutants and per- and polyfluoroalkyl substances (PFASs) and mammographic density in postmenopausal women. Int J Environ Res Public Health 17: 606. http://dx.doi.org/10.3390/ijerph17020606.

Lee, ES; Han, S; Oh, JE. (2016). Association between perfluorinated compound concentrations in cord serum and birth weight using multiple regression models. Reprod Toxicol 59: 53-59. http://dx.doi.org/10.1016/j.reprotox.2015.10.020.

Lenters, V; Portengen, L; Rignell-Hydbom, A; Jönsson, BA; Lindh, CH; Piersma, AH; Toft, G; Bonde, JP; Heederik, D; Rylander, L; Vermeulen, R. (2016). Prenatal phthalate, perfluoroalkyl acid, and organochlorine exposures and term birth weight in three birth cohorts: multi-pollutant models based on elastic net regression. Environ Health Perspect 124: 365-372. http://dx.doi.org/10.1289/ehp.1408933.

Li, A; Hou, J; Fu, J; Wang, Y; Hu, Y; Zhuang, T; Li, M; Song, M; Jiang, G. (2023a). Association between serum levels of TSH and free T4 and per- and polyfluoroalkyl compounds concentrations in pregnant women. J Environ Sci 124: 11-18. http://dx.doi.org/10.1016/j.jes.2021.10.026.

Li, H; Chen, J; Jingchao, L; Yang, J; Tan, Z; Li, L; Xiao, F; An, Z; Ma, C; Liu, Y; Wang, L; Zhang, X; Guo, H. (2023b). Association of exposure to perfluoroalkyl substances and risk of the acute coronary syndrome: A case-control study in Shijiazhuang Hebei Province. Chemosphere 313: 137464. http://dx.doi.org/10.1016/j.chemosphere.2022.137464.

Li, J; Cai, D; Chu, C; Li, QQ; Zhou, Y; Hu, LW; Yang, BY; Dong, GH; Zeng, XW; Chen, D. (2020a). Transplacental Transfer of Per- and Polyfluoroalkyl Substances (PFASs): Differences between Preterm and Full-Term Deliveries and Associations with Placental Transporter mRNA Expression. Environ Sci Technol 54: 5062-5070. http://dx.doi.org/10.1021/acs.est.0c00829.

Li, J; Yang, L; He, G; Wang, B; Miao, M; Ji, H; Wen, S; Cao, W; Yuan, W; Liang, H. (2022a). Association between prenatal exposure to perfluoroalkyl substances and anogenital distance in female neonates. Ecotoxicol Environ Saf 245: 114130. http://dx.doi.org/10.1016/j.ecoenv.2022.114130.

Li, J; Yao, J; Xia, W; Dai, J; Liu, H; Pan, Y; Xu, S; Lu, S; Jin, S; Li, Y; Sun, X; Zhang, B; Zheng, T; Jiang, Y; Jing, T. (2020b). Association between exposure to per- and polyfluoroalkyl substances and blood glucose in pregnant women. Int J Hyg Environ Health 230: 113596. http://dx.doi.org/10.1016/j.ijheh.2020.113596.

Li, M; Zeng, XW; Qian, ZM; Vaughn, MG; Sauvé, S; Paul, G; Lin, S; Lu, L; Hu, LW; Yang, BY; Zhou, Y; Qin, XD; Xu, SL; Bao, WW; Zhang, YZ; Yuan, P; Wang, J; Zhang, C; Tian, YP; Nian, M; Xiao, X; Fu, C; Dong, GH. (2017). Isomers of perfluorooctanesulfonate (PFOS) in cord serum and birth outcomes in China: Guangzhou Birth Cohort Study. Environ Int 102: 1-8. http://dx.doi.org/10.1016/j.envint.2017.03.006.

Li, QQ; Huang, J; Cai, D; Chou, WC; Zeeshan, M; Chu, C; Zhou, Y; Lin, L; Ma, HM; Tang, C; Kong, M; Xie, Y; Dong, GH; Zeng, XW. (2023c). Prenatal exposure to legacy and alternative per- and polyfluoroalkyl substances and neuropsychological development trajectories over the first

3 years of life. Environ Sci Technol 57: 3746-3757. http://dx.doi.org/10.1021/acs.est.2c07807.

Li, S; Cirillo, P; Hu, X; Tran, V; Krigbaum, N; Yu, S; Jones, DP; Cohn, B. (2019). Understanding mixed environmental exposures using metabolomics via a hierarchical community network model in a cohort of California women in 1960's. Reprod Toxicol 92: 57-65. http://dx.doi.org/10.1016/j.reprotox.2019.06.013.

Li, X; Song, F; Liu, X; Shan, A; Huang, Y; Yang, Z; Li, H; Yang, Q; Yu, Y; Zheng, H; Cao, XC; Chen, D; Chen, KX; Chen, X; Tang, NJ. (2022b). Perfluoroalkyl substances (PFASs) as risk factors for breast cancer: a case-control study in Chinese population. Environ Health 21: 83. http://dx.doi.org/10.1186/s12940-022-00895-3.

Liang, D. (2022). Re: [External] Chang et al study on PFAS and BWT. Available online at (accessed

Liang, JL; Tiwari, T; Moro, P; Messonnier, NE; Reingold, A; Sawyer, M; Clark, TA. (2018). Prevention of pertussis, tetanus, and diphtheria with vaccines in the United States: Recommendations of the Advisory Committee on Immunization Practices (ACIP). MMWR Recomm Rep 67: 1-44. http://dx.doi.org/10.15585/mmwr.rr6702a1.

Liang, Y; Zhou, H; Zhang, J; Li, S; Shen, W; Lei, L. (2023). Exposure to perfluoroalkyl and polyfluoroalkyl substances and estimated glomerular filtration rate in adults: a cross-sectional study based on NHANES (2017-2018). Environ Sci Pollut Res Int. http://dx.doi.org/10.1007/s11356-023-26384-9.

Liao, Q; Tang, P; Fan, H; Song, Y; Liang, J; Huang, H; Pan, D; Mo, M; Leilei; Lin, M; Chen, J; Wei, H; Long, J; Shao, Y; Zeng, X; Liu, S; Huang, D; Qiu, X. (2023). Association between maternal exposure to per- and polyfluoroalkyl substances and serum markers of liver function during pregnancy in China: A mixture-based approach. Environ Pollut 323: 121348. http://dx.doi.org/10.1016/j.envpol.2023.121348.

Liao, Q; Tang, P; Pan, D; Song, Y; Lei, L; Liang, J; Liu, B; Lin, M; Huang, H; Mo, M; Huang, C; Wei, M; Liu, S; Huang, D; Qiu, X. (2022a). Association of serum per- and polyfluoroalkyl substances and gestational anemia during different trimesters in Zhuang ethnic pregnancy women of Guangxi, China. Chemosphere 309: 136798. http://dx.doi.org/10.1016/j.chemosphere.2022.136798.

Liao, Q; Tang, P; Song, Y; Liu, B; Huang, H; Liang, J; Lin, M; Shao, Y; Liu, S; Pan, D; Huang, D; Qiu, X. (2022b). Association of single and multiple prefluoroalkyl substances exposure with preterm birth: Results from a Chinese birth cohort study. Chemosphere 307: 135741. http://dx.doi.org/10.1016/j.chemosphere.2022.135741.

Liew, Z; Luo, J; Nohr, EA; Bech, BH; Bossi, R; Arah, OA; Olsen, J. (2020). Maternal plasma perfluoroalkyl substances and miscarriage: a nested case-control study in the Danish National Birth Cohort. Environ Health Perspect 128: 47007. http://dx.doi.org/10.1289/EHP6202.

Limpert, E; Stahel, WA; Abbt, M. (2001). Log-normal Distributions across the Sciences: Keys and Clues: On the charms of statistics, and how mechanical models resembling gambling machines offer a link to a handy way to characterize log-normal distributions, which can provide deeper insight into variability and probability—normal or log-normal: That is the question. Bioscience 51: 341-352. http://dx.doi.org/10.1641/0006-3568(2001)051[0341:LNDATS]2.0.CO;2.

Lin, M; Liao, Q; Tang, P; Song, Y; Liang, J, un; Li, J; Mu, C; Liu, S; Qiu, X; Yi, R, ui; Pang, Q; Pan, D; Zeng, X; Huang, D. (2022). Association of maternal perfluoroalkyl substance exposure with postpartum haemorrhage in Guangxi, China. Ecotoxicol Environ Saf 245: 114078. http://dx.doi.org/10.1016/j.ecoenv.2022.114078.

Linakis, MW; Landingham, CW; Gasparini, A; Longnecker, MP. (2021). Re-expressing coefficients from regression models for inclusion in a meta-analysis. Linakis, MW; Landingham, CW; Gasparini, A; Longnecker, MP. http://dx.doi.org/10.1101/2021.11.02.466931.

Lind, DV; Priskorn, L; Lassen, TH; Nielsen, F; Kyhl, HB; Kristensen, DM; Christesen, HT; Jørgensen, JS; Grandjean, P; Jensen, TK. (2017). Prenatal exposure to perfluoroalkyl substances and anogenital distance at 3 months of age in a Danish mother-child cohort. Reprod Toxicol 68: 200-206. http://dx.doi.org/10.1016/j.reprotox.2016.08.019.

Lind, PM; Salihovic, S; Stubleski, J; Kärrman, A; Lind, L. (2018). Changes in plasma levels of perfluoroalkyl substances (PFASs) are related to increase in carotid intima-media thickness over 10 years - a longitudinal study. Environ Health 17: 59. http://dx.doi.org/10.1186/s12940-018-0403-0.

Liu, H; Pan, Y; Jin, S; Sun, X; Jiang, Y; Wang, Y; Ghassabian, A; Li, Y; Xia, W; Cui, Q; Zhang, B; Zhou, A; Dai, J; Xu, S. (2020a). Associations between six common per- and polyfluoroalkyl substances and estrogens in neonates of China. J Hazard Mater 407: 124378. http://dx.doi.org/10.1016/j.jhazmat.2020.124378.

Liu, J; Gao, X; Wang, Y; Leng, J; Li, J; Zhao, Y; Wu, Y. (2020b). Profiling of emerging and legacy per-/polyfluoroalkyl substances in serum among pregnant women in China. Environ Pollut 271: 116376. http://dx.doi.org/10.1016/j.envpol.2020.116376.

Liu, J; Li, J; Liu, Y; Chan, HM; Zhao, Y; Cai, Z; Wu, Y. (2011). Comparison on gestation and lactation exposure of perfluorinated compounds for newborns. Environ Int 37: 1206-1212. http://dx.doi.org/10.1016/j.envint.2011.05.001.

Liu, X; Zhang, L; Chen, L; Li, J; Wang, Y; Wang, J; Meng, G; Chi, M; Zhao, Y; Chen, H; Wu, Y. (2019). Structure-based investigation on the association between perfluoroalkyl acids exposure and both gestational diabetes mellitus and glucose homeostasis in pregnant women. Environ Int 127: 85-93. http://dx.doi.org/10.1016/j.envint.2019.03.035.

Liu, Y; Zhang, Z; Han, D; Zhao, Y; Yan, X; Cui, S. (2022). Association between environmental chemicals co-exposure and peripheral blood immune-inflammatory indicators. Front Public Health 10: 980987. http://dx.doi.org/10.3389/fpubh.2022.980987.

Luo, D; Wu, WX; Pan, YA; Du, BB; Shen, MJ; Zeng, LX. (2021). Associations of prenatal exposure to per- and polyfluoroalkyl substances with the neonatal birth size and hormones in the growth hormone/insulin-like growth factor axis. Environ Sci Technol 55: 11859-11873. http://dx.doi.org/10.1021/acs.est.1c02670.

Luo, F; Chen, Q; Yu, G; Huo, X; Wang, H; Nian, M; Tian, Y; Xu, J; Zhang, J; Zhang, J. (2022a). Exposure to perfluoroalkyl substances and neurodevelopment in 2-year-old children: A prospective cohort study. Environ Int 166: 107384. http://dx.doi.org/10.1016/j.envint.2022.107384.

Luo, K; Huang, W; Zhang, Q; Liu, X; Nian, M; Wei, M; Wang, Y; Chen, D; Chen, X; Zhang, J. (2022b). Environmental exposure to legacy poly/perfluoroalkyl substances, emerging alternatives and isomers and semen quality in men: A mixture analysis. Sci Total Environ 833: 155158. http://dx.doi.org/10.1016/j.scitotenv.2022.155158.

Luo, K; Liu, X; Zhou, W; Nian, M; Qiu, W; Yang, Y; Zhang, J. (2022c). Preconception exposure to perfluoroalkyl and polyfluoroalkyl substances and couple fecundity: A couple-based exploration. Environ Int 170: 107567. http://dx.doi.org/10.1016/j.envint.2022.107567.

Ma, S; Xu, C; Ma, J; Wang, Z; Zhang, Y; Shu, Y; Mo, X. (2019). Association between perfluoroalkyl substance concentrations and blood pressure in adolescents. Environ Pollut 254: 112971. http://dx.doi.org/10.1016/j.envpol.2019.112971.

Ma, X; Cui, L; Chen, L; Zhang, J; Zhang, X; Kang, Q; Jin, F; Ye, Y. (2021). Parental plasma concentrations of perfluoroalkyl substances and In Vitro fertilization outcomes. Environ Pollut 269: 116159. http://dx.doi.org/10.1016/j.envpol.2020.116159.

Maekawa, R; Ito, R; Iwasaki, Y; Saito, K; Akutsu, K; Takatori, S; Ishii, R; Kondo, F; Arai, Y; Ohgane, J; Shiota, K; Makino, T; Sugino, N. (2017). Evidence of exposure to chemicals and heavy metals during pregnancy in Japanese women. Reproductive Medicine and Biology 16: 337-348. http://dx.doi.org/10.1002/rmb2.12049.

Mamsen, LS; Björvang, RD; Mucs, D; Vinnars, MT; Papadogiannakis, N; Lindh, CH; Andersen, CY; Damdimopoulou, P. (2019). Concentrations of perfluoroalkyl substances (PFASs) in human embryonic and fetal organs from first, second, and third trimester pregnancies. Environ Int 124: 482-492. http://dx.doi.org/10.1016/j.envint.2019.01.010.

Mamsen, LS; Jönsson, BAG; Lindh, CH; Olesen, RH; Larsen, A; Ernst, E; Kelsey, TW; Andersen, CY. (2017). Concentration of perfluorinated compounds and cotinine in human foetal organs, placenta, and maternal plasma. Sci Total Environ 596-597: 97-105. http://dx.doi.org/10.1016/j.scitotenv.2017.04.058.

Manzano-Salgado, CB; Casas, M; Lopez-Espinosa, MJ; Ballester, F; Iñiguez, C; Martinez, D; Costa, O; Santa-Marina, L; Pereda-Pereda, E; Schettgen, T; Sunyer, J; Vrijheid, M. (2017). Prenatal exposure to perfluoroalkyl substances and birth outcomes in a Spanish birth cohort. Environ Int 108: 278-284. http://dx.doi.org/10.1016/j.envint.2017.09.006.

Maranhao Neto, GA; Polcrova, AB; Pospisilova, A; Blaha, L; Klanova, J; Bobak, M; Gonzalez-Rivas, JP. (2022). Associations between Per- and Polyfluoroalkyl Substances (PFAS) and Cardiometabolic Biomarkers in Adults of Czechia: The Kardiovize Study. Int J Environ Res Public Health 19: 13898. http://dx.doi.org/10.3390/ijerph192113898.

Marks, KJ; Cutler, AJ; Jeddy, Z; Northstone, K; Kato, K; Hartman, TJ. (2019). Maternal serum concentrations of perfluoroalkyl substances and birth size in British boys. Int J Hyg Environ Health 222: 889-895. http://dx.doi.org/10.1016/j.ijheh.2019.03.008.

Mehta, SS; Applebaum, KM; James-Todd, T; Coleman-Phox, K; Adler, N; Laraia, B; Epel, E; Parry, E; Wang, M; Park, JS; Zota, AR. (2020). Associations between sociodemographic characteristics and exposures to PBDEs, OH-PBDEs, PCBs, and PFASs in a diverse, overweight population of pregnant women. J Expo Sci Environ Epidemiol 30: 42-55. http://dx.doi.org/10.1038/s41370-019-0173-y.

Mehta, SS; James-Todd, T; Applebaum, KM; Bellavia, A; Coleman-Phox, K; Adler, N; Laraia, B; Epel, E; Parry, E; Wang, M; Park, JS; Zota, AR. (2021). Persistent organic pollutants and maternal glycemic outcomes in a diverse pregnancy cohort of overweight women. Environ Res 193: 110551. http://dx.doi.org/10.1016/j.envres.2020.110551.

Meng, Q; Inoue, K; Ritz, B; Olsen, J; Liew, Z. (2018). Prenatal exposure to perfluoroalkyl substances and birth outcomes; An updated analysis from the Danish national birth cohort. Int J Environ Res Public Health 15: 1832. http://dx.doi.org/10.3390/ijerph15091832.

Minatoya, M; Itoh, S; Miyashita, C; Araki, A; Sasaki, S; Miura, R; Goudarzi, H; Iwasaki, Y; Kishi, R. (2017). Association of prenatal exposure to perfluoroalkyl substances with cord blood adipokines and birth size: The Hokkaido Study on environment and children's health. Environ Res 156: 175-182. http://dx.doi.org/10.1016/j.envres.2017.03.033.

Mitro, SD; Sagiv, SK; Fleisch, AF; Jaacks, LM; Williams, PL; Rifas-Shiman, SL; Calafat, AM; Hivert, MF; Oken, E; James-Todd, TM. (2020a). Pregnancy per- and polyfluoroalkyl substance concentrations and postpartum health in project viva: A prospective cohort. J Clin Endocrinol Metab 105: e3415–e3426. http://dx.doi.org/10.1210/clinem/dgaa431.

Mitro, SD; Sagiv, SK; Rifas-Shiman, SL; Calafat, AM; Fleisch, AF; Jaacks, LM; Williams, PL; Oken, E; James-Todd, TM. (2020b). Per- and polyfluoroalkyl substance exposure, gestational weight gain, and postpartum weight changes in Project Viva. Obesity (Silver Spring) 28: 1984-1992. http://dx.doi.org/10.1002/oby.22933.

Monroy, R; Morrison, K; Teo, K; Atkinson, S; Kubwabo, C; Stewart, B; Foster, WG. (2008). Serum levels of perfluoroalkyl compounds in human maternal and umbilical cord blood samples. Environ Res 108: 56-62. http://dx.doi.org/10.1016/j.envres.2008.06.001.

Morgan, S; Mottaleb, MA; Kraemer, MP; Moser, DK; Worley, J; Morris, AJ; Petriello, MC. (2023). Effect of lifestyle-based lipid lowering interventions on the relationship between circulating levels of per-and polyfluoroalkyl substances and serum cholesterol. Environ Toxicol Pharmacol 98: 104062. http://dx.doi.org/10.1016/j.etap.2023.104062.

Morken, NH; Travlos, GS; Wilson, RE; Eggesbø, M; Longnecker, MP. (2014). Maternal glomerular filtration rate in pregnancy and fetal size. PLoS ONE 9: e101897. http://dx.doi.org/10.1371/journal.pone.0101897.

Mwapasa, M; Huber, S; Chakhame, BM; Maluwa, A; Odland, ML; Rollin, H; Choko, A; Xu, S; Odland, JO. (2023). Serum Concentrations of Selected Poly- and Perfluoroalkyl Substances (PFASs) in Pregnant Women and Associations with Birth Outcomes. A Cross-Sectional Study from Southern Malawi. Int J Environ Res Public Health 20: 1689. http://dx.doi.org/10.3390/ijerph20031689.

Nair, AS; Ma, ZQ; Watkins, SM; Wood, SS. (2021). Demographic and exposure characteristics as predictors of serum per- and polyfluoroalkyl substances (PFASs) levels - A community-level biomonitoring project in Pennsylvania. Int J Hyg Environ Health 231: 113631. http://dx.doi.org/10.1016/j.ijheh.2020.113631.

Needham, LL; Grandjean, P; Heinzow, B; Jørgensen, PJ; Nielsen, F; Patterson, DG; Sjödin, A; Turner, WE; Weihe, P. (2011). Partition of environmental chemicals between maternal and fetal blood and tissues. Environ Sci Technol 45: 1121-1126. http://dx.doi.org/10.1021/es1019614.

Newsome, PN; Cramb, R; Davison, SM; Dillon, JF; Foulerton, M; Godfrey, EM; Hall, R; Harrower, U; Hudson, M; Langford; Mackie, A; Mitchell-Thain, R; Sennett, K; Sheron, NC; Verne, J; Walmsley, M; Yeoman, A. (2018). Guidelines on the management of abnormal liver blood tests. Gut 67: 6-19. http://dx.doi.org/10.1136/gutjnl-2017-314924.

Nian, M; Li, QQ; Bloom, M; Qian, ZM; Syberg, KM; Vaughn, MG; Wang, SQ; Wei, Q; Zeeshan, M; Gurram, N; Chu, C; Wang, J; Tian, YP; Hu, LW; Liu, KK; Yang, BY; Liu, RQ; Feng, D; Zeng, XW; Dong, GH. (2019). Liver function biomarkers disorder is associated with exposure to perfluoroalkyl acids in adults: Isomers of C8 Health Project in China. Environ Res 172: 81-88. http://dx.doi.org/10.1016/j.envres.2019.02.013.

Nian, M; Luo, K; Luo, F; Aimuzi, R; Huo, X; Chen, Q; Tian, Y; Zhang, J. (2020). Association between prenatal exposure to PFAS and fetal sex hormones: Are the short-chain PFAS safer? Environ Sci Technol 54: 8291-8299. http://dx.doi.org/10.1021/acs.est.0c02444.

Noyes, PD; Paul-Friedman, KP; Haselman, JT; Barone Jr., S; Crofton, KM; Gilbert, ME; Hornung, MW; Laws, SC; Simmons, SO; Stoker, TE; Tietge, JE; Degitz, SJ. (2019). Evaluating chemicals for thyroid disruption: Opportunities and challenges with in vitro testing and adverse outcome pathway approaches. Environ Health Perspect 127: 95001. http://dx.doi.org/10.1289/EHP5297.

NTP (National Toxicology Program). (2018). 28-day evaluation of the toxicity (C04049) of perfluorononaoic acid (PFNA) (375-95-1) on Harlan Sprague-Dawley rats exposed via gavage [NTP]. http://dx.doi.org/10.22427/NTP-DATA-002-02655-0003-0000-3.

Ode, A; Rylander, L; Lindh, CH; Källén, K; Jönsson, BA; Gustafsson, P; Olofsson, P; Ivarsson, SA; Rignell-Hydbom, A. (2013). Determinants of maternal and fetal exposure and temporal trends of perfluorinated compounds. Environ Sci Pollut Res Int 20: 7970-7978. http://dx.doi.org/10.1007/s11356-013-1573-5.

Oh, J; Bennett, DH; Tancredi, DJ; Calafat, AM; Schmidt, RJ; Hertz-Picciotto, I; Shin, HM. (2022a). Longitudinal Changes in Maternal Serum Concentrations of Per- and Polyfluoroalkyl Substances from Pregnancy to Two Years Postpartum. Environ Sci Technol 56: 11449-11459. http://dx.doi.org/10.1021/acs.est.1c07970.

Oh, J; Shin, HM; Kannan, K; Busgang, SA; Schmidt, RJ; Schweitzer, JB; Hertz-Picciotto, I; Bennett, DH. (2022b). Childhood exposure to per- and polyfluoroalkyl substances and neurodevelopment in the CHARGE case-control study. Environ Res 215: 114322. http://dx.doi.org/10.1016/j.envres.2022.114322.

Ohmori, K; Kudo, N; Katayama, K; Kawashima, Y. (2003). Comparison of the toxicokinetics between perfluorocarboxylic acids with different carbon chain length. Toxicology 184: 135-140. http://dx.doi.org/10.1016/S0300-483X(02)00573-5.

Ouidir, M; Buck Louis, GM; Kanner, J; Grantz, KL; Zhang, C; Sundaram, R; Rahman, ML; Lee, S; Kannan, K; Tekola-Ayele, F; Mendola, P. (2020). Association of maternal exposure to persistent organic pollutants in early pregnancy with fetal growth. JAMA Pediatr 174: 149-161. http://dx.doi.org/10.1001/jamapediatrics.2019.5104.

Oulhote, Y; Coull, B; Bind, MA; Debes, F; Nielsen, F; Tamayo, I; Weihe, P; Grandjean, P. (2019). Joint and independent neurotoxic effects of early life exposures to a chemical mixture: A multi-pollutant approach combining ensemble learning and g-computation. Environmental Epidemiology 3: e063. http://dx.doi.org/10.1097/ee9.0000000000000063.

Pacifico, L; Ferraro, F; Bonci, E; Anania, C; Romaggioli, S; Chiesa, C. (2013). Upper limit of normal for alanine aminotransferase: Quo vadis? 422: 29-39. http://dx.doi.org/10.1016/j.cca.2013.03.030.

Padula, AM; Ning, X; Bakre, S; Barrett, ES; Bastain, T; Bennett, DH; Bloom, MS; Breton, CV; Dunlop, AL; Eick, SM; Ferrara, A; Fleisch, A; Geiger, S; Goin, DE; Kannan, K; Karagas, MR; Korrick, S; Meeker, JD; Morello-Frosch, R. (2023). Birth outcomes in relation to prenatal exposure to per-and polyfluoroalkyl substances and stress in the environmental influences on child health outcomes (echo) program [Supplemental Data]. Environ Health Perspect 131: (037006) 037001-037011. http://dx.doi.org/10.1289/EHP10723.

Pan, Y; Cui, Q; Wang, J; Sheng, N; Jing, J; Yao, B; Dai, J. (2019). Profiles of emerging and legacy per-/polyfluoroalkyl substances in matched serum and semen samples: New implications for human semen quality. Environ Health Perspect 127: 127005. http://dx.doi.org/10.1289/EHP4431.

Pan, Y; Zhu, Y; Zheng, T; Cui, Q; Buka, SL; Zhang, B; Guo, Y; Xia, W; Yeung, LW; Li, Y; Zhou, A; Qiu, L; Liu, H; Jiang, M; Wu, C; Xu, S; Dai, J. (2017). Novel Chlorinated Polyfluorinated Ether Sulfonates and Legacy Per-/Polyfluoroalkyl Substances: Placental Transfer and Relationship with Serum Albumin and Glomerular Filtration Rate. Environ Sci Technol 51: 634-644. http://dx.doi.org/10.1021/acs.est.6b04590.

Pan, Z; Guo, Y; Zhou, Q; Wang, Q; Pan, S; Xu, S; Li, L. (2023). Perfluoroalkyl substance exposure is associated with asthma and innate immune cell count in US adolescents stratified by sex. Environ Sci Pollut Res Int 30: 52535-52548. http://dx.doi.org/10.1007/s11356-023-26065-7.

Park, JH; Choi, J; Jun, DW; Han, SW; Yeo, YH; Nguyen, MH. (2019). Low Alanine Aminotransferase Cut-Off for Predicting Liver Outcomes; A Nationwide Population-Based Longitudinal Cohort Study. J Clin Med 8. http://dx.doi.org/10.3390/jcm8091445.

Park, SK; Wang, X; Ding, N; Karvonen-Gutierrez, CA; Calafat, AM; Herman, WH; Mukherjee, B; Harlow, SD. (2022). Per- and polyfluoroalkyl substances and incident diabetes in midlife women: the Study of Women's Health Across the Nation (SWAN). Diabetologia 65: 1157-1168. http://dx.doi.org/10.1007/s00125-022-05695-5.

Passen, EL; Andersen, BR. (1986). Clinical tetanus despite a protective level of toxin-neutralizing antibody [Case Report]. JAMA 255: 1171-1173. http://dx.doi.org/10.1001/jama.1986.03370090093029.

Patel, JC; Mehta, BC. (1999). Tetanus: Study of 8,697 cases. Indian J Med Sci 53: 393-401.

Peterson, AK; Eckel, SP; Habre, R; Yang, T; Faham, D; Amin, M; Grubbs, BH; Farzan, SF; Kannan, K; Robinson, M; Lerner, D; Al-Marayati, LA; Walker, DK; Grant, EG; Breton, CV; Bastain, TM. (2022). Detected prenatal perfluorooctanoic acid (PFOA) exposure is associated with decreased fetal head biometric parameters in participants experiencing higher perceived stress during pregnancy in the MADRES cohort. 9. http://dx.doi.org/10.1016/j.envadv.2022.100286.

Petro, EM; D'Hollander, W; Covaci, A; Bervoets, L; Fransen, E; De Neubourg, D; De Pauw, I; Leroy, JL; Jorssen, EP; Bols, PE. (2014). Perfluoroalkyl acid contamination of follicular fluid and its consequence for in vitro oocyte developmental competence. Sci Total Environ 496: 282-288. http://dx.doi.org/10.1016/j.scitotenv.2014.07.028.

Petroff, RL; Cavalcante, RG; Langen, ES; Dolinoy, DC; Padmanabhan, V; Goodrich, JM. (2023). Mediation effects of DNA methylation and hydroxymethylation on birth outcomes after prenatal per- and polyfluoroalkyl substances (PFAS) exposure in the Michigan mother-infant Pairs cohort. Clinical Epigenetics 15: 49. http://dx.doi.org/10.1186/s13148-023-01461-5.

Pirard, C; Dufour, P; Charlier, C. (2020). Background contamination of perfluoralkyl substances in a Belgian general population. Toxicol Lett 333: 13-21. http://dx.doi.org/10.1016/j.toxlet.2020.07.015.

Poothong, S; Thomsen, C; Padilla-Sanchez, JA; Papadopoulou, E; Haug, LS. (2017). Distribution of novel and well-known poly- and perfluoroalkyl substances (PFASs) in human serum, plasma, and whole blood. Environ Sci Technol 51: 13388-13396. http://dx.doi.org/10.1021/acs.est.7b03299.

Porter, AK; Kleinschmidt, SE; Andres, KL; Reusch, CN; Krisko, RM; Taiwo, OA; Olsen, GW; Longnecker, MP. (2022). Antibody response to COVID-19 vaccines among workers with a wide range of exposure to per- and polyfluoroalkyl substances. Environ Int 169: 107537. http://dx.doi.org/10.1016/j.envint.2022.107537.

Portier, K; Tolson, JK; Roberts, SM. (2007). Body weight distributions for risk assessment. Risk Anal 27: 11-26. http://dx.doi.org/10.1111/j.1539-6924.2006.00856.x.

Preston, EV; Rifas-Shiman, SL; Hivert, MF; Zota, AR; Sagiv, SK; Calafat, AM; Oken, E; James-Todd, T. (2020). Associations of per- and polyfluoroalkyl substances (PFAS) with glucose tolerance during pregnancy in project viva. J Clin Endocrinol Metab 105: E2864-E2876. http://dx.doi.org/10.1210/clinem/dgaa328.

Qu, J; Zhao, Y; Zhang, L; Hu, S; Liao, K; Zhao, M; Wu, P; Jin, H. (2022). Evaluated serum perfluoroalkyl acids and their relationships with the incidence of rheumatoid arthritis in the general population in Hangzhou, China. Environ Pollut 307: 119505. http://dx.doi.org/10.1016/j.envpol.2022.119505.

Ramli, MR; Yoneda, M; Ali Mohd, M; Mohamad Haron, DE; Ahmad, ED. (2020). Level and determinants of serum perfluoroalkyl acids (PFAAs) in a population in Klang Valley, Malaysia. Int J Hyg Environ Health 223: 179-186. http://dx.doi.org/10.1016/j.ijheh.2019.09.005.

Rantakokko, P; Männistö, V; Airaksinen, R; Koponen, J; Viluksela, M; Kiviranta, H; Pihlajamäki, J. (2015). Persistent organic pollutants and non-alcoholic fatty liver disease in morbidly obese patients: A cohort study. Environ Health 14: 79. http://dx.doi.org/10.1186/s12940-015-0066-z.

Reyes, L; Mañalich, R. (2005). Long-term consequences of low birth weight [Review]. Kidney Int Suppl 68: S107-S111. http://dx.doi.org/10.1111/j.1523-1755.2005.09718.x.

Rivera-Núñez, Z; Kinkade, CW; Khoury, L; Brunner, J; Murphy, H; Wang, C; Kannan, K; Miller, RK; O'Connor, TG; Barrett, ES. (2023). Prenatal perfluoroalkyl substances exposure and maternal sex steroid hormones across pregnancy. Environ Res 220: 115233. http://dx.doi.org/10.1016/j.envres.2023.115233.

Robledo, CA; Yeung, E; Mendola, P; Sundaram, R; Maisog, J; Sweeney, AM; Barr, DB; Louis, GM. (2015). Preconception maternal and paternal exposure to persistent organic pollutants and birth size: the LIFE study. Environ Health Perspect 123: 88-94. http://dx.doi.org/10.1289/ehp.1308016.

Rokoff, LB; Rifas-Shiman, SL; Coull, BA; Cardenas, A; Calafat, AM; Ye, X; Gryparis, A; Schwartz, J; Sagiv, SK; Gold, DR; Oken, E; Fleisch, AF. (2018). Cumulative exposure to environmental

pollutants during early pregnancy and reduced fetal growth: the Project Viva cohort. Environ Health 17: 19. http://dx.doi.org/10.1186/s12940-018-0363-4.

Rosen, EM; Kotlarz, N; Knappe, DRU; Lea, CS; Collier, DN; Richardson, DB; Hoppin, JA. (2022). Drinking water-associated PFAS and fluoroethers and lipid outcomes in the GenX exposure study. Environ Health Perspect 130: 97002. http://dx.doi.org/10.1289/EHP11033.

Ru, H; White, S. (2024). Dose-response modeling files for the PFNA IRIS Assessment [Computer Program].

Rylander, C; Phi, DT; Odland, JØ; Sandanger, TM. (2009). Perfluorinated compounds in delivering women from south central Vietnam. J Environ Monit 11: 2002-2008. http://dx.doi.org/10.1039/b908551c.

Sagiv, SK; Rifas-Shiman, SL; Fleisch, AF; Webster, TF; Calafat, AM; Ye, X; Gillman, MW; Oken, E. (2018). Early Pregnancy Perfluoroalkyl Substance Plasma Concentrations and Birth Outcomes in Project Viva: Confounded by Pregnancy Hemodynamics? Am J Epidemiol 187: 793-802. http://dx.doi.org/10.1093/aje/kwx332.

Salihović, S; Dickens, AM; Schoultz, I; Fart, F; Sinisalu, L; Lindeman, T; Halfvarson, J; Orešič, M; Hyötyläinen, T. (2019). Simultaneous determination of perfluoroalkyl substances and bile acids in human serum using ultra-high-performance liquid chromatography-tandem mass spectrometry. Anal Bioanal Chem 412: 2251-2259. http://dx.doi.org/10.1007/s00216-019-02263-6.

Salvatier, J; Wiecki, TV; Fonnesbeck, C. (2016). Probabilistic programming in Python using PyMC3. PeerJ Computer Science 2: e55. http://dx.doi.org/10.7717/peerj-cs.55.

Sanghavi, M; Rutherford, JD. (2014). Cardiovascular physiology of pregnancy. Circulation 130: 1003-1008. http://dx.doi.org/10.1161/CIRCULATIONAHA.114.009029.

Schillemans, T; Iszatt, N; Remy, S; Schoeters, G; Fernández, MF; D'Cruz, SC; Desalegn, A; Haug, LS; Lignell, S; Lindroos, AK; Fábelová, L; Murinova, LP; Kosjek, T; Tkalec, Ž; Gabriel, C; Sarigiannis, D; Pedraza-Díaz, S; Esteban-López, M; Castaño, A; ... Åkesson, A. (2022). Cross-sectional associations between exposure to per- and polyfluoroalkyl substances and body mass index among European teenagers in the HBM4EU aligned studies. Environ Pollut 316: 120566. http://dx.doi.org/10.1016/j.envpol.2022.120566.

Schlosser, P. (2024). Model Code for the Classical Pharmacokinetic Modeling and Alternate Dosimetric Analyses of PFNA, PFDA and PFHxS in Support of IRIS Toxicological Reviews [Computer Program].

Schumann, G; Bonora, R; Ceriotti, F; Férard, G; Ferrero, CA; Franck, PFH; Gella, FJ; Hoelzel, W; Jørgensen, PJ; Kanno, T; Kessner, A; Klauke, R; Kristiansen, N; Lessinger, JM; Linsinger, TPJ; Misaki, H; Panteghini, M; Pauwels, J; Schiele, F; Schimmel, HG. (2002). IFCC primary reference procedures for the measurement of catalytic activity concentrations of enzymes at 37°C. Part 4. Reference procedure for the measurement of catalytic concentration of alanine aminotransferase. Clin Chem Lab Med 40: 718-724. http://dx.doi.org/10.1515/CCLM.2002.124.

Schumann, G; Klauke, R. (2003). New IFCC reference procedures for the determination of catalytic activity concentrations of five enzymes in serum: preliminary upper reference limits obtained in hospitalized subjects. 327: 69-79. http://dx.doi.org/10.1016/s0009-8981(02)00341-8.

Selgrade, MK. (2007). Immunotoxicity: The risk is real [Review]. Toxicol Sci 100: 328-332. http://dx.doi.org/10.1093/toxsci/kfm244.

Shearer, JJ; Callahan, CL; Calafat, AM; Huang, WY; Jones, RR; Sabbisetti, VS; Freedman, ND; Sampson, JN; Silverman, DT; Purdue, MP; Hofmann, JN. (2021). Serum concentrations of per- and polyfluoroalkyl substances and risk of renal cell carcinoma. J Natl Cancer Inst 113: 580-587. http://dx.doi.org/10.1093/jnci/djaa143.

Sheng, N; Li, J; Liu, H; Zhang, A; Dai, J. (2016). Interaction of perfluoroalkyl acids with human liver fatty acid-binding protein. Arch Toxicol 90: 217-227. http://dx.doi.org/10.1007/s00204-014-1391-7.

Shi, S; Ding, Y; Wu, B; Hu, P; Chen, M; Dong, N; Vinturache, A; Gu, H; Dong, X; Ding, G. (2023). Association of perfluoroalkyl substances with pulmonary function in adolescents (NHANES 2007-2012). Environ Sci Pollut Res Int. http://dx.doi.org/10.1007/s11356-023-26119-w.

Shi, Y; Yang, L; Li, J; Lai, J; Wang, Y; Zhao, Y; Wu, Y. (2017). Occurrence of perfluoroalkyl substances in cord serum and association with growth indicators in newborns from Beijing. Chemosphere 169: 396-402. http://dx.doi.org/10.1016/j.chemosphere.2016.11.050.

Shiue, I. (2015a). Arsenic, heavy metals, phthalates, pesticides, hydrocarbons and polyfluorinated compounds but not parabens or phenols are associated with adult remembering condition: US NHANES, 2011-2012. Environ Sci Pollut Res Int 22: 6381-6386. http://dx.doi.org/10.1007/s11356-015-4261-9.

Shiue, I. (2015b). Urinary heavy metals, phthalates and polyaromatic hydrocarbons independent of health events are associated with adult depression: USA NHANES, 2011-2012. Environ Sci Pollut Res Int 22: 17095-17103. http://dx.doi.org/10.1007/s11356-015-4944-2.

Shiue, I. (2015c). Urinary heavy metals, phthalates, perchlorate, nitrate, thiocyanate, hydrocarbons, and polyfluorinated compounds are associated with adult hearing disturbance: USA NHANES, 2011-2012. Environ Sci Pollut Res Int 22: 20306-20311. http://dx.doi.org/10.1007/s11356-015-5546-8.

Shiue, I. (2015d). Urinary heavy metals, phthalates, phenols, thiocyanate, parabens, pesticides, polyaromatic hydrocarbons but not arsenic or polyfluorinated compounds are associated with adult oral health: USA NHANES, 2011-2012. Environ Sci Pollut Res Int 22: 15636-15645. http://dx.doi.org/10.1007/s11356-015-4749-3.

Shoaff, J; Papandonatos, GD; Calafat, AM; Chen, A; Lanphear, BP; Ehrlich, S; Kelsey, KT; Braun, JM. (2018). Prenatal exposure to perfluoroalkyl substances: Infant birth weight and early life growth. Environmental Epidemiology 2: e010. http://dx.doi.org/10.1097/EE9.0000000000000010.

Sood, S; Ojo, AO; Adu, D; Kannan, K; Ghassabian, A; Koshy, T; Vento, SM; Pehrson, LJ; Gilbert, JF; Arogundade, FA; Ademola, AD; Salako, BO; Raji, Y; Osafo, C; Antwi, S; Trachtman, H; Trasande, L; Ajayi, S; Burke, D; Cooper, R; Gbadegesin, R; Ilori, T; Mamven, M; Olanrewaju, T; Parekh, R; Rhule, J; Salako, T; Tayo, B; Ulasi, I; Investigators, HAKDRN. (2019). Association Between Perfluoroalkyl Substance Exposure and Renal Function in Children With CKD Enrolled in H3Africa Kidney Disease Research Network. 4: 1641-1645. http://dx.doi.org/10.1016/j.ekir.2019.07.017.

Starling, AP; Adgate, JL; Hamman, RF; Kechris, K; Calafat, AM; Ye, X; Dabelea, D. (2017). Perfluoroalkyl substances during pregnancy and offspring weight and adiposity at birth: Examining mediation by maternal fasting glucose in the healthy start study. Environ Health Perspect 125: 067016. http://dx.doi.org/10.1289/EHP641.

Steenland, K; Barry, V; Savitz, D. (2018a). Serum perfluorooctanoic acid and birthweight: an updated meta-analysis with bias analysis. Epidemiology 29: 765-776. http://dx.doi.org/10.1097/EDE.0000000000000903.

Steenland, K; Kugathasan, S; Barr, DB. (2018b). PFOA and ulcerative colitis. Environ Res 165: 317-321. http://dx.doi.org/10.1016/j.envres.2018.05.007.

Taibl, KR; Liang, D; Dunlop, AL; Barr, DB; Smith, MR; Steenland, K; Tan, Y; Ryan, PB; Panuwet, P; Everson, T; Marsit, CJ; Kannan, K; Jones, DP; Eick, SM. (2023). Pregnancy-related hemodynamic biomarkers in relation to trimester-specific maternal per - and polyfluoroalkyl substances exposures and adverse birth outcomes. Environ Pollut 323: 121331. http://dx.doi.org/10.1016/j.envpol.2023.121331.

Tailleur, RG. (2008). Deactivation of WNiPd/TiO2Al2O3 catalyst during the upgrading of LCO. Fuel 87: 2551-2562. http://dx.doi.org/10.1016/j.fuel.2008.01.025.

Tan, Y; Zeng, Z; Liang, H; Weng, X; Yao, H; Fu, Y; Li, Y; Chen, J; Wei, X; Jing, C. (2022). Association between Perfluoroalkyl and Polyfluoroalkyl Substances and Women's Infertility, NHANES 2013-2016. Int J Environ Res Public Health 19. http://dx.doi.org/10.3390/ijerph192215348.

Tatum-Gibbs, K; Wambaugh, JF; Das, KP; Zehr, RD; Strynar, MJ; Lindstrom, AB; Delinsky, A; Lau, C. (2011). Comparative pharmacokinetics of perfluorononanoic acid in rat and mouse. Toxicology 281: 48-55. http://dx.doi.org/10.1016/j.tox.2011.01.003.

Thulin, P; Nordahl, G; Gry, M; Yimer, G; Aklillu, E; Makonnen, E; Aderaye, G; Lindquist, L; Mattsson, CM; Ekblom, B; Antoine, DJ; Park, BK; Linder, S; Harrill, AH; Watkins, PB; Glinghammar, B; Schuppe-Koistinen, I. (2014). Keratin-18 and microRNA-122 complement alanine aminotransferase as novel safety biomarkers for drug-induced liver injury in two human cohorts. Liver Int 34: 367-378. http://dx.doi.org/10.1111/liv.12322.

Tian, M, .; Reichetzeder, C, .; Li, J, .; Hocher, B, . (2019a). Low birth weight, a risk factor for diseases in later life, is a surrogate of insulin resistance at birth. J Hypertens 37: 2123-2134. http://dx.doi.org/10.1097/HJH.0000000000002156.

Tian, YP; Zeng, XW; Bloom, MS; Lin, S; Wang, SQ; Yim, SHL; Yang, M; Chu, C; Gurram, N; Hu, LW; Liu, KK; Yang, BY; Feng, D; Liu, RQ; Nian, M; Dong, GH. (2019b). Isomers of perfluoroalkyl substances and overweight status among Chinese by sex status: Isomers of C8 Health Project in China. Environ Int 124: 130-138. http://dx.doi.org/10.1016/j.envint.2019.01.006.

Tillaut, H; Monfort, C; Giton, F; Warembourg, C; Rouget, F; Cordier, S; Laine, F; Gaudreau, E; Garlantezec, R; Saint-Amour, D; Chevrier, C. (2022). Persistent organic pollutant exposure and thyroid function among 12-year-old children. Neuroendocrinology. http://dx.doi.org/10.1159/000528631.

Tsai, MS; Miyashita, C; Araki, A; Itoh, S; Bamai, YA; Goudarzi, H; Okada, E; Kashino, I; Matsuura, H; Kishi, R. (2018). Determinants and temporal trends of perfluoroalkyl substances in pregnant women: The Hokkaido study on environment and children's health. Int J Environ Res Public Health 15: 989. http://dx.doi.org/10.3390/ijerph15050989.

U.S. EPA (U.S. Environmental Protection Agency). (2005). Guidelines for carcinogen risk assessment [EPA Report]. (EPA630P03001F). Washington, DC. https://www.epa.gov/sites/production/files/2013-09/documents/cancer_guidelines_final_3-25-05.pdf.

U.S. EPA (U.S. Environmental Protection Agency). (2011). Exposure factors handbook: 2011 edition [EPA Report]. (EPA/600/R-090/052F). Washington, DC: U.S. Environmental Protection Agency, Office of Research and Development, National Center for Environmental Assessment. https://nepis.epa.gov/Exe/ZyPURL.cgi?Dockey=P100F2OS.txt.

U.S. EPA (U.S. Environmental Protection Agency). (2012). Benchmark dose technical guidance [EPA Report]. (EPA100R12001). Washington, DC: U.S. Environmental Protection Agency, Risk Assessment Forum. https://www.epa.gov/risk/benchmark-dose-technical-guidance.

U.S. EPA (U.S. Environmental Protection Agency). (2020). ORD staff handbook for developing IRIS assessments (public comment draft) [EPA Report]. (EPA/600/R-20/137). Washington, DC: U.S. Environmental Protection Agency, Office of Research and Development, Center for Public Health and Environmental Assessment. https://cfpub.epa.gov/ncea/iris_drafts/recordisplay.cfm?deid=350086.

U.S. EPA (U.S. Environmental Protection Agency). (2022). Re: Workman et al supplemental data. Available online at (accessed

Valenti, L, . Pelusi, S,. Bianco, C,. Ceriotti, F,. Berzuini, A,. Iogna Prat, L,. Trotti, R,. Malvestiti, F,. D'Ambrosio, R,. Lampertico, P,. Colli, A,. Colombo, M,. Tsochatzis, E,. A. Fraquelli, M,. Prati,

D.,. (2021). Definition of Healthy Ranges for Alanine Aminotransferase Levels: A 2021 Update. Hematology 5: 1824-1832. http://dx.doi.org/10.1002/hep4.1794.

Valvi, D; Oulhote, Y; Weihe, P; Dalgård, C; Bjerve, KS; Steuerwald, U; Grandjean, P. (2017). Gestational diabetes and offspring birth size at elevated environmental pollutant exposures. Environ Int 107: 205-215. http://dx.doi.org/10.1016/j.envint.2017.07.016.

van Beek, JHD, A; de Moor, MHM; de Geus, E, coJC; Lubke, GH; Vink, JM; Willemsen, G; Boomsma, DI. (2013). The Genetic Architecture of Liver Enzyme Levels: GGT, ALT and AST. Behav Genet329-339. http://dx.doi.org/10.1007/s10519-013-9593-y.

van Larebeke, N; Koppen, G; Decraemer, S; Colles, A; Bruckers, L; Den Hond, E; Govarts, E; Morrens, B; Schettgen, T; Remy, S; Coertjens, D; Nawrot, T, im; Nelen, V; Baeyens, W; Schoeters, G. (2022). Per- and polyfluoroalkyl substances (PFAS) and neurobehavioral function and cognition in adolescents (2010-2011) and elderly people (2014): Results from the Flanders Environment and Health Studies (FLEHS). Environ Sci Eur 34: 98. http://dx.doi.org/10.1186/s12302-022-00675-3.

Wambaugh, JF; Setzer, RW; Pitruzzello, AM; Liu, J; Reif, DM; Kleinstreuer, NC; Wang, NC; Sipes, N; Martin, M; Das, K; Dewitt, JC; Strynar, M; Judson, R; Houck, KA; Lau, C. (2013). Dosimetric anchoring of in vivo and in vitro studies for perfluorooctanoate and perfluorooctanesulfonate. Toxicol Sci 136: 308-327. http://dx.doi.org/10.1093/toxsci/kft204.

Wang, B; Chen, Q; Shen, L; Zhao, S; Pang, W; Zhang, J. (2016a). Perfluoroalkyl and polyfluoroalkyl substances in cord blood of newborns in Shanghai, China: Implications for risk assessment [Review]. Environ Int 97: 7-14. http://dx.doi.org/10.1016/j.envint.2016.10.008.

Wang, H; Li, W; Yang, J; Wang, Y; Du, H; Han, M; Xu, L; Liu, S; Yi, J; Chen, Y; Jiang, Q; He, G. (2023a). Gestational exposure to perfluoroalkyl substances is associated with placental DNA methylation and birth size. Sci Total Environ 858: 159747. http://dx.doi.org/10.1016/j.scitotenv.2022.159747.

Wang, J; Yan, S; Zhang, W; Zhang, H; Dai, J. (2015). Integrated proteomic and miRNA transcriptional analysis reveals the hepatotoxicity mechanism of PFNA exposure in mice. J Proteome Res 14: 330-341. http://dx.doi.org/10.1021/pr500641b.

Wang, W; Zhou, W; Wu, S; Liang, F; Li, Y; Zhang, J; Cui, L; Feng, Y; Wang, Y. (2019). Perfluoroalkyl substances exposure and risk of polycystic ovarian syndrome related infertility in Chinese women. Environ Pollut 247: 824-831. http://dx.doi.org/10.1016/j.envpol.2019.01.039.

Wang, Y; Adgent, M; Su, PH; Chen, HY; Chen, PC; Hsiung, CA; Wang, SL. (2016b). Prenatal exposure to perfluorocarboxylic acids (PFCAs) and fetal and postnatal growth in the Taiwan maternal and infant cohort study. Environ Health Perspect 124: 1794-1800. http://dx.doi.org/10.1289/ehp.1509998.

Wang, Z; Zhang, J; Dai, Y; Zhang, L; Guo, J; Xu, S; Chang, X; Wu, C; Zhou, Z. (2023b). Mediating effect of endocrine hormones on association between per- and polyfluoroalkyl substances exposure and birth size: Findings from sheyang mini birth cohort study. Environ Res 226: 115658. http://dx.doi.org/10.1016/j.envres.2023.115658.

Weaver, YM; Ehresman, DJ; Butenhoff, JL; Hagenbuch, B. (2010). Roles of rat renal organic anion transporters in transporting perfluorinated carboxylates with different chain lengths. Toxicol Sci 113: 305-314. http://dx.doi.org/10.1093/toxsci/kfp275.

Weiss, JM; Andersson, PL; Lamoree, MH; Leonards, PEG; van Leeuwen, SPJ; Hamers, T. (2009). Competitive Binding of Poly- and Perfluorinated Compounds to the Thyroid Hormone Transport Protein Transthyretin. Toxicol Sci 109: 206-216. http://dx.doi.org/10.1093/toxsci/kfp055.

Weisskopf, MG; Seals, RM; Webster, TF. (2018). Bias amplification in epidemiologic analysis of exposure to mixtures. Environ Health Perspect 126. http://dx.doi.org/10.1289/EHP2450.

Wen, HJ; Wang, SL; Chen, PC; Guo, YL. (2019). Prenatal perfluorooctanoic acid exposure and glutathione s-transferase T1/M1 genotypes and their association with atopic dermatitis at 2 years of age. PLoS ONE 14: e0210708. http://dx.doi.org/10.1371/journal.pone.0210708.

Whitworth, KW; Haug, LS; Baird, DD; Becher, G; Hoppin, JA; Skjaerven, R; Thomsen, C; Eggesbo, M; Travlos, G; Wilson, R; Longnecker, MP. (2012). Perfluorinated compounds and subfecundity in pregnant women. Epidemiology 23: 257-263. http://dx.doi.org/10.1097/EDE.0b013e31823b5031.

Whitworth, KW; Haug, LS; Sabaredzovic, A; Eggesbo, M; Longnecker, MP. (2016). Brief Report: Plasma Concentrations of Perfluorooctane Sulfonamide and Time-to-pregnancy Among Primiparous Women. Epidemiology 27: 712-715. http://dx.doi.org/10.1097/EDE.0000000000000524.

Wielsøe, M; Eiberg, H; Ghisari, M; Kern, P; Lind, O; Bonefeld-Jørgensen, EC. (2018). Genetic variations, exposure to persistent organic pollutants and breast cancer risk - a greenlandic case-control study. Basic & Clinical Pharmacology & Toxicology Online Pharmacology Online 123: 335-346. http://dx.doi.org/10.1111/bcpt.13002.

Wielsøe, M; Kern, P; Bonefeld-Jørgensen, EC. (2017). Serum levels of environmental pollutants is a risk factor for breast cancer in Inuit: a case control study. Environ Health 16: 56. http://dx.doi.org/10.1186/s12940-017-0269-6.

Wikström, S; Lin, PI; Lindh, CH; Shu, H; Bornehag, CG. (2020). Maternal serum levels of perfluoroalkyl substances in early pregnancy and offspring birth weight. Pediatr Res 87: 1093-1099. http://dx.doi.org/10.1038/s41390-019-0720-1.

Wolf, CJ; Zehr, RD; Schmid, JE; Lau, C; Abbott, BD. (2010). Developmental effects of perfluorononanoic acid in the mouse are dependent on peroxisome proliferator-activated receptor-alpha. PPAR Research 2010. http://dx.doi.org/10.1155/2010/282896.

Woodcroft, MW; Ellis, DA; Rafferty, SP; Burns, DC; March, RE; Stock, NL; Trumpour, KS; Yee, J; Munro, K. (2010). Experimental characterization of the mechanism of perfluorocarboxylic acids' liver protein bioaccumulation: the key role of the neutral species. Environ Toxicol Chem 29: 1669-1677. http://dx.doi.org/10.1002/etc.199.

Woods, MM; Lanphear, BP; Braun, JM; McCandless, LC. (2017). Gestational exposure to endocrine disrupting chemicals in relation to infant birth weight: A Bayesian analysis of the HOME Study. Environ Health 16: 115. http://dx.doi.org/10.1186/s12940-017-0332-3.

Workman, CE; Becker, AB; Azad, MB; Moraes, TJ; Mandhane, PJ; Turvey, SE; Subbarao, P; Brook, JR; Sears, MR; Wong, CS. (2019). Associations between concentrations of perfluoroalkyl substances in human plasma and maternal, infant, and home characteristics in Winnipeg, Canada. Environ Pollut 249: 758-766. http://dx.doi.org/10.1016/j.envpol.2019.03.054.

Wright, JM; Larsen, A; Rappazzo, K; Ru, H; Radke, EG; Bateson, TF. (2023). Systematic review and meta-analysis of birthweight and PFNA exposures. Environ Res115357. http://dx.doi.org/10.1016/j.envres.2023.115357.

Xie, Z; Tan, J; Fang, G; Ji, H; Miao, M; Tian, Y; Hu, H; Cao, W; Liang, H; Yuan, W. (2022). Associations between prenatal exposure to perfluoroalkyl substances and neurobehavioral development in early childhood: A prospective cohort study. Ecotoxicol Environ Saf 241: 113818. http://dx.doi.org/10.1016/j.ecoenv.2022.113818.

Xiong, X; Chen, B; Wang, Z; Ma, L; Li, S; Gao, Y. (2022). Association between perfluoroalkyl substances concentration and bone mineral density in the US adolescents aged 12-19 years in NHANES 2005-2010. Front Endocrinol (Lausanne) 13: 980608. http://dx.doi.org/10.3389/fendo.2022.980608.

Xu, C; Yin, S; Liu, Y; Chen, F; Zhong, Z; Li, F; Liu, K; Liu, W. (2019). Prenatal exposure to chlorinated polyfluoroalkyl ether sulfonic acids and perfluoroalkyl acids: Potential role of maternal determinants and associations with birth outcomes. J Hazard Mater 380: 120867. http://dx.doi.org/10.1016/j.jhazmat.2019.120867.

Xu, C; Zhang, L; Zhou, Q; Ding, J; Yin, S; Shang, X; Tian, Y. (2022). Exposure to per- and polyfluoroalkyl substances as a risk factor for gestational diabetes mellitus through interference with glucose homeostasis. Sci Total Environ 838: 156561. http://dx.doi.org/10.1016/j.scitotenv.2022.156561.

Xu, H; Zhou, Q; Zhang, J; Chen, X; Zhao, H; Lu, H; Ma, B; Wang, Z; Wu, C; Ying, C; Xiong, Y; Zhou, Z; Li, X. (2020). Exposure to elevated per- and polyfluoroalkyl substances in early pregnancy is related to increased risk of gestational diabetes mellitus: A nested case-control study in Shanghai, China. Environ Int 143: 105952. http://dx.doi.org/10.1016/j.envint.2020.105952.

Yang, D; Han, J; Hall, DR; Sun, J; Fu, J; Kutarna, S; Houck, KA; Lalone, CA; Doering, JA; Ng, CA; Peng, H. (2020). Nontarget screening of per- and polyfluoroalkyl substances binding to human liver fatty acid binding protein. Environ Sci Technol 54: 5676-5686. http://dx.doi.org/10.1021/acs.est.0c00049.

Yang, J; Wang, H; Du, H; Xu, L; Liu, S; Yi, J; Qian, X; Chen, Y; Jiang, Q; He, G. (2019). Factors associated with exposure of pregnant women to perfluoroalkyl acids in North China and health risk assessment. Sci Total Environ 655: 356-362. http://dx.doi.org/10.1016/j.scitotenv.2018.11.042.

Yang, L; Ji, H; Liang, H; Yuan, W; Song, X; Li, X; Niu, J; Shi, H; Wen, S; Miao, M. (2022a). Associations of perfluoroalkyl and polyfluoroalkyl substances with gestational hypertension and blood pressure during pregnancy: A cohort study. Environ Res 215: 114284. http://dx.doi.org/10.1016/j.envres.2022.114284.

Yang, L; Li, J; Lai, J; Luan, H; Cai, Z; Wang, Y; Zhao, Y; Wu, Y. (2016a). Placental transfer of perfluoroalkyl substances and associations with thyroid hormones: Beijing prenatal exposure study. Sci Rep 6: 21699. http://dx.doi.org/10.1038/srep21699.

Yang, L; Wang, Z; Shi, Y; Li, J; Wang, Y; Zhao, Y; Wu, Y; Cai, Z. (2016b). Human placental transfer of perfluoroalkyl acid precursors: Levels and profiles in paired maternal and cord serum. Chemosphere 144: 1631-1638. http://dx.doi.org/10.1016/j.chemosphere.2015.10.063.

Yang, Z; Men, K; Guo, J; Liu, R; Liu, H; Wei, J; Zhang, J; Liu, L; Lin, X; Zhang, M; Liu, Y; Chen, Y; Tang, NJ. (2022b). Association between exposure to perfluoroalkyl substances and uric acid in Chinese adults. Chemosphere 312: 137164. http://dx.doi.org/10.1016/j.chemosphere.2022.137164.

Yao, J; Pan, Y; Sheng, N; Su, Z; Guo, Y; Wang, J; Dai, J. (2020). Novel perfluoroalkyl ether carboxylic acids (PFECAs) and sulfonic acids (PFESAs): Occurrence and association with serum biochemical parameters in residents living near a fluorochemical plant in China. Environ Sci Technol 54: 13389-13398. http://dx.doi.org/10.1021/acs.est.0c02888.

Yao, Q; Gao, Y; Zhang, Y; Qin, K; Liew, Z; Tian, Y. (2021). Associations of paternal and maternal per- and polyfluoroalkyl substances exposure with cord serum reproductive hormones, placental steroidogenic enzyme and birth weight. Chemosphere 285: 131521. http://dx.doi.org/10.1016/j.chemosphere.2021.131521.

Ye, WL; Chen, ZX; Xie, YQ; Kong, ML; Li, QQ; Yu, S; Chu, C; Dong, GH; Zeng, XW. (2021). Associations between serum isomers of perfluoroalkyl acids and metabolic syndrome in adults: Isomers of C8 Health Project in China. Environ Res 196: 110430. http://dx.doi.org/10.1016/j.envres.2020.110430.

Yu, Y; Qin, XD; Bloom, MS; Chu, C; Dai, X; Li, QQ; Chen, ZX; Kong, ML; Xie, YQ; Meng, WJ; Yang, BY; Hu, LW; Zeng, XW; Zhao, XM; Zhou, Y; Dong, GH. (2022). Associations of prenatal exposure to perfluoroalkyl substances with preterm birth: A family-based birth cohort study. Environ Res 214: 113803. http://dx.doi.org/10.1016/j.envres.2022.113803.

Zeng, X; Chen, T; Cui, Y; Zhao, J; Chen, Q; Yu, Z; Zhang, Y; Han, L; Chen, Y; Zhang, J. (2023). In utero exposure to perfluoroalkyl substances and early childhood BMI trajectories: A mediation

analysis with neonatal metabolic profiles. Sci Total Environ 867: 161504. http://dx.doi.org/10.1016/j.scitotenv.2023.161504.

Zhang, JJ. (2022). RE: Prenatal exposure to perfluoroalkyl and polyfluoroalkyl substances and birth outcomes: A longitudinal cohort with repeated measurements. Available online at (accessed

Zhang, T; Sun, H; Lin, Y; Qin, X; Zhang, Y; Geng, X; Kannan, K. (2013). Distribution of poly- and perfluoroalkyl substances in matched samples from pregnant women and carbon chain length related maternal transfer. Environ Sci Technol 47: 7974-7981. http://dx.doi.org/10.1021/es400937y.

Zhang, Y; Chen, R; Gao, Y; Qu, J; Wang, Z; Zhao, M; Bai, X; Jin, H. (2023a). Human serum poly- and perfluoroalkyl substance concentrations and their associations with gestational diabetes mellitus. Environ Pollut 317: 120833. http://dx.doi.org/10.1016/j.envpol.2022.120833.

Zhang, Y; Mustieles, V; Sun, Y; Oulhote, Y; Wang, YX; Messerlian, C. (2022). Association between serum per- and polyfluoroalkyl substances concentrations and common cold among children and adolescents in the United States. Environ Int 164: 107239. http://dx.doi.org/10.1016/j.envint.2022.107239.

Zhang, Y; Mustieles, V; Wang, YX; Sun, Q; Coull, B; Sun, Y; Slitt, A; Messerlian, C. (2023b). Red blood cell folate modifies the association between serum per- and polyfluoroalkyl substances and antibody concentrations in U.S. adolescents. Environ Sci Technol 57: 2445-2456. http://dx.doi.org/10.1021/acs.est.2c07152.

Zhao, W; Zitzow, JD; Weaver, Y; Ehresman, DJ; Chang, SC; Butenhoff, JL; Hagenbuch, B. (2017). Organic anion transporting polypeptides contribute to the disposition of perfluoroalkyl acids in humans and rats. Toxicol Sci 156: 84-95. http://dx.doi.org/10.1093/toxsci/kfw236.

Zhao, X; Lin, JY; Dong, WW; Tang, ML; Yan, SG. (2022). Per- and polyfluoroalkyl substances exposure and bone mineral density in the U.S. population from NHANES 2005-2014. J Expo Sci Environ Epidemiol. http://dx.doi.org/10.1038/s41370-022-00452-7.

Zhou, Y; Li, Q; Wang, P; Li, J; Zhao, W; Zhang, L; Wang, H; Cheng, Y; Shi, H; Li, J; Zhang, Y. (2023). Associations of prenatal PFAS exposure and early childhood neurodevelopment: Evidence from the Shanghai Maternal-Child Pairs Cohort. Environ Int 173: 107850. http://dx.doi.org/10.1016/j.envint.2023.107850.

Zong, G; Grandjean, P; Wang, X; Sun, Q. (2016). Lactation history, serum concentrations of persistent organic pollutants, and maternal risk of diabetes. Environ Res 150: 282-288. http://dx.doi.org/10.1016/j.envres.2016.06.023.

Zurlinden, T. (2024). Model Code for the Hierarchical Bayesian Pharmacokinetic Analysis in Support of the IRIS Toxicological Review of PFNA [Computer Program].